Fall 10-1-2021

The Development of Mathematical Methods for Tackling Problems in Non-Perturbative Quantum Field Theory, Cosmology, and Gravity

Daniel Berkowitz
Yale University Graduate School of Arts and Sciences, db2505@nyu.edu

Abstract

The Development of Mathematical Methods for Tackling Problems in Non-Perturbative Quantum Field Theory, Cosmology, and Gravity

Daniel Berkowitz

2021

We have extended two recently developed theoretical methods, the Quantum Finite Elements (QFE) and the Euclidean-signature semi-classical method (ESSCM). The QFE is a technique for constructing lattice field theories (LFTs) on curved Riemannian manifolds. We extended the applicability of the QFE to formulating LFTs on certain three and four dimensional Riemannian manifolds such as $\mathbb{S}^3$ and $\mathbb{R} \times \mathbb{S}^3$. This was done by first constructing a novel simplicial approximation to $\mathbb{S}^3$. Then, after correctly computing the weights of the links and vertices that make up this simplicial approximation, we defined a Laplacian on it, whose low lying spectrum was observed to approach the known continuum limit as we further refined our simplicial complex. To facilitate a comparison between the QFE and the bootstrap, we calculated an estimate of the fourth-order Binder cumulant using CFT data extracted from the conformal bootstrap.

The ESSCM is a methodology for facilitating the use of already known mathematical theorems/results to approach Lorentzian signature problems in bosonic field theory and quantum gravity in terms of their Euclidean-signature analogs. We further developed this method by applying it in a novel fashion to quantum cosmological models with matter sources. In particular, for the Taub models, we proved for the first time the existence of a countably infinite number of well behaved 'excited' state solutions when Λ is present. Both methods are promising and have applications for field theory, beyond standard model physics, and quantum gravity.

The Development of Mathematical Methods for Tackling Problems in Non-Perturbative Quantum Field Theory, Cosmology, and Gravity

A Dissertation
Presented to the Faculty of the Graduate School
of
Yale University
in Candidacy for the Degree of
Doctor of Philosophy

by
Daniel Berkowitz

Dissertation Director: George Tamminga Fleming and Vincent Edward Moncrief

December 2021

Contents

List of Figures

Chapter 1

Acknowledgments

I graciously thank the committee for their time and patience during the preparation of this dissertation and for reading it. Furthermore I thank them for their commitment to the proliferation of the study of physics. The guidance of my advisers, George Fleming and Vincent Moncrief, has been a true blessing in my life. I have learned so much from working under them. This experience has helped me grow much as a physicist and as a person.

This dissertation is in memory of my loving parents, Susan Orchan Berkowitz and Jonathan Berkowitz. If it weren't for them I wouldn't be where I am today. I owe everything to them. My mom till her dying day did everything she could to ensure I would succeed at Yale. No matter how much her cancer progressed she always put my interests first. She knew how badly I wanted to become a physicist, and with vigor continuously supported me as I pursued that endeavor. Her strength was indescribable. I love her very much and greatly miss her. My dad also supported me till his dying day. Every decision he made was with my best interest at heart. I certainly wouldn't have majored in physics if it wasn't for my father. He instilled in me such a love for science and math when I was young. Those endless lists of science questions I would always ask him, and the brilliant answers he gave were pivotal in

(a) My mom: Susan Berkowitz

(b) My dad: Jonathan Berkowitz

(c) Paul Gass

me deciding to become a physicist. I love you very much dad and miss you immensely. Thanks mom and dad for everything. No tribute can escapulate how amazing you both were as parents.

I also commemorate this dissertation in memory of Paul Gass. I must also thank Cecilia Santos Berkowitz for all her love and support over the years. Throughout this process I have also been blessed to have lots of friends who care about me. Thank you. Finally I must thank Yale university for facilitating this journey.

If I am not for myself, who will be for me? And being only for myself, what am 'I'?

Hillel The Elder

If you believe that you can destroy, believe that you can repair.

Rebbe Nachman of Breslov

Chapter 2

In Regards To Notation

For tensors we generally follow Wald's [233] convention for using the Latin alphabet to denote tensors and use the Greek alphabet to denote the components of a tensor expressed in a given basis. If we deviate from this convention at all for a certain few calculations then the new convention will be stated in the calculation.

Chapter 3

Introductory Remarks

We further developed mathematical methods that can be directly applied to problems in high energy physics, quantum cosmology, and quantum gravity. The two methods we developed and built upon were the Quantum Finite Elements (QFE) and the Euclidean-signature semi-classical method.

The QFE was further developed by extending its applicability to lattice field theories formulated on certain three and four dimensional Riemannian manifolds such as $\mathbb{S}^3$ and $\mathbb{R} \times \mathbb{S}^3$. This was done by first tessellating the 600-cell, which possesses the largest discrete subgroup of isometries belonging to $\mathbb{S}^3$, by using two different types of tetrahedrons and then projecting the resultant vertices to $\mathbb{S}^3$. Using those vertices we constructed a convex hull on $\mathbb{S}^3$ and figured out how to compute the correct weights associated with the links belonging to the plethora of tetrahedrons that form our simplicial approximation to $\mathbb{S}^3$, that were created as a result of the positive curvature inherent to $\mathbb{S}^3$ which distorts the two types of tetrahedrons we originally used to tessellate the 600-cell. Using these correct values of the weights we were able to formulate the Laplace operator on our simplicial approximation to $\mathbb{S}^3$ and compute its spectrum at a given level of refinement. What we found was that as we increased the level of refinement of our simplicial approximation to $\mathbb{S}^3$, the low lying spectrum we

computed by approximately diagonalizing our discretized Laplacian using its known eigenfunctions, the hyperspherical harmonics, is converging to the known continuum limit. In addition we further tested our method for constructing a simplicial approximation to $\mathbb{S}^3$ by formulating a discretized Laplacian on a certain type of tetrahedron, known as the K tetrahedron, whose spectrum was analytically calculated in closed form, and showed that our estimated spectrum is converging to the known continuum limit as we increase our level of refinement.

Beyond testing the validity of our application of Discrete Exterior Calculus (DEC) to the tessellation of $\mathbb{S}^3$ we began taking the following steps to apply the geometric program we will describe in detail in this dissertation to ϕ^4 theory on $\mathbb{S}^3$. We oriented our simplices by finding a correct ordering of their vertices so that the discrete version of the boundary operator, ∂, when it is applied to our simplicial approximation of $\mathbb{S}^3$ vanishes, $\partial\mathcal{K} = 0$, as one would expect in the continuum limit. Furthermore using conformal bootstrap data we computed an estimate of the fourth-order Binder cumulant for the critical 3D Ising model mapped on to $\mathbb{S}^3$. The estimate we computed is $U_4 = 0.39220$ with an error of ± 0.00011. We intend to compare this result and other CFT data such as scaling dimensions and correlation functions to what the QFE predicts when we apply it to ϕ^4 theory on $\mathbb{S}^3$ at its Wilson-Fisher critical fixed point.

If the upcoming test of this program of ϕ^4 theory on $\mathbb{S}^3$ is successful then we will be significantly closer to applying the QFE to novel problems in non-perturbative quantum field theory on curved manifolds. Thus the work presented in this dissertation is an important step towards realizing the study of these incredibly fascinating topics.

We have further advanced the Euclidean-signature semi-classical method by applying it to the quantum Bianchi II, $\text{VII}_{h=0}$, VIII, IX, and Taub models when a plethora of matter sources were present; thus resulting in a large number of new and novel

solutions to their Lorentzian signature Wheeler DeWitt (WDW) equations. These matter sources include a cosmological constant, aligned electromagnetic field, a free homogeneous scalar field, an exponential homogeneous scalar field and stiff matter, which can be thought of as a perfect fluid whose ratio of energy density to pressure is $\frac{\rho}{P} = \gamma = 1$.

These new solutions were obtained using a different application of the Euclidean-signature semi-classical method than what J.Bae employed to prove that an asymptotic solution exists for the vacuum diagonal Bianchi IX WDW equation. Rather than integrating the solutions of flow equations that one obtains from the Euclidean-signature Hamilton Jacobi equation, we were able to take advantage of the symmetries that are present in some of these models and directly prove the existence of smooth and globally defined solutions to the infinite sequence of transport equations this modified semi-classical method yields.

In particular we were able to prove the existence of a countably infinite number of smooth and globally defined 'excited' state solutions to the Taub WDW equation when a cosmological constant is present and argue that we can easily perform the same feat when both a cosmological constant and aligned electromagnetic field are present. In addition we proved the existence of asymptotic solutions to both the vacuum Bianchi II and 'no boundary' Taub WDW equations by directly reducing the problem of solving the infinite sequence of transport equations into an algebraic problem. By proving the existence of solutions to these equations using novel applications of the Euclidean-signature semi-classical method we have shown new ways it can be applied to other finite dimensional Lorentzian signature problems.

The Euclidean-signature semi-classical method naturally is able to connect the solutions of the Euclidean-signature equations its application yields to the solutions of the Lorentzian signature problem it is applied to without having to invoke a Wick rotation. This same method can be modified so it can be applied to problems in

bosonic field theory and quantum gravity while retaining the same advantageous properties we just described. For those two applications the absence of a need to apply a Wick rotation is a huge advantage given the problems associated with the traditional Euclidean-signature path integral approach. An advantage of this method for bosonic field theory in particular is that it doesn't require splitting the theory up into one part which is linear (non-interacting) and another part which is a nonlinear (interacting) perturbation. This allows the fully interacting nature of the field theory to be present at every level of its analysis. Thus by expanding upon the ways this method can be applied to prove the existence of smooth and globally defined solutions to Lorentzian signature equations we inspire further development of this method which in the future can prove to be a powerful tool to tackle non-trivial problems in quantum gravity and bosonic relativistic theory, including Yang-Mills theory.

Beyond the significance this dissertation has for mathematical physics, in terms of theoretical quantum cosmology the solutions we have found possess some interesting qualities that are not present in other known solutions to the WDW equation. These qualities include, the creation of additional geometric states that our quantum universes can tunnel into when an aligned electromagnetic field is "weak", the destruction of states when the aligned electromagnetic field becomes too "strong, and a clear manifestations of how a quantum universe which possesses many likely states that it can tunnel in and out of becomes a semi-classical universe with only one likely geometric state it can be in when it becomes too large in size as dictated by its scale factor α.

The interesting aesthetic characteristics of our wave functions imply certain effects on primordial cosmological evolution which should be chronicled as possible effects that a toy model of quantum gravity can induce. In addition, due to the inclusion of matter sources such as a cosmological constant and an electromagnetic field, the wave functions we have obtained can be the basis for future work, which we will elaborate

on towards the end of this dissertation, such as understanding potential perturbations in the CMB that originated from a primordial magnetic field, and the relationship between Anti de Sitter space and de Sitter space in a quantum cosmology context.

Chapter 4

Conformal Invariance and the Ising Model on $\mathbb{S}^3$ in Connection With the Quantum Finite Elements

4.1 The Importance Of Studying Conformal Field Theory

Conformal field theories (CFTs) are a class of field theories which are conformally invariant. Conformal invariance in this context means that the correlation functions of a CFT, expressed in a certain coordinate system, $\mathbf{x}_i$, can be evaluated in a conformally related coordinate system, $\mathbf{x}_i \to \mathbf{x'}_i$. The exact manner in how this is done, will be explicitly demonstrated later when we compute the fourth-order Binder cumulant of the critical 3D Ising model on $\mathbb{S}^3$. Conformal transformations in general are angle preserving maps in space which locally look like a rotation accompanied by either a position independent or dependent dilation. A property that CFTs possess is that they are scale invariant [193, 194]. A theory is scale invariant if it behaves the same regardless of the energy scale it is being studied at. Quantum field theories studied at

their fixed point are scale invariant theories. However not all scale invariant theories are CFTs [183, 203].

CFTs can be used to study how certain QFTs behave when their coupling constants approach a conformal fixed point. Thus their study possesses foundational significance for understanding the nature of quantum field theories in general. Due to their nature, CFTs aid in the development of numerical methods that can be used to study non-perturbative quantum field theories on curved Riemannian manifolds. This is the case because a CFT defined on $\mathbb{R}^n$, which is an infinite volume domain, can be mapped to $\mathbb{S}^n$, which has a finite volume. This is a very useful feature because it allows one to numerically study a CFT, which was originally formulated on an infinite domain, on a compact manifold, thus eliminating any possible finite volume artifacts that are associated with studying field theories on finite sub-regions of $\mathbb{R}^n$. Furthermore conformal symmetry allows one to perform radial quantization [50, 52, 53, 171] from $\mathbb{R}^n$ to $\mathbb{R} \times \mathbb{S}^{n-1}$, which is the cylindrical boundary of AdS^{n+1} space which facilities the utilization of AdS/CFT correspondence.

In 3D, conformal mapping can possess the following form

$$ds^2 = \Omega\left(x_i\right)^2 \left(dr^2 + r^2 d\theta^2 + r^2 \sin^2\theta d\phi^2\right) = ds^2_{\mathbb{M}}, \tag{4.1}$$

where $ds^2_{\mathbb{M}}$ is the metric of any 3D Riemannian manifold whose Cotton tensor

$$C_{ijk} = \nabla_k R_{ij} - \nabla_j R_{ik} + \frac{1}{4}\left(\nabla_j R g_{ik} - \nabla_k R g_{ij}\right), \tag{4.2}$$

where R_{ij}, the Ricci tensor, vanishes. Examples of such manifolds include $\mathbb{R} \times \mathbb{S}^2$ and $\mathbb{S}^3$. In addition, $\Omega\left(x_i\right)$ is the Weyl or conformal factor, and is a function of the metric variables. Any manifold whose metric can be expressed as a product of a function of only the metric variables and the metric of $\mathbb{R}^n$ is conformally flat and can have a CFT defined on it.

Due to the strength of conformal symmetry, the form that correlation functions associated with CFTs can possess are limited. As a result of this restrictiveness, the correlation functions of a CFT can be defined by a set of numbers that are referred to as CFT data. This data can be computed using the conformal bootstrap techniques [87, 88, 215] or by the QFE [56]. For example, in the 2D critical Ising model, conformal invariance constrains [194] the form of the scalar two-point function to be

$$g(1,2) = \langle \phi(\vec{r}_1)\, \phi(\vec{r}_2) \rangle_{\text{plane}} = B\, |\vec{r}_2 - \vec{r}_1|^{-2X}, \tag{4.3}$$

where B is just an arbitrary constant and X is a number known as the scaling dimension. For the 2D critical Ising model, the scaling dimension is $X = \frac{1}{8}$. Furthermore the four-point function can be expressed completely in terms of the two-point function

$$\begin{aligned} g(1,2,3,4) = & \frac{1}{2} \Bigg\{ \left[\frac{g(1,2)g(2,3)g(3,4)g(4,1)}{g(1,3)g(2,4)} \right]^2 + (2 \leftrightarrow 3) \\ & + (3 \leftrightarrow 4) \Big\}^{1/2}. \end{aligned} \tag{4.4}$$

In higher dimensions, the four-point function typically cannot be expressed exactly in closed form. However it can be expressed as an OPE expansion in terms of known functions called conformal blocks and CFT data extracted from either the bootstrap or the QFE.

In any number of dimensions, nth-point correlation functions corresponding to CFTs formulated on $\mathbb{R}^n$ can be mapped to a nth dimension conformally flat manifold by just knowing its Weyl factor

$$\langle \phi(x_1) \cdots \phi(x_n) \rangle_{g_{uv}} = \frac{1}{\Omega(x_1)^X} \cdots \frac{1}{\Omega(x_n)^X} \langle \phi(x_1) \cdots \phi(x_n) \rangle_{\text{flat}} . \tag{4.5}$$

The ability to map CFTs to conformally flat manifolds and the restrictive forms their correlation functions possess makes them a valuable tool for developing methods

for formulating lattice field theories on curved Riemannian manifolds. This is because if one knows the relevant data, such as the scaling dimensions, for the operators associated with a CFT formulated on $\mathbb{R}^n$, and the form of its correlation functions, then one can compare those known values and functions with the data that is obtained from a particular lattice formulation of that same CFT on a conformally flat manifold. For 2D we know that the CFT which exists for ϕ^4 theory on $\mathbb{S}^2$ at its strong coupling Wilson-Fisher critical fixed point is in the same universality class [208] as the critical 2D Ising model on $\mathbb{R}^2$. Thus if we study ϕ^4 theory using a new method for formulating lattice field theories on curved Riemannian manifolds we can compare the results produced by this new method to known CFT data for the exact 2D critical Ising model. This type of comparison was done [54] using the QFE for ϕ^4 theory and it was found that the numerical results for the two and four-point correlation functions, and the Binder cumulants up to 12th order were in agreement with the exact [187] analytical results of the 2D critical Ising model. Because of the power and versatility of conformal invariance, CFTs are a valuable tool to test the validity of new methods designed to study non-perturbative quantum field theories on curved manifolds. Prior to applying the QFE to novel problems such as two-dimensional condensed matter systems such as graphene sheets, four-dimensional gauge theories, and beyond the standard model (BSM) strong dynamics we need to ensure that it can reproduce known results which recent advances [120, 144, 191] in the study of CFT has given us. Only once we have reproduced a sufficient number of results pertaining to CFTs can we confidently apply the QFE to quantum field theories which are not CFTs.

Beyond using CFTs to check the validity of the QFE and other numerical techniques which are in development, thanks to AdS/CFT correspondence, the study of certain CFTs can shed much light on other fascinating problems in physics. The AdS/CFT correspondence was first proposed [163] by J.Maldacena and is a conjecture which posits that there is a relationship between theories of gravity defined on the

bulk region of AdS space-time and conformal field theories living on the boundary of AdS space-time. After this conjecture was proposed, certain physically relevant identifications were made between CFTs and tractable theories of gravity on the bulk of AdS.

The most notable was the application of AdS/CFT correspondence to the study of quark-gluon plasma. In theory the dynamics of a quark-gluon plasma can be described using QCD. However due to the extreme density and temperature required for quark-gluon plasma to exist, perturbative QCD is not applicable. Thus a non-perturbative approach is required. AdS/CFT correspondence was able to help us study [147] quark-gluon plasma by making an identification between the non-perturbative field theory which describes this exotic state of matter and five dimensional AdS black holes. They found that the ratio between the viscosity η and the entropy s associated with a quark-gluon plasma is approximately equal to the following combination of universal constants

$$\frac{\eta}{s} \approx \frac{\hbar}{4\pi k}. \tag{4.6}$$

The estimate of this ratio was facilitated by AdS/CFT correspondence and it was later found to agree with experimental results [159]. The physical significance of this finding is very profound because we have good reason to believe that very shortly after the big bang, $\approx 10^{-11}s$, that quark-gluon plasma was present in the early universe. Thus we now have reason to believe that AdS/CFT correspondence can help us understand the dynamics of our universe at some of its earliest moments of existence. Beyond the AdS/CFT correspondence which has already proven to be a powerful tool to help us understand certain non-perturbative problems, other correspondences have been proposed such as dS/CFT correspondence [221], Kerr/CFT correspondence [107], and a relationship [75] between Liouville CFT and (2+1) quantum gravity. Hence the focus we will give to CFTs in this dissertation, even though we don't live in a

world which physically respects conformal symmetry is emphatically justified.

4.2 Introductory Remarks And Four-Point Function For The Critical 3D Ising model

In three dimensions powerful techniques have been developed to calculate conformal blocks [120, 144, 191] for CFTs. These conformal blocks show up when trying to calculate four-point functions in 3D and are a sum of the contributions of the relevant operators that are part of the CFT in question. The development of these new techniques was necessitated by the fact that the conformal group in 3D has only a finite number of parameters as opposed to the 2D conformal group. Thus conformal symmetry in 3D is less restrictive than it is in 2D. At the forefront of new techniques designed to evaluate conformal blocks and operator product expansions(OPE) is the conformal bootstrap [145], which has given us highly precise calculations in regards CFT data such as the spin, dimension and coefficients of operators appearing in OPE for the critical 3D Ising model [87, 141, 144]. S.Rychkov, D.Simmons-Duffin and B. Zan [209] used recently compiled CFT bootstrap data to analyze the non-gaussianity of the four-point function of the 3D critical Ising model. Using their result for the four-point function we can further extend the work done by Youjin Deng and Henk W. J. Blote [81] in 2D, to 3D, and compute an estimate of the Binder cumulant for the critical 3D Ising model mapped to $\mathbb{S}^3$ using Monte Carlo integration of the two-point and four-point functions. By computing the fourth-order Binder cumulant in this fashion we'll have an additional piece of data that we can later compare to the QFE [55] when it is applied to ϕ^4 theory on $\mathbb{S}^3$ at its Wilson Fisher critical fixed point. The QFE has already been successfully applied to ϕ^4 theory on $\mathbb{S}^2$ [54] and $\mathbb{R} \times \mathbb{S}^2$ [56] at their Wilson-Fisher critical fixed point and the results they yielded matches very nicely with known CFT data for the critical 2D and 3D Ising models.

Conformal symmetry restricts the form of the four-point function for the critical 3D Ising model as is shown below

$$\langle \phi(x_1)\phi(x_2)\ \phi(x_3)\ \phi(x_4)\rangle_{flat} = \frac{g(u,v)}{|x_1-x_2|^{2\Delta_\sigma}\,|x_3-x_4|^{2\Delta_\sigma}}, \tag{4.7}$$

where x_i is a point in $\mathbb{R}^3$ and u and v are the following conformally invariant cross ratios

$$\begin{aligned} u &= \frac{(x_{12}^2 x_{34}^2)}{(x_{13}^2 x_{24}^2)} \\ v &= \frac{(x_{32}^2 x_{14}^2)}{(x_{13}^2 x_{24}^2)}. \end{aligned} \tag{4.8}$$

For our four-point function (4.7), Δ_σ is the scaling dimension of $\phi(\hat{x}_i)$ and its value [146] estimated by the conformal bootstrap is $\Delta_\sigma = 0.5181489(10)$. The numerator of (4.7), $g(u,v)$, can be expressed as an OPE in terms of conformal blocks

$$g(r,\eta) = 1 + \sum_{\mathscr{O}\in\sigma\times\sigma} C^2_{\sigma\sigma\mathscr{O}} g_{\Delta_\mathscr{O},\ell_\mathscr{O}} g(r,\eta), \tag{4.9}$$

where

$$\begin{aligned} r &= \sqrt{\frac{z\bar{z}}{\left(\sqrt{1-z}+1\right)^2\left(\sqrt{1-\bar{z}}+1\right)^2}} \\ \eta &= \frac{\frac{z}{\left(\sqrt{1-z}+1\right)^2} + \frac{\bar{z}}{\left(\sqrt{1-\bar{z}}+1\right)^2}}{2\left(\frac{z\bar{z}}{\left(\sqrt{1-z}+1\right)^2\left(\sqrt{1-\bar{z}}+1\right)^2}\right)^{\frac{1}{2}}} \\ u &= z\bar{z} \\ v &= (1-z)(1-\bar{z}). \end{aligned} \tag{4.10}$$

These coordinates were chosen so our results are in concord with what was previously done on this subject [121, 144].

The sum in (4.9) is over the operators(excluding the unit operator) that are present in the $\phi(x_i)\times\phi(x_j)$ OPE of dimension $\Delta_\mathscr{O}$ and spin $\ell_\mathscr{O}$. The scale dimensions

and spins for these operators are provided in table 1 of [141]. To evaluate (4.9) we use following recursion relation which was first reported in [145]

$$
\begin{aligned}
&(4r)^{\Delta} h_{\Delta,\ell}(r,\eta) \equiv \; g_{\Delta,\ell}(r,\eta) \\
&h_{\Delta,\ell}(r,\eta) = h_{\ell}^{(\infty)}(r,\eta) + \sum_{k} \frac{c_1 r^{n_1}}{\Delta - \Delta_1} h_{\Delta_1+n_1,\ell_1}(r,\eta) + \sum_{k} \frac{c_2 r^{n_2}}{\Delta - \Delta_2} h_{\Delta_2+n_2,\ell_2}(r,\eta) \\
&+ \sum_{k} \frac{c_3 r^{n_3}}{\Delta - \Delta_3} h_{\Delta_3+n_3,\ell_3}(r,\eta)
\end{aligned}
\tag{4.11}
$$

where information on what $h_{\ell}^{(\infty)}(r,\eta)$, c_i, n_i, ℓ_i, and Δ_i are is described in [144].

This recursion relation converges quickly and is easy to evaluate using a computer algebra system like Mathematica. For our purposes we evaluate $h_{\Delta,\ell}$ to 12th order in r where $h_{\ell}^{(\infty)}$ is not expanded in terms of r. The result of using this recursion relation (4.11) to compute $h(r,\eta)$ up to nth order should be a nth order polynomial in r whose coefficients include $h_{\ell}^{(\infty)}(r,\eta)$. In the appendix, there will be a Mathematica code that evaluates (4.9) as a sum over the operators present in table 1 of [141] up to any order in r.

4.3 Conformal Invariance of an 3D Spheroid

4.3.1 Conformal Invariance of $\mathbb{S}^3$

In this section we will furnish a conformal mapping between a general 3D spheroid and $\mathbb{R}^3$. We will later use the resultant Weyl factor to obtain an estimate of the fourth-order Binder cumulant for the critical 3D Ising model on $\mathbb{S}^3$. Our spheroid can be defined as a set of points embedded in $\mathbb{R}^4$ which satisfies the following relation in Cartesian coordinates

$$\frac{x^2}{a^2}+\frac{y^2}{a^2}+\frac{z^2}{a^2}+\frac{w^2}{b^2}=1 \quad (a,b>0). \tag{4.12}$$

When $b \to 0$ our spheroid approaches the 3D analogue of a disc or a 2-ball, which is a 3-ball. Technically speaking this 3-ball will be the superposition of two 3-balls superimposed onto each other at their boundaries. This will be discussed in more detail later. In the opposite limit when $b \to \infty$ our spheroid can be understood to approach $\mathbb{R} \times \mathbb{S}^2$. In an earlier calculation ϕ^4 theory at its Wilson-Fisher fixed point was analyzed [56] on $\mathbb{R} \times \mathbb{S}^2$ using the QFE. When $b \to a$ the spheroid approaches $\mathbb{S}^3$, which is the next manifold we wish to study ϕ^4 theory on using the QFE.

A set of equations which satisfy (4.12) and encapsulates all of the cases we just outlined and everything else in-between are

$$\begin{aligned} x &= a \sin\psi \sin\theta \cos\phi, \\ y &= a \sin\psi \sin\theta \sin\phi, \\ z &= a \sin\psi \cos\theta, \\ w &= b \cos\psi, \end{aligned} \tag{4.13}$$

where ψ and θ range from 0 to π, and ϕ ranges from 0 to 2π. Intuitively this set of coordinates can be deduced by noticing that as one goes up a dimension from the circle, $\mathbb{S}^1$, to the sphere, $\mathbb{S}^2$, that an extra parameter, θ, is introduced which ranges from 0 to π in the following manner

$$\begin{aligned} x_{\mathbb{S}^2} &= \sin\theta x_{\mathbb{S}^1}, \\ y_{\mathbb{S}^2} &= \sin\theta y_{\mathbb{S}^1}, \\ z_{\mathbb{S}^2} &= \cos\theta. \end{aligned} \tag{4.14}$$

For the coordinates originally associated with the lower dimensional sphere, a factor of $\sin\theta_i$, where θ_i ranges from 0 to π is included and represents a new degree of freedom

present on the higher dimensional sphere. The new independent Cartesian coordinate which differentiates the higher dimensional embedding space from the one dimension lower space is parameterized by $\cos\theta_i$. We see that carrying out this construction from the $\mathbb{S}^2$, parameterized using standard spherical coordinates, to the $\mathbb{S}^3$ results in (4.13). Extending this to arbitrary dimensions results in the following parameterization for a n-sphere with radius r,

$$\begin{aligned} x_1 &= r\cos(\theta_1) \\ x_2 &= r\sin(\theta_1)\cos(\theta_2) \\ x_3 &= r\sin(\theta_1)\sin(\theta_2)\cos(\theta_3) \\ &\vdots \\ x_{n-1} &= r\sin(\theta_1)\cdots\sin(\theta_{n-2})\cos(\phi) \\ x_n &= r\sin(\theta_1)\cdots\sin(\theta_{n-2})\sin(\phi)\,. \end{aligned} \tag{4.15}$$

Because the n-sphere and in turn the n-spheroid can be parameterized in a convenient coordinate system the results in this paper can be generalized to n dimensions.

Using (4.13) we obtain the following metric representation for a 3D spheroid

$$ds^2_{sph} = \left(b^2\sin^2\psi + a^2\cos^2\psi\right)d\psi^2 + a^2\sin^2\psi(d\theta^2 + \sin^2\theta d\phi^2). \tag{4.16}$$

Using the following change in coordinates inspired by [81], $w = \int\sqrt{b^2\sin^2\psi + a^2\cos^2\psi}d\psi$, we can rewrite (5.31) as

$$ds^2_{sph} = dw^2 + f(w)^2(d\theta^2 + \sin^2\theta d\phi^2), \tag{4.17}$$

where $f(w) = a\sin\psi$. This metric can be related conformally to the following metric on $\mathbb{R}^3$

$$ds^2_{flat} = (dr^2 + r^2 d\theta^2 + r^2 \sin^2\theta d\phi^2), \tag{4.18}$$

by introducing this functional dependency, $r = e^{g(w)}$, which results in

$$ds^2_{flat} = e^{2g(w)} \left(\frac{dg}{dw}\right)^2 \left(dw^2 + \left(\frac{1}{\frac{dg}{dw}}\right)^2 \left(d\theta^2 + \sin^2\theta d\phi^2\right)\right). \tag{4.19}$$

We can now set

$$\left(\frac{1}{\frac{dg}{dw}}\right) = a \sin\psi(w) \tag{4.20}$$

and obtain $g(w) = \int \frac{1}{a} \csc\psi dw$. Going back to the original coordinate transformation we applied to (5.31), we can rewrite $g(w)$ as

$$g(w) = \int \frac{1}{a} \csc\psi \sqrt{b^2 \sin^2\psi + a^2 \cos^2\psi} d\psi = \int \sqrt{\frac{b^2}{a^2} + \cot^2\psi} d\psi. \tag{4.21}$$

By doing so we recover the following metric which is conformal to (4.17)

$$ds^2_{flat} = \frac{e^{2g(w)}}{a^2 \sin^2\psi} \left(dw^2 + f(w)^2 (d\theta^2 + \sin^2\theta d\phi^2)\right). \tag{4.22}$$

By comparing (4.22) to (4.17) we can deduce that the Weyl factor of our 3D spheroid is

$$\Omega_{spheroid}(x_i) = a \sin\psi e^{-\int \sqrt{\frac{b^2}{a^2} + \cot^2\psi} d\psi}. \tag{4.23}$$

For the case of $\mathbb{S}^3$ when $b = a = 1$ this reduces to

$$\Omega_{\mathbb{S}^3}(x_i) = 2\cos^2\frac{\psi}{2}. \tag{4.24}$$

Going back to how we parameterized r in (4.18) and setting $b = a = 1$ we obtain the

following mapping between a point on $\mathbb{S}^3$ and a point in $\mathbb{R}^3$

$$\begin{aligned} z &= \tan\left(\frac{\psi}{2}\right)\cos\theta, \\ y &= \tan\left(\frac{\psi}{2}\right)\sin\theta\sin\phi, \\ x &= \tan\left(\frac{\psi}{2}\right)\sin\theta\cos\phi. \end{aligned} \tag{4.25}$$

From a geometric perspective our conformal mapping of $\mathbb{S}^3$ to $\mathbb{R}^3$ is the exact higher dimensional analogue of the standard stereographic projection commonly performed from $\mathbb{S}^2$ to $\mathbb{R}^2$. For the general case this mapping can be accomplished by placing a $\mathbb{S}^n$ on $\mathbb{R}^n$ with its south pole centered on the origin of $\mathbb{R}^n$ and drawing lines from the north pole which intersect both $\mathbb{S}^n$ and $\mathbb{R}^n$. Each one of those lines are oriented by a set of n angles and their intersection with $\mathbb{S}^n$ and $\mathbb{R}^n$ provides a one to one mapping between $\mathbb{S}^n$ and $\mathbb{R}^n$. The north pole itself cannot be mapped using only a single cover because in the limiting case the line that would intersect the north pole becomes parallel to $\mathbb{R}^n$ and hence never intersects it. That is why $\mathbb{S}^n$ can be thought of as a one point compactification of $\mathbb{R}^n$. A picture of this stereographic projection is provided in Fig. 5.11.

4.3.2 Conformal Invariance of $R \times \mathbb{S}^2$

As we previously mentioned, in the limit, $b \to \infty$, (4.12) gives the equation for a 3D cylinder which is topologically equivalent to $R \times \mathbb{S}^2$. One way of seeing this is to examine what happens to (4.12) as $b \to \infty$ and $-\infty < w < \infty$. In the limit of, $b \to \infty$, and w being finite, (4.12) reduces to

$$\frac{x^2}{a^2} + \frac{y^2}{a^2} + \frac{z^2}{a^2} = 1. \tag{4.26}$$

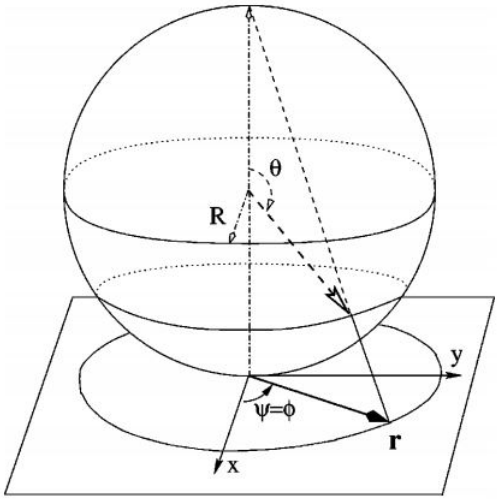

(a)

Figure 4.1 Illustration of the conformal mapping between an infinite plane and $\mathbb{S}^2$ with the polar angle shifted in the following manner, $\theta \to \pi - \theta$, compared to what we have in (4.24). This imagine originally appeared in [81]

Despite the disappearance of w the manifolds which (4.26) admits are still embedded in $\mathbb{R}^4$. Thus w can be parameterized independently of x, y, and z in an arbitrary fashion. Because we wish to recover $R \times \mathbb{S}^2$ we will set $w = t$, where t ranges from $(-\infty, \infty)$ and parameterize x, y, and z using standard spherical coordinates. Doing so results in the following metric

$$\begin{aligned} ds^2_{3-cyl} &= dx^2 + dy^2 + dz^2 + dw^2, \\ ds^2_{3-cyl} &= dt^2 + a^2(d\theta^2 + \sin^2\theta d\phi^2), \end{aligned} \tag{4.27}$$

where a is the radius of $\mathbb{S}^2$. Using (4.15), this metric can be generalized to $R \times \mathbb{S}^n$

$$ds^2_{n-cyl} = dt^2 + d\Omega^2_{n-1}, \tag{4.28}$$

where $d\Omega^2_{n-1}$ is the metric of $\mathbb{S}^{n-1}$ which can be obtained for any n using (4.15). As the reader can verify $dt^2 + a^2(d\theta^2 + \sin^2\theta d\phi^2)$ is conformally related to $(dr^2 + r^2 d\theta^2 + r^2 \sin^2\theta d\phi^2)$ through the following Weyl factor

$$\Omega^2_{3-cyl} = e^{-2t/a}, \tag{4.29}$$

generated by defining r as

$$r = ae^{\frac{t}{a}}. \tag{4.30}$$

It should be mentioned that setting b equal to a positive, real, finite number does not result in the geometry of a finite length $\mathbb{R} \times \mathbb{S}^2$. Rather the resultant geometry is a 3D ellipsoid. Only in the limit as $b \to \infty$ is $\mathbb{R} \times \mathbb{S}^2$ realized.

Because $\mathbb{R} \times \mathbb{S}^2$ isn't a compact manifold using integration to find the Binder cumulant (4.39) isn't trivial. To obtain an estimate of the Binder cumulant for this non-compact geometry one can perform a single point compactification of $\mathbb{R} \times \mathbb{S}^2$ which results in $\mathbb{S}^1 \times \mathbb{S}^2$ and define a lattice field theory on that manifold. Once a lattice field theory is defined on $\mathbb{S}^1 \times \mathbb{S}^2$ one can perform a Monte Carlo simulation to compute an estimate of the Binder cumulant on that compactified geometry as was done in [57]. When this compactification is done the manifold is defined by two radii $r1$ and $r2$, where $r1$ denotes the radius of $\mathbb{S}^1$ and, $r2$ is the radius of $\mathbb{S}^2$. In the limit as $r1 \to \infty$, $\mathbb{S}^1 \times \mathbb{S}^2$ approaches $\mathbb{R} \times \mathbb{S}^2$. Therefore if one has a method, such as the QFE, which allows them to formulate lattice field theories on curved manifolds they can study the critical 3D Ising model on $\mathbb{S}^1 \times \mathbb{S}^2$ as $r1 \to \infty$ and observe what the Binder cumulant approaches.

4.3.3 Conformal Invariance of 3-Ball

Before we move on to calculating the Binder cumulant on $\mathbb{S}^3$ it is prudent to talk about how one would do the corresponding calculation for the 3-ball. The 3-ball is imminently related to $\mathbb{S}^3$. One can construct $\mathbb{S}^3$ by superimposing two 3-balls and defining an equivalence class which identifies all of the points which make up the shared boundaries of this superimposed ball. In other words, the points which

make up the boundary of the two superimposed 3-balls, which are two 2-spheres, are identified as a single point. This identification of the boundary with a single point can be realized by projecting out the boundary of this superimposed 3-ball into a higher dimensional space in which the boundary points of the 2-spheres merge at the north pole; thus resulting in a newly formed $\mathbb{S}^3$.

Mathematically we see a hint of this construction by setting, $b = 0$, and obtaining the following r from our earlier coordinate transformation

$$r = \lim_{b\to 0} e^{\int \sqrt{\frac{b}{a}+\cot^2\psi}d\psi} = \sin\psi. \tag{4.31}$$

As it can be seen when $b \to 0$ our r doesn't cover the whole plane $\mathbb{R}^3$ because r only ranges from 0 to 1. This is because these coordinates only map points located on the lower hemisphere and excludes points located on our 3-ball's upper hemisphere. This is an artifact of $\mathbb{S}^3$ being a construction of two superimposed 3-balls with their shared boundaries being glued together at a single point. The total mapping can be realized by noticing that we could have defined our functional dependency right above (4.19) as $r = e^{-g(w)}$. Such a functional dependency would have allowed us to obtain a different Weyl factor, $\Omega(x_i)$, which nonetheless yields the exact same Binder cumulant for the case of $\mathbb{S}^3$ as the one we previously calculated. However it would also result in the following radius

$$r = \lim_{b\to 0} e^{-\int \sqrt{\frac{b}{a}+\cot^2\psi}d\psi} = \csc\psi. \tag{4.32}$$

which ranges from 1 to ∞. Thus in order to compute the two and four-point functions for the superimposed 3-ball one must differentiate between points on the northern hemisphere and points on the southern hemisphere because they both have different radial coordinates, (4.31) and (4.32). The resulting calculation involves group averaging the four-point function over all of the different combination of points that can

be on one hemisphere and the opposite hemisphere. More information of this group averaging for the 2-ball which can be extrapolated to the 3-ball can be found in [81].

Preliminary results obtained using the five operators reported in table 1 of [142] and setting $\frac{b}{a} = 10^{-5}$ yields, $U_4 = 0.38703 \pm .0.00570$, which suggests that the Binder cumulant for these two superimposed 3-balls is similar to the Binder cumulant for $\mathbb{S}^3$ as we show in section IV. This similarity between the Binder cumulant of the superimposed 3-ball and $\mathbb{S}^3$ are in concord with the similarity found in [81] between the Binder cumulant of the superimposed 2-ball (disc) and $\mathbb{S}^2$.

For the related case of the interior of a single, non-superimposed sphere that was considered in [74] one has to take into account the boundary. This is done by studying the boundary conformal field theory (BCFT) [62, 63] which has its own scaling dimensions and operators associated with it. For the case with a free boundary on $\mathbb{S}^2$ the scaling dimension of the relevant operator was found to be [82, 85, 99, 113] $\Delta_{\tilde{\sigma}} = 1.276(2)$. Thus in computing the Binder cumulant of a 3-ball with a boundary one must differentiate between pairs of points which are either both on the boundary, inside the bulk or where one point is inside the bulk and the other is on the boundary. The need to differentiate the location of points on the two aforementioned manifolds is a similarity that the two-superimposed 3-balls and the single 3-ball with boundary share with each other.

Using the known values of the scaling dimensions on the boundary of a 3-ball and its interior allows one in theory to use the formalism we presented in this paper to compute an estimate of the fourth-order Binder cumulant. An estimate of the fourth-order Binder cumulant for the critical 3D Ising model on a 3-ball with a boundary computed by integrating its two and four-point functions can be compared with the estimate obtained in [74]. Comparing this hypothetical estimate to what was obtained in [74] can increase our understanding of how to study BCFTs via numerical simulations. In the future we plan to do the calculation we outlined in this section in

the limit when, $\frac{b}{a} = 0$, and perform a comparison of the value of the Binder cumulant obtained from direct integration to [74]. Furthermore in the future the QFE can be extended to apply to quantum field theories formulated on curved manifolds with boundaries.

4.4 Binder Cumulant Estimate

Using the Weyl factor, $\Omega(x_i) = 2\cos^2\left(\frac{\psi_i}{2}\right)$, we obtained earlier we can map the two and four-point functions of the critical 3D Ising model from $\mathbb{R}^3$ to $\mathbb{S}^3$ as is shown below in

$$\begin{aligned}
&\langle\phi(x_1)\,\phi(x_2)\rangle_{g_{uv}} = \frac{1}{\Omega(x_1)^{\Delta_\sigma}}\frac{1}{\Omega(x_2)^{\Delta_\sigma}}\langle\phi(x_1)\,\phi(x_2)\rangle_{\text{flat}} \\
&\langle\phi(x_1)\,\phi(x_2)\,\phi(x_3)\,\phi(x_4)\rangle_{g_{uv}} \\
&= \frac{1}{\Omega(x_1)^{\Delta_\sigma}}\ldots\frac{1}{\Omega(x_4)^{\Delta_\sigma}}\langle\phi(x_1)\ldots\phi(x_4)\rangle_{\text{flat}}\ .
\end{aligned} \tag{4.33}$$

We will use these variables in (4.25) to construct our two and four-point functions

As it can be seen below conformal symmetry greatly restricts the form of the following two-point function

$$\langle\phi(x_1)\,\phi(x_2)\rangle_{flat} = \frac{1}{x_{12}^{2\Delta}}, \tag{4.34}$$

where $x_{ij} = |x_i - x_j|$. The two quantities we need to find by integrating our two and four-point functions over $\mathbb{S}^3$ in order to obtain our fourth-order Binder cumulant are the following magnetization densities

$$\begin{aligned}
\langle\sigma^2\rangle &= \rho^2\int \mathrm{d}S_1\ \mathrm{d}S_2\,\langle\phi(x_1)\,\phi(x_2)\rangle_{g_{uv}}\,, \\
\langle\sigma^4\rangle &= \rho^4\int \mathrm{d}S_1\cdots\mathrm{d}S_4\,\langle\phi(x_1)\,\phi(x_2)\,\phi(x_3)\,\phi(x_4)\rangle_{g_{uv}}\,,
\end{aligned} \tag{4.35}$$

where ρ is the areal density of the spins, and $\mathrm{d}S_i$ represents the number of spins in an infinitesimal area. For the $\mathbb{S}^3$, ρ, and $\mathrm{d}S_i$ can respectively be expressed as $\frac{1}{2\pi^2}$ and

$\sin^2\psi_i \sin\theta_i d\psi_i d\theta_i d\phi_i$. We can reduce the computational cost of integrating our two and four-point functions by taking advantage of the SO(4) symmetry of $\mathbb{S}^3$. Because SO(4) has six generators, which corresponds to six independent rotations, we can rotate our $\mathbb{S}^3$ in such a way that some of the angles that we would normally need to integrate over are fixed; thus reducing the computational cost of our multidimensional Monte Carlo integration. This can be seen because SO(4) is locally isomorphic to $SO(3) \otimes SO(3)$. Thus there are six independent rotations for $\mathbb{S}^3$ three for each SO(3). This can be seen by noticing that the Lie Algebra of SO(4) can be represented as two copies of the Lie Algebra of SO(3).

The key for efficiently evaluating these integrals (4.35) is to use the SO(4) symmetry of $\mathbb{S}^3$. For the two-point function we can naively evaluate a 6th dimensional integral over these points on its surface, $(\psi_1, \theta_1, \phi_1)$ and $(\psi_2, \theta_2, \phi_2)$. By rotating $\mathbb{S}^3$ we can set the first point to be $(0, 0, 0)$ and the second point to be $(\psi_2, 0, 0)$. This results in the following integral for the 2nd order magnetization density.

$$\left\langle \sigma^2 \right\rangle = \int_0^\pi \frac{\left((2\pi^2)\,(4\pi)\sin^2(\psi_2)\right)\left(\frac{1}{2\pi^2}\right)^2}{\left(2\cos^2\left(\frac{\psi_2}{2}\right)\right)\left(\frac{\sin^2(\psi_2)}{(1+\cos(\psi_2))^2}\right)^{0.518149}} d\psi_2 \tag{4.36}$$

which yields from Mathematica's INTEGRATE function

$$\left\langle \sigma^2 \right\rangle = 0.847359 \tag{4.37}$$

The four-point function can be ultimately expressed using the following coordinates $(\psi_1, \theta_1, \phi_1)$, $(\psi_2, \theta_2, \phi_2)$, $(\psi_3, \theta_3, \phi_3)$, $(\psi_4, \theta_4, \phi_4)$. Using the SO(4) group we can reduce the dimensionality of our integral for $\langle \sigma^4 \rangle$ from twelve to six by fixing the following coordinates $(0, 0, 0), (\psi_2, 0, 0), (\psi_3, \theta_3, 0), (\psi_4, \theta_4, \phi_4)$. Using Mathematica NINTEGRATE, we preformed 10,000 Monte Carlo evaluations and obtained the following

estimate of the fourth-order magnetization and its associated statistical error

$$\left\langle \sigma^4 \right\rangle = 1.59083 \pm 0.00016. \tag{4.38}$$

We now have all that we need to compute an estimate of the fourth-order Binder cumulant.

$$U_4 = \frac{3}{2}\left(1 - \frac{1}{3}\frac{\langle \sigma^4 \rangle}{\langle \sigma^2 \rangle^2}\right) \tag{4.39}$$

$$U_4 = 0.39220 \pm 0.00011. \tag{4.40}$$

For now we exclude sources of error orientating from uncertainty inherent to the CFT data obtained through the bootstrap.

This result must be understood within the context of the OPE representation of the four-point function. Infinitely many operators of varying scaling dimension and spin exist which must be summed in order to obtain an exact expression for the four-point function of the critical 3D Ising model. The finite number of operators whose CFT data has been obtained from the bootstrap are the leading order operators which contribute the most to the four-point function. However, because we only took into account data pertaining to eleven of those operators a systematic error will be present in our calculation as a result of us not being able to integrate the exact four-point function. The remainder of the operators posses a higher spin and/or scaling dimension. Thus their inclusion would allow us to more accurately compute the four point function when the points are very close to each other.

The range of this systematic error can be estimated by taking the difference between the Binder cumulant computed using the eleven operators listed in table 2 of [216] and the resultant cumultant one obtains if they use only ten of the operators. There is no definitive answer for which ten operators one should include. Thus we performed this estimate using two similar, but different methodologies. The first methodology involves computing a sequence of Binder cumulants as operators are

added to the OPE in the order of their scaling dimension. This means first computing the Binder cumulant while only including the operator with the lowest scaling dimension, ϵ, in the OPE representation of the four-point function and than including the operator with the next lowest scaling dimension, $T_{\mu,\nu}$, until ten of the eleven operators are included in the four-point function. The next methodology is similar except operators are included sequentially into the OPE in order of increasing spin.

In terms of increasing scaling dimension and spin, one respectively obtains the following Binder cumulants and potential estimates for the systemic error

$$\begin{aligned} U_{Scaling} &= 0.39216 \pm 0.00011 \\ \Delta U_{4-Scaling} &= U_4 - U_{Scaling} = 0.00004, \end{aligned} \tag{4.41}$$

$$\begin{aligned} U_{Spin} &= 0.39165 \pm 0.00011 \\ \Delta U_{4-Spin} &= U_4 - U_{Spin} = 0.00141. \end{aligned} \tag{4.42}$$

One way to interpret the magnitude of the systematic errors that we obtained using bootstrap data is to compare it to the magnitude of the systematic error generated by doing the analogous calculation using the QFE. A direct comparison of such nature cannot be done at the moment because we haven't had a chance to apply the QFE to ϕ^4 theory on $\mathbb{S}^3$. However it is reasonable to expect that the relative error that we will obtain when we do the aforementioned calculation will be similar to the relative error obtained for the analogous calculation [95, 174] on $\mathbb{S}^2$ which has already been done.

Below are the statistical(58) and systematic(90) errors for an estimate of the fourth-order Binder cumulant of ϕ^4 theory at its Wilson-Fisher conformal fixed point on $\mathbb{S}^2$ computed using the QFE (Monte Carlo Values) [95, 174] and direct integration (Analytic CFT Values).

$$\begin{aligned} &\text{Monte Carlo Values:} \qquad U_{4,cr} = 0.85020(58)(90) \\ &\text{Analytic CFT Values:} \qquad U_4^* = 0.8510207(63). \end{aligned} \tag{4.43}$$

If we compute the relative error of the above QFE result we obtain

$$\delta U_{4,cr} = \frac{9 \times 10^{-4}}{0.85020} \approx 10^{-3}. \tag{4.44}$$

This is a reasonable estimate of the systematic error that we expect our QFE calculation on $\mathbb{S}^3$ to yield. Therefore in order to interpret the magnitude of the relative error that the bootstrap presently yields for the fourth-Binder cumulant of the critical 3D Ising model we should compare it to (4.44).

$$\delta U_{4,scaling-dim} \approx 9 \times 10^{-5}, \tag{4.45}$$

$$\delta U_{4,spin} \approx 3.6 \times 10^{-3}. \tag{4.46}$$

If the systematic error in our calculation is closer to (4.45) that would suggest that the current CFT data that we have from the bootstrap is enough to compute an accurate estimate of the four-point function relative to the implementation of the QFE that was used in [54]. However if the systematic error is much closer to (4.46), that would indicate that the current bootstrap results aren't enough to match the accuracy of the QFE and that additional data on higher order operators is needed so that the accuracy of the two calculations can be in agreement with each other.

To demonstrate the convergence of the Binder cumulant as we add terms to the four-point function we show in figure 2 the Binder cumulant as a function of these operators for both methodologies. We used Monte-Carlo integration and 1,000 iterations to compute each Binder cumulant. We are confident that our range is representative of the systematic error because it is evident that as we include operators in the OPE that our results are converging to a definitive value. The difference between

preceding cumulants have a tendency to shrink as we include more operators, thus the inclusion of more operators will allow us to further minimize the systematic error. Thus in order to compute a more accurate estimate of the fourth-Binder cumulant using integration we need additional bootstrap results for higher order operators and to include more Monte Carlo iterations.

Figure 2b shows an interesting phenomenon. Excluding when only the operator with both the lowest scaling dimension and spin is included, the inclusion of an operator with higher spin results in the value of U_4 jumping. When the highest operator included in the four-point function has spin 2 the values of U_4 varies little as additional spin 2 operators are included. It is only when spin 4 operators are included that we see such a jump and again see that the value of U_4 varies very little when additional spin 4 operators are included. We see a similar jump when we include a spin 6 operator. The jump though decreases in magnitude as higher and higher spin operators are included. This suggests that the value of the Binder cumulant approaches some definitive number as we increase the operators in the OPE representation of the four point function. The origin of this phenomenon deserves to be investigated.

As a check that our procedure for evaluating the four-point function on $\mathbb{S}^3$ is correct we calculated the Binder cumulant for the free theory. The correlation functions for a free CFT are given in [106] and its Binder cumulant should be zero. Using Monte Carlo integration, 10,000 iterations, and accuracy goal 15, we calculated

$$U_4 = -1.9176 \times 10^{-6} \pm 4.7357 \times 10^{-5}. \tag{4.47}$$

Our result is very comfortably within the range of the expected result of 0 for the Binder cumulant. We hope to check our results for the Binder cumulant of the critical 3D Ising model on $\mathbb{S}^3$ using the QFE in the near future.

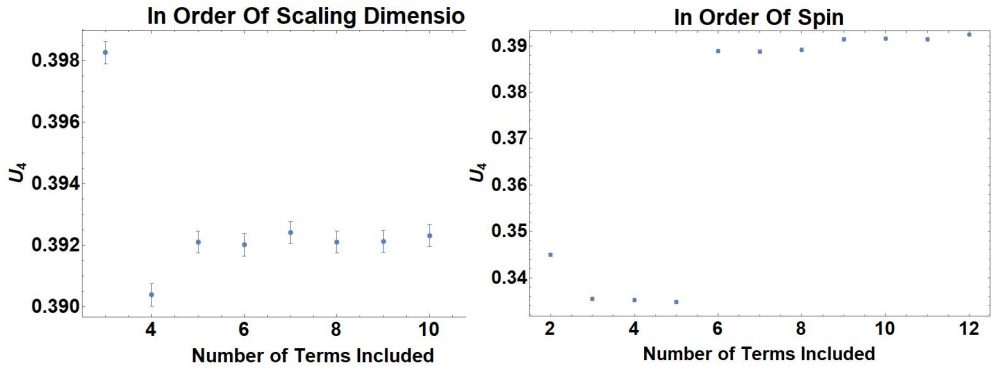

(a) Binder cumulant plot in order of scaling dimension

(b) Binder cumulant plot in order of increasing spin

Figure 4.2 Plots of the Binder cumultant as we include operators into the OPE of the four-point function in order of their scaling dimension and spin. We count the unit operator as the first term included. We started with the 3rd operator plot in order of scaling dimension. The statistical error bars don't show in the spin graph because of the large difference in values of the Binder cumulant when only spin zero operator are included versus when spin $2 >$ operators are included. The statistical errors for all of the points in our spin graph are around $\approx .0004$.

4.5 Further Remarks

Using the data of the critical 3D Ising model computed using the conformal bootstrap method, we integrated the approximate two and four-point functions to obtain an estimate of the fourth-order Binder cumulant. We also showed how this approach could be used to estimate the Binder cumulants for the 3-ball and other 3D spheroids. Our approach is an extension of the work by Deng and Blote [81] to three dimensions and we showed how it could be extended further to higher dimensional spheroids. The immediate application of our result is to compare this estimate of the Binder cumulant with one computed in an upcoming calculation of ϕ^4 theory on $\mathbb{S}^3$ using quantum finite elements (QFE). A favorable comparison of the two methods would give us further confidence that QFE is a correct framework for computing non-perturbative quantum field theories on curved manifolds.

Chapter 5

The Quantum Finite Elements

5.1 Brief History of the Quantum Finite Elements

Lattice field theory has proven to be a powerful non-perturbative approach to quantum field theory [10]. However, the lattice regulator has generally been restricted to flat Euclidean space, $\mathbb{R}^4$, discretized on hypercubic lattices with a uniform ultraviolet (UV) cutoff, $\Lambda_{UV}=\frac{\pi}{a}$, in terms of the lattice spacing, a. This formalism is not ideal to study quantum field theories at their conformal fixed points. One issue, [95] is that correlations functions associated with certain field theories grow without bound as one numerically tunes them to their conformal fixed points. This results in finite volume artifacts compromising the integrity of the calculation being performed. Another issue is that at conformal fixed points, correlation functions generally scale as fixed power law functions as opposed to an exponential. This makes it difficult to extract accurate eigenvalues, scaling dimensions, and other CFT data using traditional lattice methods.

A way to partially amend the above situation is to perform radial quantization. As was previously discussed, a CFT on $\mathbb{R}^d$ can be mapped to $\mathbb{R} \times \mathbb{S}^{d-1}$. This conformal

mapping at a geometric level takes the form of

$$ds^2_{\mathbb{R}^d} = dr^2 + r^2 d\Omega^2_{d-1} = e^{2t}\left(dt^2 + d\Omega^2_{d-1}\right) \to dt^2 + d\Omega^2_{d-1} = ds^2_{\mathbb{R}\times\mathbb{S}^{d-1}}, \tag{5.1}$$

where the coordinates r and t are related to each other by an exponential map $r = e^t$ and the Weyl factor is $\Omega = e^t$. This exponential factor results in the correlation function of the theory being studied at its conformal fixed point to behave in an exponential fashion.

In order to study field theory numerically on $\mathbb{R} \times \mathbb{S}^{d-1}$ a compaction of the time axis $\mathbb{R}$ must take place. This is done by employing periodic boundary conditions, thus transforming $\mathbb{R} \times \mathbb{S}^{d-1}$ to $\mathbb{S} \times \mathbb{S}^{d-1}$. Despite this progress towards applying traditional lattice methods to field theories at their conformal fixed points a problem still remained. It was pointed out by Cardy that applying radial quantization for the case when $d > 2$ raises a problem [64] because no regular lattice refinement scheme was known for the temporal cross sections of $\mathbb{R} \times \mathbb{S}^{d-1}$.

Thus the problem of studying field theories at their conformal fixed points became a problem of formulating lattice field theories on curved Riemannian manifolds. Before one can proceed to tackle this problem, the question of whether a renormalizable quantum field theory in flat space-time is perturbatively renormalizable on a curved space-time must be answered. Fortunately, thanks to a large amount of research [60, 125, 126, 157] conducted in the 70s and 80s this question was answered. That research concluded that any UV complete theory in flat space is perturbatively renormalizable on a curved Riemannian manifold and its counter terms are invariant under diffeomorphism of the manifold that the theory is on.

With this in mind we can begin to talk about attempts to formulate what is now known as the QFE. In 2012 R. Brower, G. Fleming and H. Neuberger embarked on an investigation [58] of the critical 3D Ising model using radial quantization. In

the process of their investigation, they constructed a simplicial approximation of $\mathbb{S}^2$ using a regular icosahedron. In spite of some qualitative success, small defects were observed at the $l = 3$ level which persisted as the continuum limit was approached. Nonetheless much was learned from this exercise. In the coming years, the method was improved upon [52, 53] by figuring how to include position (lattice) dependent quantum counter terms to remedy any artifacts as a result of working on a non-uniform lattice and by studying the geometric nature of the non traditional lattice that was originally constructed in 2012.

After much work, the QFE was applied to 2D ϕ^4 theory at its Wilson Fisher critical fixed point and it was found that the numerical results for the two- and four-point correlation functions, and the Binder cumulants up to 12th order were in agreement with the exact analytical results of the $c = 1/2$ CFT solutions. It was also successfully applied to ϕ^4 theory at its Wilson-Fisher critical fixed point [56] on $\mathbb{R} \times \mathbb{S}^2$ and to a free theory consisting of fermions [55]. Currently it is in the process of being applied to ϕ^4 theory on $\mathbb{S}^3$ by the author which will pave the way for it to be applied to theories on the physically relevant space of $\mathbb{R} \times \mathbb{S}^3$. This space is important to study because manifolds that can be described as $\mathbb{R} \times \mathbb{S}^3$ in a topological sense are ubiquitous in general relativity.

This chapter will consist of the following content. In the next section we will discuss how we construct our simplicial approximation of $\mathbb{S}^3$ which preserves the largest known discrete subgroup of $SO(4)$. Then we will explain how we found the correct weights for the links and vertices which make up our simplicial approximation to $\mathbb{S}^3$ and how we constructed our discrete Laplacian on $\mathcal{K}$. Afterwards we will discuss how we were able to order the simplices which form our simplicial approximation to $\mathbb{S}^3$ in such a way that when the discrete form of the boundary operator is applied to our ordered complex, $\mathcal{K}$, it vanishes. From there we will talk about how we compute quantum counter terms to deal with UV effects and position dependent irregularities

in our lattice.

In the next chapter we will show how the spectrum of our discretized Laplacian defined on a simplicial approximation to $\mathbb{S}^3$ appears to be converging to the known continuum limit as the refinement level of our complex is continuously increased. By doing so we are able validate our method for discretizing $\mathbb{S}^3$ which is a crucial prerequisite to formulating a lattice field theory on it.

5.2 Constructing A Simplicial Complex On $\mathbb{S}^3$

The first step to formulating a LFT on $\mathbb{S}^3$ is to construct a simplicial approximation of $\mathbb{S}^3$ in a manner which allows us to assign weights (a number) to the links and vertices which make up our simplical approximation. The largest discrete subgroup of the isometries of $\mathbb{S}^3$ is the 600-cell which is composed of 600 "equilateral" tetrahedrons glued together in such a way that each vertex is shared by 20 tetrahedrons and each edge is shared by 5 tetrahedrons. The 600-cell can be properly embedded in $\mathbb{R}^4$, just like the $\mathbb{S}^3$, and as a result will be the basis for our simplicial approximation of $\mathbb{S}^3$.

In order to discretize the 600-cell, two types of tetrahedrons can be used, "equilateral" tetrahedrons and "right" tetrahedrons. This is deduced by knowing that an 3D Euclidean-space, such as the interior of a "equilateral" tetrahedron, can be perfectly tessellated with a tetrahedral-octahedral honeycomb as shown in figure (5.1).

A point can be inserted in the center of each octahedron and then lines from the vertices of the octahedron can be connected to that point to break up the octahedron into eight "right" tetrahedrons. An image of what this looks like when it is applied to tessellating the interior of a "equilateral" tetrahedron is displayed below, where the ‘red’ vertex was inserted and the ‘red’ links connect the original ‘black’ vertices of the octahedron to the ‘red’ vertex that we inserted into the center of the octahedron. The higher our level of discretization k is, the more refined our tessellation of the

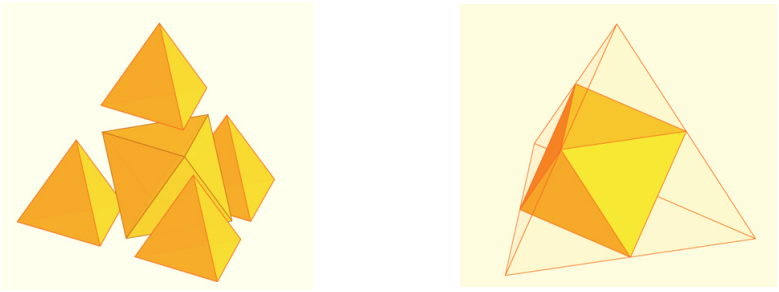

(a) **(b)**

Figure 5.1 Tetrahedral-octahedral honeycomb tessellation of an equilateral tetrahedron. These images were sourced from https://www.cosmic-core.org/free/article-48-geometry-platonic-solids-part-9-the-octahedron/

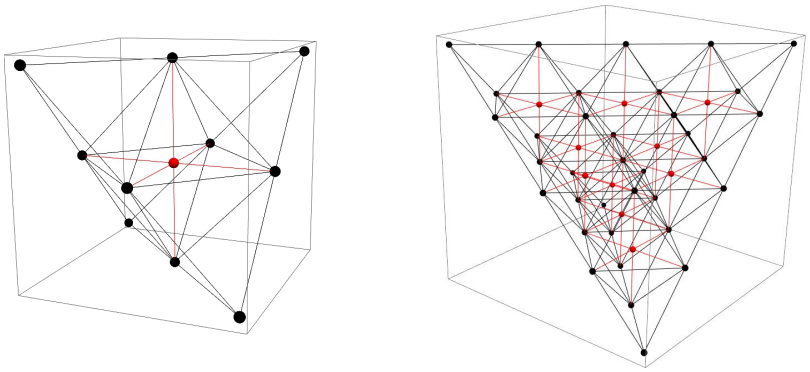

(a) Refined tetrahedron:k=2 **(b)** Further refined tetrahedron:k=4

Figure 5.2 Refined tetrahedrons

tetrahedron in figure (5.2) becomes.

To further illustrate how we are discretizing the 600-cell an image of a right tetrahedron and an equilateral tetrahedron are presented in figure 5.3.

The "right" tetrahedron is named so because three out of four of its triangular faces are right triangles and the "equilateral" tetrahedron is named so because all of its faces are equilateral triangles.

After refining the tessellation of the 600-cell to a desired level we project all of the vertices of the refined 600-cell to the surface of $\mathbb{S}^3$. By using a program called `qhull` [25] a Delaunay triangulation is constructed on the surface of the $\mathbb{S}^3$ from the vertices we projected onto it. A Delaunay triangulation is a tessellation in which no vertices

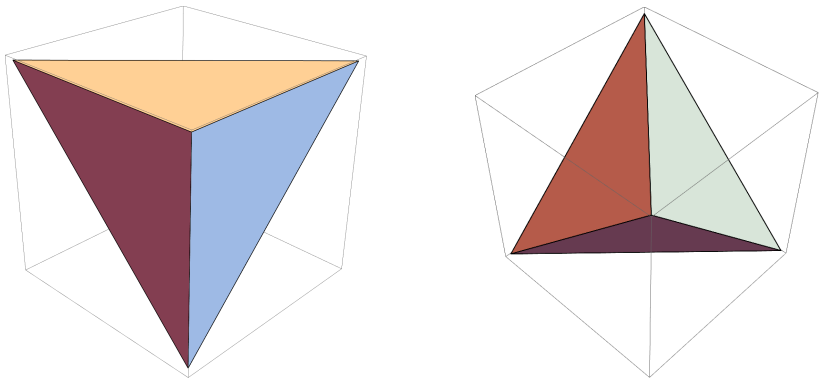

(a) Right tetrahedron **(b)** Equilateral tetrahedron

Figure 5.3 Tetrahedrons we used to tessellate the 600-cell

not associated with a simplex are contained within the circumcircle of that simplex. Some images [72] illustrating this in 2D are shown in figure (5.4) and (5.5).

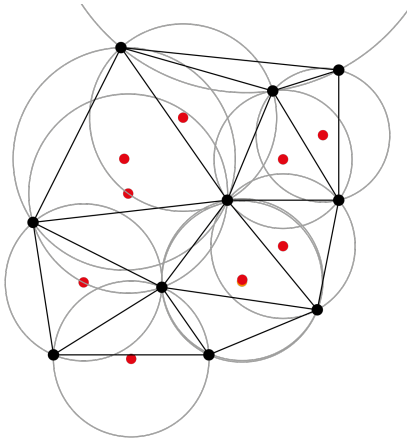

Figure 5.4 The 'red' vertices are the centers of the circumcircle

Due to the positive curvature, the tetrahedrons which are constructed from this new triangulation are distorted. Because we started out with the 600-cell, this discretization of the $\mathbb{S}^3$ preserves the symmetry of the 600-cell, which as we mentioned before, is the largest discrete subgroup which preserves the isometries of the $\mathbb{S}^3$. An image of one of these tessellated distorted tetrahedrons of the $\mathbb{S}^3$ projected down to $\mathbb{R}^3$ is shown in figure (5.6).

Another way of viewing this construction which allows notions from discrete ex-

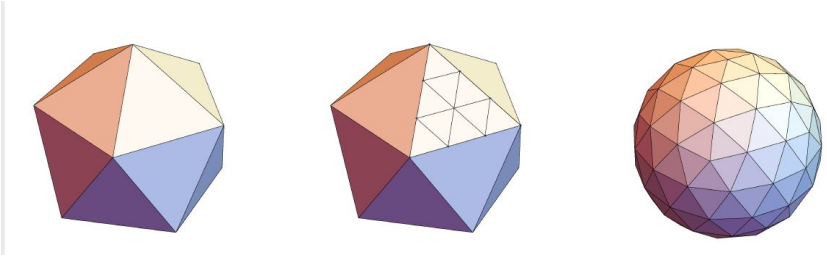

Figure 5.5 The left picture is of an Icosahedron. The middle picture shows one of the faces of the Icosahedron being tessellated using equilateral triangles. The picture on the right is the result of projecting the vertices of a fully tessellated Icosahedron on to $\mathbb{S}^2$ and then constructing a Delaunay triangulation out of it. These pictures originally appeared in [54, 95].

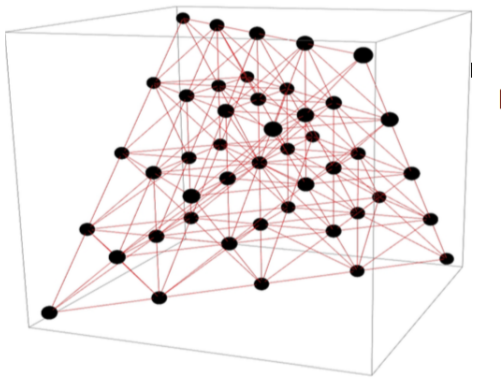

Figure 5.6 A refined portion of the simplicial approximation to the $\mathbb{S}^3$ projected down to $\mathbb{R}^3$

terior calculus to manifest more clearly is the following: a pure simplicial complex, $\mathcal{K}$, consists of a set of d -dimensional simplices (designated by σ_d) "glued" together at shared faces (boundaries) consisting of (d-1) -dimensional simplices (σ_{d-1}), this iteratively gives the sequence of simplices: $\sigma_d \to \sigma_{d-1} \to \cdots \sigma_1 \to \sigma_0$. This hierarchy of boundaries/simplices is specified by the boundary operator,

$$\partial\sigma_n\left(i_0 i_1 \cdots i_n\right) = \sum_{k=0}^{n}(-1)^k \sigma_{n-1}\left(i_0 i_1 \cdots \widehat{i i_k} \cdots i_n\right) \tag{5.2}$$

where $\widehat{i i_k}$ means to exclude the vertices of the simplex. Each simplex $\sigma_n\left(i_0 i_1 \cdots i_n\right)$ is an anti-symmetric function of the vertices it is composed of. To properly construct a

lattice field theory on a Riemannian manifold which itself has no boundary such as the $\mathbb{S}^3$, the vertices of the $\sigma_n\left(i_0 i_1 \cdots i_n\right)$s must be ordered so that the boundary operator over the sum of all the n-simplices $\left(\sigma_n\left(i_0 i_1 \cdots i_n\right)\right)$ vanishes. This to ensure that the continuum result of the $\mathbb{S}^3$ not possessing a boundary is shared by its simplicial approximation, $\mathcal{K}$.

The next step in our discretization is to construct the dual to the Delaunay triangulation, the Voronoï dual lattice. In general it is constructed as follows. One first identifies the circumcenters of the links of the simplicial complex. Normals are drawn from the circumcenters/midpoints of the links into the interior of each 2-simplex. Inside of each 2-simplex, the three normals intersect at exactly one point which is the circumcenter of the 2-simplex. From there normals are drawn from the now known circumcenters of the 2-simplices which intersect inside the 3-simplices. The points at which they intersect are the circumcenters of the 3-simplices. This procedure continues iteratively. Once the circumcenters of all (k-1) -simplices are identified, normals are drawn from them into the interior of each k-simplex. The (k+1) normals intersect at exactly one point inside each k-simplex which is its circumcenter. The collection of circumcenters and normal lines constructed in this manner form the graph of the Voronoï dual lattice. A picture of what this construction looks like in two-dimensions on top of a simplicial complex can be seen below in figure (5.7).

The Voronoï dual lattice has the same hierarchical structure, in which it is composed of polytopes, $\sigma_0^* \leftarrow \sigma_1^* \leftarrow \cdots \leftarrow \sigma_d^*$, where σ_n^* has dimension $d-n$ as illustrated in figure (5.7). These two constructions are orthogonal to each other in the sense that each σ_n is orthogonal to its dual polytope σ_n^*. The main consequence of this is that the volume of the hybrid cells which are shaded in blue in figure (5.7) have the following simple form

$$\left|\sigma_n \wedge \sigma_n^*\right| = \frac{n!\,(d-n)!}{d!}\left|\sigma_n\right|\left|\sigma_n^*\right|. \tag{5.3}$$

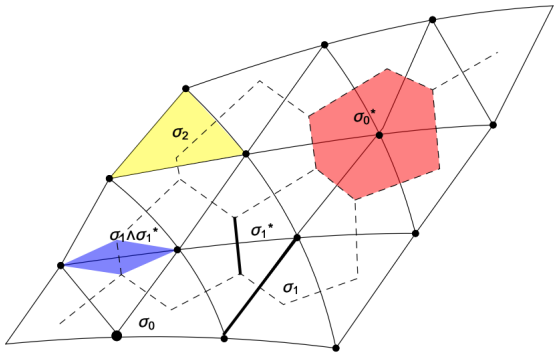

Figure 5.7 A 2-d simplicial complex with points (σ_0), edges (σ_1) and triangle (σ_2) (illustrated in yellow). At each vertex (σ_0) there is a dual polytope (σ_0^*) (illustrated in red), and at each link, σ_1, there is a dual link (σ_1^*) and its associated hybrid cell $\sigma_1 \wedge \sigma_1^*$ (illustrated in blue). This image was sourced from [54].

Ultimately we will use these hybrid cells constructed from the circumcenters of $\sigma_d \rightarrow \sigma_{d-1} \rightarrow \cdots \sigma_1 \rightarrow \sigma_0$. to form our discrete approximation to $\mathbb{S}^3$.

To find a hybrid cell for our discrete approximation to $\mathbb{S}^3$, one can start by choosing an arbitrary link. Next a vertex σ_0 of that link is identified. From there the circumcenter (midpoint) of that link σ_1 is found. Then the circumcenter of one of the two triangular faces (σ_2) of the tetrahedral cell (σ_3) whose boundary contains the link (σ_1) is found. Finally the circumcenter of the tetrahedral cell (σ_3) associated with that link is found. These four circumcenters form a tetrahedron, the same construction is done for the other vertex of the link and for the other triangular face whose boundary contains that link, which in total yields four tetrahedrons. These four tetrahedrons are one of the hybrid cells which ultimately discretize our $\mathbb{S}^3$, they are the three dimensional analogue to the two dimensional hybrid cells of figure (5.7). The aforementioned construction is shown in figure (5.8). More information on the discrete analogues of common operations that are applied to differential forms can be found in [95].

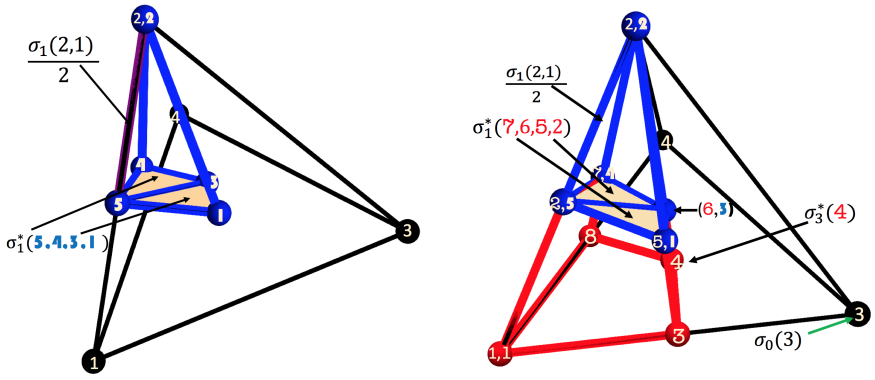

(a) Portion of Hybrid cell **(b)** Hybrid cell and Voronoï dual

Figure 5.8 The thick blue lines outline a portion of the hybrid cell, the thinner black lines outline an equilateral tetrahedron cell, σ_3, of the Delaunay triangulation and the red thick red lines outline a portion of the Voronoï dual σ_0^*. The different fonts used to label the vertices distinguish between the common vertices of these cells. Furthermore the arrows point to geometric structures of interest, such as the portion of the link which is orthogonal to the surface/boundary of a portion of the Voronoï dual. In 7a it is shown how the hybrid cell is formed from the circumcenters of the simplices σ_3, σ_2, σ_1, and σ_0 of the cell. In 7b the orthogonal nature between σ_1^* and σ_1 is displayed.

5.3 Constructing The Discretized Laplacian

Now that we have explained how we constructed our simplicial approximation to $\mathbb{S}^3$ we can discuss obtaining the matrix representation of the scalar Laplacian for a given level of refinement of our simplicial complex. Using the methods of discrete exterior calculus [9, 12, 83, 174] the action for a free massless scalar field theory on a surface discretized in the manner described earlier was elegantly expressed by [68–70] as

$$S_\sigma[\phi] = \frac{1}{2}\sum_{\langle i,j\rangle} V_{ij}\frac{(\phi_i - \phi_j)^2}{l_{ij}^2}. \tag{5.4}$$

For (5.4) V_{ij} is $|\sigma_1(ij) \wedge \sigma_1^*(ij)| = l_{ij}S_{ij}/d$, which is the product of the length of the link l_{ij} times the volume of the (d-1)-dimensional "surface", $S_{ij} = |\sigma_1^*(ij)|$ of the dual polytope normal to the link $\langle i,j\rangle$. This can be seen visually in figure (5.8b). We can rewrite the action (5.4) as the following

$$\frac{1}{2}\sum_{\langle i,j\rangle}\frac{V_{ij}}{l_{ij}^2}\left(\phi_i-\phi_j\right)^2=\frac{1}{2}\overrightarrow{\phi_i}^T M_{ij}\overrightarrow{\phi_j}, \tag{5.5}$$

where M_{ij} is a symmetric matrix with the following as its elements

$$M_{ii}=\sum_{j=1}^{n}\frac{V_{ij}}{l_{ij}^2}, \tag{5.6}$$

$$M_{ij}=-\frac{V_{ij}}{l_{ij}^2}\ when\ i\neq j. \tag{5.7}$$

The volumes of our hybrid cells must satisfy the following condition

$$\frac{1}{2}\sum_{i=1}^{4}\sum_{i\neq j}V_{ij}=\sigma_3(1,2,3,4). \tag{5.8}$$

This condition (5.8) states that the sum of the volumes of the hybrid cells over the links of an arbitrary tetrahedral cell in our simplicial complex must equal the volume of that cell. For the case of an equilateral tetrahedron it is easy to show how this manifests itself geometrically. As can be seen in figure (5.9a) and extrapolated from the symmetries present in the equilateral tetrahedron, all of the components of the hybrid cells occupy a unique portion of the interior volume of the tetrahedron. Thus if we were to sum up the volumes of all 24 components of the hybrid cells in figure (5.9a), we would obtain the ordinary volume of the equilateral tetrahedron; which means all of the contributions to the weights are positive.

For the right tetrahedron this is not the case because some portions of the hybrid cells lie entirely outside of the interior volume as can be seen in figure (5.9b). Thus if we were to simply sum up the volumes of all of the hybrid cells we would obtain a result greater then the volume of the right tetrahedron. In order to satisfy the aforementioned condition we must allow contributions to the weights for our links to be negative. For the right tetrahedron all of the negative contributions to the weights

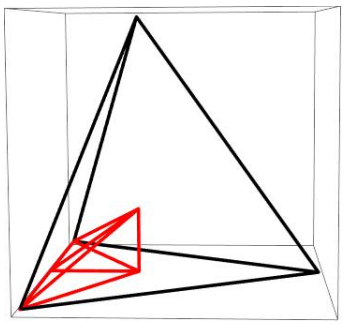

(a) Portion of Hybrid Cell For Equilateral Tetrahedron

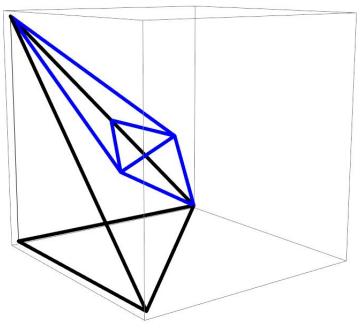

(b) Portion of Hybrid Cell For Right Tetrahedron

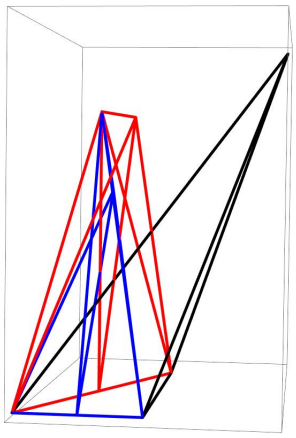

(c) Portion of Hybrid Cell For Obtuse Tetrahedron

Figure 5.9 In 8a the red polytope is a portion of the hybrid cell for a particular link of our equilateral tetrahedron. It can be clearly seen that it is contained entirely within the tetrahedron and thus its contribution to the weight of the link is positive. The portion of the hybrid cell in 8b, which is colored blue, lies entirely outside of the right tetrahedron. It results in a negative contribution to the weight of its respective link. For 8c the two portions of the hybrid cell which are both individually colored blue and red intersect which makes it difficult to determine which one gives a positive or negative contribution to the weight of the link.

are those who hybrid cells lie entirely outside of the interior of the tetrahedron. The positive contributions come from portions of the hybrid cells which start from the interior of the tetrahedron but extend outside of it. This results in the negative contributions canceling out the portions of the volumes of the positive contributions which extend outside of the tetrahedron, leading to the sum of the weights equaling the total volume of the right tetrahedron.

If we look back at the 600-cell which we refined using only "equilateral" and "right" tetrahedrons it becomes apparent that we need to calculate the weights of links which are shared among multiple tetrahedrons. This is accomplished by computing the signed components of the common link weights for each individual tetrahedron and then summing them all up. Because we choose a Delaunay construction for our simplicial complex the sum of the contributions from all of the neighboring tetrahedrons always results in a positive link weight.

These rules for determining the signs of the contributions to a given weight are pretty straightforward. However they only apply when our tetrahedrons are approximately "equilateral" or "right." The positive curvature which distorts the tetrahedrons which make up our refined 600-cell that we project onto $\mathbb{S}^3$ results in highly distorted tetrahedrons where one cannot easily eyeball which contributions to the links are positive or negative. An example of such a distorted tetrahedron can be seen in figure (5.9c). In figure (5.9c) the two portions of the hybrid cells overlap with each other. This makes it difficult to disentangle the two portions of the hybrid cells and determine which one cancels out the portion of the volume required for the condition (5.8) to be met.

To overcome the ambiguities in determining the signs of the contributions to the weights associated with highly distorted tetrahedrons we first used the fact that despite there being 24 portions of the hybrid cell for each tetrahedron, only 12 yield unique contributions to the weights. As can be seen in figures (5.7) and (5.9a), the

volume of a portion of the hybrid cell constructed from our previously mentioned hierarchy of simplices/circumcenters is the same under permuting the two vertices of the link whose circumcenter we used to construct that portion of the hybrid cell. In other words, if we look at the hybrid cell shaded blue in figure (5.8a) and imagine choosing our first circumcenter in our hierarchy to be vertex 1 instead of 2 of the tetrahedral cell, while keeping all of the other circumcenters the same, we would obtain a portion of the hybrid cell which possesses the same volume. Thus we only need to compute the signs of 12 portions of the hybrid cell which can either be plus or minus. Therefore there are 4096 different possible combinations of signed hybred cell volumes and we are looking for the combinations that satisfy the condition that their sum equals the volume of the cell in our simplicial complex which they are derived from.

With that said we must stress that the sum of the signed hybrid cell volumes of the hybrid cells equaling the volume of the tetrahedral cell is only a necessary, but not a sufficient condition for successfully constructing our discretized Laplcian. This is because for certain tetrahedrons multiple combinations of hybrid cell signed volumes exist which lead to our necessary condition being satisfied and not all of them result in a discretized Laplacian whose low lying spectrum approaches the continuum limit as we increase the refinement of our simplicial complex. In order to consistently pick the correct combination we had to come up with a way of classifying the plethora of tetrahedrons that were used to construct our simplicial approximation of $\mathbb{S}^3$ and figure out how to pick out the single correct combination for each class.

We found that each tetrahedron in our simplicial complex can be classified by the barycentric coordinates of its bulk circumcenter and the circumcenters of its four faces (boundaries). Thus we classified each tetrahedron using following set of barycentric coordinates

$$[[\lambda_1, \lambda_2, \lambda_3, \lambda_4], [\lambda_5, \lambda_6, \lambda_7, \lambda_8], [\lambda_9, \lambda_{10}, \lambda_{11}, \lambda_{12}], [\lambda_{13}, \lambda_{14}, \lambda_{15}, \lambda_{16}], [\lambda_{17}, \lambda_{18}, \lambda_{19}, \lambda_{20}]] \tag{5.9}$$

where the first set are the barycentric coordinates of the bulk and the other four sets are the barycentric coordinates of the faces (boundaries). In addition we reparameterized λ_i by setting it equal to 1 if it is greater or equal to zero and setting it equal to 0 if it is less than zero. In terms of this classification scheme the authors found that 47 different types of tetrahedrons make up our simplicial complex at k=20. However we were able to dramatically reduce that number in practice by realizing that within this classification scheme equivalence classes for tetrahedrons exist by sorting all of the elements, λ_i, within the sets of (5.9) from least to greatest and ordering all of the sets themselves associated with the four faces in order from least to greatest determined by the sum of all of their elements. For example two tetrahedrons which can be classified as the following in (5.10) belong to the same equivalence class in (5.11)

$$\begin{aligned}&[[1,0,0,1],[1,1,1,1],[1,0,1,1],[1,1,1,1],[1,1,1,1]],\\&[[0,1,0,1],[1,1,1,1],[1,1,1,1],[1,1,1,1],[1,1,0,1]],\end{aligned} \tag{5.10}$$

$$[[0,0,1,1],[0,1,1,1],[1,1,1,1],[1,1,1,1],[1,1,1,1]]. \tag{5.11}$$

Overall this reduces our 47 unique tetrahedrons we had to consider to only 6.

By applying the same methodology to a large swath of tetrahedrons the authors found that we were able to form these equivalence classes because all of the tetrahedrons up to k=20 which appear in our complex have a very specific property that can be inferred from their barycentric coordinates. All of the zeros in the unordered sets corresponding to the faces of our 47 classes of tetrahedrons are all in the same position as the zeros which are contained within the set corresponding to the bulk

of the tetrahedral cell. Every time a zero appears in our classification scheme that means the circumcenter for that face or bulk is outside of the tetrahedral cell. It is only when this alignment is present that the equivalence classes that we mentioned exist. The conditionality of our equivalence classes points to some interesting geometric properties of 3D simplicial complexes, Voronoï duals, and the hybrid cells constructed from them that deserve to be investigated more thoroughly.

Using this classification scheme we first applied our combinatorial procedure to a tetrahedron in our simplicial complex which belongs to an equivalence class to obtain candidates for the correct signs for the contributions to its link weights. If this procedure leads to a single viable set because all of the other 4095 combinations result in a gross violation of (5.8) which cannot be explained via numerical noise/imprecision then we can say that we successfully found the correct signs to the contributions to the link weights of that cell. Assuming only a single set is viable we can find relationships between the signs of its contributions to the weights and the barycentric coordinates of the circumcenters of the links, faces and bulk of our tetrahedral cell which form the vertices of the hybrid cell. An example of such a relationship associated with tetrahedrons within the equivalence class shown in (5.11) will be given below.

From examining the set of signs (± 1) given by brute force combinatorics, we posit that if a portion of the hybrid cell is constructed using the circumcenter of a face, whose unordered barycentric coordinates satisfies the property, that the position of its negative barycentric coordinate$\big([-\frac{1}{4}, 0, \frac{1}{2}, \frac{3}{4}]\big)$ is in the same position as one of the non zero $\big([\frac{1}{2}, 0, \frac{1}{2}, 0]\big)$ barycentirc coordinates of the circumcenter/midpoint of the link that is used in constructing that portion of the hybrid cell, then the sign of the contributions to the weights from that portion is negative. Once we deduce all of our relationships we test them out on a plethora of random tetrahedrons belonging to the equivalence class we are studying and see if they without fail compute the correct signs of our hybrid volumes to ensure that (5.8) is satisfied. If all of our relationships

correctly calculate the signs for those random tetrahedrons we then move on to the next class.

In the case when multiple candidates emerge via combinatorics which satisfy (5.8), we can narrow down our list to one viable set by constructing a plethora of random tetrahedrons belonging to the class in question and finding the ones which only have one combination of (± 1) which satisfy (5.8) and then follow the procedure we just outlined. In the end, we obtain a method for computing the signs of all of the contributions to the weights without having to use brute force combinatorics. As we will show in the coming sections, this method allowed us to construct a discretized Laplcian on $\mathbb{S}^3$ which gives a low lying spectrum which very well matches the continuum limit.

5.4 Tessellation In Relation To The Cubic Lattice

We can relate our method for discretizing the interior of 3D objects using two types of tetrahedrons to the traditional cubic lattice by tessellating a unit cube in a well known fashion. By examining 5.3b we see that a cube can be tessellated by constructing an equilateral tetrahedron whose vertices are located at four of the cube's eight vertices and then filling the remaining space with four "right" tetrahedrons. This construction is clearly illustrated in 5.10c.

As can be seen in 5.10a and 5.10b the process of tessellating a tetrahedron results in cubes being formed whose edges are 'colored red' and whose vertices are colored 'black', and 'red'. As we previously mentioned, we begin our tessellation by first breaking up the interior of our tetrahedrons using a space-filling tetrahedral-octahedral honeycomb. All of the vertices and links used in this construction of our honeycomb are considered 'black'. Afterwards we insert 'red' vertices into the center of each of our octahedrons and then connect those 'red' vertices to the 'black' vertices

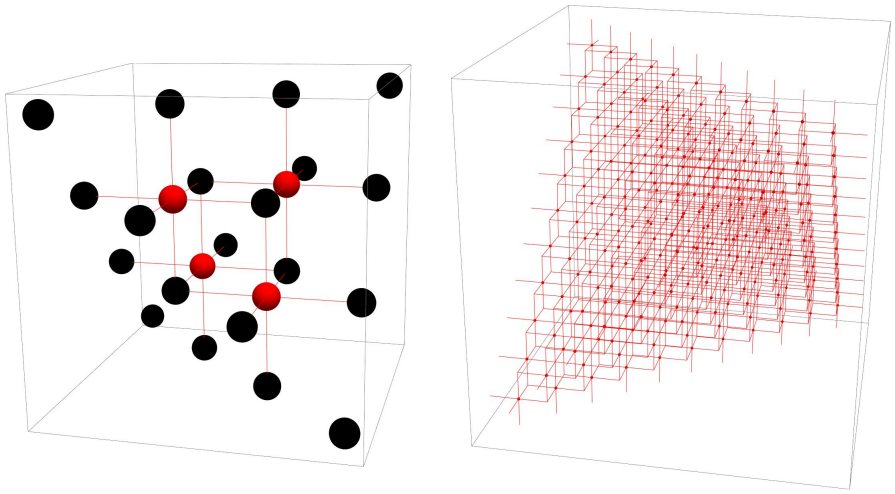

(a) Partial discretization of equilateral tetrahedron

(b) Cubic discretization of equilateral tetrahedron using only 'red' links and vertices

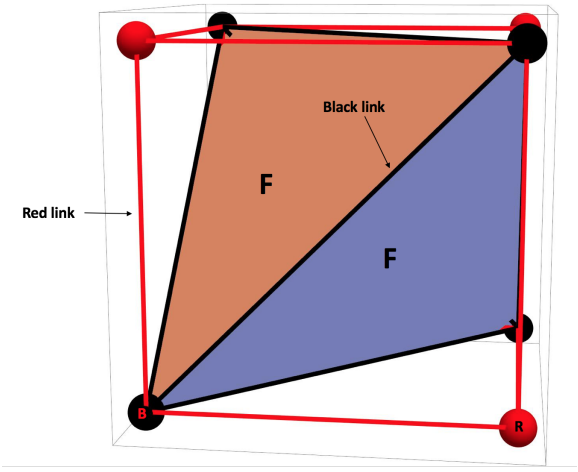

(c) Labeled tessellation of unit cube.

Figure 5.10 Figure 9a is a discertization of an equilateral tetrahedron where the 'black links' originally belonging to the tetrahedral-octohedreal honeycomb are not shown. The labels in figure 9c correspond to the following. Capital f indicates that this is one of the faces of our equilateral tetrahedron whose links and vertices are 'black'. The capital r indicates a 'red' vertex and the capital b indicates a 'black' vertex.

of the octahedrons, breaking them up into 8 "right" tetrahedrons. The links which connect the 'red' vertices to the 'black' vertices are 'red' links. 'Black' vertices and links are the remnants of our original tetrahedral-octahedral honeycomb. As can be seen in 5.10b if we only use 'red' links and vertices we obtain a cubic tessellation of the bulk region of our tetrahedrons.

If we include all of the 'black' and 'red' vertices, and links, the cubes present in 5.10a and 5.10b look like 5.10c. Using our knowledge of the signs for the contributions to the weights of shared links for right and equilateral tetrahedrons we can deduce that the weights of the 'black' diagonal links of our cube vanishes. This is the case because in 5.10c each 'black' link belongs to the edge of one equilateral tetrahedron and two "right" tetrahedrons. The 'black' links of our "right" tetrahedrons in 5.10c have negative weights because the portions of the hybrid cells that can be formed from then using the aforementioned hierarchies of circumcenters exist solely outside of the volume of the right tetrahedron as is shown in 5.9b. On the other hand the portions of the hybrid volume constructed from the 'black' links of our equilateral tetrahedrons all exist in the interior of its volume as can be seen in 5.9a.

Using this understanding of the signs of the contributions to the weights, the reader can easily verify that the sum of the weight of the 'black' link of our equilateral tetrahedron and the weights of the two 'black' links of our "right" tetrahedrons **vanishes**. The 'red' links which form the boundary of our cube don't vanish at all. Thus our tessellation in 5.10c is equivalent to the cubic tessellation employed in standard lattice field theory because only the weights of the sides of the cube are non vanishing while all of the diagonal links possess vanishing weights. For the case of tessellating a tetrahedron in flat space as can be seen in 5.2b all of the internal black links have vanishing weight. Therefore for the case of a tetrahedron in Euclidean space the only non vanishing links are the 'red' links, which are equivalent to a cubic discretization of the bulk of the tetrahedron, and the 'black' links which form the

boundary of the faces of the tetrahedron. The addition of the weights belonging to these 'black' links which form the boundary of our faces results in an increased rate of convergence of our results to the continuum as the level of refinement is increased indefinitely. In curved space, this cancelling of the bulk 'black' links doesn't always occur due to tetrahedrons being heavily distorted to the point that they resemble the tetrahedrons in 5.9c.

5.5 Ordering The 3-Simplices Of $\mathcal{K}$

Before we can use the values of the weights of our links and vertices to obtain estimates for the nth-order Binder cumulants, and n-point correlation functions for ϕ^4 theory, we need to order all of the vertices of our 3-simplices (σ_3) so that the discrete form of the boundary operator acting on our simplicial approximation to $\mathbb{S}^3$, $\mathcal{K}$, yields the same result as when the continuous form of the boundary operator (∂) acts on $\mathbb{S}^3$.

$$\partial\mathbb{S}^3 = 0. \tag{5.12}$$

Because we are approximating $\mathbb{S}^3$ as a simplicial complex, it can be thought of as a sum of 3-simplices glued together in accordance with the aforementioned hierarchies of circumcenters belonging to lower dimensional simplices. As the level of refinement of our simplicial complex increases so too does the number of simplices required to construct it. In addition, as our complex becomes increasingly refined its, rotational symmetry approaches the SO(4) rotational symmetry of $\mathbb{S}^3$. We previously defined the boundary operator acting on a single simplex in our simplicial complex. Using the discrete form of the boundary operator, the discrete analogue of 5.12 is

$$\partial\mathcal{K} = \sum_{n=1}^{N} \partial\sigma_3^n(i_0 i_1 i_2 i_3) = \sum_{n=1}^{N} \left(\sum_{k=0}^{3} (-1)^k \sigma_2^n \left(i_0 i_1 \cdots \widehat{i i_k} \cdots i_3 \right) \right) = 0, \tag{5.13}$$

where N is the total number of cells present for a given level of refinement of our simplicial complex and n is a superscript which indicates which cell the boundary operator is acting on. As previously mentioned, $\widehat{ii}_k$ means to exclude the vertices of the simplex and $\sigma_n\left(i_0 i_1 \cdots i_n\right)$ is an anti-symmetric function of the vertices it is composed of. Because the boundary operator is anti-symmetric, applying the boundary operator twice to any manifold yields a null result

$$\partial\partial\ \mathbb{M} = 0. \tag{5.14}$$

In equation 5.13 σ_2, are the triangular faces of our tetrahedral 3-simplices which make up our simplicial complex. Each face (σ_2) of a tetrahedron can only be shared by one other tetrahedron; as opposed to an edge (σ_1) which can be shared by multiple tetrahedrons such as in the case of the 600 cell. Trivially the common face between two tetrahedrons are identically the same. Thus their $|\sigma_2|$ are the same values as well.

In order to satisfy 5.13, all of the vertices of the $\sigma_3^n(i_0 i_1 i_2 i_3)$'s, must be ordered in such a way, that the common $\sigma_2^n(i_0 i_1 i_2)$ between a pair of $\sigma_3^n(i_0 i_1 i_2 i_3)$'s, which border each other, must cancel each other out. This cancellation is possible due to the anti-symmetric nature of the $\sigma_2^n(i_0 i_1 i_2)$'s and the $(-1)^k$ term in 5.13. To show what this entails in practice let's assume we have two $\sigma_3^n(i_0 i_1 i_2 i_3)$'s, $\sigma_3^1(1,2,3,4)$ and $\sigma_3^2(2,3,4,5)$. If we apply the boundary operator to these two 3-simplices we obtain

$$\begin{aligned}
\partial\sigma_3^1(1,2,3,4) &= \sigma_2^1(2,3,4) - \sigma_2^1(1,3,4) + \sigma_2^1(1,2,4) - \sigma_2^1(1,2,3) \\
\partial\sigma_3^2(2,3,4,5) &= \sigma_2^2(3,4,5) - \sigma_2^2(2,4,5) + \sigma_2^2(2,3,5) - \sigma_2^2(2,3,4).
\end{aligned} \tag{5.15}$$

Because $\sigma_2^1(2,3,4)$ and $\sigma_2^2(2,3,4)$ are defined using the same three vertices, they geometrically represent two identical triangular faces of $\sigma_3^1(1,2,3,4)$ and $\sigma_3^2(2,3,4,5)$; therefore $|\sigma_2^1(2,3,4)| = |\sigma_2^2(2,3,4)|$. Thus, due to the anti-symmetric nature of the

boundary operator and how the vertices of our 3-simplices were ordered, we see that if we were to add $\partial\sigma_3^1(1,2,3,4)$ and $\partial\sigma_3^2(2,3,4,5)$ together, that their shared triangular faces $\sigma_2^1(2,3,4)$ and $\sigma_2^2(2,3,4)$ would cancel.

The end goal is to order all of the vertices of the $\sigma_3^n(i_0i_1i_2i_3)$'s, in such a way, that the sum of $\partial\sigma_3^n(i_0i_1i_2i_3)$'s, vanishes for each level of refinement of our simplicial complex. In other words, after properly ordering all of the $\sigma_3^n(i_0i_1i_2i_3)$'s, when the boundary operator ∂ is applied to each one of them, for every resultant $\sigma_2^n(i_0i_1i_2)$, there should exist another $\sigma_2^n(i_0i_1i_2)$ which possesses the exact same ordering of its vertices, but has an opposite sign due to the anti-symmetric nature of ∂. When this condition is met $\partial\mathcal{K} = 0$.

To accomplish this, the author created a code in Mathematica using the following thought process. As the reader can easily convince themselves, there is no unique ordering of vertices which satisfies 5.13. Thus we are at liberty to pick the orientation of any one tetrahedral cell which makes up our simplicial complex. In practice, this one cell is the first cell which appears in the list of cells generated by Q-hull. After picking that single orientation, the orientations of the rest of the cells must be determined, they cannot be arbitrarily picked up to an even permutation.

To determine the orientation of the other cells, we need to compare how the boundary operator acts on our first cell to how it acts on another cell(s) which shares a face(s) with our first cell. This may be done by searching from the list of un-oriented cells, which make up our simplical complex, a cell, which shares a face with the first cell that we already oriented. If the resultant shared faces produced by our boundary operators on the two cells have opposite signs determined by $(-1)^k$, then the orientation of the second cell does not need to be altered. If their shared faces have the same orientation, then an odd permutation needs to be applied to the vertices of the second cell. Once the second cell has been oriented, the two oriented cells are deleted from the list of cells which make up our complex. This is to ensure

no duplicates arise in our list of oriented cell. From there one can find a third cell which shares a face with either the first or second cell and do the same comparison to determine its orientation. This procedure can in principle be carried about for all of the cells which make up our simplical complex.

An issue arises though orienting the tetrahedral cells this way. If one insists on starting with the first cell and then comparing it to the second cell, and then comparing it to the third cell, and so on, one may find a cell whose four faces are already shared by four other previously oriented cells. To continue orienting the remainder of the cells of the simplical complex, one would need to search the list of already oriented cells to find ones whose faces are not currently shared by any other oriented cells. This requires searching the list and greatly increases the run time of the code. For each even level of refinement (k=2, 4, 6, 8....) the numbers of additional cells increases cubically. In addition, the act of deleting cells from a initially long list of cells is computationally expensive, so is appending an element to an already long list.

To ensure the code scales linearly in the number of cells that make up our simplical complex $\mathcal{K}$, we can alternatively construct it as follows. Like before, we start by orienting the first cell that appears in our list of cells produced by Q-hull. Afterwards, we build a list of all of the triangular faces which form the boundaries of the cells which make up our complex. Then we in advance determine the location of the cells, in our list of cells which make up our complex, whose boundary contains each face in our aforementioned list of faces. Once we know the location of each cell which possess a face in our list of faces, we save that information as a function of each face. In other words, we construct a function such that when the three vertices which make up a face (σ_2) are inserted into it, the function gives the numerical location of the 3-simplices in the list of un-ordered 3-simplices, whose boundary contains that face. That way when it comes time to search the list of cells for the cells which share a

common face with our first cell, we already know their locations and don't have to search the whole list every time. The initial search only needs to be done once and is an "embarrassingly" parallel process whose speed increases linearly in the number of cores one has available.

In addition we know the final length that the list of oriented cells will have and thus can form a list of said length that contains only zeros. That way after orienting a cell, instead of appending it to a long list, the zero in our ficidual list can be replaced by that oriented cell. This is computationally far less intensive for Mathematica then appending our oriented cells to a list whose length is constantly changing.

From there, instead of only searching for a cell which shares a single face with our original cell, we locate all four cells which share the four faces of our first oriented cell and orient those four cells in the way previously described. Afterwards our list of oriented cells possesses five elements. Instead of deleting those elements from the list of cells which make up our complex, we take advantage of already knowing their positions in our list of cells, thanks to having computed the locations of all of our faces in the list of cells which make up our complex in advance, by replacing those five cells in our list of un-oriented cells by the number zero. Doing this prevents us from searching those cells again when we look for the remainder of the neighboring cells for the second tetrahedron in our list of oriented simplices, thus preventing any duplicates from being appended.

Because each face forms the boundary of two neighboring tetrahedrons, and we do not want any duplicates in our list, we code a simple criteria to determine which tetrahedron we will compare to our second oriented tetrahedron. If the first location given by our function we built in advance corresponds to a zero that we retroactively inserted to prevent duplicates, then we will choose the tetrahedron in the second location, if not then we will choose the tetrahedron in the first location.

As a result of our method picking four tetrahedrons at a time, and knowing that

at least one face of the second tetrahedron is already in our oriented list, at least one place-holder zero from our list of un-oriented tetrahedrons will be "compared" to the faces of the second tetrahedron produced by the boundary operator. Before we replace the ficidual zeros with the outcome of these comparisons we delete the inevitable "zero comparisons". By knowing how many non-zero comparisons we have performed, we know how many ficidual zeros to replace accordingly. We then apply the same procedure to the third tetrahedron and so on until all of the elements in our original ficidual list have been replaced. This results in the vertices of all of our cells that make up our complex, being ordered in such a manner, that when you apply the boundary operator to the list, the sum of all of the faces vanishes, which equates to a vanishing boundary; thus satisfying the discrete version of 5.12.

5.6 The "Finite Elements" of Quantum Finite Elements

So far we have discussed in detail how we constructed our simplicial approximation to $\mathbb{S}^3$ so we can formulate lattice field theories on it using the QFE. After clarifying the geometric aspects of our program we shall now discuss how we handle the scalar fields which define ϕ^4 theory.

In the classical limit, the field theory we wish to study using the QFE has the following action in the continuum limit

$$S_{cont} = \int_{\mathbb{S}^3} d^3x\sqrt{g}\left[\frac{1}{2}g^{\mu\nu}\partial_\mu\phi(x)\partial_\nu\phi(x) + \frac{1}{2}\xi_0\mathbf{Ric}\phi^2(x) + \frac{1}{2}m^2\phi^2(x) + \frac{1}{2}\lambda\phi^4(x)\right], \tag{5.16}$$

where $g^{\mu\nu}$ is the inverse of the metric tensor for $\mathbb{S}^3$, $\sqrt{g}$ is the square root of the determinant of the metric tensor, ξ_0 is $(d-2)/(4(d-1))$ for $d \geq 3$ and couples the

scalar field to the Ricci scalar, $\mathbf{Ric} = (d-1)(d-2)/R^2$, m is mass, and λ is the self interaction coupling constant. The inclusion of the Ricci term is optional and amounts to a shift in the mass. However its inclusion has been shown [56] to increase the rate of convergence of our numerical calculations. Our task is to formulate an action on our simplicial complex so that it converges to (5.16) as the continuum limit is approached.

To begin this task we will define a coordinate system which will allow us to interpolate the value of the scalar field ϕ within the interior of our flat 3-simplices which make up $\mathcal{K}$. The coordinate system we will choose are the barycentric coordinates. We will define them for a 3-simplex, but this definition can be easily generalized to a nth dimensional simplex.

The barycentric coordinates for a 3-simplex embedded in $\mathbb{R}^4$ with the following vertices $(\vec{v_0}, \vec{v_1}, \vec{v_2}, \vec{v_3})$ are defined as follows

$$\begin{aligned}
x &= \xi^0(\vec{v_0} \cdot \hat{e_x}) + \xi^1(\vec{v_1} \cdot \hat{e_x}) + \xi^2(\vec{v_2} \cdot \hat{e_x}) + \xi^3(\vec{v_3} \cdot \ \hat{e_x}), \\
y &= \xi^0(\vec{v_0} \cdot \hat{e_y}) + \xi^1(\vec{v_1} \cdot \hat{e_y}) + \xi^2(\vec{v_2} \cdot \hat{e_y}) + \xi^3(\vec{v_3} \cdot \ \hat{e_y}), \\
z &= \xi^0(\vec{v_0} \cdot \hat{e_z}) + \xi^1(\vec{v_1} \cdot \hat{e_z}) + \xi^2(\vec{v_2} \cdot \hat{e_z}) + \xi^3(\vec{v_3} \cdot \ \hat{e_z}), \\
w &= \xi^0(\vec{v_0} \cdot \hat{e_w}) + \xi^1(\vec{v_1} \cdot \hat{e_w}) + \xi^2(\vec{v_2} \cdot \hat{e_w}) + \xi^3(\vec{v_3} \cdot \ \hat{e_w}), \\
\xi^0 &+ \xi^1 + \xi^2 + \xi^3 = 1,
\end{aligned} \tag{5.17}$$

where $\hat{e_i}$ is a unit vector in Cartesian coordinates and (x, y, z, w) are the coordinates of the embedding space, $\mathbb{R}^4$. By their nature we can also call barycentric coordinates, center of mass coordinates because if you specified a set of them to be masses you would be able to calculate the center of mass $(x_{cm}, y_{cm}, z_{cm}, w_{cm})$ of a 3-simplex.

Next we have to define the metric tensor, $g_{\mu\nu}$, of our simplicial complex. In the continuum limit, the metric tensor defines the totality of the geometric information one can extract from a manifold $\mathbb{M}$. Thus it follows, that in order to construct the metric of a simplicial complex, one needs to specify the lengths of all of its links. If

one has the lengths of its links then one can find a coordinate system which specifies the location of any point on any of its simplices. Using the barycentric coordinates (5.17) as a guide we can construct the following coordinate system

$$\vec{r} = \sum_{n=0}^{d} \xi^n \vec{v}_n = \sum_{i=1}^{d} \xi^i \vec{l}_{i0} + \vec{v}_0, \tag{5.18}$$

where the unity constraint among the barycentric coordinates was employed and $\vec{v}_i$ are the locations of the vertices of a particular simplex. Using this coordinate system (5.18) and the standard definition of the metric tensor we obtain

$$G_{ij} = \frac{\partial \vec{r}}{\partial \xi^i} \cdot \frac{\partial \vec{r}}{\partial \xi^j} \equiv \vec{l}_{i0} \cdot \vec{l}_{j0}, \tag{5.19}$$

where we take our derivatives with respect to the barycentric coordinates ξ^i. Now that we can define the metric for each simplex we can rewrite the action (5.16) as a sum over the tetrahedrons which make up our complex

$$S_\sigma = \sum_{\sigma \in \sigma_3} \int_\sigma d^3\xi \sqrt{G_\sigma} \left[\frac{1}{2} G_\sigma^{ij} \partial_i \phi(\xi) \partial_j \phi(\xi) + \frac{1}{2} \left(m^2 + \xi_0 \mathbf{Ric} \right) \phi^2(\xi) + \frac{1}{2} \lambda \phi^4(\xi) \right], \tag{5.20}$$

where G_σ^{ij} is the usual inverse metric and $\sqrt{G_\sigma}$ is the determinant of our matrix (5.19).

Using (5.17) we expand our scalar fields, $\phi(x)$, as a finite element basis on each simplex σ_3

$$\phi(x) \to \phi_\sigma(\xi) = \xi^0 \phi_0 + \xi^1 \phi_1 + \xi^2 \phi_2 + \xi^3 \phi_3, \tag{5.21}$$

where ϕ_i is defined on the vertices of each simplex and interpolation is used to extrapolate the values of the field inside each simplex. Inserting this finite dimensional representation of the scalar fields into our action (5.20) and integrating over each simplex results in

$$S\left[\phi_i\right] = \frac{1}{2}\phi_i M_{i,j}\phi_j + \frac{1}{2}\left(m^2 + \frac{1}{4R^2}\right)\sqrt{g_i}\phi_i^2 + \frac{1}{2}\lambda\sqrt{g_i}\phi_i^4, \tag{5.22}$$

where we inserted in the numerical value of the Ricci term and its coupling constant for $d = 3$, $M_{i,j}$ is the scalar Laplacian we constructed earlier and $\sqrt{g_i}$ is the Voronoï dual volume (σ_0^*). This action possesses a numerical value on each vertex which makes up our simplicial complex.

To prep our action (5.22) for a numerical simulation we perform a change of variables which makes all of our parameters and fields dimensionless. Starting with $\sqrt{g_i}$ and ϕ_i we make the following substitution

$$\sqrt{g_i} = A^*\sqrt{\tilde{g}_i} \quad , \quad \phi_i = \tilde{\phi}_i / Z_0 \tag{5.23}$$

where A^* is some quantity with units of volume and Z_0 has units of length $L^{-\frac{1}{2}}$. There is no single unique choice for A^* and Z_0. A natural candidate for A^* would be the average value of the Voronoï dual volumes, σ_0^*, $\langle\sqrt{g_i}\rangle$. But another possibility would be the average volumes of the tetrahedrons, σ_3, or the average values over the length of the link which make up our complex cubed. For now we will set $A^* = \langle\sqrt{g_i}\rangle = na^3$, where a is a single number which roughly characterizes the lengths of the links and n is a constant. By setting A^* we shall set Z_0 as $Z_0^2 = na$. We will make our parameters dimensionless, (m, λ), by redefining them as $\frac{m_0}{a} = m$ and $\lambda = \frac{n\lambda}{a}$. Performing the above dimensionless reparameterization results in the following action

$$S_\sigma[\phi] = \frac{1}{2}\phi_i M_{i,j}\phi_j + \frac{1}{2}m_0^2\sqrt{g_i}\phi_i^2 + \frac{a^2}{8R^2}\sqrt{g_i}\phi_i^2 + \frac{1}{2}\lambda_0\sqrt{g_i}\phi_i^4, \tag{5.24}$$

where we removed the tilde ˜ notation and summed over like indices.

5.7 The "Quantum" of Quantum Finite Elements

The action we have written in the last section is perfectly capable of being used to numerically calculate observables for classical ϕ^4 theory formulated on $\mathbb{S}^3$. However, due to our lattice not being uniform as a result of the positive curvature of $\mathbb{S}^3$, applying standard renormalization techniques that are employed for quantum field theories on cubic lattices are not sufficient [58] for recovering the known continuum limit as we further refine our complex. In order to obtain the correct continuum limit we have to study the geometric aspects of renormalization on a non-uniform simplicial complex.

The procedures we will outline for obtaining the correct continuum limit for ϕ^4 theory on a non-uniform lattice are difficult to rigorously justify. Instead we will appeal to the fact that theses procedures have enabled the construction of an action for ϕ^4 theory on $\mathbb{S}^2$ and $\mathbb{R} \times \mathbb{S}^2$ which has successfully [54, 56] converged to the known continuum limit, the universality class of the critical 2D and 3D Ising models respectively. We have no reason to believe these techniques won't work again for ϕ^4 theory on $\mathbb{S}^3$. In addition, the procedures we will outline are closely related to standard [158] techniques which are employed for renormalizing field theories and studying non-perturbative conformal field theories on uniform cubic lattices.

To construct our QFE action which will converge to the known continuum limit of the critical 3D Ising model we will employ both perturbative and non-perturbative techniques such as calculating Feynman diagrams and tuning the theory to its critical surface in parameter space, $(m_0\, \lambda_0)$, each time we refine our simplicial complex. At criticality, the renormalized values of our dimensionless mass and coupling constant goes to zero as correlations functions become as large as the finite size of $\mathbb{S}^3$ allows them to. Tuning the theory to the critical surface allows us to eliminate position independent divergences which can be extrapolated from UV divergent Feynman diagrams by group averaging them as we will explain shortly.

Before we discuss the perturbative aspect of renormalization on a non-uniform

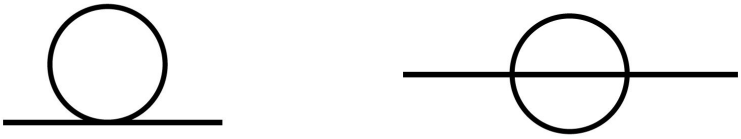

(a) 1-Loop **(b)** 2-Loop

Figure 5.11 Divergent Feynman diagrams for ϕ^4 theory in two and three dimensions

lattice we put forward some assumptions which have held true during previous applications of the QFE.

1. Only UV divergent diagrams are position dependent in the continuum limit.

2. The group averaged divergent portion of UV diagrams are universal in the sense that they are independent of position.

The first assumption ensures that we can eliminate non-uniform lattice artifacts using only a finite number of counter terms for super-renormalizable theories. The second assumption guarantees us that we can eliminate divergent position independent portions of Feynman diagrams by tuning our theory to the critical surface for each level of refinement all the way up to the continuum limit.

With these assumptions in mind, we can begin to analyze the divergent diagrams of ϕ^4 theory in 3D. In 3D, ϕ^4 theory is super-renormalizable and as a result only has a finite number of divergent Feynman diagrams. A convenient way to determine if a particular Feynman diagram in lattice field theory is divergent or not was introduced by Reisz [199–202]. Reisz defined a lattice degree of divergence $Deg(\boldsymbol{I})$ for a Feynman integral $\boldsymbol{I}$ which is the lattice analog of the superficial degree of divergence from continuum field theory, and proves that any integral with $Deg(\boldsymbol{I}) < 0$ is finite and given by the expected continuum limit as lattice spacing $a \to 0$.

For the single loop Feynman diagram of ϕ^4 theory in d dimensions which is shown in 5.11a the degree of divergence is $\mathrm{Deg}\,(\boldsymbol{I_1}) = d - 2$. This means for $d \geq 2$ the one loop diagram of ϕ^4 theory is always divergent. For $d = 2$ it diverges logarithmically

and for $d = 3$ it diverges linearly. For $d = 2$ this logarithmic divergence was recovered [54, 95] numerically and matches the known continuum limit.

For the two loop diagram the degree of divergence is $\mathrm{Deg}\,(\boldsymbol{I_1}) = 2d-6$. Therefore for $d = 2$, the two loop diagram is not divergent and should be independent of position. This was found [54, 95] to be the case which further bolsters the validity of our assumptions. However for $d = 3$ the two loop diagram is divergent and is position dependent as was shown in [56, 95]. For $d = 2$ and $d = 3$ the three and higher order loop diagrams are all convergent and thus we assume they are independent of position.

In standard lattice field theory with a uniform cutoff, a, the one loop diagram in any dimension, d, for ϕ^4 theory can be represented in momentum space as the following Feynman integral

$$I_1(k, m; a) = \frac{\lambda}{2} \int_{-\pi/a}^{\pi/a} \frac{d^d q}{(2\pi)^d} \frac{1}{\tilde{q}^2 + m^2}, \tag{5.25}$$

where $\tilde{q}^2 = (2/a)^2 \sum_\mu \sin\left(aq_\mu/2\right)^2$ is the standard momentum factor appearing in the propagator. Our momentum variable here is k. The absence of k implies a conservation of momentum within the loop which means our propagator is translationally invariant on the lattice. Due to our 1-loop diagram being independent of momentum we can cancel out this divergent integral by introducing a universal momentum independent counter term.

For the two loop diagram in standard lattice field theory the situation is slightly more complicated

$$I_2(k, m; a) = \frac{\lambda^2}{3} \int_{-\pi/a}^{\pi/a} \frac{d^d q}{(2\pi)^2} \frac{d^d q'}{(2\pi)^2} \frac{1}{\tilde{q}^2 + m^2} \frac{1}{(q'-q)^{2^*} + m^2} \frac{1}{(q'-k)^{2^*} + m^2}, \tag{5.26}$$

where both the $\tilde{}$ and '*' is the same $q^{2^*} = \tilde{q}^2 = (2/a)^2 \sum_\mu \sin\left(aq_\mu/2\right)^2$ as in (5.25).

This two loop integral contains an explicit momentum dependence k. For perturbative renormalization on a standard cubic lattice, integrals of this kind are handled by breaking them up into two parts. The first part is independent of momentum and is found by setting $k = 0$ in (5.26). We label it by as $I_2(0, m; a) = \hat{I}_2(m; a)$. The second piece we define to be $D_2(k, m; a) = I_2(k, m; a) - \hat{I}_2(m; a)$, and as a result $I_2(k, m; a) = I_2(0, m; a) + D_2(k, m; a)$. Using Reisz's method for classifying Feynman integrals in lattice field theories it can be shown that $I_2(0, m; a)$ is divergent as the UV cutoff, a, approaches zero and $D_2(k, m; a)$ is convergent. Thus on a cubic lattice one can cancel the divergent contribution, $I_2(0, m; a)$, to the 2-loop diagram using a universal momentum independent counter term. The finite piece, $D_2(k, m; a)$, uniformly approaches its continuum limit as the lattice is indefinitely refined.

Because the lattice spacing, a, of our simplicial complex is not uniform due to the positive curvature of $\mathbb{S}^3$, our lattice is not translationally invariant. As a result of our lattice not possessing translation invariance we cannot express our 1 or 2-loop diagrams in momentum space. Thus we are confined to work in position space. Another consequence of our lattice not being uniform is that high energy modes of our theory don't evenly contribute to the propagator. UV divergent diagrams are sensitive to all length scales present in the theory. This is evident by the lattice spacing cut off, a, in the Feynman integrals we recently wrote down. Because our simplicial complex is composed of a plethora of tetrahedrons which possess different sizes and shapes our simplicial complex admits a multitude of different length scales which contribute to the renormalized mass. Thus the finite portions of the 1-loop and 2-loop integrals on our simplicial complex don't naively converge to the continuum limit like they do on a cubic lattice with only one length scale. To remedy this irregularity due to the multitude of length scales present in our complex we must introduce position dependent counter terms which allow our lattice field theory to recover $SO(4)$ symmetry in the continuum limit.

In position space we can rewrite the simplicial representation of the integrals associated with the 1 and 2-loop diagrams in the following manner

$$\begin{aligned} I(x,m;a) &= \bar{I}(m;a) + D(x_i,m;a), \\ \bar{I}(m;a) &= \sum_i \sqrt{g_i} I(x_i,m;a) / \sum_i \sqrt{g_i}, \end{aligned} \tag{5.27}$$

where $\sqrt{g_i}$ is the Voronoï volume of a particular vertex in our complex, and $D(x,m;a) = I(x,m;a) - \bar{I}(m;a)$. The term $\bar{I}(m;a)$ is the average of $I(x,m;a)$ over the $SO(4)$ group and diverges as the characteristic lattice spacing, a, approaches zero. The difference term, $D(x,m;a)$, is the result of projecting out $SO(4)$ symmetry from $I(x,m;a)$ and is the term we need to negate using a counter term.

If our assumptions hold, then a UV divergent diagram should possess a position independent divergent part and a position sensitive/dependent finite part. The divergent part, $\bar{I}(m;a)$, can be handled non-perturbatively by setting our theory to the critical surface in parameter space for each level of refinement. However the finite position dependent portion, $D(x,m;a)$, which doesn't possess any trace of $SO(4)$ symmetry is sensitive to the irregularities present in our lattice. As a result unlike the case encountered in cubic lattice field theory, this term does not converge to the exact continuum limit.

To remedy this situation we have to introduce a position dependent counter term to our action (5.24) which is proportional to $\propto -D(x,m;a)$. This counter term will remove the irregular contributions to our UV diagrams and ensure that our lattice field theory admits $SO(4)$ symmetry in the continuum limit.

Working in perturbatively in position space results in the lattice propagator, G_{ij}, of our simplicial complex being defined as the inverse of our Laplacian whose construction we have already detailed

$$G_{ij} = [M_{ij}^{-1}], \tag{5.28}$$

where M_{ij} is exactly the matrix in (5.5). Using a standard perturbative expansion in powers of the coupling constants and quantities associated with the free field theory, such as the Laplacian, results in the following second order in λ_0 effective action

$$S_{eff} = S + 6\lambda_0\sqrt{g_i}G_{ii}\phi_i^2 - 24\lambda_0^2\sqrt{g_i}\phi_i G^3_{i\ j}\phi_j\sqrt{g_j}. \tag{5.29}$$

Because ϕ^4 theory in 3D has divergent 1 and 2-loop diagrams we need to compute counter terms associated with both perturbative contributions to the effective action. For the first counter term we group average G_{ii} over our simplicial approximation to $\mathbb{S}^3$ and subtract out the resultant $SO(4)$ invariant quantity to reexpress G_{ii} as

$$G_{ii} = \frac{1}{N}\sum_i \sqrt{g_i}G_{ii} + \left(G_{ii} - \frac{1}{N}\sum_i \sqrt{g_i}G_{ii}\right), \tag{5.30}$$

where $N = \sum_i \sqrt{g_i}$. By rewriting G_{ii} in this fashion we can identify the counter term that negates the position dependence of our effective action (5.29) up to first order in λ_0, which if left alone, will prevent our field theory from manifesting $SO(4)$ symmetry in the continuum limit

$$\delta G_i = \left(G_{ii} - \frac{1}{N}\sum_i \sqrt{g_i}G_{ii}\right). \tag{5.31}$$

Because the 2-loop diagram has a non-local term, $\phi_i\phi_j$, we have to be mindful when applying this procedure to it. After group averaging over the pair of points, $(i\,j)$, of our complex and keeping in mind how we rescaled our parameters with respect to a, we notice that non-local terms of our total quantum correction to the action are exponentially damped as the lattice spacing approaches zero. Keeping this observation in mind our second counter term is

$$\delta G_i^{(3)} = \sum_j \sqrt{g_j}\left[G^3_{ij} - \frac{1}{N}\sum_{i=1}^{N}\sqrt{g_i}G^3_{ij}\right]. \tag{5.32}$$

Using these two counter terms we can finally construct our QFE action

$$S_{QFE} = S_{eff} - \sum_i \sqrt{g_i} \left[6\lambda_0 \delta G_i - 24\lambda_0^2 \delta G_i^{(3)} \right] \phi_i^2. \tag{5.33}$$

As of the writing of this dissertation, we haven't had a chance to employ the code which will use these counter terms and our known Laplacian to compute CFT data that we can then compare to data extracted from the critical 3D Ising model using the conformal bootstraps. However to give an idea of how these counter term allow us to recover a defined continuum limit we will go over results which were obtained for ϕ^4 theory on $\mathbb{R} \times \mathbb{S}^2$.

The 4th-order Binder cumulant, as we previously discussed, is a number which characterizes the criticality of a field theory. The 4th-order Binder cumulant on our simplicial approximation to $\mathbb{S}^3$ in terms of the 4th and 2nd order magnetization is the following

$$\begin{aligned} U_4\left(K, m_0, \lambda_0\right) &= \frac{3}{2}\left[1 - \frac{\langle M^4 \rangle}{3\langle M^2 \rangle^2}\right] \\ M &= \sum_i \sqrt{g_i}\phi_i. \end{aligned} \tag{5.34}$$

This quantity is computed by performing a Monte Carlo simulation over random field configurations. We choose this normalization so that the cumulant is 0 in the disorderly phase and 1 in the ordered phase of our field theory. For a field theory on its critical surface the Binder cumluant is some number between 0 and 1. A clear sign that the theory described by the action we are using is approaching a conformal field theory in the continuum limit is if the Binder cumulant converges monotonically to a specific value as we continuously tune its parameters, (m_0, λ_0), to the critical surface.

For the top plot in 5.12, we see that for values of $m_0^2 > -.026906$, our Binder cumulant is not monotonically converging. Instead what we see is the Binder cumulant beginning to behave as an oscillatory function as the lattice space, a, is made con-

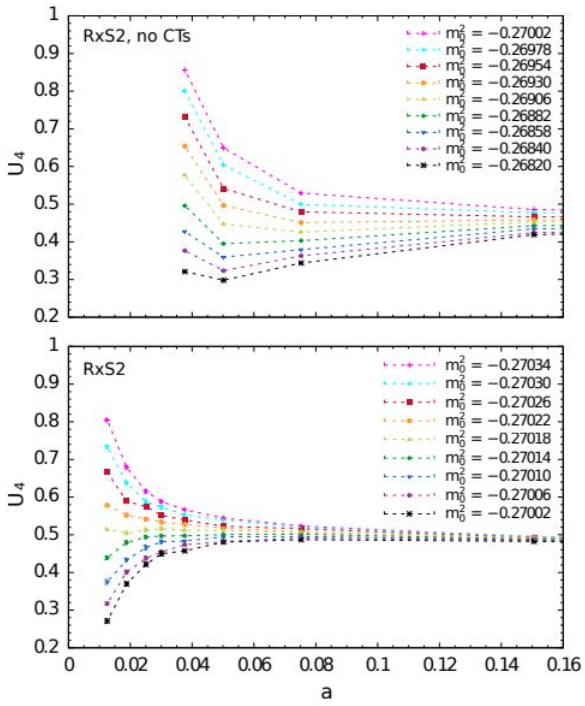

Figure 5.12 The convergence of the 4th-order Binder cumulant as a function of the characteristic lattice spacing, a. For plots we varied m_0 while holding fixed $\lambda_0 = .2$. This plot originally appeared in [56]

.

tinuously smaller. This indicates that our theory does not possess a critical surface and therefore is not converging to the critical 3D Ising model in the continuum limit. However when we include our counter terms (CT) in our action we see a monotonic convergence for all our sampled values of m_0^2 which is a sign that our lattice field theory is indeed approaching the correct continuum limit.

Chapter 6

Spectrum Fidelity On $\mathbb{S}^3$

6.1 Spectrum Of A Particle Trapped Inside A K Tetrahedral Box

Before we use the method we outlined to compute the estimated low lying spectrum of the Laplcian on $\mathbb{S}^3$, it is instructive to apply our tetrahedral-octahedral tessellation, to a particle trapped inside a K tetrahedral box and compare the estimated low lying spectrum it yields to the known exact spectrum. The exact eigenvalues and eigenfunctions associated with the K tetrahedron were first computed [148] by mapping the "4 hard cores" problem to the vertices of the following tetrahedron $(-\frac{\pi}{\sqrt{2}}, -\frac{\pi}{\sqrt{2}}, -\frac{\pi}{2})$, $(\frac{\pi}{\sqrt{2}}, -\frac{\pi}{\sqrt{2}}, \frac{\pi}{2})$; $(-\frac{\pi}{\sqrt{2}}, \frac{\pi}{\sqrt{2}}, \frac{\pi}{2})$ and $(\frac{\pi}{\sqrt{2}}, \frac{\pi}{\sqrt{2}}, -\frac{\pi}{2})$, which resulted in suitable boundary conditions which were used to modify the solution to the "4 hard cores" problem to that of a particle trapped in the aforementioned tetrahedral box. The problem was later explored [224] by utilizing the fact that like the equilateral triangle in 2D, the K tetrahedron possesses a space-filling property which allows it to tessellate an 3D space.

The eigenfunctions and eigenvalues of a particle trapped inside a K tetrahedral box are the following respectively

$$\phi_{lmn}(x,y,z) =$$

$$\begin{vmatrix} 1 & 1 & 1 & 1 \\ \exp\left[\mathrm{i}l\left(\frac{x}{\sqrt{2}}+\frac{z}{2}+\frac{3\pi}{4}\right)\right] & \exp\left[\mathrm{i}l\left(\frac{y}{\sqrt{2}}-\frac{z}{2}+\frac{\pi}{4}\right)\right] & \exp\left[\mathrm{i}l\left(-\frac{x}{\sqrt{2}}+\frac{z}{2}-\frac{\pi}{4}\right)\right] & \exp\left[\mathrm{i}l\left(-\frac{y}{\sqrt{2}}-\frac{z}{2}-\frac{3\pi}{4}\right)\right] \\ \exp\left[\mathrm{i}m\left(\frac{x}{\sqrt{2}}+\frac{z}{2}+\frac{3\pi}{4}\right)\right] & \exp\left[\mathrm{i}m\left(\frac{y}{\sqrt{2}}-\frac{z}{2}+\frac{\pi}{4}\right)\right] & \exp\left[\mathrm{i}m\left(-\frac{x}{\sqrt{2}}+\frac{z}{2}-\frac{\pi}{4}\right)\right] & \exp\left[\mathrm{i}m\left(-\frac{y}{\sqrt{2}}-\frac{z}{2}-\frac{3\pi}{4}\right)\right] \\ \exp\left[\mathrm{i}n\left(\frac{x}{\sqrt{2}}+\frac{z}{2}+\frac{3\pi}{4}\right)\right] & \exp\left[\mathrm{i}n\left(\frac{y}{\sqrt{2}}-\frac{z}{2}+\frac{\pi}{4}\right)\right] & \exp\left[\mathrm{i}n\left(-\frac{x}{\sqrt{2}}+\frac{z}{2}-\frac{\pi}{4}\right)\right] & \exp\left[\mathrm{i}n\left(-\frac{y}{\sqrt{2}}-\frac{z}{2}-\frac{3\pi}{4}\right)\right] \end{vmatrix}, \tag{6.1}$$

$$E_{lmn} = \left(\frac{\hbar^2}{8M}\right)\left[3\left(l^2+m^2+n^2\right) - 2lm - 2\ln -2mn\right], \tag{6.2}$$

where (l,m,n) are positive, distinct non-vanishing integers. Because we know the exact eigenfunctions for the particle trapped inside a K tetrahedral box, we can evaluate them on each lattice point in our tessellation of the K tetrahedron and thus approximately diagonalize the resultant Laplace operator (5.6) and (5.7). The diagonal components of this matrix are

$$E_{lmn} = \frac{\phi^*_{lmn}(\hat{r}_x)\, M_{xy} \phi_{lmn}(\hat{r}_y)}{\sum_x \sqrt{g_x}\phi^*_{lmn}(\hat{r}_x)\,\phi_{lmn}(\hat{r}_x)}, \tag{6.3}$$

where M_{xy} is (5.5) and (5.6), and $\sqrt{g_x} = \sigma_0^*$ is the volume of the Voronoï duel at the lattice site we evaluate (6.1) at. After expressing our Laplacian in a basis which is a finite dimensional representation of (6.1) we compute its diagonal elements (6.3) at various levels of refinement and obtain the two graphs shown in figure (6.1) which indicate that our numerical results are converging to the continuum limit (6.2). In other words, as we increase the level of refinement for our simplicial approximation to the K tetrahedron, the symmetries that are associated with it which are described in [148, 153], monotonically become closer to being fully restored.

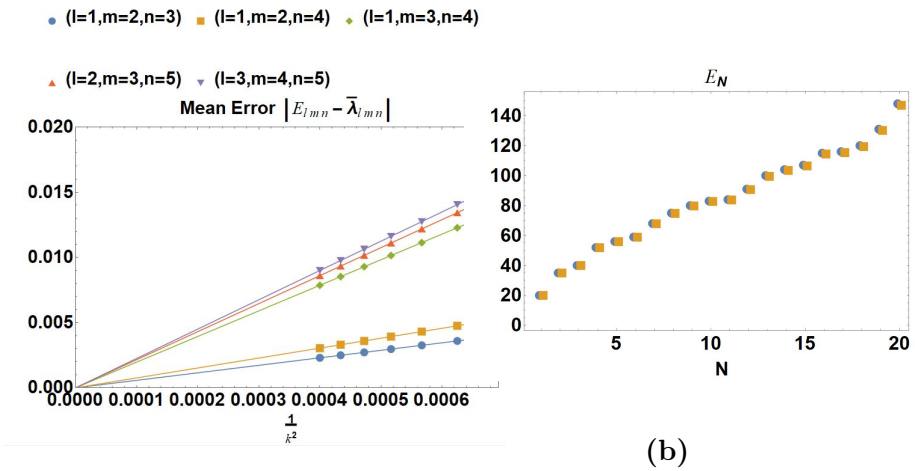

Figure 6.1 Figure 10(a) shows how the difference between the exact spectrum, (6.2), and the average, $(\overline{\lambda}_{lmn})$, over the degeneracy of our numerically computed spectrum, λ_{lmn}, appears to approach zero as our level of refinement "k" increases. In figure 10(b) we compare the first exact 20 eigenvalues in order of increasing energy to the first 20 eigenvalues we computed numerically at refinement level 'k=60'. The blue circle corresponds to exact eigenvalues and the yellow squares are the numerically estimated eigenvalues.

6.2 Spectral Fidelity on $\mathbb{S}^3$

To obtain our results we will utilize the fact that we know the exact eigenfunctions, the hyperspherical harmonics, for the scalar Laplacian on $\mathbb{S}^3$. In terms of hyperspherical coordinates they can be expressed as

$$Y\,(j,l,m) = \left(2^l\sqrt{\frac{2}{\pi}}l!\,\sqrt{\frac{(j+1)(j-l)!}{(j+l+1)!}}\right)\sin^l(\psi)C_{j-l}^{(l+1)}(\cos(\psi))y_l^m(\theta,\phi), \tag{6.4}$$

where $y_l^m(\theta,\phi)$ are the ordinary spherical harmonics which satisfy

$$\frac{1}{y_l^m}\left(\frac{1}{\sin\theta}\frac{\partial}{\partial\theta}\left(\sin\theta\frac{\partial y_l^m}{\partial\theta}\right)+\frac{1}{\sin^2\theta}\frac{\partial^2 y_l^m}{\partial\phi^2}\right) = -l(l+1), \tag{6.5}$$

and $C_{j-l}^{(l+1)}(\cos(\psi))$ are the Gegenbauer polynomials. For our hyperspherical harmonics our quantum numbers are restricted to the following range $j \geq 0$, $j \geq l$, and

$l \geq |m|$. The hyperspherical harmonics are the eigenfunctions of the generalization of (6.5) to $\mathbb{S}^3$ and have associated with them the following eigenvalues and degeneracies

$$\begin{aligned} \lambda_{continuum} &= j(j+2), \\ degeneracies &= (j+1)^2. \end{aligned} \tag{6.6}$$

We evaluated the hyperspherical harmonics, $Y_{jlm}(\hat{r}_x)$, at our lattice sites, $\hat{r}_x$, so we can estimate the eigenvalues of the discretized Laplcian operator whose construction we previously outlined by computing the diagonal elements against j

$$E_{j,l,m} = \frac{Y^*_{jlm}(\hat{r}_x)\, M_{xy} Y_{jlm}(\hat{r}_y)}{\sum_x \sqrt{g_x} Y^*_{jlm}(\hat{r}_x)\, Y_{jlm}(\hat{r}_x)}. \tag{6.7}$$

In equation (6.7), $\sqrt{g_x} = \sigma_0^*$, which is the volume of the Voronoï duel at the lattice site we evaluate our hyperspherical harmonics on.

As can be seen in figure (6.2a), when $k = 2$, the degeneracies of our low lying spectrum splits noticeably while at much higher levels of refinement, such as $k = 18$, as is shown in figure (6.2b), our low lying spectrum's degeneracies practically match that of the continuum limit. Geometrically this indicates that the rotational symmetry of our simplicial complex as we continue to refine it approaches the rotational invariance of $\mathbb{S}^3$. Another interesting feature in figures 11(a) and 11(b) is that the degeneracies of the first five energy levels match that of the continuum even at low levels of refinements such as $k = 2$. This is an artifact of us starting with the refined 600-cell, which preserves the largest discrete subgroup of the isometries of $\mathbb{S}^3$ and then projecting those points onto $\mathbb{S}^3$.

In terms of convergence, we see that in figure (6.3), the estimated low lying spectrum practically matches the continuum limit of $j(j+2)$ and that it is converging at a linear rate as a function of one over the level of refinement squared. The convergence of our estimated low lying spectrum to the continuum limit is a theoretical

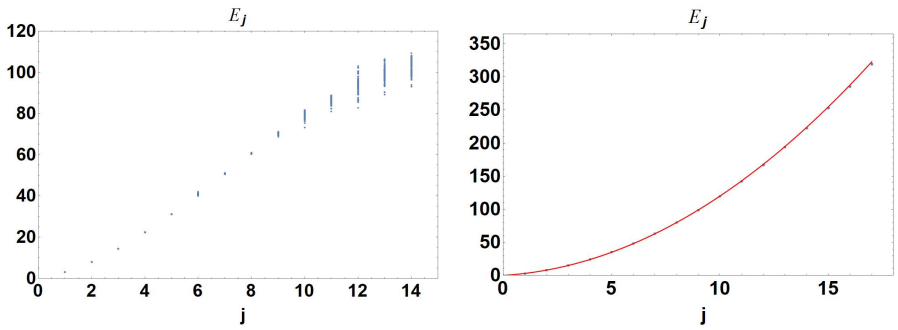

(a) **(b)**

Figure 6.2 Figure 6.2a shows the splitting of the degeneracy which is present for the first 14 energy levels at a $k = 2$ level of refinement of our simplicial complex on $\mathbb{S}^3$. Figure 6.2b is the same type of graph except for the first 17 levels with the $k = 18$ level of refinement. To show that as we increase our level of refinement that the symmetry of our simplicial complex approaches the rotational invariance of $\mathbb{S}^3$ we superimposed on it a plot of the continuum spectrum, $j(j+2)$, which it matches quite well.

consequence of FEM convergence theorems for shape regular linear elements as the diameter goes uniformly to zero [220]. Even though we used the DEC [12] prescription for constructing our discretized Laplacian we will assume without proof that this property holds.

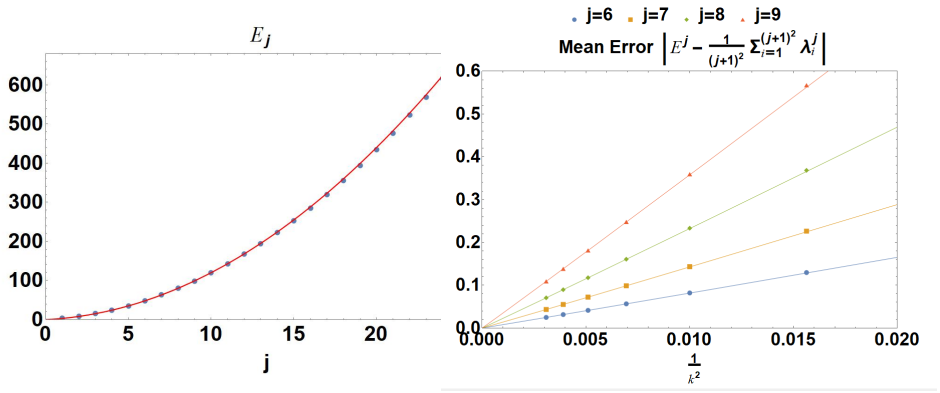

(a) **(b)**

Figure 6.3 Figure 6.3a is a graph of our estimated eigenvalues for the first 25 energy levels averaged over their degeneracies superimposed over $j(j+2)$. Figure 6.3b is a graph of the mean error for a particular set of energy levels as a function of our level of refinement, k, which demonstrates the rate of convergence of our low lying spectrum to the continuum limit for the levels of refinements $k = 8$ to $k = 18$. For figure 6.2a, E^j are the eigenvalues, $j(j+2)$, in the continuum limit, while λ_i^j are our estimated eigenvalues for a given energy level, j, averaged over their degeneracies. From our mean errors as functions of k for the $k = 18$ and $k = 16$ refinement levels we were able to construct the following functions which we overlaid on our graph for each energy level we considered. In order of increasing j they are $8.781\left(\frac{1}{k}\right)^{2.0316}$, $15.29\left(\frac{1}{k}\right)^{2.03}$, $24.82\left(\frac{1}{k}\right)^{2.03}$, and $37.73\left(\frac{1}{k}\right)^{2.02}$.

6.3 Concluding Remarks

In the past two chapters we have laid the groundwork for an exciting test of the QFE on ϕ^4 theory on $\mathbb{S}^3$. We have discussed in length how to construct a simplicial approximation to $\mathbb{S}^3$, related our simplicial complex to the conventional cubic lattice, figured out how to properly order the simplices which make up our complex, shown how to renormalize a quantum field theory on a non-uniform lattice, and demonstrated the validity of our approach for computing the weights of the links which make up our simplical complex by showing that our estimated spectrums appear to be converging to their known continuum limits.

Because our counter terms are dependent upon the Laplacian and we have given ample evidence that we can correctly construct a Laplacian on our complex the stage is set for this non-trivial test of the QFE. In this test we seek to compute two and four point correlation functions as was done on $\mathbb{S}^2$ [54] and extrapolate from them the Binder cumulants [36], and other data that we can compare to conformal bootstrap results [87, 141, 209, 215] for the critical 3D Ising model. Regardless of the outcome, performing this comparison will further develop the tools we have available to study quantum field theories non-perturbatively. In addition, just the ability to construct a simplicial approximation to $\mathbb{S}^3$ is an important step towards being able to study numerically novel classical or quantum field theories on curved Riemannian manifolds in three and four dimensions. Towards the end of our dissertation we will discuss the importance of $\mathbb{R} \times \mathbb{S}^3$ and how our present work is related to formulating lattice field theories on it.

If our upcoming test of the QFE for ϕ^4 theory on $\mathbb{S}^3$ is successful it will give us further confidence that we have a viable method that we can apply to more novel lattice field theories formulated on Riemannian manifolds. The applications of studying such lattice field theories includes two-dimensional condensed matter systems such as graphene sheets [51], four-dimensional gauge theories for beyond the standard model

(BSM) strong dynamics [11, 152], and perhaps even quantum effects in a space-time near massive systems such as black holes. Thus the work presented so far is an important step towards realizing the study of these incredibly fascinating topics.

Chapter 7

From Quantum Gravity To Quantum Cosmology

7.1 Hamiltonian of Constrained Systems

It is well known that the Hamiltonian formulation of a classical system can be quantized $\left(p_i \to \hat{p}_i = -i\hbar\frac{\partial}{\partial x_i}\,, x_i \to \hat{x}_i\right)$, thus resulting in a Schrödinger like equation which governs the dynamical behavior of the quantum analog of the classical system originally in question. Thus if one wishes to study quantum gravity, and in turn quantum cosmology, it is natural to seek a Hamiltonian formulation of general relativity. To begin constructing such a Hamiltonian formulation we first must ask what does it mean for a Hamiltonian formulation of general relativity to exist? This question is necessitated because unlike other classical theories which seek to analyze the dynamics of either particle(s) or field(s) in a known, a priori, space-time, general relativity describes the dynamics of space-time itself as is encapsulated by the Einstein field equations (EFE)

$$R_{ab} - \frac{1}{2}Rg_{ab} + \Lambda g_{ab} = \frac{8\pi G}{c^4}T_{ab}. \tag{7.1}$$

From (7.1) it is clear that the nature of the geometry of space-time, g_{ab}, is coupled to the nature of matter, T_{ab}, and vice versa. Furthermore no a priori space-time is assumed in general relativity unlike other classical theories. As a result general relativity is fundamentally different from classical theories which assume the existence of a space-time background and whose dynamical/canonical variables, (p_i, q_i), live on a symplectic manifold.

One of the hallmarks of general relativity is that space and time are in a sense treated on an equal footing. This can be understood by how both time and spatial components of the metric tensor are equally unknown quantities in the EFE. In other words the 'time' variable is treated as just another variable whose evolution can be described using the same arbitrary clock, $f(\tau)$, as the spatial variables in a natural fashion. This feature of general relativity should cause one to pause before formulating a Hamiltonian version of it. In Hamiltonian mechanics the conjugate momentum, $p_i = \frac{\partial \mathscr{L}}{\partial \dot{x}_i}$, is defined with respect to only the partial derivative of the time derivative of the configuration variables and not with respect to their spatial derivatives. This preferential treatment of the time variable in defining the conjugate momentum is at odds with the equal footing the EFE gives to both space and time.

Despite this arguably undesirable preferential treatment of time over space, the most commonly employed Hamiltonian formulation of general relativity known as the ADM formalism [13, 14] yields equations of motion which are formally equivalent to the EFE (7.1). As a result we will seek to quantize this Hamiltonian to obtain a theory of quantum gravity which we will use to motivate constructing a theory of quantum cosmology. Furthermore in the ADM formalism the original equal footing of space and time is somewhat preserved by the fact that the Hamiltonian we obtain is for a constrained system. For the case of spatially closed universes and the cosmological models we will be considering in this dissertation the Hamiltonian itself is a constraint which equals zero $H = 0$. When asymptotic flatness is demanded additional boundary

terms [197, 198] need to be taken into account which results in the Hamiltonian constraint not vanishing.

To give a sense of what we mean by a constrained Hamiltonian let's start [205] with the case of a single particle under the influence of an arbitrary potential $V(x)$. The action of such a simple system is given below

$$\begin{aligned} S &= \int_{t_i}^{t_f} \mathscr{L}[\dot{x}\ x(t)]dt, \\ \mathscr{L}[\dot{x}\ x] &= \frac{m}{2}\dot{x}^2 - V(x(t)). \end{aligned} \tag{7.2}$$

Now let's introduce a 'time' dependency in the time parameter, t, thus changing it to a dependent variable like, $x(t)$, by introducing an arbitrary clock, $f(\tau)$, where τ is an evolution parameter. As a result (7.2) becomes

$$\begin{aligned} S &= \int_{\tau_i}^{\tau_f} \mathscr{L}[\dot{x}\ x(t(\tau))]\frac{df}{d\tau}\frac{dt}{df}d\tau, \\ \dot{t} &= \frac{df}{d\tau}\frac{dt}{df}, \\ \mathscr{L}[\dot{x}\ x] &= \frac{m}{2}\frac{\dot{x}^2}{\dot{t}} - V(x(t(f(\tau))))\dot{t}, \end{aligned} \tag{7.3}$$

where the dot, $\dot{}$, now represents $\frac{d}{d\tau}$, where τ is our arbitrary evolution parameter. As it can be seen, our Lagrangian now has two configuration variables (t, x) as opposed to one. Both the time variable, t, and the spatial variable, x, are on equal footing. This simple example can tell us something about what a Hamiltonian formalism of general relativity will look like because presently both space and time are treated on an equal footing at the Lagrangian level.

Treating, ($t(\tau)$, $x(\tau)$), as our configuration space we can obtain the following equations of motions from the Euler Lagrange equation

$$\frac{d}{d\tau}\frac{\partial \mathscr{L}}{\partial \dot{q}_i} = \frac{\partial \mathscr{L}}{\partial q_i}, \tag{7.4}$$

$$\begin{aligned}
&\frac{d}{d\tau}\left(\frac{m\dot{x}}{\dot{t}}\right)+\frac{dV(x(t(f(\tau))))}{dx(t(f(\tau)))}\dot{t}=0,\\
&\frac{d}{d\tau}\left(\frac{m\dot{x}^2}{2\dot{t}^2}+V(x(t(f(\tau))))\right)=0.
\end{aligned} \tag{7.5}$$

The top equation in (7.5) can be identified with Newton's equation of motion $m\frac{d\dot{x}}{dt} = -\nabla V$, while the bottom of (7.5) can be identified as conservation of energy. The fact that these two equations are not independent suggests that the introduction of an arbitrary evolution parameter has caused a redundancy in our configuration space. The arbitrariness in the manner in which our clock, $f(\tau)$, ticks has introduced a gauge invariance in our system. This gauge invariance in how 'time' is defined is an intrinsic feature of general relativity and will play a big role in how we interpret its final Hamiltonian formalism. To get a glimpse of what that final formalism will look like, let's construct the Hamiltonian of (7.3).

$$\begin{aligned}
p_x &= \frac{\partial \mathscr{L}}{\partial \dot{x}} = \left(\frac{m\dot{x}}{\dot{t}}\right),\\
p_t &= \frac{\partial \mathscr{L}}{\partial \dot{t}} = \left(-\frac{m\dot{x}^2}{2\dot{t}^2} - V(x(t(f(\tau))))\right),
\end{aligned} \tag{7.6}$$

$$H = p_x\dot{x} + p_t\dot{t} - \left(\frac{m}{2}\frac{\dot{x}^2}{\dot{t}} - V(x(t(f(\tau))))\dot{t}\right) = 0. \tag{7.7}$$

As a result of introducing a gauge invariance, $f(\tau)$, we obtain a vanishing Hamiltonian. It is important to keep in mind that this does not mean the energy of our single particle under the influence of an arbitrary potential is zero. Instead this indicates that the dynamics of our system depends on the relationship between the evolution of, $x(f(\tau))$ to $t(f(\tau))$. This relational-dynamics between the configuration variables is different from what we usually see in classical systems in which the dynamics in question are expressed as the evolution of dependent variables with respect to some independent parameter we call time. This is a sign that there is redundancy in our configuration space as a result of time and space being treated on an equal footing. If we conclude

this is the result of the gauge invariance associated with treating time and space on an equal footing we would expect the quantity denoted as the Hamiltonian in general relativity to vanish as well. This indeed is the case.

This shows that despite the Hamiltonian formalism giving preferential treatment to the 'time' variable it is also able to preserve or sublate the general relativistic notion that time and space are on an equal footing by the generation of a Hamiltonian constraint. The ability to preserve this notion will have important consequences for quantization that we will discuss in the upcoming sections. Now that we have an idea of what our end product will look like we shall proceed to illuminate how one repeats the same procedure we did above to this one dimensional system to a formally infinite dimensional theory of space-time/gravity.

7.2 Initial Value Formulation of General Relativity

To begin constructing a Hamiltonian formalism of general relativity we need to express general relativity in a way that makes it more in concord with other classical theories. Typically a classical theory describes a plethora (infinite number) of trajectories that some quantity such as the position of a particle can trace in space-time. If the equations of motion are second order, one picks out a unique trajectory that the theory admits by specifying a pair of initial conditions at some arbitrary point in time. An initial value problem consists of a collection of m, nth order ordinary differential equations and m*n initial conditions for them. We will not rigorously prove the existence and uniqueness of solutions to the EFE. Instead we explain and motivate the variables which are used in the initial value formulation of general relativity. We will use these variables to construct a Hamiltonian for general relativity. For a rigorous proof of a well-posed initial value formulation for general relativity we refer the reader to these sources [15, 91, 181].

The main quantity one finds using the EFE is the metric tensor, g_{ab}, in which both space and time count towards the dimensions of the space-time described by g_{ab}. Therefore it makes no sense to talk about the time evolution of the whole metric tensor because the metric encapsulates both space and time. However if we dissect the metric tensor, g_{ab}, we may obtain a quantity which can be described as evolving as a function of time. Because the metric tensor, g_{ab}, is associated to a four-dimensional space-time manifold, $\mathbb{M}$, it induces a Riemannian metric on any lower dimensional spacelike manifold embedded in that higher dimensional space-time. If this manifold, Σ_t, is an 3D spacelike surface we call it a hypersurface. We choose to denote this 3D spatial surface, Σ_t, because it is effectively a cross section in time, t, of the four-dimensional manifold, $\mathbb{M}$, with metric g_{ab}.

From the first fundamental form of differential geometry we know that a hypersurface, Σ_t, has the following metric induced on it from the higher dimensional space-time, g_{ab}, it is embedded in

$$h_{ab} = g_{ab} + n_a n_b, \tag{7.8}$$

where n_a is the unit vector, $n^a n_a = -1$, normal to the hypersurface, Σ_t, with Riemannian metric, h_{ab}. As a result $h_{ab}n^a = 0$. Because the metric, h_{ab}, is associated to a time slice, Σ_t, of $\mathbb{M}$ we can compare it to the metric, h_{ab}, of an adjacent time slice, Σ_{t+dt}. To do that though we need to define a quantity which denotes the flow from one hypersurface to another. Because these are spatial hypersurfaces it makes sense for this quantity to be related to 'time', t. Thus we shall define this general vector which describes moving from one spatial slice to another as

$$t^a \nabla_a t = 1. \tag{7.9}$$

Because we are assuming that space-time, $(\mathbb{M}, g_{ab})$, can be decomposed into hyper-

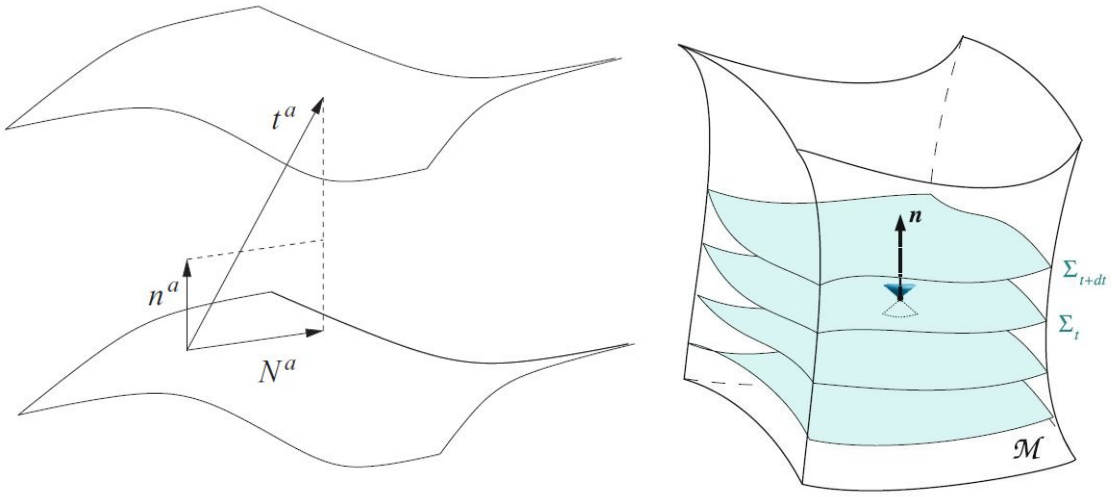

(a) Decomposition of t^a from Σ_t to Σ_{t+dt}

(b) A flotation of space-time.

Figure 7.1 Figure a is from [48] and figure b is from [182]

surfaces/slices, Σ_t, the 'time' vector, t^a, should be a space-time vector. This means it should encapsulate the change in both space and time that a particle/observer may experience as it/they travel from one hypersurface, Σ_t, to another, Σ_{t+dt}. We can decompose t^a into two quantities which are orthogonal to each other

$$t^a = Nn^a + N^a. \tag{7.10}$$

In this decomposition the quantity N is called the lapse and n^a is the unit vector normal to Σ_t that we introduced earlier and N^a which lies in the tangent space of Σ_t is called the shift. In 2D one can visualize our time slices, Σ_t, and our 'time' vector, t^a, in a manner depicted by the figures above. As it is shown in (7.1a) N^a describes the change in spatial position while traversing to the hypersurface, Σ_{t+dt}, relative to one's spatial position on Σ_t; while N is a measurement of how time is measured as one transverses from one hypersurface to another. Thus the t^a gives a space-time description of how one transverses the hypersurfaces belonging to a particular

foliation of space-time.

It must be pointed out that neither the lapse, N, nor the shift, N^a, are necessarily unique quantities. One can foliate space-time in an arbitrary way as a result of the inherent diffeomorphism invariance of general relativity. Thus the foliation shown in (7.1b) is not unique and can be substituted with any other geometric foliation. The result of how one foliates space-time has no bearings on the observables that one can compute and measure on it. Thus N and the components of N^a at least in the case when no exotic anisotropic matter sources are present, can be set to any value. This is akin to how earlier in our one dimensional example we introduced an arbitrary evolution parameter which could represent the tick of an arbitrary clock. Thus N and N^a represent the gauge freedom present in general relativity. As a result of N and N^a being gauge variables they cannot be the dynamical quantities that evolve as functions of time that we need to define an initial value formulation of general relativity.

Using (7.8) and (7.10) we obtain the following relationship between the metric, g_{ab}, and the quantities we just introduced

$$g^{ab} = h^{ab} - n^a n^b = h^{ab} - \frac{1}{N^2}\left(t^a - N^a\right)\left(t^b - N^b\right). \tag{7.11}$$

From the above it is clear that (h_{ab}, N, N^a) contains all of the information present in g_{ab}, and thus form the configuration space of general relativity. As a result of our foliation of space-time it is easy to see how h_{ab} is a quantity which changes as one transverses along t^a from one spatial slice of $\mathbb{M}$ to another. Thus h_{ab} plays the role of a quantity which puts general relativity in concordance with other classical theories. Geometrically this means we can envision space-time as the time evolution of a spatial metric, $h(t)_{ab}$, on some abstract hypersurface, Σ_0. The gauge variables, (N, N^a), represent a non-trivial redundancy in our configuration space which will ultimately

result in us obtaining a Hamiltonian constraint for general relativity similar to the one we obtained in the last section.

In order to adequately describe the evolution of $h(t)_{ab}$ we need some quantity that takes into account that our hypersurface, Σ_0, is embedded in a higher dimensional curved space-time. Thus we need to define extrinsic curvature. In order to obtain a notion of extrinsic curvature we need to define a derivative operator associated with $h(t)_{ab}$. This is analogous to how a derivative operator associated with g_{ab} is required when defining the Riemannian curvature tensor $R_{abc}{}^{d}$.

To motivate the upcoming definition of this derivative operator let's imagine a space-time vector, $v^a = Cn^a + v^a_{tangent}$, where C is a constant, n^a is perpendicular to some spatial hypersurface, Σ_0, and, $v^a_{tangent}$ lies entirely in the tangent space of Σ_0. If we apply the spatial metric, h_{ab}, to the space-time vector, v^a, we obtain $h^b_a v^a = v^b_{tangent}$ where the index of the spatial metric was raised using g^{ab}. Thus we see that h_{ab} acts as a projection operator from the tangent space of $\mathbb{M}$ to the tangent space of the spatial hypersurface Σ_0.

This notion of a projection operator from a space-time vector to a vector on a one dimension lower spatial surface can be generalized to tensors in the following manner

$$T^{a_1\ldots a_k}_{b_1\ldots b_l} = h^{a_1}_{d_1}\cdots h^{a_k}_{d_k} h^{e_1}_{b_1}\cdots h^{e_l}_{b_l}\, T^{d_1\ldots d_k}_{e_1\ldots e_l}. \tag{7.12}$$

Using this generalized notion of a projection operator from a space-time tensor to a spatial tensor we can define our derivative operator in terms of the well known covariant derivative ∇_a. Going back to vectors, if we are applying the covariant derivative to a spatial vector $\nabla_a v^b_{tangent}$ we immediately see a problem. Due to the vector, v^a, having its components which are orthogonal to the hypersurface it is tangent to being projected out; we have no information on how they vary as we leave the spatial hypersurface. However if we apply the projection operator, h_{ab}, to the

covariant derivative itself, we project out the portion of the covariant derivative which measures how a tangent vector changes in a direction perpendicular to the surface it is tangent to. Thus for the space-time vector, v^a, we can define the following derivative operator associated with, h_{ab}, on it

$$D_a v_b = h_a^c h_b^d \nabla_c v_d. \tag{7.13}$$

The generalization of this derivative operator to an arbitrary space-time tensor is

$$D_c T^{a_1 \ldots a_k}_{b_1 \ldots b_l} = h^{a_1}_{d_1} \cdots h^{a_k}_{d_k} h^{e_1}_{b_1} \cdots h^{e_l}_{b_l} \; h_c^f \nabla_f T^{d_1 \ldots d_k}_{e_1 \ldots e_l}. \tag{7.14}$$

This derivative operator, D_c, satisfies the metric compatibility condition for, h_{ab}, as is demonstrated below

$$\begin{aligned} &D_c h_{ab} = h_c^d h_a^e h_b^f \nabla_d h_{ef}, \\ &h_c^d h_a^e h_b^f \nabla_d \left(g_{ef} + n_e n_f \right) = h_c^d h_a^e h_b^f \nabla_d \left(n_e n_f \right) = 0. \end{aligned} \tag{7.15}$$

This results was arrived at by taking advantage of the fact that ∇_d is compatible with g_{ef} and that $h_a^e n_e = 0$.

Now that we have an appropriate derivative operator we can properly define a notion of extrinsic curvature for our metric h_{ab}. The extrinsic curvature should measure the change that a vector orthogonal to the hypersurface, Σ_0, experiences as it is parallel transported along a curve in the tangent bundle of Σ_0. Graphically this is demonstrated below.

From this logic it follows that a natural definition of the extrinsic curvature is simply

$$K_{ab} = h_a^c h_b^d \nabla_c n_d = D_a n_b. \tag{7.16}$$

We will state without proof that this tensor is symmetric. We will prove though that

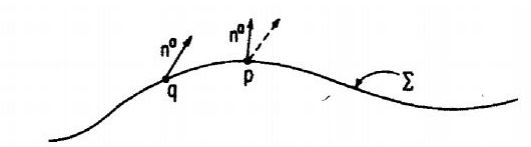

Figure 7.2 This image shows a vector initially on the hypersurface, Σ, at point, q, being parallel transported along some curve on the hypersurface which passes through point p. If the hypersurface was embedded in a flat, higher dimensional space-time, the vector, n^σ, would possess the same orientation at point, p, as the dashed line does. However if the hypersurface is embedded in a curved, higher dimensional space-time, the orientation of the vector at point, p, would be different. That difference is what the extrinsic curvature measures. This image is originally from [233].

it can be expressed in an alternative form which will allow us to relate the extrinsic curvature, K_{ab}, to $\dot{h}_{ab}$ and thus allow us to construct our initial value formulation of general relativity. We first will show that $K_{ab} = h_a^c \nabla_c n_b$

$$\begin{aligned} K_{ab} &= h_a^c h_b^d \nabla_c n_d, \\ &= h_a^c \left(g_b^d + n^d n_b \right) \nabla_c n_d, \\ &= h_a^c \nabla_c n_b + h_a^c n_b n^d \nabla_c n_d, \\ &= h_a^c \nabla_c n_b + h_a^c n_b g^{ed} n_e \nabla_c n_d, \\ &= h_a^c \nabla_c n_b + h_a^c n_b \frac{1}{2} \nabla_c g^{ed} n_e n_d = 0, \\ &= h_a^c \nabla_c n_b. \end{aligned} \tag{7.17}$$

In our derivation we used the metric compatibility of g^{ed} and ∇_c and $n^e n_e = -1$.

Next we will demonstrate that $K_{ab} = h_a^c \nabla_c n_b = \frac{1}{2} \mathcal{L}_n h_{ab}$ where $\mathcal{L}_n h_{ab}$ is the Lie derivative of the spatial metric with respect to the unit vector orthogonal to the surface which the spatial metric is associated with. The Lie derivative, $\mathcal{L}_\xi$, can be thought of as the change of a vector or tensor that is defined on a manifold as the manifold is subjected to a diffeomorphism generated by the vector ξ^a. Lie derivatives can also be generalized to maps acting on manifolds generated by tensors. First we will manipulate the right hand side of this equality in the following manner

$$\begin{aligned}\frac{1}{2}\left(h_a^c\nabla_c n_b + h_b^c\nabla_c n_a\right) &= \frac{1}{2}\left(n^c\nabla_c h_{ab} + h_{cb}\nabla_a n^c + h_{ac}\nabla_b n^c\right), \\ &= \frac{1}{2}\left(n^c\nabla_c h_{ab} - n^c\nabla_a h_{cb} - n^c\nabla_b h_{ca}\right), \\ &= \frac{1}{2}\left(n^c\nabla_c h_{ab} - n^c\nabla_a n_c n_b - n^c\nabla_b n_c n_a\right), \\ &= \frac{1}{2}\left(n^c\nabla_c h_{ab} + \nabla_a n_b + \nabla_b n_a\right).\end{aligned} \tag{7.18}$$

Next we will manipulate the left hand side

$$\begin{aligned}\frac{1}{2}\left(h_a^c\nabla_c n_b + h_b^c\nabla_c n_a\right) &= \frac{1}{2}\left(\nabla_a n_b + \nabla_b n_a + n^c n_a\nabla_c n_b + n^c n_b\nabla_c n_a\right), \\ &= \frac{1}{2}\left(\nabla_a n_b + \nabla_b n_a + n^c\nabla_c\left(n_a n_b\right)\right), \\ &= \frac{1}{2}\left(\nabla_a n_b + \nabla_b n_a + n^c\nabla_c h_{ab}\right).\end{aligned} \tag{7.19}$$

Equating (7.18) and (7.19) demonstrates that $K_{ab} = h_a^c\nabla_c n_b = \frac{1}{2}\mathcal{L}_n h_{ab}$. In this proof we used the metric compatibility associated with g_{ab} and (7.8).

The usual initial conditions one uses to determine the dynamics of a 2nd order classical system are $x(0) = c_1$ and $x'(0) = c_2$ where x is the dependent variable and x' is the derivative of x with respect to time or the evolution parameter. If we want to do something analogous for general relativity we need to define $\dot{h}_{ab}$. Starting from $K_{ab} = \frac{1}{2}\mathcal{L}_n h_{ab}$ we will derive below $K_{ab} = \frac{1}{2N}\left(\dot{h}_{ab} - D_a N_b - D_b N_a\right)$.

$$\begin{aligned}K_{ab} &= \frac{1}{2}\mathcal{L}_n h_{ab}, \\ &= \frac{1}{2}\left(n^c\nabla_c h_{ab} + h_{cb}\nabla_a n^c + h_{ac}\nabla_b n^c\right), \\ &= \frac{1}{2}\left(\frac{1}{N}\left(t^c - N^c\right)\nabla_c h_{ab} + h_{cb}\nabla_a\frac{1}{N}\left(t^c - N^c\right) + h_{ac}\nabla_b\frac{1}{N}\left(t^c - N^c\right)\right), \\ &= \frac{1}{2N}\left(\mathcal{L}_t h_{ab} - \mathcal{L}_N h_{ab}\right), \\ &= \frac{1}{2N}\left(\dot{h}_{ab} - \mathcal{L}_N h_{ab}\right).\end{aligned} \tag{7.20}$$

To obtain this result we took advantage of the linear nature of the Lie derivative

operator and (7.10). We now need to prove that $D_a N_b + D_b N_a = \mathcal{L}_N h_{ab}$.

$$\begin{aligned} h^{ab}\left(D_a N_b + D_b N_a\right) &= h^{ab}\left(\mathcal{L}_N h_{ab}\right), \\ &= h^{ab}\left(N^c \nabla_c h_{ab} + h_{cb}\nabla_a N^c + h_{ac}\nabla_b N^c\right), \\ &= h^{ab} N^c \nabla_c h_{ab} + 2\nabla_c N^c, \\ &= \frac{1}{2} N^c \nabla_c \left(h^{ab} h_{ab}\right) + 2\nabla_c N^c, \\ &= 2\nabla_c N^c, \\ &= 2 D_c N^c, \\ &= 2 h^x_c h^c_d \nabla_x N^d, \\ &= 2\delta^x_d \nabla_x N^d, \\ &= 2\nabla_c N^c \end{aligned} \tag{7.21}$$

In this derivation we took advantage of the fact that $h_{ab}h^{ab} = 3$ which one can obtain by using the well known identity $g_{ab}g^{ab} = 4$ and (7.8). In addition we used the compatibility $D_a h_{bc} = 0$. We were able to utilize compatibility in this fashion because the shift, N_a, is a spatial vector. As the reader can verify if N_a was a space-time vector like n_a we wouldn't be able to employ compatibility in the manner we just did.

We have provided motivation for using the following quantities, $(\Sigma_0, h_{ab}, K_{ab})$, to define an initial value formulation of general relativity where we have related K_{ab} to $\dot{h}_{ab}$. We will use these variables in the next section to obtain the ADM Hamiltonian formalism of general relativity which we will quantize to obtain a theory of quantum gravity. To facilitate the derivation of the Hamiltonian constraint in the next section we will state the Gauss Codazzi equations without proof

$$^{(3)}R_{abc}{}^{d} = h^f_a h^g_b h^k_c h^d_j R_{fgk}{}^{j} - K_{ac}K^d_b + K_{bc}K^d_a \tag{7.22}$$

$$D_a K^a_b - D_b K^a_a = R_{cd} n^d h^c_b \tag{7.23}$$

In equation (7.22) ${}^{(3)}R_{abc}{}^d$ is the Riemann curvature tensor for the spatial manifold, Σ_0, with metric h_{ab}. It can be defined using the derivative operator associated with h_{ab}

$$D_a D_b w_c - D_b D_a w_c = {}^{(3)}R_{abc}{}^d w_d. \tag{7.24}$$

In the next section using the Gauss Codazzi equations and our definitions of h_{ab} and K_{ab} we will write out a Hamiltonian formalism for general relativity.

7.3 Hamiltonian And Quantization Of General Relativity

In order to construct a Hamiltonian for general relativity we need to find an appropriate Lagrangian to apply a Legendre transformation to. The Lagrangian whose variation with respect to δg^{ab} yields the EFE is

$$S = \int \left[\frac{1}{2\kappa} R + \mathcal{L}_{\mathrm{M}} \right] \sqrt{-g}\ \mathrm{d}^4 x, \tag{7.25}$$

where $\kappa = 8c^{-3}G$, R is the Ricci scalar, $\mathcal{L}_{\mathrm{M}}$ is the Lagrangian associated with a matter source such as a perfect fluid, homogeneous scalar field or electromagnetic field, and, $\sqrt{-g}$, is the square root of minus the determinant of the space-time metric. For the remainder of this section we shall set $\mathcal{L}_{\mathrm{M}} = 0$. Later when we consider canonical quantization in the simplified setting of cosmology we will introduce a cosmological constant, an electromagnetic field and a free homogeneous scalar field. To obtain a Hamiltonian from this Lagrangian we need to rewrite it using the variables we introduced and motivated in the previous section.

We will first begin with $\sqrt{-g}$. We note from (7.11) and the inherent spatial characteristic of the shift vector, N^a, and h^{ab} that $g^{00} = -\frac{1}{N^2}$. We can express the general metric tensor, g_{ab}, as

$$g_{ab} = \begin{bmatrix} -N^2 + N_a N^a & N_a \\ N_b & h_{ab}. \end{bmatrix}$$

Using the formula $(g_{ab})^{-1} = (-1)^{a+b}\frac{C_{ab}}{detg}$, for the components of the inverse metric, where, C_{ab}, is minor of, g_{ab}, we can use the fact that we know $g^{00} = -\frac{1}{N^2}$ to obtain

$$\begin{aligned} (g_{00})^{-1} &= (-1)^{a+b}\frac{C_{00}}{detg}, \\ -\frac{1}{N^2} &= \frac{deth}{detg}, \\ detg &= -N^2 deth, \\ \sqrt{-g} &= N\sqrt{deth} = N\sqrt{h}. \end{aligned} \tag{7.26}$$

This identity, $\sqrt{-g} = N\sqrt{h}$, is the first step towards deriving a Hamiltonian from our Lagrangian (7.25). The next step is to express the Ricci scalar in terms of $(h_{ab}, \dot{h}_{ab})$. This can be accomplished by first doing the following evaluation

$$\begin{aligned} R_{\text{abcd}}\, h^{ac}h^{bd} &= R_{abcd}\left(g^{ac} + n^a n^c\right)\left(g^{bd} + n^b n^d\right), \\ &= R + 2R_{ac}n^a n^c, \\ &= 2G_{ac}n^a n^c, \end{aligned} \tag{7.27}$$

where $R_{abcd}n^a n^b n^c n^d = 0$ as a result of $R_{abcd} = -R_{bacd}$ and $R_{abcd} = -R_{abdc}$. Using the first Gauss Codazzi equation (7.22) and multiplying each side by $h^b_d h_{ab}$ we obtain

$$\begin{aligned} 0 &= G_{ab}n^a n^b, \\ &= \frac{1}{2}\left\{{}^{(3)}R + (K^a_a)^2 - K_{ab}K^{ab}\right\}. \end{aligned} \tag{7.28}$$

From this we can express R as

$$R = {}^{(3)}R + (K_a^a)^2 - K_{ab}K^{ab} - 2R_{ac}n^a n^c. \tag{7.29}$$

To fully express R in terms of the variables we introduced in the last section we need to simplify $2R_{ac}n^a n^c$.

$$R_{abc}{}^d n_d = (\nabla_a \nabla_b - \nabla_b \nabla_a) n_c = R_{abcd}n^d = -R_{abdc}n^d, \tag{7.30}$$

$$\begin{aligned} n^a g^{bc} R_{abdc} n^d &= -n^a g^{bc} (\nabla_a \nabla_b - \nabla_b \nabla_a) n_c, \\ R_{ad} n^a n^d &= -n^a (\nabla_a \nabla_c - \nabla_c \nabla_a) n^c. \end{aligned} \tag{7.31}$$

Now that we have $R_{ac}n^a n^c$ in terms of n^i and ∇_i we can express it as a combination of extrinsic curvatures and divergences,

$$\begin{aligned} n^a (\nabla_c \nabla_a) n^c &= \nabla_c \nabla_a (n^c n^a) - \nabla_c (n^c \nabla_a n^a) - (\nabla_c n^a)(\nabla_a n^c), \\ n^a (\nabla_a \nabla_c) n^c &= \nabla_a \nabla_c (n^c n^a) - \nabla_a (n^c \nabla_c n^a) - (\nabla_a n^a)(\nabla_c n^c), \end{aligned} \tag{7.32}$$

which results in

$$R_{ab}n^a n^b = K^2 - K_{ac}K^{ac} - \nabla_a (n^a \nabla_c n^c) + \nabla_c (n^a \nabla_a n^c). \tag{7.33}$$

As a result of $K_{ab} = h_a^c \nabla_b n_c$ and $n^a K_{ab} = 0$ we can treat K_{ab} as a spatial tensor. Thus we can raise its indices using h^{ab} and use the identity $h_{ab}h^{ac} = \delta_b^c$. We define $K = h^{ab}K_{ab}$. This allows us to represent our derivatives of n^i in terms of contractions of the extrinsic curvature. Thus our action and Lagrangian density are respectively

$$\begin{aligned} S &= \frac{1}{2\kappa} \int N\sqrt{h} \left({}^{(3)}R + K_{ab}K^{ab} - K^2 \right) \ \mathrm{d}^4 x, \\ \mathcal{L}_G &= \frac{1}{2\kappa} N\sqrt{h} \left({}^{(3)}R + K_{ab}K^{ab} - K^2 \right), \end{aligned} \tag{7.34}$$

where we used Stokes's law to transform the divergences into boundary terms and then throw them away. If we require δh_{ab} and its first derivatives to vanish on the boundary we can always throw away these boundary terms which arise out of divergences. For the work contained in this dissertation we can always disregard boundary terms. However for the general case where we only demand that the variation of h_{ab} and not its first derivative vanishes on the boundary, we have to add the Gibbons–Hawking–York boundary term,

$$S_{GHY} = \frac{1}{\kappa} \int \sqrt{h} K \ \ \mathrm{d}^3 x, \tag{7.35}$$

to our action (7.34).

We will now compute $\pi^{ab} = \frac{\delta \mathcal{L}_G}{\delta \dot{h}_{ab}}$ using $K_{ab} = \frac{1}{2N}\left(\dot{h}_{ab} - D_a N_b - D_b N_a\right)$ from the previous section.

$$\begin{aligned}
\mathcal{L}_G &= \frac{1}{2\kappa} N \sqrt{h} \left({}^{(3)}R + h^{xc} h^{yd} K_{xy} K_{cd} - \left(h^{xy} K_{xy}\right)^2 \right), \\
Z_{ab} &= D_a N_b + D_b N_a, \\
\mathcal{L}_G &= \frac{1}{2\kappa} N \sqrt{h} \left({}^{(3)}R + \frac{1}{4N^2} h^{xc} h^{yd} \left(\dot{h}_{xy} - Z_{xy}\right)\left(\dot{h}_{cd} - Z_{cd}\right) - \frac{1}{4N^2}\left(h^{xy}\left(\dot{h}_{xy} - Z_{xy}\right)\right)^2 \right), \\
\frac{\delta \mathcal{L}_G}{\delta \dot{h}_{ab}} &= \frac{1}{2\kappa}\sqrt{h}\left(\frac{1}{2N}\left(\dot{h}^{ab} - Z^{ab}\right) - \frac{1}{2N} h^{xy}\left(\dot{h}_{xy} - Z_{xy}\right) h^{ab}\right), \\
\frac{\delta \mathcal{L}_G}{\delta \dot{h}_{ab}} &= \frac{1}{2\kappa}\sqrt{h}\left(K^{ab} - K h^{ab}\right), \\
\pi^{ab} = \frac{\delta \mathcal{L}_G}{\delta \dot{h}_{ab}} &= \frac{1}{2\kappa}\sqrt{h}\left(K^{ab} - K h^{ab}\right).
\end{aligned} \tag{7.36}$$

Using this expression for our canonical momentum we can express K terms of our

canonical variables π^{ab} and h_{ab}.

$$\begin{aligned} h_{ab}\pi^{ab} &= \frac{1}{2\kappa} h_{ab}\sqrt{h}\left(K^{ab} - Kh^{ab}\right), \\ \pi &= \frac{1}{2\kappa}\sqrt{h}\left(K - 3K\right), \\ \frac{-\kappa\pi}{\sqrt{h}} &= K. \end{aligned} \tag{7.37}$$

From this we can express the extrinsic curvature K_{ab} and $\dot{h}_{ab}$ entirely in terms of canonical variables

$$\begin{aligned} \pi^{ab} &= \frac{\delta\mathcal{L}_G}{\delta\dot{h}_{ab}} = \frac{1}{2\kappa}\sqrt{h}\left(K^{ab} + \frac{\kappa\pi}{\sqrt{h}}h^{ab}\right), \\ K^{ab} &= \frac{2\kappa\pi^{ab}}{\sqrt{h}} - \frac{\kappa\pi}{\sqrt{h}}h^{ab}, \\ \dot{h}_{ab} &= 2N\left(\frac{2\kappa\pi^{ab}}{\sqrt{h}} - \frac{\kappa\pi}{\sqrt{h}}h^{ab}\right) + D_aN_b + D_bN_a. \end{aligned} \tag{7.38}$$

Now we have all of the tools required to compute the ADM Hamiltonian

$$\begin{aligned} H_{ADM} &= \pi^{ab}\dot{h}_{ab} - \frac{1}{2\kappa}N\sqrt{h}\left({}^{(3)}R + K_{ab}K^{ab} - K^2\right), \\ &= \pi^{ab}\dot{h}_{ab} - \frac{1}{2\kappa}N\sqrt{h}\left({}^{(3)}R + \left(\frac{2\kappa\pi_{ab}}{\sqrt{h}} - \frac{\kappa\pi}{\sqrt{h}}h_{ab}\right)\left(\frac{2\kappa\pi^{ab}}{\sqrt{h}} - \frac{\kappa\pi}{\sqrt{h}}h^{ab}\right) - \frac{\kappa^2\pi^2}{h}\right), \\ &= \pi^{ab}\left(2N\left(\frac{2\kappa\pi^{ab}}{\sqrt{h}} - \kappa\frac{\pi}{\sqrt{h}}h^{ab}\right) + D_aN_b + D_bN_a\right) - \frac{1}{2\kappa}N\sqrt{h}\left({}^{(3)}R + 4\kappa^2\frac{\pi_{ab}\pi^{ab}}{h} - 2\kappa^2\frac{\pi^2}{h}\right), \\ H_{ADM} &= 2\kappa N\frac{\pi^{ab}\pi_{ab}}{\sqrt{h}} - \kappa N\frac{\pi^2}{\sqrt{h}} - \frac{1}{2\kappa}N\sqrt{h}{}^{(3)}R + 2\pi^{ab}D_aN_b, \\ &= h^{\frac{1}{2}}\left(N\left[2\kappa h^{-1}\pi^{ab}\pi_{ab} - \kappa h^{-1}\pi^2 - {}^{(3)}\frac{1}{2\kappa}R\right] - 2N_b\left[D_a\left(h^{-\frac{1}{2}}\pi^{ab}\right)\right] + 2D_a\left(h^{-\frac{1}{2}}N_b\pi^{ab}\right)\right). \end{aligned} \tag{7.39}$$

In the last line we decomposed the $2\pi^{ab}D_aN_b$ term so we can isolate a total divergence which we can eliminate. If we vary H_{ADM} with respect to the lapse, N, and the shift, N_a, we respectively obtain the following constraints

$$-\frac{1}{2\kappa}{}^{(3)}R + 2\kappa h^{-1}\pi^{ab}\pi_{ab} - \kappa h^{-1}\pi^2 = 0, \tag{7.40}$$

$$D_a\left(h^{-1/2}\pi^{ab}\right) = 0, \tag{7.41}$$

as a result of the both $\dot{N}$ and $\dot{N}_a$ being absent from (7.39).

Equation (7.40) is known as the Hamiltonian constraint while (7.41) is known as the diffeomorphism constraint. (7.41) is called the diffeomorphism constraint because it describes the fact that two metrics $\Phi * h_{ab} \to q_{ab}$ which can be transformed into one another via a diffeomorphism, Φ, describe the same physics. This means that our configuration space as it is currently formulated possesses a redundancy because not every unique spatial metric corresponds to a unique physical situation. However this redundancy can be remedied by defining the configuration space to only consist of equivalence classes between spatial metrics that can be transformed into one another via a diffeomorphism. We call this redefinition of the configuration space of general relativity superspace [235]. This redefinition has the following mathematical consequences. Let's assume the vector field, v_b, is an infinitesimal generator of diffeomorphisms on h_{ab}. If both h_{ab} and $\Phi * h_{ab}$ describe the exact same physics where Φ is generated by v_b, then it follows that

$$\int \pi^{ab}\left(\delta h_{ab} + \frac{1}{2}\left(D_a v_b + D_b v_a\right)\right) = \pi^{ab}\delta h_{ab}. \tag{7.42}$$

This is true when

$$D_a\left(h^{-1/2}\pi^{ab}\right) = 0. \tag{7.43}$$

Thus defining the configuration space of general relativity as the equivalence class of spatial metrics, h_{ab}, which can be transformed into each other via a diffeomorphism always ensures that the momenta, π^{ab}, always satisfies the diffeomorphism constraint (7.41).

This way of defining the phase space ensures (7.41) is always satisfied. The Hamiltonian constraint (7.40) shares a resemblance to the reparameterized one particle Hamiltonian we worked out earlier. This is a result of 'time' being treated on an

equal footing to space in general relativity just as it was when we previously reparameterized that one particle system. Physically this constraint is a result of the gauge freedom present in how one chooses to foliate space-time using hypersurfaces Σ_t. Unlike (7.7) our constraint is not linear in the conjugate momentum of the 'time' variable/coordinate. For (7.7) we could solve (7.5) to obtain the true time evolution of the system and recover a non-vanishing Hamiltonian. Doing the analogous calculation is not trivial for (7.40). This means that we will be quantizing a Hamiltonian constraint as opposed to a regular Hamiltonian. Our constraint will annihilate any physically realizable quantum state of gravity/geometry.

To facilitate the quantization of (7.40) we shall express it in the following form

$$\begin{aligned} &2\kappa h^{-1} G_{abcd}\pi^{ab}\pi^{cd} - \frac{1}{2\kappa}{}^{(3)}R = 0, \\ &G_{abcd} = \frac{1}{2}\left(h_{ac}h_{bd} + h_{ad}h_{bc} - h_{ab}h_{cd}\right), \end{aligned} \tag{7.44}$$

where we introduced the DeWitt supermetric G_{abcd}. One can use Dirac's prescription for quantization and promote π^{ab} and h_{ab} to operators as we have done below

$$\begin{aligned} &\pi^{ab} \to \hat{\pi}^{ab} = -i\hbar\frac{\delta}{\delta h_{ab}}, \\ &h_{ab} \to \hat{h}_{ab}. \end{aligned} \tag{7.45}$$

Before we can quantize (7.44) though we have to talk about the ambiguity inherent in ordering its operators. To illustrate this let's introduce a much simpler Hamiltonian $H = ap_a$ where a is the sole degree of freedom and p_a is its conjugate momentum. Classically these three Hamiltonians, $H = ap_a$, $H = p_a a$, and $H = p_a^{\frac{1}{2}} a p_a^{\frac{1}{2}}$ represent the same system. However if we quantize these Hamiltonians and require that our wave function satisfies $\hat{H}\psi(a) = 0$ we immediately notice that these three Hamiltonians don't yield equivalent quantum systems. As a matter of fact one of the operator orderings, $H = p_a^{\frac{1}{2}} a p_a^{\frac{1}{2}}$, doesn't even yield a trivial Hamiltonian due its momentum being raised to a fractional power. The same issue present for this initially innocuous

Hamiltonian is present for our exceedingly more complicated ADM Hamiltonian.

There is no universally accepted operator ordering for the Wheeler DeWitt (WDW) equation and thus we will simply choose the simplest one for illustration purposes,

$$\left(2\hbar^2\kappa h^{-1}G_{abcd}\frac{\delta}{\delta h_{ab}}\frac{\delta}{\delta h_{cd}}+\frac{1}{2\kappa}{}^{(3)}R\right)\Psi\left(h_{ab}\right)=0. \tag{7.46}$$

The formal WDW equation, $\hat{\mathcal{H}}_{constraint}\left(h_{ab},\frac{\hbar}{i}\frac{\delta}{\delta h_{ab}}\right)$, understood in its abstract sense in which a factor ordering has not been prescribed has inspired a lot of thought into the nature of quantum gravity. First of all an equation whose argument is $\Psi(h_{ab})$ can be interpreted as yielding a probability density which in theory may permit us to calculate the probability that a certain space-time configuration is realizable given a set of boundary conditions. This suggests that we can view quantum gravity in a probabilistic manner somewhat akin to ordinary quantum mechanics. However the applicability of this analogy is limited because in quantum gravity there are no external observers unlike in ordinary quantum mechanics. In addition it has motivated the introduction of path integrals [110, 114, 115] to the study of quantum gravity and all of the interpretational descriptions of the wave function of the universe, $\Psi(h_{ab})$, that comes from them.

Despite some progress in understanding the WDW equation written in these ADM variables no known formal solutions of it have been proven to exist. One avenue which can shed light on the WDW equation despite not knowing what operator ordering it should be expressed in is the Euclidean-signature semi-classical method. As we will show in the upcoming next, regardless of which operator ordering one chooses, one can recover in the WDW equation's semiclassical limit a Euclidean-signature functional Hamilton-Jacobi equation. A proof that formal solutions exist for this Euclidean-signature functional Hamilton-Jacobi equation may be arrived at using known mathematical methods in a manner which isn't possible with its Lorentzian

signature counterpart for reasons we will discuss in detail soon.

7.4 Quantum Cosmology

As we previously mentioned, there is no known way of solving (7.46) in closed form. In theory though, if one could solve the functional WDW equation expressed in an operator ordering where the commutator between the Hamiltonian constraint and the diffeomorphism constraint closes then one could potentially find a wave function which describes the evolution of a universe that is in concord with the isotropic and homogeneous FLRW model which is currently our best model for the history of the universe after the Planck epoch. The complete freezing out of inhomogeneous modes though is not permissible due to the uncertainty principle that naturally originates from (7.45).

The difficulty of solving the WDW equation can be seen as a result of it naturally including inhomogeneous modes. This is so because inhomogeneous fields have a non-vanishing number of degrees of freedom present at each point in space-time. Therefore any inhomogeneous field theory defined on a continuous manifold is going to have infinitely many degrees of freedom and thus an infinite dimensional phase space. Because our theory at the classical level admits inhomogeneous space-times/modes its Hamiltonian formalism is complicated which in turns results in an exceedingly complicated WDW equation after quantization.

From this understanding one may argue that a way to obtain a simpler equation of quantum gravity would be to freeze out inhomogeneous space-times at the ***classical*** level and then quantize the resulting theory. Doing so is called symmetry reduction. At the classical level this is usually applied to the EFE when one is trying to find an isotropic and homogeneous solution to them. For our purposes we are going to do this at the Lagrangian level and then obtain a Hamiltonian from our reduced

Lagrangian. Doing so will give us a finite dimensional Hamiltonian and thus will result in a partial differential equation that may be solvable. The solutions of this equation though would not possess all of the quantum information that analogous solutions of (7.46) would possess. Nonetheless, its formulation would serve as a useful toy model of quantum gravity that can help us understand certain qualitative features of it. Furthermore these toy models of quantum gravity can allow us to test mathematical methods which have applications beyond quantum cosmology such as the Euclidean-signature semi-classical method.

To exclude at the classical level inhomogeneous space-times we first have to define what it means for a space-time to be homogeneous. To do this we will borrow heavily from [48, 233]. A space-time, $(\mathbb{M}, g_{ab})$, is homogeneous if there exists a set of isometries for each foliating hypersurface, Σ_t, of the space-time such that these isometries map any point on the hypersurface, $p \in \Sigma_t$, to any other point on the hypersurface, $q \in \Sigma_t$. This set of isometries forms a Lie group, $\mathbb{G}$, where the elements of the Lie group, $s \in \mathbb{G}$, are space-time isometries $s * g_{ab} = g_{ab}$. This Lie group, $\mathbb{G}$, is an "m" dimensional continuous manifold which can be mapped onto any hypersurface, Σ_t, which foliates the homogeneous space-time. Furthermore this Lie group is a subgroup belonging to the group of diffeomorphisms that can act on $(\mathbb{M}, g_{ab})$.

Let's pick an arbitrary point on an arbitrary time-slice of space-time $p \in \Sigma_t$. If our space-time is homogeneous then there exists an isometry which maps our point, $p \in \Sigma_t$, to any other point on Σ_t. Therefore for each point on our hypersurface, $q \in \Sigma_t$, there is a corresponding element, $s \in \mathbb{G}$, of our Lie Group which maps p into it, $s(p) = q$, where p and q are any two points on Σ_t. This mapping means that our Lie group acts transitively on any Σ_t. If this mapping is one-to-one then our Lie group acts simply transitively. For our purposes of analyzing only the Bianchi models we can restrict ourselves to simply transitive Lie groups without losing any generality [160]. This ability to map the elements of $\mathbb{G}$ to each Σ_t which foliates

our space-time suggests that the dimensions of $\mathbb{G}$ and the dimensions of Σ_t are the same $dim\,\Sigma_t = dim\,\mathbb{G} = 3$. Thus in addition to our Lie group acting in a simply transitive manner on the hypersurfaces it is also a finite dimensional manifold. In the language of group theory, a group is smooth and continuous if there exists a spectrum of elements which are infinitesimally close to the group's identity element, $s = I + \epsilon_a \xi^a + O(\epsilon^2) \in \mathbb{G}$, and any other arbitrary element in the group can be reached by multiplying these infinitesimal elements/transformations with each other.

In our expansion around the identity element of our Lie group, ξ^a are vector fields which act as generators of the group and ϵ_a are the infinitesimal group parameters. Vector fields in general are the generators of diffeomorphisms, which include our isometries that act on the hypersurfaces that foliate space-time in the manner we described above. A Lie group and its elements are obtained by exponentiating their generators which are vector fields, ξ^a, which themselves have to form a Lie algebra. We will provide a heuristic argument for this statement.

The composition of two infinitesimal group transformations generated by ξ^a obeys the following intuitive property $\Phi^\xi_\epsilon \circ \Phi^\xi_\epsilon = \Phi^\xi_{2\epsilon}$. If we act upon an arbitrary point, x^a, using an infinitesimal transformation around the identity element we obtain $\Phi^\xi_\epsilon(x^a) = x^a + \epsilon\ \xi^a + \epsilon^2 Y^a + O(\epsilon^3)$ where Y^a is an unknown quantity we wish to deduce. First we will evaluate the left hand side of our composition

$$\begin{aligned}
\Phi^\xi_\epsilon(\Phi^\xi_\epsilon(x^a)) &= \Phi^\xi_\epsilon(x^a + \epsilon\ \xi^a + \epsilon^2 Y^a) + O(\epsilon^3), \\
&= x^a + \epsilon\ \xi^a + \epsilon^2 Y^a + \epsilon \xi^a \left(x^b + \epsilon \xi^b\right) + \epsilon^2 Y^a + O(\epsilon^3), \\
&= x^a + 2\epsilon \xi^a + \epsilon^2 \left(2Y^a + \xi^b \partial_b \xi^a\right) + O(\epsilon^3).
\end{aligned} \tag{7.47}$$

Now we will evaluate the right hand side

$$\Phi^\xi_{2\epsilon}(x^a) = x^a + 2\epsilon \xi^a + 4\epsilon^2 Y^a + O(\epsilon^3). \tag{7.48}$$

We can equate (7.47) with (7.48) if we set $Y^a = \frac{1}{2}\xi^b\partial_b\xi^a$. This results in $\Phi^\xi_\epsilon(x^a) = x^a + \epsilon\ \xi^a + \epsilon^2\frac{1}{2}\xi^b\partial_b\xi^a + O(\epsilon^3)$. Carrying out the above expansion and comparison to higher order results in the following representation for the elements which make up our Lie group of isometries

$$\begin{aligned}\Phi^\xi_\epsilon &= \sum_{n=0}^{\infty}\frac{1}{n!}\epsilon^n\left(\xi^b\partial_b\right)^n = e^{\epsilon\boldsymbol{\xi}},\\ \boldsymbol{\xi} &= \xi^b\partial_b.\end{aligned} \tag{7.49}$$

The partial derivatives were introduced by using the fact that in order to recover the notion of a vector space on a curved manifold without referencing its embedding space one may define directional derivatives on each tangent space of the manifold associated with each point on it. These directional derivatives on the tangent spaces of a curved manifold allows one to recover a notion of a vector space.

In order for the elements that are generated by exponentiating vectors to form a Lie group the vectors themselves have to satisfy a certain algebraic relation. This algebra can be ascertained by using the expansion we just employed to evaluate $\Phi^{\xi_1}_{\epsilon 1}\Phi^{\xi_2}_{\epsilon 2}\Phi^{\xi_1}_{-\epsilon 1}\Phi^{\xi_2}_{-\epsilon_2}$ up to second order in the infinitesimal group parameters. Doing so results in $\Phi^{\xi_1}_{\epsilon 1}\Phi^{\xi_2}_{\epsilon 2}\Phi^{\xi_1}_{-\epsilon 1}\Phi^{\xi_2}_{-\epsilon_2} = x^a + \epsilon 1\epsilon 2\left[\xi_1,\xi_2\right]^a + O(\epsilon^n)$, where the commutator is $\left[\xi_1,\xi_2\right]^a = \xi^b_1\partial_b\xi^a_2 - \xi^b_2\partial_b\xi^a_1$. The commutator is anti-symmetric and linear in both of its arguments.

Because the product of two or more elements of a group is itself an element of the group we know that $\Phi^{\xi_1}_{\epsilon 1}\Phi^{\xi_2}_{\epsilon 2}\Phi^{\xi_1}_{-\epsilon 1}\Phi^{\xi_2}_{-\epsilon_2} = \Phi^{\xi_3}_{\epsilon 3}$. Evaluating the left and the right sides of the expression we just wrote down allows one to eventually deduce the following algebraic relationship between these three vectors

$$\left[\xi_a,\xi_b\right] = -\tilde{C}^c_{ab}\xi_c, \tag{7.50}$$

where $\tilde{C}^c_{ab}$ is antisymmetric in a and b, and $\tilde{C}^c_{ab} = -\tilde{C}^c_{ba}$. The antisymmetric quan-

tity, $\tilde{C}^c_{ab}$, are the structure constants of the algebra. As a result of the commutator being anti-symmetric and linear in its arguments the following Jacobi identity can be obtained from evaluating $[\xi_a, [\xi_b, \xi_c]]$ and using (7.50)

$$\tilde{C}^e_{ab}\tilde{C}^d_{ec} + \tilde{C}^e_{bc}\tilde{C}^d_{ea} + \tilde{C}^e_{ca}\tilde{C}^d_{eb} = 0. \tag{7.51}$$

Equations (7.50) and (7.51) completely define the Lie algebra of our vector fields which generate isometries.

Because the elements of our Lie group are isometries they are generated by Killing vector fields. The Killing vector fields associated with a manifold are a set of vectors which generate infinitesimal transformations which preserve all distances on the manifold. For example a set of vectors which point clockwise and are the same length on a circle can generate an infinitesimal flow which preserves the distances between all points on the circle as it rotates clockwise. Therefore our Killing vector fields which satisfy (7.50) and (7.51) also satisfy the Killing equation

$$\mathbb{L}_\xi g_{ab} = \nabla_a \xi_b + \nabla_b \xi_a = 0. \tag{7.52}$$

To move forward with our construction we need to find a basis which is invariant with respect to the group of isometries which define homogeneous space-times. A set of basis vector fields which are invariant under the action of our Killing vector fields can be found by solving the following equation

$$0 = [\xi_I, V_J]^a = \left(\xi^b_I \partial_b V^K_J\right) \xi^a_K - V^K_J \tilde{C}^L_{IK} \xi^a_L. \tag{7.53}$$

This equation can be obtained by considering the action, $\Phi_\epsilon * V^a(x^b) = \frac{\partial \Phi^a_{-\epsilon}}{\partial x^c} V^c \left(\Phi_\epsilon(x^b)\right)$, of an isometry, Φ^ξ_ϵ, on a vector, $V^a(x^b)$, defined on a hypersurface where we notionally suppressed the Killing vector ξ. By writing this equation out and expressing

our unknown invariant basis vectors, V_j^k, in terms of a set of known Killing vectors, $V_j^a = V_j^k \xi_k^a$, which themselves form a basis on the tangent space, one can arrive at (7.53). The integration of this equation globally over the hypersurface is not trivial. However it can be shown locally, in a Euclidean patch of Σ_t that invariant vector fields exist which is sufficient for our purposes.

These invariant vector fields, V_j^a, themselves form a Lie algebra

$$[V_a, V_b] = C_{ab}^c V_c. \tag{7.54}$$

If these invariant vector fields exist and represent an independent non degenerate set of basis vectors, then there must also exist on the cotangent space of our manifold a set of invariant dual basis vector fields, ω_a^g, which satisfy $\omega_a^g V_j^a = \delta_j^g$. Our invariant dual basis fields satisfy the Maurer–Cartan relations

$$\mathrm{d}\boldsymbol{\omega}^c = \frac{1}{2} C_{ab}^c \omega^a \wedge \omega^b, \tag{7.55}$$

where C_{ab}^c are the same structure constants which define the Lie algebra of our invariant vector fields in (7.54). Using this basis of invariant one forms we can construct the following class of homogeneous spatial metrics

$$h_{ab} = \frac{L^2}{6\pi} h_{ij} \omega_a^i \omega_b^j, \tag{7.56}$$

where h_{ij} is a symmetric 3 by 3 matrix composed of coefficients which only depend on time. The L^2 term is a constant with units of length, the exact units such a meters or parsecs are immaterial at the moment. See equation (9.1) for more info on L. The dual basis can be subjected to coordinate transformations for each group of isometries we will consider in such a way that h_{ij} can be diagonalized and expressed

as the following

$$(h_{ij}) = \text{diag}\left(e^{2\alpha(t)+2\beta_+(t)+2\sqrt{3}\beta_-(t)}, e^{2\alpha(t)+2\beta_+(t)-2\sqrt{3}\beta_-(t)}, e^{2\alpha(t)-4\beta_+(t)}\right), \tag{7.57}$$

where $(\alpha, \beta_+, \beta_-)$ are the Misner variables [169, 170]. The two beta variables measure the anisotropy present in space-time while α is related to either its absolute or relative volume.

As a result of (7.57) all we need are a set of three invariant basis one forms which obey (7.55). If we can specify all of the structure constants that would be of interest to us then we can in principle solve for the one forms. Because our Lie group of isometries has three dimensions, it is generated by a set of three Killing vector fields ξ^1, ξ^2, and ξ^3 which obey (7.50) where a, b, and c range from 1 to 3. As a result the invariant vector fields in (7.54) have the exact same cardinality. From this we can infer that $C^c_{[ab]} = C^c_{ab}$ admits up to nine independent constants. By decomposing, C^c_{ab}, into its symmetric and antisymmetric components we can recover the Bianchi classification of all real three dimensional Lie algebras.

First we will express C^c_{ab} as the sum of two 3 by 3 matrices, one symmetric and one antisymmetric, by contracting the structure constants with the antisymmetric Levi-Cevita symbol

$$\frac{1}{2}C^c_{ab}\epsilon^{abd} =: n^{(cd)} + A^{[cd]} = n^{cd} + \epsilon^{cde}v_e, \tag{7.58}$$

where v_e is a vector with three independent components. Using this equation we can express the structure constants as

$$C^c_{ab} = \frac{1}{2}\left(C^c_{ab} - C^c_{ba}\right) = \frac{1}{2}C^c_{de}\epsilon^{def}\epsilon_{fab} = \epsilon_{fab}n^{cf} + \delta^c_b v_a - \delta^c_a v_b. \tag{7.59}$$

We can insert this into the Jacobi identity (7.51) to obtain the surprisingly simple

	Group type	k	n^1	n^2	n^3
Class A	I	0	0	0	0
	II	0	+	0	0
	VII $_0$	0	+	+	0
	VI $_0$	0	+	−	0
	IX	0	+	+	+
	VIII	0	+	+	−
Class B	V	+	0	0	0
	IV	+	0	0	+
	VII $_\eta$	+	0	+	+
	VI $_\eta$	+	0	+	−

Table 7.1 Classifications of Bianchi algebras taken from [48] where n^i are the diagonal elements of n^{ab}.

relation

$$n^{ab}v_b = 0. \tag{7.60}$$

Because $n^{ab}$is a symmetric 3 by 3 matrix (7.58) we can interpret v_b as its kernel and as an eigenvector. As a result we can diagonalize n^{ab} and set $v_b = (k, 0, 0)$. From this reparameterization of C^c_{ab} we are left with only four independent constants. From these four independent constants we can classify 9 types of Lie algebras. The form of these constants can be further reduced to be either, -1, 0, or 1 by rescaling the invariant basis of vector fields in (7.54).

For the case when $v_b = (0, 0, 0)$ there are six distinct diagonal three by three matrices, n^{ab}, which have unique ranks and signatures. These are outlined in the table below and correspond to the class A Bianchi models. When $k \neq 0$ the symmetric matrix n^{ab} at most can be rank two and from this we have four class B Bianchi models. We will only consider in this dissertation Bianchi A models. Reasons for this will be given at the end of this section.

Using this classification scheme we can express (7.54) for general Bianchi A and B models as

$$
\begin{aligned}
[V_1, V_2] &= -kV_2 + n_3V_3 \\
[V_2, V_3] &= n_1V_1 \\
[V_3, V_1] &= kV_3 + n_2V_2.
\end{aligned}
\tag{7.61}
$$

In this dissertation we will only consider the Bianchi A models. This is so because only the Bianchi A models satisfy the principle of symmetric criticality due to the nature of the structure constants which define the Lie algebras that generate their space-times isometries. Symmetric criticality means that reducing the degrees of freedom at the Lagrangian level is equivalent to reducing the degrees of freedom at the level of the equations of motion (Einstein field equations). This enables a straightforward quantization procedure. Despite not satisfying the principle of symmetric criticality, Bianchi B models can be quantized [207] using a more complicated procedure. Thus the Euclidean-signature semi-classical method which we will describe in the next section can possibly be applied to the Bianchi B models as well. Doing so would constitute an interesting future project which can facilitate expanding the scope of the Euclidean-signature semi-classical method.

If we include a cosmological constant, an aligned electromagnetic field, and a free homogeneous scalar field into (7.34) we will obtain the following classical action which will ultimately result in the WDW equation we will be analyzing in this dissertation

$$
S = \frac{1}{2\kappa}\int N\sqrt{h}\left({}^{(3)}R + K_{ab}K^{ab} - K^2 - 2\Lambda - \frac{\kappa}{8\pi}F_{ab}F^{ab} - \kappa\partial_a\phi\partial^a\phi\right) \ \mathrm{d}^4x,
\tag{7.62}
$$

where F_{ab} is the classical electromagnetic tensor and ϕ is a free homogeneous scalar field. If we insert (7.56) into (7.62) while temporarily ignoring the electromagnetic contribution and setting $L = \sqrt{6\pi}$, the following Lagrangian density is obtained

$$\mathcal{L}_{GS} = \frac{6}{2\kappa}\frac{1}{N}e^{3\alpha}\left(-\dot{\alpha}^2 + \dot{\beta}_+^2 + \dot{\beta}_-^2\right) + e^{3\alpha}\frac{1}{2N}\dot{\phi}^2 - Ne^{3\alpha}\frac{\Lambda}{\kappa} - \frac{1}{2\kappa}Ne^{3\alpha}V(\alpha,\beta_+,\beta_-), \tag{7.63}$$

where the upper-dot, $\dot{}$, signifies a time derivative and $V(\alpha,\beta_+,\beta_-)$ is ${}^{(3)}R$, and its form depends on the structure constants associated with the Bianchi A models we are interested in. Also GS stands for "Gravity-Scalar". In addition we eliminated a total derivative by insisting that variations at the boundary vanish and the lapse, N, is a function of time only and never vanishes.

If we apply the standard Legendre transformation to (7.63) we obtain

$$\begin{aligned} H_{GS} &= p_\alpha\dot{\alpha} + p_{\beta_+}\dot{\beta_+} + p_{\beta_-}\dot{\beta_-} + p_\phi\dot{\phi} - \mathcal{L}_{Gravity}, \\ H_{GS} &= \frac{e^{-3\alpha}\mathrm{N}\left(6e^{6\alpha}(V(\alpha,\beta_+,\beta_-)+2\Lambda) + \kappa \quad \left(\kappa\left(-p_\alpha^2 + p_{\beta_+}^2 + p_{\beta_-}^2\right) + 6p_\phi^2\right)\right)}{12\kappa}. \end{aligned} \tag{7.64}$$

Varying (7.64) with respect to the lapse and reinstating L results in the vanishing Hamiltonian constraint for the gravity-scalar components of the theory

$$H_{GS-Constraint} = 36\pi^3\kappa \quad \left(\kappa\left(-p_\alpha^2 + p_{\beta_+}^2 + p_{\beta_-}^2\right) + 6p_\phi^2\right) + L^6(V(\alpha,\beta_+,\beta_-) + 12\Lambda e^{6\alpha}) = 0, \tag{7.65}$$

where we absorbed the constant into the potential term, $V(\alpha,\beta_+,\beta_-)$, and the α term. For any Bianchi A model this Hamiltonian constraint can be quantized using Dirac's prescription to obtain the WDW equation. The electromagnetic field portion in (7.62) contributes to the potential in (7.65) and can be computed separately from the gravitational sector by solving Maxwell's equations in a Bianchi A space-time.

For the following calculations we will be working in units in which $\kappa = \frac{1}{2}$. We will compare two methods for obtaining the electromagnetic contribution to (7.65)

and ultimately the WDW equations we will be considering. The first method will be based on directly quantizing the class of classical Hamiltonians for Bianchi A models that was developed in [234]. This will lead to a semi-classical treatment of our electromagnetic degree of freedom and will give us the exact WDW equations we will be considering for the rest of this dissertation. However we will also do a full quantum treatment of the electromagnetic degree of freedom and compare the two approaches. We will assume that all of our electric and magnetic fields are parallel to each other as was done in [124, 234]. We will only consider the case when a single aligned electromagnetic field is present. It would be of practical interest though to study the quantum cosmology of Bianchi I models when a pure magnetic field is present due to recent evidence [184, 223] for the existence of a femto Gauss strength intergalactic magnetic field that has been uncovered by observing gamma rays. semi-classical methods such as the Euclidean-signature semi-classical method can certainly aid in that proposed program.

With this in mind our first task is to obtain solutions for Maxwell's equations for the following class of diagonal Bianchi A space-times

$$ds^2 = -N^2 dt^2 + \frac{L^2}{6\pi} h_{ab} \omega^a \omega^b, \tag{7.66}$$

where N is the lapse, h_{ab} is (7.57), L is a quantity which has units of length, of which the exact units are immaterial for our purposes, and ω^a are a basis of one forms which are invariant under the action of the Lie group generated by the Bianchi A Lie algebra in question. For now we will set $L = \sqrt{6\pi}\ell$ where ℓ is a quantity which has a magnitude of unity and has units of 'length'. Starting from

$$\boldsymbol{A} = A_0 dt + A_1 \omega^1 + A_2 \omega^3 + A_3 \omega^3 \tag{7.67}$$

and using the fact that $d\omega^c = \frac{1}{2} C^c_{ab} \omega^a \wedge \omega^b$ to aide us in computing $\boldsymbol{F} = d\boldsymbol{A} =$

$\frac{1}{2}F_{ab}\omega^a \wedge \omega^b$ results in the following expression for F_{ab}

$$F_{ab} = A_{b,a} - A_{a,b} + A_c C^c_{ab}. \tag{7.68}$$

In (7.68) differentiation is done through a vector dual acting on our one forms ω^a which we denote as X_a. Thus $A_{b,a} = X_a A_b$. The action for the electromagnetic contribution (7.69) is the following

$$\mathcal{S}_{matter} = \int N\sqrt{h}\left(-\frac{1}{16\pi}F_{ab}F^{ab}\right)dx^4. \tag{7.69}$$

Writing the action (7.69) in terms of its vector potential A and our structure constants results in the Lagrangian density which was derived in [234]

$$\begin{aligned}
\mathscr{L} &= \Pi^s A_{s,0} - NH, \\
\mathscr{L} &= \Pi^s A_{0,s} - N\frac{2\pi}{\sqrt{h}}\Pi^s\Pi^p h_{sp} \\
&- \frac{N\sqrt{h}}{16\pi}h^{ik}h^{sl}\left(2A_{[i,s]} + A_m C^m_{is}\right)\left(2A_{[k,l]} + A_m C^m_{kl}\right),
\end{aligned} \tag{7.70}$$

where

$$\Pi^s = \frac{\partial\mathscr{L}}{\partial\left(X_0 A_s\right)} = \frac{h^{sj}\sqrt{h}}{4N\pi}\left(-A_{0,j} + A_{j,0} + A_\alpha C^\alpha_{0j}\right). \tag{7.71}$$

We allow the shift N^k to vanish because we are only considering diagonal Bianchi A models. If we invoke the homogeneity of (7.66) then we can say that $A_{i,j} = 0$, and $A_{0,j} = 0$, where both i and j are restricted to run from 1 to 3, which results in (7.70) simplifying to

$$\mathscr{L} = \Pi^s A_{s,0} - N\left[\frac{2\pi}{\sqrt{h}}\Pi^s\Pi^p h_{ps} + \frac{\sqrt{h}}{16\pi}h^{ik}h^{sl}C^m_{kl}C^n_{is}A_m A_n\right]. \tag{7.72}$$

To ensure we are only considering an aligned electromagnetic field we will shall set A_2, A_3, Π^2, and Π^3 to zero and only consider the electromagnetic field produced

by A_1 and Π^1; doing so results in the following Lagrangian density

$$\mathscr{L} = \Pi^1 A_{1,0} - N\left[\frac{2\pi}{\sqrt{h}}\Pi^1\Pi^1 h_{11} + \frac{\sqrt{h}}{16\pi}h^{ik}h^{sl}C^1_{kl}C^1_{is}A_1A_1\right]. \tag{7.73}$$

Due to the form that the structure constants of the Bianchi A models possess $C^a_{bc} = 0$ where a does not equal either b or c and our spatial metrics being diagonal, it can be easily shown that $h^{ik}h^{sl}C^1_{kl}C^1_{is} = \frac{2h_{11}}{h}$, where h is the determinant of (7.57). This allows us to obtain the following set of Maxwell's equations when A_1 and Π^1 are varied in (7.73)

$$\dot{A}_1 - 4N\pi\frac{1}{\sqrt{h}}\Pi^1 h_{11} = 0 \tag{7.74}$$

and

$$\dot{\Pi}^1 + N\frac{1}{4\pi}\frac{1}{\sqrt{h}}h_{11}A_1 = 0. \tag{7.75}$$

For the last equation we applied an integration by parts to the term $\Pi^1 A_{1,0}$ and dropped the total derivative which vanishes at the spatial boundary. The solutions for (7.74) and (7.75) are

$$A_1 = \sqrt{2}B_0 cos(\theta(t)) \tag{7.76}$$

$$\Pi^1 = \frac{1}{2\sqrt{2}\pi}B_0 sin(\theta(t)) \tag{7.77}$$

where $\theta(t)$ is an integral which is immaterial for our purposes and B_0 is an integration constant. Inserting (7.76) and (7.77) back into (7.73) results in

$$\begin{aligned}\mathscr{L} =& \Pi^1 A_{1,0} - N\frac{B_0^2}{4\pi\sqrt{h}}h_{11}\left(sin(\theta(t))^2 + cos(\theta(t))^2\right) \\ =& \Pi^1 A_{1,0} - N\frac{B_0^2}{4\pi}e^{-\alpha(t)+2\beta_+(t)+2\sqrt{3}\beta_-(t)},\end{aligned} \tag{7.78}$$

From (7.70) we can easily identify the electromagnetic Hamiltonian as

$$H_{em} = \frac{B_0^2}{4\pi}e^{-\alpha(t)+2\beta_+(t)+2\sqrt{3}\beta_-(t)}, \tag{7.79}$$

which can be added to resultant Hamiltonian constraint one obtains if they apply standard canonical techniques to both the purely gravitational and free homogeneous scalar field coupled to gravity sectors of the Lagrangian we had earlier in (7.65)

$$e^{-3\alpha(t)}\left(-p_{\alpha}^{2}+p_{\beta_{+}}^{2}+p_{\beta_{-}}^{2}+12p_{\phi}^{2}\right)+e^{3\alpha}V(\alpha,\beta_{+},\beta_{-})+\frac{B_{0}^{2}}{4\pi}e^{-\alpha(t)+2\beta_{+}(t)+2\sqrt{3}\beta_{-}(t)}=0. \tag{7.80}$$

Quantizing (7.80) using the semi general factor ordering proposed by Hartle-Hawking [110], multiplying each side by $e^{3\alpha(t)}$, and rescaling B_0 results in the following WDW equation with the electromagnetic potential

$$\begin{aligned}&\frac{\partial^{2}\psi}{\partial\alpha^{2}}-B\frac{\partial\psi}{\partial\alpha}-\frac{\partial^{2}\psi}{\partial\beta_{+}^{2}}-\frac{\partial^{2}\psi}{\partial\beta_{-}^{2}}-12\frac{\partial^{2}\psi}{\partial\phi^{2}}\\&+e^{6\alpha}V(\alpha,\beta_{+},\beta_{-})\psi+48\Lambda e^{6\alpha}\psi+2b^{2}e^{2\alpha+2\beta_{+}+2\sqrt{3}\beta_{-}}\psi=0,\end{aligned} \tag{7.81}$$

where B can be any real number.

As the reader can verify for the cases when $A_1 = 0$, $A_3 = 0$, $\Pi^1 = 0$, and $\Pi^3 = 0$ the resulting electromagnetic term is

$$U_{2\ em}=2b^{2}e^{2\alpha+2\beta_{+}-2\sqrt{3}\beta_{-}}, \tag{7.82}$$

and the case when $A_1 = 0$, $A_2 = 0$, $\Pi^1 = 0$, and $\Pi^2 = 0$ results in the term reported in [234]

$$U_{3\ em}=2b^{2}e^{2\alpha-4\beta_{+}}. \tag{7.83}$$

These three aligned electromagnetic fields which exist when their respective structure constants are non-zero for the models under consideration yield the following WDW equations for the Bianchi A models

$$\frac{\partial^2\psi}{\partial\alpha^2} - B\frac{\partial\psi}{\partial\alpha} - \frac{\partial^2\psi}{\partial\beta_+^2} - \frac{\partial^2\psi}{\partial\beta_-^2} - 12\frac{\partial^2\psi}{\partial\phi^2} + V(\alpha,\beta_+,\beta_-)\psi + 48\Lambda e^{6\alpha}\psi + 2b^2e^{2\alpha-4\beta_+} \vee 2b^2e^{2\left(\alpha\pm\sqrt{3}\beta_-+\beta_+\right)}\psi = 0, \tag{7.84}$$

where we list the potentials and possible electromagnetic field configurations of all of the Bianchi A models below. The symbol $\vee$ is the logical 'or' operator.

Neglecting the free homogeneous scalar field for now, if we start with (7.73) and directly quantize our component of the total Hamiltonian constraint which is proportional to the lapse N we obtain a similar, but slightly different contribution to the potential. Simplifying the term in brackets of (7.73) via (7.57) results in the following contribution to the Hamiltonian constraint derived from (7.62)

$$H_{em} = N\left[\frac{e^{-\alpha+2\beta_++2\sqrt{3}\beta_-}\left(16\pi^2\Pi^1\Pi^1 + A_1^2\right)}{8\pi}\right]. \tag{7.85}$$

The term $(16\pi^2\Pi^1\Pi^1 + A_1^2)$ commutes with our total Hamiltonian constraint $H_{Gravity-Constraint}+$ H_{em}. Thus we can solve the following WDW equation constructed by directly quantizing (7.85) and adding it to the rest of our constraint (7.66)

$$\frac{\partial^2\Psi}{\partial\alpha^2} - \frac{\partial^2\Psi}{\partial\beta_+^2} - \frac{\partial^2\Psi}{\partial\beta_-^2} - 12\frac{\partial^2\Psi}{\partial\phi^2} - e^{2\alpha+2\beta_++2\sqrt{3}\beta_-}\left(-2\pi\frac{\partial^2\Psi}{\partial A_1^2} + \frac{1}{8\pi}A_1^2\Psi\right) + V(\alpha,\beta_+,\beta_-)\Psi + 48\Lambda e^{6\alpha}\Psi = 0, \tag{7.86}$$

by first solving this eigenvalue problem

$$-2\pi\frac{\partial^2\Psi}{\partial A_1^2} + \frac{1}{8\pi}A_1^2\Psi = b_n\Psi, \tag{7.87}$$

where Ψ is a function of α, β_+, β_-, and A_1^2. This is simply the Schrödinger equation

Bianchi Type	$V(\alpha, \beta_+, \beta_-)$
I	0
II	$\frac{1}{3}e^{4\left(\alpha+\beta_+ +\sqrt{3}\beta_-\right)}$
VI $_{h=-1}$	$\frac{4}{3}e^{4\alpha+4\beta_+}$
VII $_{h=0}$	$\frac{4}{3}e^{4(\alpha+\beta_+)}\sinh^2\left(2\sqrt{3}\beta_-\right)$
VIII	$\frac{1}{3}e^{4\alpha-8\beta_+}\left(4e^{12\beta_+}\sinh^2\left(2\sqrt{3}\beta_-\right)+4e^{6\beta_+}\cosh\left(2\sqrt{3}\beta_-\right)+1\right)$
IX	$\frac{1}{3}e^{4\alpha-8\beta_+}\left(4e^{12\beta_+}\sinh^2\left(2\sqrt{3}\beta_-\right)-4e^{6\beta_+}\cosh\left(2\sqrt{3}\beta_-\right)+1\right)$

Table 7.2 The potentials for of the Bianchi A models in terms of Misner variables.

for a harmonic oscillator whose eigen-solutions are well known

$$\begin{aligned}\Psi &= \psi\left(\alpha, \beta_+, \beta_-\right) e^{-\frac{A_1^2}{8\pi}} H_{b_n-\frac{1}{2}}\left(\frac{A_1}{2\sqrt{\pi}}\right) \\ b_n &= \frac{1}{2}\left(1+2n\right).\end{aligned} \tag{7.88}$$

Inserting our Ψ from (7.88) into (7.86) yields

$$\begin{aligned}&\frac{\partial^2\psi}{\partial\alpha^2} - B\frac{\partial\psi}{\partial\alpha} - \frac{\partial^2\psi}{\partial\beta_+^2} - \frac{\partial^2\psi}{\partial\beta_-^2} - 12\frac{\partial^2\psi}{\partial\phi^2} \\ &+ V(\alpha, \beta_+, \beta_-)\psi + 48\Lambda e^{6\alpha}\psi + 2b_n e^{2\alpha-4\beta_+} \vee 2b_n e^{2\left(\alpha\pm\sqrt{3}\beta_- +\beta_+\right)}\psi = 0,\end{aligned} \tag{7.89}$$

where the ordering parameter B has been reinstated. This WDW equation is similar to what we had before except for the fact that the strength b_n of the electromagnetic field is now quantized thanks to (7.88). This feature wasn't present before because we first solved the A_i equations (7.74) in terms of the Misner variables and thus eliminated the electromagnetic field degree of freedom as opposed to quantizing it first. For now though working with (7.84) is sufficient for what will follow.

The WDW equation (7.84) is analogous to the time dependent Schrödinger equations for Bianchi A quantum cosmology. Viewing the WDW equation as $\hat{\mathcal{H}}_\perp\psi = 0$ and trying to relate it to the conventional Schrödinger equation results in the problem of time manifesting itself as

$$i\hbar\frac{\partial\psi}{\partial t} = N\hat{\mathcal{H}}_\perp\psi = 0, \tag{7.90}$$

where $\frac{\partial \psi}{\partial t} = 0$. Due to the absence of the time derivative term of the Schrödinger equation in the WDW equation, the construction of a unitary time evolution operator is not trivial, thus leading to the potential breakdown of a simple probabilistic interpretation of the wave function of the universe.

A Klein-Gordon current

$$\mathcal{J} = \frac{i}{2}\left(\psi^* \nabla \psi - \psi \nabla \psi^*\right) \tag{7.91}$$

can be defined [179, 230] which could be used to construct a probability density. It however, possesses unattractive features such as it vanishing when the wave function used to construct the current is purely real or imaginary and not always being positive definite.

To deal with the problem of time we will choose one of our variables $(\alpha, \beta_+, \beta_-, \phi)$ to act as an evolution parameter [84]. The Misner variable, α, is a good candidate to be our "clock" for various reasons. The scale factor, α, would be an intuitive clock to use because it corresponds to the size of our models and thus is fundamentally intrinsic to them. In addition if we look at the kinetic portion of (7.84) we can rewrite it as

$$\begin{aligned} & e^{-3\alpha} p^i G_{ij} p^j \\ & \vec{p} = \left(p_\alpha, p_{\beta_+}, p_{\beta_-}, p_\phi\right) \\ & G_{ij} = \text{diag}\left(-1, 1, 1, 12\right), \end{aligned} \tag{7.92}$$

where the signature associated with p_α in our symmetry reduced DeWitt supermetric has the same sign as the time component of our metric (7.66). A downside to using α as an internal clock though is that classically Bianchi universes can experience a transition from an expansionary epoch to contractionary one which causes α to "tick" backwards. An alternative is to use p_ϕ as our internal clock as has been done in loop quantum cosmology [16–18]. If p_ϕ is a conserved quantity then classically ϕ always

increases monotonically and thus in a quantum cosmological context emerges as a candidate for time. In this dissertation we will use both α and ϕ, as our internal clocks depending on what points the author wishes to elucidate.

Chapter 8

The Euclidean-Signature Semi-Classical Method

8.1 A Family Of Modified Semi-Classical Methods

As we previously alluded to, the Euclidean-signature semi-classical method is far more than a standalone mathematical technique one can apply to the symmetry-reduced WDW equation in hopes of solving it. Instead it is a methodology towards carrying out semi-classical calculations for a plethora of different theories. These theories range from one dimensional problems in ordinary quantum mechanics, to bosonic relativistic field theories and to formal quantum gravity. Depending on the complexity of the problem, the exact steps one needs to take after applying the Euclidean-signature semi-classical method to fully solve it is still a work in progress. Nonetheless this method has already generated some interesting results for quantum anharmonic oscillators and a class of relativistic scalar field theories [164, 176]. As we will demonstrate, the nature by which these results have been obtained provides us with good reasons to further develop this method and apply it towards more complicated finite and infinite dimensional problems.

In order for the applications of this method to quantum cosmology to be understood in their proper context we will, in moderate detail, illuminate the applications that the Euclidean-signature semi-classical method has for ordinary quantum mechanics and bosonic relativistic field theory. We will discuss how a variant of this semi-classical method can be successfully applied to a class of nonlinear oscillators to obtain a set of asymptotic expansions which converge faster to the known exact solution than the corresponding expansions found using conventional (Rayleigh/Schrödinger) perturbation theory. We will also show how this method applies to bosonic relativistic field theories and to the formal WDW equation.

The quantum anharmonic oscillators are an important set of systems in their own right. On a basic level, the bosonic quantum field theories we will introduce later can be understood as a continuum of quantum anharmonic oscillators present at each point in Minkowski space-time. As a result of the importance of this general class of models it can be used to motivate and showcase the utility of our class of modifications to standard semi-classical methods. We will briefly summarize the work conducted in [176] to highlight the methodological nature of the techniques that the author employed to study a variety of WDW equations with.

The Hamiltonian for the anharmonic oscillators is

$$\hat{H} = \frac{-\hbar^2}{2m} \sum_{i=1}^{n} \frac{\partial^2}{\partial x_i^2} + \frac{1}{2} m \sum_{i=1}^{n} \omega_i^2 \left(x_i\right)^2 + A(\mathbf{x}), \tag{8.1}$$

where x_i are independent Cartesian coordinates, ω_i are the oscillation frequencies along the x_i Cartesian coordinate axis, and $A(\mathbf{x})$ is a function whose zeroth, first and second order Taylor series expansion around $\mathbf{x} = 0$ vanishes

$$A(0, \ldots, 0) = \frac{\partial A(0, \ldots, 0)}{\partial x^i} = \frac{\partial^2 A(0, \ldots, 0)}{\partial x^i \partial x^j} = 0. \tag{8.2}$$

We will require that the potential, $\frac{1}{2} m \sum_{i=1}^{n} \omega_i^2 \left(x_i\right)^2 + A(\mathbf{x})$, satisfies a convexity

condition and that it only possesses a unique global minimum at $\mathbf{x} = 0$. In addition a coercivity condition is imposed on $A(\mathbf{x})$ to bound it from below and the oscillation frequencies, ω_i, satisfy an optional [176] non resonance condition. We will denote the potential in (8.1) as

$$V = \frac{1}{2} m \sum_{i=1}^{n} \omega_i^2 \left(x_i\right)^2 + A(\mathbf{x}), \tag{8.3}$$

Given our Hamiltonian (8.2) we can construct the following ground state time independent Schrödinger equation

$$\hat{H}\psi_\hbar = E_\hbar \psi_\hbar. \tag{8.4}$$

We can propose that the wave function/eigenfunction which satisfies (8.4) can be expressed in the following form

$$\psi_\hbar(\mathbf{x}) = N_\hbar e^{-\mathcal{S}_\hbar(\mathbf{x})/\hbar}, \tag{8.5}$$

where $N_\hbar$ is a normalization constant and $\mathcal{S}_\hbar$ itself can be expanded as a series of functions which are proportional to ever increasing powers of $\hbar$

$$\mathcal{S}_\hbar(\mathbf{x}) \simeq \mathcal{S}_{(0)}(\mathbf{x}) + \hbar \mathcal{S}_{(1)}(\mathbf{x}) + \frac{\hbar^2}{2!}\mathcal{S}_{(2)}(\mathbf{x}) + \cdots + \frac{\hbar^n}{n!}\mathcal{S}_{(n)}(\mathbf{x}). \tag{8.6}$$

Inserting (8.6) into the left hand side of (8.4) results in a sequence of expressions which are proportional to powers of $\hbar$. If we expand our ground state eigenvalue, $E_\hbar$, in powers of $\hbar$ then we can match the expressions on the right hand side to the expressions on the left hand side which share the same power of $\hbar$. The expansion of $E_\hbar$ in powers of $\hbar$ is the following

$$E_\hbar := \hbar^{(0)}\mathcal{E}_\hbar \simeq \hbar\left(\mathcal{E}_{(0)} + \hbar\mathcal{E}^{(0)}_{(1)} + \frac{\hbar^2(0)}{2!}\mathcal{E}_{(2)} + \cdots + \frac{\hbar^n(0)}{n!}\mathcal{E}_{(n)} + \cdots\right), \tag{8.7}$$

where $\mathcal{E}_{(i)}$ are constants which we will have to solve for each order of $\hbar$. Equating both sides in the manner we described above results in the following sequence of equations

$$\frac{1}{2m}\nabla\mathcal{S}_{(0)}\cdot\nabla\mathcal{S}_{(0)} - V = 0, \tag{8.8}$$

$$-\frac{1}{m}\nabla S_{(0)}\cdot\nabla S_{(1)} + \frac{1}{2m}^{(n)}\Delta S_{(0)} = \mathcal{E}_{(0)} \tag{8.9}$$

$$-\frac{1}{m}\nabla S_{(0)}\cdot\nabla S_{(2)} - \frac{1}{m}\nabla S_{(1)}\cdot\nabla S_{(1)} + \frac{1}{m}^{(n)}\Delta S_{(1)} = 2\mathcal{E}_{(1)} \tag{8.10}$$

$$-\frac{1}{m}\nabla S_{(0)}\cdot\nabla S_{(3)} - \frac{3}{m}\nabla S_{(1)}\cdot\nabla S_{(2)} + \frac{3}{2m}^{(n)}\Delta S_{(2)} = 3\mathcal{E}_{(2)}, \tag{8.11}$$

and for arbitrary, $k \geq 2$

$$-\frac{1}{m}\nabla S_{(0)}\cdot\nabla S_{(k)} - \frac{1}{2m}\sum_{j=1}^{k-1}\frac{k!}{j!\,(k-j)!}\nabla S_{(j)}\cdot\nabla S_{(k-j)} + \frac{k}{2m}(n)\Delta S_{(k-1)} = k\mathcal{E}_{(k-1)}. \tag{8.12}$$

As we will demonstrate soon, in order for $S_{(k\geq 1)}$ to be smooth and globally defined we will need to set $\mathcal{E}_{(i)}$ to be the following unique constants

$$\mathcal{E}_{(0)} = \left[\frac{1}{2m}^{(n)}\Delta S_{(0)}\right](0,\ldots,0), \tag{8.13}$$

$$\mathcal{E}_{(1)} = \left[\frac{1}{2m}^{(n)}\Delta S_{(1)} - \frac{1}{2m}\nabla S_{(1)}\cdot\nabla S_{(1)}\right](0,\ldots,0), \tag{8.14}$$

$$\overset{(0)}{\mathcal{E}}_{(k-1)}= \left[\frac{1}{2m}{}^{(n)}\Delta S_{(k-1)} - \frac{1}{2m}\sum_{j=1}^{k-1} \frac{(k-1)!}{j!\,(k-j)!}\nabla S_{(j)}\cdot\nabla S_{(k-j)} \right](0,\ldots,0). \qquad (8.15)$$

When we introduce the form of the Euclidean-signature semi-classical method tailored for quantum cosmology we will discuss in depth the construction of excited states using this method.

When the ansatz (8.5) and expansions (8.6), and (8.7) are inserted into the time independent Schrödinger equation (8.4) the resultant zeroth order in $\hbar$ equation (8.8) is the vanishing energy Hamilton Jacobi equation with an inverted potential $-V$. Despite the Hamilton Jacobi equation having an inverted potential, our ansatz (8.5) naturally relates solutions of the inverted potential Hamilton Jacobi equation to solutions for the non-inverted potential time independent Schrödinger equation. If a smooth and globally defined solution to (8.8) can be proven to exist then known microlocal methods [71, 90, 116, 117, 176] can be used to integrate the higher order $S_{(k\geq 1)}$ linear transport equations. In the context of quantum mechanics the solutions of the higher order transport equations yield quantum corrections to the wave function, $e^{-\mathcal{S}_0(\mathbf{x})/\hbar}$, which can be computed sequentially after obtaining a smooth and globally defined solution to (8.8).

As a result of the properties we imposed on the original potential, V, this inverted potential, $V_{ip} = -V$, has properties which allows us to invoke certain mathematical theorems we otherwise wouldn't be able to invoke for the original non-inverted potential problem. Using these mathematical theorems which apply to the inverted potential Hamilton Jacobi equation it can be proven [176] that smooth and globally defined solutions of it exist. We will reveal what these theorems are and how they were used to prove the existence of smooth and globally defined solutions to (8.8).

In general the solutions, $S(\mathbf{x}_0, t_i, t_f)$, of the Hamilton Jacobi equation are equal to

the classical actions, $S(\mathbf{x}_0, t_i, t_f) = \int_{t_i}^{t_f} L(\mathbf{x}(t), \dot{\mathbf{x}}(t))dt$, of their corresponding system. Thus if we want to prove the existence of smooth and globally defined solutions to (8.8) it is natural to start with the classical action for our inverted potential anharmonic oscillators

$$\mathcal{S}(\mathbf{x}_0) := \int_{-\infty}^{0} \left\{ \frac{1}{2} m \sum_{i=1}^{n} \left[\left(\dot{x}^i(t) \right)^2 + \omega_i^2 \left(x^i(t) \right)^2 \right] + A(\mathbf{x}) \right\} dt. \tag{8.16}$$

If we can prove that solutions which satisfy certain properties exist for this action's corresponding Euler-Lagrange equations then we can prove that smooth and globally defined solutions to (8.8) exist. The type of solution curves in configuration space whose existence we wish to prove are those which begin at $t = 0$ at some arbitrary point, $\mathbf{x}_0$, with a unique initial velocity, $\mathbf{v}_0$, which then asymptotically approach as $t \to -\infty$ the global maximum of V_{ip} which is the origin, $\mathbf{x} = 0$. As a result of the Hamilton Jacobi equation describing a system with total energy zero the velocity must also asymptotically approach zero as $t \to -\infty$.

The curves we just described which approach the origin as $t \to -\infty$ reside in the following affine space of curves

$$\begin{aligned} \mathcal{D}_{\mathbf{x}} := \{ & \gamma \in H^1(I, \mathbb{R}^n) \mid I = (-\infty, 0] \\ & \gamma(t) = \mathbf{x}(t), \lim_{t \to 0} \gamma(t) = \mathbf{x}_0 \in \mathbb{R}^n \} \end{aligned} \tag{8.17}$$

where $H^1(I, \mathbb{R}^n)$ are the distribution of curves in the Sobolov space with norm

$$\|\gamma(\cdot)\|_{H^1(I,\mathbb{R}^n)} := \left\{ \int_{-\infty}^{0} \sum_{i=1}^{n} \left[\left(\dot{x}^i(t) \right)^2 + \omega_i^2 \left(x^i(t) \right)^2 \right] dt \right\}^{1/2}. \tag{8.18}$$

As a result of our modified semi-classical method yielding an inverted potential Hamilton Jacobi equation we can invoke the Sobolov embedding theorem [46, 61] which states that these curves have a finite norm

$$\|\gamma(\cdot)\|_{L^{\infty}(I,\mathbb{R}^n)} := \sup_{t\in I} \sqrt{\sum_{i=1}^{n} \left(x^i(t)\right)^2} < \infty, \tag{8.19}$$

and that these curves vanish at infinity

$$\lim_{t\searrow -\infty} |\gamma(t)| = \lim_{t\searrow -\infty} \sqrt{\sum_{i=1}^{n} \left(x^i(t)\right)^2} = 0. \tag{8.20}$$

From the consequences of the Sobolov embedding theorem it can be proven [176] that minimizers of the action (8.16) or solutions to the corresponding inverted potential Euler-Lagrange equations do exist and that solutions which satisfy the above properties also always satisfy

$$\begin{aligned} E_{ip}(\mathbf{x}(t), \dot{\mathbf{x}}(t)) &:= \frac{m}{2} \sum_{i=1}^{n} \left(\dot{x}^i(t)\right)^2 + V_{ip}(\mathbf{x}(t)) \\ &= \frac{m}{2} \sum_{i=1}^{n} (\dot{x}(t))^2 - V(\mathbf{x}(t)) \\ &= 0. \end{aligned} \tag{8.21}$$

Thus we can denote

$$\mathcal{S}_{(0)}(\mathbf{x}) = \mathcal{S}_{ip}\left[\gamma_{\mathbf{x}}\right] \tag{8.22}$$

as the minimizers of our action (8.16) where $\gamma_{\mathbf{x}}$ is a curve in the configuration space of our anharmonic oscillator which satisfies the properties we listed above and at $t = 0$ equals some arbitrary point in $\mathbb{R}^n$.

Using the Banach space version of the implicit function theorem [1] it can be shown [176] that the class of minimizers denoted by (8.22) are smooth and globally defined solutions of the inverted potential Hamilton Jacobi equation (8.8). In addition the Banach space version of the implicit function theorem allows us to show that the gradient of the action can be used to find the second set of initial conditions once we know $\mathbf{x}_0$

$$\begin{aligned}\mathbf{p}_0 &:= \left(\frac{\partial \mathcal{S}}{\partial x^1}, \ldots, \frac{\partial \mathcal{S}}{\partial x^n}\right) \mathbf{x}_0 \\ &= m\mathbf{v}_0.\end{aligned} \tag{8.23}$$

In general the gradient of our action or solution to (8.8) according to the aforementioned implicit function theorem yields the family of curves which asymptotically approach the origin whose proof we lightly sketched out above

$$m\frac{dx^i(t)}{dt} = \frac{\partial \mathcal{S}}{\partial x^i}\left(x^1(t), \ldots, x^n(t)\right), \tag{8.24}$$

where $(x^1(0), \ldots, x^n(0)) = \mathbf{x}_0$.

Using (8.24) and the chain rule of calculus we can rewrite our linear transport equations (8.9), (8.10), and (8.12) as

$$\frac{dS_{(1)}}{dt}\left(x^1(t), \ldots, x^n(t)\right) = \left(\frac{1}{2m}^{(n)} \Delta S_{(0)} - \mathcal{E}_{(0)}\right)\left(x^1(t), \ldots, x^n(t)\right), \tag{8.25}$$

$$\frac{dS_{(2)}}{dt}\left(x^1(t), \ldots, x^n(t)\right) = \left(\frac{1}{m}^{(n)} \Delta S_{(1)} - \frac{1}{m}\nabla S_{(1)} \cdot \nabla S_{(1)} - 2\mathcal{E}^{(0)}_{(1)}\right)\left(x^1(t), \ldots, x^n(t)\right), \tag{8.26}$$

and for $k \geq 2$

$$\begin{aligned}&\tfrac{dS_{(k)}}{dt}\left(x^1(t), \ldots, x^n(t)\right) \\ &= \left(\tfrac{k}{2m}^{(n)} \Delta S_{(k-1)} - \tfrac{1}{2m}\textstyle\sum_{j=1}^{k-1} \tfrac{k!}{j!(k-j)!} \nabla S_{(j)} \cdot \nabla S_{(k-j)} - k\mathcal{E}_{(k-1)}\right)\left(x^1(t), \ldots, x^n(t)\right)\end{aligned} \tag{8.27}$$

It can be seen that in order for the time integral of the right side of these equations to converge that the constants, $\mathcal{E}_{(i)}$, which when summed approach the eigenvalue for our ground state solution must satisfy (8.13), (8.14), and (8.15).

Using a smooth and globally defined $S_{(0)}$ the higher order transport equations can be integrated to generate smooth and globally defined quantum corrections to the quantum anharmonic oscillators. These collections of results can be used to prove

that an asymptotic solution exists for the time independent Schrödinger equation when its potential has the same properties of the anharmonic oscillators we just analyzed. One such system is the Mathieu oscillator which the author obtained some preliminary results for. The terms the author obtained for its ground state appear to have properties which suggest that they are Borel summable. We will discuss soon what these properties are. The Mathieu oscillator has been the subject recently for the exact WKB method [122].

For the specific cases of the quartic, sectic, octic, and dectic oscillators the potential is given below

$$V_\kappa(x) = \frac{1}{2} m\omega_o^2 x^2 + g x^{2\kappa}, \tag{8.28}$$

where κ is respectively, 2, 3, 4, and 5, and g in the context of perturbation theory is a perturbative parameter, but for our purposes is just a constant of arbitrary size. For this model it was observed that the wave function computed using the above method possessed the more-rapid-than-Gaussian decay known to hold for the exact solutions to these problems. This behavior begins to manifest itself at leading order in $N_\hbar e^{-\mathcal{S}_\hbar(\mathbf{x})/\hbar}$. In addition the eigenvalues found using this method matched those found using conventional Rayleigh/Schrödinger perturbation theory.

The quartic case proved to be especially interesting because the 25 terms which were computed in closed form possessed the following properties. The derivatives, $\left\{\frac{dS_{(0)}}{dx}, \ldots, \frac{dS_{(25)}}{dx}\right\}$, are all odd in x and have uniformly definite sign on each of the intervals $(\infty, 0)$ and $(0, \infty)$. Also the following quantum corrections, $\left\{S_{(\ell)}(x), \ell = 2, 3, 4, \ldots, 25\right\}$, satisfy the property that their signs on the intervals which they are defined on alternate with ℓ and that they decay from their global maximum as $|x| \to \infty$. Furthermore it was observed that that the sequence of ratios $\left\{-\frac{S_{(\ell)}(0)}{\mathcal{E}_{(\ell)}^{(0)}}, \ell = 2, 3, \ldots, 25\right\}$ decreases monotonically with increasing ℓ.

If the remaining countably infinite number of terms which make up (8.6) also

possess these aforementioned properties then the series in (8.6) can be Borel summed

$$\sum_{\ell=2}^{\infty} \frac{S_{(\ell)}(x)\hbar^{\ell}}{\ell!} \tag{8.29}$$

which would result in an exact closed form solution

$$\overset{(0)}{\psi}(x) := Ne^{-\frac{s_{(0)}(x)}{\hbar} - S_{(1)}(x) - \frac{S(x)}{\hbar} - \sum_{\ell=2}^{\infty} \frac{S_{(\ell)}(x)\hbar^{\ell}}{\ell!}} \tag{8.30}$$

to (8.4) for the $\kappa = 2$ potential of (8.28). These same properties were observed by the author when he did the analogous calculation for the Mathieu oscillator

$$\hat{H} = \frac{-\hbar^2}{2m} \frac{\overset{(0)}{\psi}\, \partial^2}{\partial x^2} + V_{(0)} \left(\cosh \frac{x}{2L} - 1 \right) \overset{(0)}{\psi}, \tag{8.31}$$

which was previously investigated recently using the exact WKB method. In (8.31) V_0 is a positive constant and L is constant with units of 'length'. The proof that the remaining terms also possess these properties is a work in progress.

In light of the terms which make up (8.6) for the quartic oscillator's wave function appearing to be Borel summable, and the fact that all of the anharmonic oscillators analyzed with this modified semi-classical method so far exhibit this expected faster-than-Gaussian decay it is fruitful to perform a leading order comparison between the traditional WKB method and the modified semi-classical one we detailed above.

If we insert

$$\psi_{\hbar}(\mathbf{x}) = N_{\hbar} e^{i\mathcal{S}_{WKB}(\mathbf{x})/\hbar}, \tag{8.32}$$

into (8.4) and apply the standard textbook WKB procedure we obtain at leading order

$$\frac{1}{2m} \left(\frac{\partial S_{WKB}}{\partial x} \right)^2 + \frac{1}{2} m\omega_o^2 x^2 + gx^4 = E_n. \tag{8.33}$$

If one tried to directly solve this equation via integration they would obtain a very non-

trivial expression for S_{WKB}. Because the quartic anharmonic oscillator is a potential well, one can try to obtain an estimate of its energy using the standard connection formula

$$\int_{\sqrt{\frac{\sqrt{8E_n gm+m^4\omega^4}}{4gm}-\frac{m\omega^2}{4g}}}^{\sqrt{\frac{\sqrt{8E_n gm+m^4\omega^4}}{4gm}-\frac{m\omega^2}{4g}}} S_{WKB}dx = \left(n+\frac{1}{2}\right)\pi\hbar. \tag{8.34}$$

Given how complicated this integral is, it isn't even clear if such an expression is inevitable for E_n. In addition, due to the concavity of the potential in (8.33) we cannot indirectly tackle this problem using the vast array of mathematical theorems we previously employed for the general anharmonic oscillators. This example suggests that the standard WKB method is not a simple and natural formalism for tackling many important problems in physics.

However if we insert (8.5) into (8.4) we obtain

$$\frac{1}{2m}\left(\frac{\partial S_{IP}}{\partial x}\right)^2 - \frac{1}{2}m\omega_o^2 x^2 - gx^4 = 0 \tag{8.35}$$

which corresponds to a classical system with a total energy of zero, but one that admits a negative potential energy. As a result the kinetic energy of this system can be positive when its potential energy is negative or zero when the potential energy is zero. Thus the solutions of this equation can correspond to the dynamics of a real classical system. In particular its leading order solution is

$$S_{ip} = \frac{(4mgx^2+2m^2w^2)^{3/2}}{12\sqrt{2}mg} \tag{8.36}$$

which manifestly demonstrates the expected rate of decay of the wave function.

From this elementary example it should be clear why in some cases our modified semi-classical method is a more versatile and natural tool than the WKB method. For the class of problems we discussed, the leading order implementation of this method yields an inverted potential Hamilton Jacobi equation whose solutions correspond

to real classical trajectories of the inverted potential system. This allows one to employ already established mathematical results to ascertain further properties of the classical action which would not be possible if one started from the standard WKB ansatz because it doesn't admit a leading order equation for this class of potentials whose solutions are purely real. As we previously mentioned the class of systems this modified method applies to are not trivial. Anharmonic oscillators form the basis of understanding infinite dimensional quantum field theories. Some QFTS can be rudimentarily understood as a space-time with an anharmonic oscillator existing at each one of its points. Therefore it is no small feat that this modified semi-classical method is technically superior to the WKB method for analyzing this class of finite dimensional problems.

Most importantly, the set of established mathematical results that the application of this modified semi-classical method allowed us to use can be generalized to infinite dimensional systems. One such system in four space-time dimensions is quantum ϕ^4 theory whose Hamiltonian can be expressed as

$$\hat{H} = \int_{\mathbb{R}^3} \left\{ -\frac{\hbar^2}{2} \frac{\delta^2}{\delta\phi^2(\mathbf{x})} + \frac{1}{2}\nabla\phi \cdot \nabla\phi(\mathbf{x}) + \frac{m^2}{2}\phi^2(\mathbf{x}) + \lambda\phi^4(\mathbf{x}) \right\} d^3x \tag{8.37}$$

where $\frac{\delta^2}{\delta\phi^2(\mathbf{x})}$ is the second functional derivative with respect to the scalar field $\phi(x)$. In order to define the full quantum theory one would need to apply regularization to the functional derivatives and let the coupling constants, (m, λ), run under the influence of a renormalization flow. However we can ignore those requirements if we only apply our method to leading order. We will begin by picking the following ground state ansatz for our wave functional

$$
\begin{aligned}
&\psi_{\hbar}[\phi(\cdot)] = N_{\hbar} e^{-\mathcal{S}_{\hbar}[\phi(\cdot)]/\hbar}, \\
&\mathcal{S}_{\hbar}[\phi(\cdot)] \simeq \mathcal{S}_{(0)}[\phi(\cdot)] + \hbar \mathcal{S}_{(1)}[\phi(\cdot)] + \frac{\hbar^2}{2!}\mathcal{S}_{(2)}[\phi(\cdot)] + \ldots, \\
&\overset{(0)}{E}_{\hbar} \simeq \hbar \left\{ \mathcal{E}_{(0)} + \hbar \mathcal{E}_{(1)} + \frac{\hbar^2(0)}{2!}\mathcal{E}_{(2)} + \ldots \right\},
\end{aligned}
\tag{8.38}
$$

which we will insert into the functional analog of (8.4). The notation, $\phi(\cdot)$, will be taken to be boundary data induced on the following Euclidean hypersurface at $t = 0$

$$
\mathbb{R}^4 = \left\{ (t, \mathbf{x}) \mid t \in \mathbb{R}, \mathbf{x} \in \mathbb{R}^3 \right\} \tag{8.39}
$$

of a scalar field, Φ, which we will take to be a generalized function defined in the following region

$$
\mathbb{R}^{4-} := (-\infty, 0] \times \mathbb{R}^3. \tag{8.40}
$$

By treating Φ as a generalized function in the same sense that the Dirac delta is a generalized function/distribution will allow us to define the map $\Phi : (-\infty, 0] \to \mathbb{R}^{\infty}$.

Inserting (8.38) into the functional version of (8.4) and only keeping terms which are independent of $\hbar$ yields the following vanishing-energy-Euclidean-signature functional Hamilton-Jacobi equation

$$
\int_{\mathbb{R}^3} \left\{ \frac{1}{2} \frac{\delta \mathcal{S}_{(0)}}{\delta \phi(\mathbf{x})} \frac{\delta \mathcal{S}_{(0)}}{\delta \phi(\mathbf{x})} - \frac{1}{2} \nabla \phi \cdot \nabla \phi(\mathbf{x}) - \frac{m^2}{2} \phi^2(\mathbf{x}) - \lambda \phi^4(\mathbf{x}) \right\} d^3x = 0. \tag{8.41}
$$

The term "Euclidean-signature" was included because if the classical analog of ϕ^4 theory in (8.37) was formulated in Euclidean-signature as opposed to Lorentzian signature and if the following substitution was made, $p_{\phi} \to \frac{\mathcal{S}_{(0)}}{\delta \phi(\mathbf{x})}$, the resulting equation would be (8.41).

The methods that we outlined for the finite dimensional case were generalized [164] to this infinite dimensional case which were then used to find a unique minimizers for

$$\mathcal{I}_{\text{es}}\left[\Phi\right] := \int_{\mathbb{R}^3}\int_{-\infty}^{0}\left\{\frac{1}{2}\dot{\Phi}^2 + \frac{1}{2}\nabla\Phi\cdot\nabla\Phi + \frac{1}{2}m^2\Phi^2 + \lambda\Phi^4\right\}dtd^3x, \tag{8.42}$$

for arbitrary boundary data, $\phi(\cdot)$, prescribed at $t = 0$. These unique minimizers resulted in the following classical action

$$\mathcal{S}_{(0)}[\phi(\cdot)] = \mathcal{I}_{es}\left[\Phi_{\phi}\right]. \tag{8.43}$$

Then using a generalized version of the Banach space implicit function theorem it was shown that this function (8.43) was smooth and globally defined in the domain of interest and that it does indeed satisfy the Euclidean-signature functional Hamilton Jacobi equation (8.41)

$$\frac{1}{2}\int_{\mathbb{R}^3}\left|\frac{\delta\mathcal{S}_{(0)}[\phi(\cdot)]}{\delta\phi(\mathbf{x})}\right|^2 d^3x = \int_{\mathbb{R}^3}\left\{\frac{1}{2}\nabla\phi\cdot\nabla\phi(\mathbf{x}) + \frac{1}{2}m^2\phi^2(\mathbf{x}) + \lambda\phi^4(\mathbf{x})\right\}d^3x. \tag{8.44}$$

Thus it was proven that a fundamental solution, $\mathcal{S}_{(0)}[\phi(\cdot)]$, exists which in theory allows one to compute the quantum corrections associated with the ground state wave functional (8.38) of ϕ^4 theory. To go from theory to practice, transport equations must be constructed which take into account the regularization of functional derivatives of the Hamiltonian and the running of the coupling constants. Such a program is a work in progress [164, 165].

As a result of this program for studying bosonic relativistic field theories not requiring splitting the theory up into one part which is a free theory and another part which contains interactions it can potentially be a useful tool to study Yang-Mill theory. This is so because the Lie algebra which generates the non-abelian Lie group which underlines Yang-Mills theory is not perfectly suited to be studied using standard perturbation theory. This is so because standard perturbation theory at

the zeroth order neglects certain interactions which results in transforming the non-abelian Lie group into an abelian one which generates multiple copies of Maxwell's theory. As one proceeds to apply perturbation theory to higher and higher orders one is attempting to recapture more and more of the non-abelian aspects of Yang-Mill theory. The Euclidean signature-semi-classical method on the other hand can preserve the structure of the non-abelian Lie group even at leading order and does so as one includes additional quantum corrections. Therefore it is hoped that one day this program may be able to shed [165] some light on the very important 'mass-gap' problem.

Given the abundance of potential applications this methodology has for physics and the fact that it is currently in an early stage of development it is important to apply the techniques we outlined in this section to a wide variety of problems. By doing so we can better ascertain the limitations of this methodology while also simultaneously highlighting its strengths which can further guide its development. The author did this by applying this methodology to a variety of finite dimensional systems found in quantum cosmology which possess different properties than those considered earlier by J.Bae [20]. In the next section we will showcase the form of the Euclidean-signature semi-classical which is tailored for quantum cosmology and show how it can potentially be applied to the formal infinite dimensional WDW equation of quantum gravity.

8.2 Euclidean-Signature Semi-Classical Method For Quantum Cosmology and Gravity

As a result of obtaining the WDW equation (7.84) from quantizing a constrained system which was subject to symmetry reduction this particular application of the Euclidean-signature semi-classical method is going to differ somewhat from what

we previously considered. The most notable difference between the WDW equation and the Schrödinger equation is that the Hamiltonian appears to annihilate, $\hat{H}\psi = 0$, any physically realizable state. As a result the crucial step we took earlier of expanding (8.7) the energy eigenvalues, E_n, in powers of $\hbar$ will be absent from this particular application of the Euclidean-signature semi-classical method. As a result our equations will be simpler but their results will be more difficult to interpret. This is especially true when it comes to delineating 'ground' states from 'excited' states. This is why from here on out we will be labeling the quantum cosmological 'ground' and 'excited' states with a ''.

The method we are about to outline was applied by Joseph Bae to the quantum diagonal Bianchi IX WDW equation [20]. Using it he was able to prove the existence of a smooth and globally defined asymptotic 'ground' state solution for any arbitrary Hartle-Hawking ordering parameter [110]. In addition he was able to investigate leading order 'excited' states of the quantum Bianchi IX models. The ability of this modified semi-classical method to facilitate a definition of 'excited' states for finite dimensional constrained theories makes it a valuable tool in quantum cosmology.

Our application of this method will be somewhat different from what was previously carried out by J.Bae. Because he was only considering a vacuum model there was no preferred length scale. As a result, in his mathematical analysis he was able to effectively reduce the degrees of freedom of the Bianchi IX minisuperspace model by one. Furthermore the solution [178] of the Euclidean-signature Hamilton Jacobi equation he was working with induced a specific flow in β space. Notably the flow induced by the 'wormhole' solution of the Bianchi IX Euclidean-signature Hamilton Jacobi equation drives [20, 22] the anisotropic variables, $\beta_+(t)$ and $\beta_-(t)$, to the origin as $t \to \infty$, irrespective of their initial location in β space, which we hold to be purely real. As a result, the equations corresponding to the quantum corrections for the Bianchi IX models were solved by integrating them along a flow induced in a subset

of minisuperspace. The integrals for the quantum corrections that were previously considered only yielded smooth and globally defined quantities if the variables, $\beta_+(t)$ and $\beta_-(t)$, being integrated vanish as $t \to \infty$.

Our approach will differ from this because we are including matter sources which pick out preferred length scales. Also our solutions to the Euclidean-signature Hamilton Jacobi equation don't induce a flow in minisuperspace which drives the β variables to the origin. Instead we will show that either the transport equations which correspond to our quantum corrections are directly solvable by picking a clever ansatz which reduces the task of solving them to an algebraic problem or that the sequence of transport equations terminates after a finite number of them have been solved. Thus our application of the Euclidean-signature semi-classical can be considered a novel one. In particular we will apply the following approach to the quantum Taub, Bianchi IX, Bianchi VIII, Bianchi VII$_{h=0}$, and Bianchi II models when a cosmological constant and aligned electromagnetic field are present.

Our outline of this method will follow closely [175]. The method described in this section and its resultant equations can in principle be used to find solutions (closed and asymptotic) to a wide class of quantum cosmological models such as all of the diagonal Bianchi A, Kantowski Sachs models, and the FLRW models. The first step is to quantize the vanishing constraint (7.65) while introducing proper units into our WDW equation by setting $\kappa = \frac{\bar{G}}{2c^3}$, where we rescaled G so that $\bar{G} = 4\pi G$. Second we will rescale L so that $\bar{L} = \sqrt{6\pi}L$. Doing these two steps results in the following WDW equation

$$\left(\frac{L_{Planck}}{\bar{L}}\right)^4 \left(\frac{\partial^2\psi}{\partial\alpha^2} - B\frac{\partial\psi}{\partial\alpha} - \frac{\partial^2\psi}{\partial\beta_+^2} - \frac{\partial^2\psi}{\partial\beta_-^2} - \hbar\left(\frac{L_{Planck}}{\bar{L}}\right)12\frac{\partial^2\psi}{\partial\phi^2}\right)$$
$$+ \bar{L}^2 e^{6\alpha} V(\alpha,\beta_+,\beta_-)\psi + 48\bar{L}^2\Lambda e^{6\alpha}\psi + \bar{L}^{-2}2b^2 e^{2\alpha-4\beta_+} \vee 2b^2 e^{2\left(\alpha\pm\sqrt{3}\beta_-+\beta_+\right)}\psi = 0, \tag{8.45}$$

where the rescaled Planck length is $L_{Planck} = \left(\frac{\bar{G}\hbar}{c^3}\right)^{1/2}$. The next step we will take in solving the WDW equation is to introduce the ansatz

$$\overset{(0)}{\Psi}_{\hbar} = e^{-S_{\hbar}/\hbar} \tag{8.46}$$

where $S_{\hbar}$ is a function of $(\alpha, \beta_+, \beta_-, \phi)$. We will rescale $S_{\hbar}$ in the following way

$$\mathcal{S}_{\hbar} := \frac{\bar{G}}{c^3 \bar{L}^2} S_{\hbar} \tag{8.47}$$

where $\mathcal{S}_{\hbar}$ is dimensionless and admits the following power series in terms of this dimensionless parameter

$$X := \frac{L^2_{\text{Planck}}}{\bar{L}^2} = \frac{\bar{G}\hbar}{c^3 \bar{L}^2}. \tag{8.48}$$

The series is given by

$$\mathcal{S}_{\hbar} = \mathcal{S}_{(0)} + X\mathcal{S}_{(1)} + \frac{X^2}{2!}\mathcal{S}_{(2)} + \cdots + \frac{X^k}{k!}\mathcal{S}_{(k)} + \cdots, \tag{8.49}$$

and as a result our initial ansatz now takes the following form

$$\overset{(0)}{\Psi}_{\hbar} = e^{-\frac{1}{X}\mathcal{S}_{(0)} - \mathcal{S}_{(1)} - \frac{X}{2!}\mathcal{S}_{(2)} - \cdots}. \tag{8.50}$$

Substituting this ansatz into the Wheeler-DeWitt equation and requiring satisfaction, order-by-order in powers of X and $\hbar$, and setting $\bar{L} = 1$ leads immediately to the sequence of equations

$$\left(\frac{\partial \mathcal{S}_{(0)}}{\partial \alpha}\right)^2 - \left(\frac{\partial \mathcal{S}_{(0)}}{\partial \beta_+}\right)^2 - \left(\frac{\partial \mathcal{S}_{(0)}}{\partial \beta_-}\right)^2 - 12\left(\frac{\partial \mathcal{S}_{(0)}}{\partial \phi}\right)^2 + U = 0, \tag{8.51}$$

$$\begin{aligned} &2\left[\frac{\partial \mathcal{S}_{(0)}}{\partial \alpha}\frac{\partial \mathcal{S}_{(1)}}{\partial \alpha} - \frac{\partial \mathcal{S}_{(0)}}{\partial \beta_+}\frac{\partial \mathcal{S}_{(1)}}{\partial \beta_+} - \frac{\partial \mathcal{S}_{(0)}}{\partial \beta_-}\frac{\partial \mathcal{S}_{(1)}}{\partial \beta_-} - 12\frac{\partial \mathcal{S}_{(0)}}{\partial \phi}\frac{\partial \mathcal{S}_{(1)}}{\partial \phi}\right] \\ &+ B\frac{\partial \mathcal{S}_{(0)}}{\partial \alpha} - \frac{\partial^2 \mathcal{S}_{(0)}}{\partial \alpha^2} + \frac{\partial^2 \mathcal{S}_{(0)}}{\partial \beta_+^2} + \frac{\partial^2 \mathcal{S}_{(0)}}{\partial \beta_-^2} + 12\frac{\partial^2 \mathcal{S}_{(0)}}{\partial \phi^2} = 0, \end{aligned} \tag{8.52}$$

$$
\begin{aligned}
&2\left[\frac{\partial\mathcal{S}_{(0)}}{\partial\alpha}\frac{\partial\mathcal{S}_{(k)}}{\partial\alpha}-\frac{\partial\mathcal{S}_{(0)}}{\partial\beta_+}\frac{\partial\mathcal{S}_{(k)}}{\partial\beta_+}-\frac{\partial\mathcal{S}_{(0)}}{\partial\beta_-}\frac{\partial\mathcal{S}_{(k)}}{\partial\beta_-}-12\frac{\partial\mathcal{S}_{(0)}}{\partial\phi}\frac{\partial\mathcal{S}_{(k)}}{\partial\phi}\right]\\
&+k\left[B\frac{\partial\mathcal{S}_{(k-1)}}{\partial\alpha}-\frac{\partial^2\mathcal{S}_{(k-1)}}{\partial\alpha^2}+\frac{\partial^2\mathcal{S}_{(k-1)}}{\partial\beta_+^2}+\frac{\partial^2\mathcal{S}_{(k-1)}}{\partial\beta_-^2}+12\frac{\partial^2\mathcal{S}_{(k-1)}}{\partial\phi^2}\right]\\
&+\sum_{\ell=1}^{k-1}\frac{k!}{\ell!\,(k-\ell)!}\left(\frac{\partial\mathcal{S}_{(\ell)}}{\partial\alpha}\frac{\partial\mathcal{S}_{(k-\ell)}}{\partial\alpha}-\frac{\partial\mathcal{S}_{(\ell)}}{\partial\beta_+}\frac{\partial\mathcal{S}_{(k-\ell)}}{\partial\beta_+}-\frac{\partial\mathcal{S}_{(\ell)}}{\partial\beta_-}\frac{\partial\mathcal{S}_{(k-\ell)}}{\partial\beta_-}-12\frac{\partial\mathcal{S}_{(\ell)}}{\partial\phi}\frac{\partial\mathcal{S}_{(k-\ell)}}{\partial\phi}\right)=0,
\end{aligned}
\tag{8.53}
$$

where U is the total potential

$$
U=e^{6\alpha}V(\alpha,\beta_+,\beta_-)\psi+48\Lambda e^{6\alpha}\psi+2b^2e^{2\alpha-4\beta_+}\vee 2b^2e^{2\left(\alpha\pm\sqrt{3}\beta_-+\beta_+\right)}. \tag{8.54}
$$

We will refer to $\mathcal{S}_{(0)}$ in our WDW wave functions as the leading order term, which can be used to construct a semi-classical approximate solution to the Lorentzian signature WDW equation, and call $\mathcal{S}_{(1)}$ the first order term. The $\mathcal{S}_{(1)}$ term can also be viewed as our first quantum correction, with the other $\mathcal{S}_{(k)}$ terms being the additional higher order quantum corrections, assuming that they are smooth and globally defined. This is reflected in the fact that the higher order transport equations depend on the operator ordering used in defining the Wheeler Dewitt equation, which is an artifact of quantization. Additionally in some cases one can find a solution to the $\mathcal{S}_{(1)}$ equation which allows the $\mathcal{S}_{(2)}$ equation to be satisfied by zero. Then one can write down the following as a solution to the WDW equation for either a particular value of the Hartle-Hawking ordering parameter, or for an arbitrary ordering parameter depending on the $\mathcal{S}_{(1)}$ which is found.

$$
\overset{(0)}{\Psi}_{\hbar}= e^{-\frac{1}{X}\mathcal{S}_{(0)}-\mathcal{S}_{(1)}} \tag{8.55}
$$

.

This can be easily shown. Let's take $\mathcal{S}_{(0)}$ and $\mathcal{S}_{(1)}$ as arbitrary known functions which allow the $\mathcal{S}_{(2)}$ transport equation to be satisfied by zero. Then the $k=3$

transport equation can be expressed as

$$2\left[\frac{\partial\mathcal{S}_{(0)}}{\partial\alpha}\frac{\partial\mathcal{S}_{(3)}}{\partial\alpha}-\frac{\partial\mathcal{S}_{(0)}}{\partial\beta_{+}}\frac{\partial\mathcal{S}_{(3)}}{\partial\beta_{+}}-\frac{\partial\mathcal{S}_{(0)}}{\partial\beta_{-}}\frac{\partial\mathcal{S}_{(3)}}{\partial\beta_{-}}-12\frac{\partial\mathcal{S}_{(0)}}{\partial\phi}\frac{\partial\mathcal{S}_{(3)}}{\partial\phi}\right]=0 \tag{8.56}$$

which is clearly satisfied by $\mathcal{S}_{(3)}$=0. The $\mathcal{S}_{(4)}$ equation can be written in the same form as (8.56) and one of its solution is 0 as well, thus resulting in the $\mathcal{S}_{(5)}$ equation possessing the same form as (8.56). One can easily convince oneself that this pattern continues for all of the $k \geq 3$ $\mathcal{S}_{(k)}$ transport equations as long as the solution of the $\mathcal{S}_{(k-1)}$ transport equation is chosen to be 0. Thus if an $\mathcal{S}_{(1)}$ exists which allows one to set the solutions to all of the higher order transport equations to zero the infinite sequence of transport equations generated by our ansatz truncates to a finite sequence of equations which allows us to construct a closed form wave function satisfying the WDW equation. Not all solutions to the $\mathcal{S}_{(1)}$ transport equation will allow the $\mathcal{S}_{(2)}$ transport equation to be satisfied by zero; however for the particular systems dealt with in this dissertation we were able to find $\mathcal{S}_{(1)}$'s which cause the $\mathcal{S}_{(2)}$ transport equation to be satisfied by zero for them, thus allowing one to set all of the solutions to the higher order transport equations to zero as shown above. This enabled us to construct new 'ground' state closed form solutions for our Lorentzian signature WDW equations for arbitrary ordering parameters.

There is still some work that needs to be done to rigorously define 'excited' states within the contexts of the quantum cosmological application of this method. However the definition which has done a satisfactory job of describing 'excited' states for the Bianchi IX models and for the Taub models [20, 39] starts with the ansatz given below

$$\Psi_{\hbar} = \phi_{\hbar} e^{-S_{\hbar}/\hbar} \tag{8.57}$$

where $\phi_{\hbar}$ and ϕ_{k} denote quantum corrections to the 'excited' states and **should not**

be confused with the free scalar field ϕ and

$$S_\hbar = \frac{c^3\bar{L}^2}{\bar{G}}\mathcal{S}_\hbar = \frac{c^3\bar{L}^2}{G}\left(\mathcal{S}_{(0)} + X\mathcal{S}_{(1)} + \frac{X^2}{2!}\mathcal{S}_{(2)} + \cdots\right)$$

is the same series expansion as before and $\phi_\hbar$ can be expressed as the following series

$$\phi_\hbar = \phi_{(0)} + X\phi_{(1)} + \frac{X^2}{2!}\phi_{(2)} + \cdots + \frac{X^{k(*)}}{k!}\phi_{(k)} + \cdots, \tag{8.58}$$

with X being the same dimensionless quantity as before. Inserting (8.57) with the expansions given by (8.49) and (8.58) into the Wheeler DeWitt equation (8.45) and by matching equations in powers of X and $\hbar$ leads to the following sequence of equations.

$$-\frac{\partial\phi_{(0)}}{\partial\alpha}\frac{\partial\mathcal{S}_{(0)}}{\partial\alpha} + \frac{\partial\phi_{(0)}}{\partial\beta_+}\frac{\partial\mathcal{S}_{(0)}}{\partial\beta_+} + \frac{\partial\phi_{(0)}}{\partial\beta_-}\frac{\partial\mathcal{S}_{(0)}}{\partial\beta_-} + 12\frac{\partial\phi_{(0)}}{\partial\phi}\frac{\partial\mathcal{S}_{(0)}}{\partial\phi} = 0, \tag{8.59}$$

$$\begin{aligned}
&-\frac{\partial\phi_{(1)}}{\partial\alpha}\frac{\partial\mathcal{S}_{(0)}}{\partial\alpha} + \frac{\partial\phi_{(1)}}{\partial\beta_+}\frac{\partial\mathcal{S}_{(0)}}{\partial\beta_+} + \frac{\partial\phi_{(1)}}{\partial\beta_-}\frac{\partial\mathcal{S}_{(0)}}{\partial\beta_-} + 12\frac{\partial\phi_{(0)}}{\partial\phi}\frac{\partial\mathcal{S}_{(0)}}{\partial\phi} \\
&+\left(-\frac{\partial\phi_{(0)}}{\partial\alpha}\frac{\partial\mathcal{S}_{(1)}}{\partial\alpha} + \frac{\partial\phi_{(0)}}{\partial\beta_+}\frac{\partial\mathcal{S}_{(1)}}{\partial\beta_+} + \frac{\partial\phi_{(0)}}{\partial\beta_-}\frac{\partial\mathcal{S}_{(1)}}{\partial\beta_-} + 12\frac{\partial\phi_{(0)}}{\partial\phi}\frac{\partial\mathcal{S}_{(1)}}{\partial\phi}\right) \\
&+\frac{1}{2}\left(-B\frac{\partial\phi_{(0)}}{\partial\alpha} + \frac{\partial^2\phi_{(0)}}{\partial\alpha^2} - \frac{\partial^2\phi_{(0)}}{\partial\beta_+^2} - \frac{\partial^2\phi_{(0)}}{\partial\beta_-^2} - 12\frac{\partial^2\phi_{(0)}}{\partial\phi^2}\right) = 0,
\end{aligned} \tag{8.60}$$

$$\begin{aligned}
&-\frac{\partial\phi_{(k)}}{\partial\alpha}\frac{\partial\mathcal{S}_{(0)}}{\partial\alpha} + \frac{\partial\phi_{(k)}}{\partial\beta_+}\frac{\partial\mathcal{S}_{(0)}}{\partial\beta_+} + \frac{\partial\phi_{(k)}}{\partial\beta_-}\frac{\partial\mathcal{S}_{(0)}}{\partial\beta_-} + 12\frac{\partial\phi_{(k)}}{\partial\phi}\frac{\partial\mathcal{S}_{(0)}}{\partial\phi} \\
&+k\left(-\frac{\partial\phi_{(k-1)}}{\partial\alpha}\frac{\partial\mathcal{S}_{(1)}}{\partial\alpha} + \frac{\partial\mathcal{S}_{(1)}}{\partial\beta_+}\frac{\partial\mathcal{S}_{(1)}}{\partial\beta_+} + \frac{\partial\phi^{(*)}_{(k-1)}}{\partial\beta_-}\frac{\partial\mathcal{S}_{(1)}}{\partial\beta_-} + 12\frac{\partial\phi^{(*)}_{(k-1)}}{\partial\phi}\frac{\partial\mathcal{S}_{(1)}}{\partial\phi}\right) \\
&+\frac{k}{2}\left(-B\frac{\partial\phi_{(k-1)}}{\partial\alpha} + \frac{\partial^2\phi^{(*)}_{(k-1)}}{\partial\alpha^2} - \frac{\partial^2\phi_{(k-1)}}{\partial\beta_+^2} - \frac{\partial^2\phi_{(k-1)}}{\partial\beta_-^2} - 12\frac{\partial^2\phi_{(k-1)}}{\partial\phi^2}\right) \\
&-\sum_{\ell=2}^{k}\frac{k!}{\ell!\,(k-\ell)!}\left(\frac{\partial\phi_{(k-\ell)}}{\partial\alpha}\frac{\partial\mathcal{S}_{(\ell)}}{\partial\alpha} - \frac{\partial\phi_{(k-\ell)}}{\partial\beta_+}\frac{\partial\mathcal{S}_{(\ell)}}{\partial\beta_+} - \frac{\partial\phi_{(k-\ell)}}{\partial\beta_-}\frac{\partial\mathcal{S}_{(\ell)}}{\partial\beta_-} - 12\frac{\partial\phi_{(k-\ell)}}{\partial\phi}\frac{\partial\mathcal{S}_{(\ell)}}{\partial\phi}\right) = 0.
\end{aligned} \tag{8.61}$$

It can be seen from computing $\frac{d\phi_{(0)}(\alpha,\beta_+,\beta_-,\phi)}{dt} = \dot{\alpha}\frac{\partial\Phi_{(0)}}{\partial\alpha} + \dot{\beta_+}\frac{\partial\Phi_{(0)}}{\partial\beta_+} + \dot{\beta_-}\frac{\partial\Phi_{(0)}}{\partial\beta_-} + \dot{\phi}\frac{\partial\Phi_{(0)}}{\partial\phi}$, and extrapolating from $(4.9,\ 4.18 - 4.20)$ of [175] what $\dot{\phi}$ is in terms of $\mathcal{S}_{(0)}$ that $\phi_{(0)}$

is a conserved quantity under the flow of S_0. This means that any function $F\left(\Phi_{(0)}\right)$ is also a solution of the equation (8.59). Wave functions constructed from these functions of ϕ_0 are only physical if they are smooth and globally defined. If we choose our ϕ_0 to have the form $f\left(\alpha,\beta_+,\beta_-,\phi\right)^{m_1} g\left(\alpha,\beta_+,\beta_-,\phi\right)^{m_2}$ where $f\left(\alpha,\beta_+,\beta_-,\phi\right)$ and $g\left(\alpha,\beta_+,\beta_-,\phi\right)$ are some functions which are conserved under the flow of $\mathcal{S}_{(0)}$ and vanish for some finite values of the Misner variables then we must restrict m_i to be either zero or a positive integer. For bound states, m_i can plausibly be interpreted as graviton excitation numbers [19]. This makes our 'excited' states akin to bound states in quantum mechanics like the harmonic oscillator whose excited states are denoted by discrete integers as opposed to a continuous index. This discretization of the quantities that denote our 'excited' states is the mathematical manifestation of quantization one would expect excited states to possess in quantum dynamics. If our conserved quantities do not vanish in minisuperspace then our 'excited' states can be interpreted as 'scattering' states akin to the quantum free particle and m_i can be any pair of real numbers.

As we will show soon, these 'excited' state transport equations can be solved in an elegant manner for the Taub and Bianchi II models. Studying both the mathematical properties of our 'excited' state transport equations and of the various models they can be applied to can shed light on how the Euclidean-signature semi-classical method can be applied to other problems in physics. In a previous study [21] the perturbations of the LRS Bianchi IX models were quantized to obtain an interpretation of the Bianchi IX model's 'excited' states; it may prove useful to do the same for the LRS Bianchi II models to show that the 'excited' states that this method can provide are indeed actual excited states. Additional information about 'excited' states can be found in [175].

We can quantize the Hamiltonian (7.40) and diffeomorphism/momentum (7.41) constraint we defined earlier in section 3 of chapter 7 irrespective of choosing their

operator ordering to obtain their quantum analogs

$$\hat{\mathcal{H}}_{\perp}\left(h_{ab}, \frac{\hbar}{i}\frac{\delta}{\delta h_{ab}}\right)\Psi[h_{ab}] = 0, \tag{8.62}$$

and

$$\hat{\mathcal{J}}_{i}\left(h_{ab}, \frac{\hbar}{i}\frac{\delta}{\delta h_{ab}}\right)\Psi[h_{ab}] = 0. \tag{8.63}$$

Technically the operator orderings one may choose for these quantized constraints are restricted by the fact that the commutator, $[\hat{\mathcal{H}}_{\perp}(\mathbf{x}), \hat{\mathcal{H}}_{\perp}(\mathbf{y})]$, should close naturally without any anomalies emerging in the form of new constraints. The solution of this problem is currently outstanding. What is known though is that the diffeomorphism constraint can be expressed in an operator ordering which allows the action of its quantized version to ensure that that physically realizable wave functions, $\Psi[h_{ab}]$, are invariant under diffeomorphism on the spatial metric

$$\Psi\left[\varphi^{*}h_{ab}\right] = \Psi[h_{ab}]. \tag{8.64}$$

Regardless of the operator ordering one chooses for these constraints one can propose the following ansatz for the 'ground' state solution to the WDW equation

$$\overset{(0)}{\Psi}_{\hbar}\left[h_{ab}\right] = e^{-S_{\hbar}[h_{ab}]/\hbar} \tag{8.65}$$

where $S_{\hbar}[h_{ab}]$ is expanded in powers of $\hbar$ in the following manner

$$S_{\hbar}[h_{ab}] = S_{(0)}[h_{ab}] + \hbar S_{1}[h_{ab}] + \frac{\hbar^{2}}{2!}S_{(2)}[h_{ab}] + \cdots + \frac{\hbar^{k}}{k!}S_{(k)}[h_{ab}] + \cdots. \tag{8.66}$$

Applying the momentum constraint to (8.65) results in each one of the terms(8.66) which make up $S_{\hbar}[h_{ab}]$ being invariant under the group of diffeomorphism of h_{ab}

$$S_{(k)}\left[\varphi^{*}\gamma\right] = S_{(k)}[\gamma], k = 0, 1, 2, \ldots . \tag{8.67}$$

Irrespective of the operator ordering one chooses for the Hamiltonian constraint, due to the operator ordering problem itself being an artifact of quantum mechanics, the zeroth order equation our ansatz (8.65) produces when it is inserted

$$\hat{\mathcal{H}}_{\perp}\left(h_{ab}, \frac{\hbar}{i}\frac{\delta}{\delta h_{ab}}\right) e^{-S_{(0)}[h_{ab}]/\hbar - S_{(1)}[\gamma] - \cdots} = 0 \tag{8.68}$$

into the Hamiltonian constraint is the functional Euclidean-signature Hamilton Jacobi equation

$$\left(\frac{16\pi G}{c^4}\right)^2 \left(h_{ac}h_{bd} - \frac{1}{2}h_{ab}h_{cd}\right) \frac{\delta S_{(0)}}{\delta h_{ab}} \frac{\delta S_{(0)}}{\delta h_{cd}} + h^{(3)}R(h_{ab}) = 0 \tag{8.69}$$

where h is the determinant of h_{ab}. In keeping with our approach of focusing for now on the zeroth order in $\hbar$ equation pertaining to infinite dimensional field theories the following question naturally arises. Is there an established mathematical method for proving the existence of a diffeomorphism invariant fundamental solution, $S_{(0)}(\varphi^{*}h_{ab}) = S_{(0)}(h_{ab})$, to the Euclidean-signature functional differential Hamilton-Jacobi equation (8.69)?

A stab at answering this question can be undertaken by generalizing the techniques we outlined for the anharmonic oscillator and the subsequent relativistic bosonic field theory. For the anharmonic oscillator we were trying to prove the existence of solutions to its inverted potential Euler Lagrange equations which satisfied an initial and asymptotic condition. For general relativity this generalizes to looking for Riemannian metrics which satisfy a certain boundary and asymptotic condition. If we can prove the existence of such a class of Riemannian metrics that would represent the first step towards proving that the classical Euclidean-signature action which

corresponds to those metrics is indeed a smooth and globally defined solution to (8.69).

We can use the fact that in a vacuum or when only conformally invariant matter sources are present that a special class of solutions to Einstein's equations exists when the four dimensional Ricci scalar vanishes, $R(g_{Eucl}) = 0$. Without loss of generality if we start our search for solutions to Einstein's equations when $R(g_{Eucl}) = 0$ our task of minimizing the corresponding Euclidean-signature action functional is simplified. In addition to simplifying our task this condition allows us to avoid the pitfalls which have plagued other approaches to quantum gravity. One such approach is based on Euclidean-signature path integrals. However it is plagued by the problem that in general the Riemannian metrics it sums over results in an action which is not bounded from below which causes the integral for the wave function to diverge. However when $R(g_{Eucl}) = 0$ the conformal degree of freedom which results in the action being unbounded [97, 98] from below is frozen and thus vanishing of the Ricci scalar is a natural condition we should impose for the method we would like to employ.

Because we can seek to minimize the relevant action when $R(g_{Eucl}) = 0$ we have a good idea of what types of Riemannian metrics we are looking for. As a result of the positive action theorem [77, 212, 237] we know that the action of any asymptotically Euclidean Riemannian metric which satisfies $R(g_{Eucl}) = 0$ is positive. On a basic level this is a result of the additional boundary terms we encountered earlier not vanishing when asymptotic flatness is a boundary condition. Thus in the same way we knew which types of curves we wanted to prove the existence of for the anharmonic oscillator we know which types of metrics corresponding to the Euclidean-signature Hamilton Jacobi equation we wish to prove the existence of. Thus the previous success of this method for proving the existence of smooth and globally defined solutions to the Euclidean-signature functional Hamilton Jacobi equation for ϕ^4 theory provides a road map for doing the same for the formal WDW equation.

In addition to having a road map which doesn't rely on previous techniques which possess long standing unresolved issues, our method has another advantage over the traditional Euclidean path integral approach. This method doesn't require the use of a Wick rotation like the Euclidean path integral approach. The Euclidean path integral approach like our method seeks to solve the Lorentzian signature WDW equation. However, performing a Euclidean path integral over Riemannian metrics and matter fields would normally result in a solution to the Euclidean signature WDW equation. Despite this drawback, proving the convergence of the path integral in Euclidean-signature is in principle easier to do than in Lorentzian signature. Most importantly though, any result obtained via a Euclidean-signature path integral can hopefully be Wick rotated retroactively to satisfy the Lorentzian signature WDW equation. The problem is that there is no generally accepted Wick rotation that can accomplish this. The form that such a Wick rotation would take is an outstanding problem in itself. However our method requires no Wick rotation. We get to take advantage of the simplicity of working with Euclidean-signature equations without having to worry about how to relate our results back to the original Lorentzian signature problem in question. Our method naturally relates the solutions of the Euclidean-signature functional Hamilton Jacobi equation of quantum gravity to the wave function of the formal Lorentzian signature WDW equation.

As we have shown in this chapter the Euclidean-signature semi-classical method can be applied to an impressive array of finite dimensional and infinite dimensional systems. In particular its applications to certain infinite dimensional systems are highly promising. The Euclidean-signature semi-classical method can potentially provide us with fascinating insights into bosonic relativistic field theory and quantum gravity that other presently known methods cannot. As a result the further development of this method is a worthy task. To aid in the development of this method in the upcoming chapters we will expand upon the types of finite dimensional systems

that this method can be applied to by considering quantum cosmological models with matter sources, which, as we previously mentioned, possess different properties than the model investigated by J.Bae [20]. In what follows we will work in a set of units in which $X = 1$, unless stated other wise.

Chapter 9

Quantum Taub Models

9.1 Introduction

Throughout the entirety of this chapter we will not consider the free scalar field and will thus drop all terms which depend upon its existence from the aforementioned formalism and the Taub WDW equation. The metric formulation of the Taub models is given below

$$\begin{aligned} ds^2 &= -N^2 dt^2 + \frac{L^2}{6\pi} e^{2\alpha(t)} \left(e^{2\beta(t)}\right)_{ab} \omega^a \omega^b, \\ \left(e^{2\beta(t)}\right)_{ab} &= \text{diag}\left(e^{2\beta_+(t)}, e^{2\beta_+(t)}, e^{-4\beta_+(t)}\right), \\ \omega^1 &= \cos\psi d\theta + \sin\psi \sin\theta d\phi, \\ \omega^2 &= \sin\psi d\theta - \cos\psi \sin\theta d\phi, \\ \omega^3 &= d\psi + \cos\theta d\phi, \end{aligned} \tag{9.1}$$

where ω^i are the one forms defined on the spatial hypersurface of the Bianchi IX models. Using these one forms and $d\omega^c = \frac{1}{2} C^c_{ab} \omega^a \wedge \omega^b$, one can recover the Bianchi IX structure constants, C^c_{ab}, listed in table 1. In addition L has units of 'length' and sets a scale for the spatial size of our cosmology. This can be seen because any shift in the scale factor $e^{\alpha(t)+\delta}$ where δ is a real number can be reabsorbed into L^2.

Beyond inspecting (9.1), it can be known that $e^{\alpha(t)}$ acts as the scale factor of the Taub models in these Misner variables by computing $\sqrt{-\det^{(4)} g}$ of the metric tensor (9.1) expressed in orthonormal coordinates, yielding $\frac{L^3}{(6\pi)^{\frac{3}{2}}} e^{3\alpha(t)}$ which measures the total volume of our closed space-time.

As (9.1) implies, the Hamiltonian formulation of the Taub models can be ascertained by starting with (7.65), setting $p_{\beta_-} = 0$, and then setting $\beta_- = 0$ for the Bianchi IX potential term, $V(\alpha, \beta_+, \beta_-)$, listed in table 2. The Bianchi IX models possess a rich history and have been studied in a multitude of different contexts. Investigations into them began with the works of Misner, Ryan, and Belinskii, Khalatnikov, and Lifshitz [32, 33, 169, 206]. What partly made these models so appealing was that they shared the 3-sphere spatial topology of the k=1 FLRW models, which were widely believed to be a good approximation for our physical universe until more precise cosmological observations [80] suggested the real possibility that our universe may indeed by flat $k = 0$. In addition the classical equations which govern the dynamics of the Bianchi IX mini-superspace variables, which we will take to be the Misner variables $(\alpha, \beta_+, \beta_-)$ [169, 170] admit chaotic solutions [28, 66, 73, 180]. It was originally thought that the chaos present near its singularity, which took the form of an erratic sequence of Kasner contractions and expansions could explain why we observe the universe to be mostly homogeneous, hence the origin of the name Mixmaster [169]. The quantum diagonalized Bianchi IX models were first studied by Misner [170], and later by Moncrief-Ryan [178]; among others in a plethora of different contexts, such as supersymmetric quantum cosmology [78, 100, 101, 161]. Recently they were investigated using the traditional WKB method [67].

The classical Taub models [222] and its extension, the Taub-NUT models have a rich history of their own, which includes being used to model the space-time around a black hole [134, 185]. Recently work has been conducted in finding new solutions to the symmetry reduced Wheeler DeWitt equation of the LRS Bianchi IX models [132]

using Killing vectors and tensors. Their quantum cosmology has also been investigated within the context of the generalized uncertainty principle [31] and using the WKB approximation [65, 79]. We will further expand upon what was previously done by proving the existence of a countably infinite number of closed form 'excited' states for the quantum Taub models when a cosmological constant is present and studying how matter sources such as an aligned electromagnetic field and a cosmological constant can affect 'excited' states of the Taub models.

Also new solutions to the Taub WDW equation will be obtained when both a cosmological constant and aligned electromagnetic field are present. The reason the author chose to include an electromagnetic field goes beyond showcasing the utility of the Euclidean-signature semi-classical method. Recent evidence [184, 223] for the existence of a femto Gauss strength intergalactic magnetic field has been uncovered by observing gamma rays. This provides further reasons to continue [89, 128, 131, 133, 140, 156, 190] studying electric/magnetic fields through the lens of quantum cosmology. Through studying the effects of electric/magnetic fields on quantum universes we can potentially better understand how seeds of anisotropy developed in our early universe which we can observe [6, 35, 118] today in the CMB. Recent work [123, 129, 173, 188] has been conducted in trying to determine what signatures a primordial magnetic field would induce on the various computable spectrum's derived from the CMB. By studying what effects electromagnetic fields induce on both 'ground' state and 'excited' state wave functions of the Taub models we can contribute to the theoretical portion of that task.

The wave functions we will obtain through this method are easiest to interpret in a qualitative manner when we allow $\Lambda < 0$. Choosing a negative cosmological constant does not necessarily make our solutions non-physical. Recently there has been some interesting work [45, 111, 112, 172, 231] done in studying inflation with a negative cosmological constant and the connection between asymptotically AdS

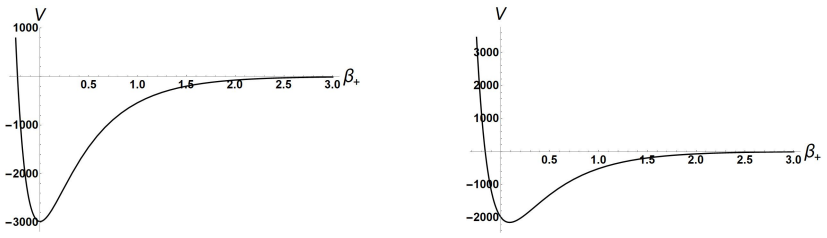

(a) $\alpha = 2 \quad \Lambda = 0 \quad b = 0$ **(b)** $\alpha = 2 \quad \Lambda = 0 \quad b = 3$

Figure 9.1 Plots of the potential as a function of β_+ in (9.2) when $\alpha = 2$.

wave functions to classical cosmological histories which exhibit phenomenology that one expects from universes with a positive cosmological constant. From a theoretical point of view it is worthwhile to study quantum cosmologies that possess a negative cosmological constant.

Using the WDW equation(7.89) we previously wrote down, throwing out its $\frac{\partial^2\psi}{\partial\beta_-^2}$ term, and setting $\beta_- = 0$ for the Bianchi IX potential in table II yields the equation which we will exclusively focus on throughout this chapter.

$$\frac{\partial^2\Psi}{\partial\alpha^2} - B\frac{\partial\Psi}{\partial\alpha} - \frac{\partial^2\Psi}{\partial\beta_+^2} + \left(\frac{e^{4\alpha-8\beta_+}}{3}\left(1-4e^{6\beta_+}\right) + \frac{2e^{6\alpha}\Lambda}{9\pi} + 2b^2e^{2\alpha-4\beta_+}\right)\Psi = 0, \quad (9.2)$$

where B is the Hartle-Hawking [110] ordering parameter, b^2 is the strength of the electromagnetic field; and Λ is normalized differently than in (7.89), and is dimensionless. Adding an electromagnetic field results in the potential well in (9.2) becoming more shallow as b^2 increases as can be seen in (9.1).

This chapter will be organized as follows. First we will apply the Euclidean-signature semi-classical method to the quantum Taub models when both a cosmological constant and a primordial electromagnetic field are present to obtain a closed form 'ground' state solution. In addition we will find two closed form 'excited' state solutions when $\Lambda = 0$ and $b \neq 0$ which demonstrate the fantastical effects an aligned electromagnetic field can induce on the 'excited' states of the Taub models.

We will then prove the existence of a countably infinite number of Taub 'excited' state solutions when a cosmological constant is present. Afterwards we will prove the existence of 'ground' state asymptotic solutions for the 'wormhole' [178] and 'no boundary' [103] cases and then comment on the mathematical differences between the two. Finally we will qualitatively discuss the large number of wave functions computed in this work and give some concluding remarks. We will interpret our wave functions by their atheistic characteristics. For example we will assume, as was done in [93], that each visible peak which is present for our wave functions represents a geometric state a quantum universe can tunnel in and out of.

9.2 Closed Form 'Ground' And 'Excited' State Solutions For The Quantum Taub Models With A Cosmological Constant And An Aligned Electromagnetic Field

The author found the following $\mathcal{S}_{(0)}$ associated with the Euclidean signature Hamilton Jacobi equation(8.51) of (9.2)

$$\mathcal{S}_{(0)} := \mathrm{b}^2(-\alpha-\beta_+) - \frac{\Lambda e^{4(\alpha+\beta_+)}}{36\pi} + \frac{1}{6}\left(2e^{6\beta_+}+1\right)e^{2\alpha-4\beta_+}, \tag{9.3}$$

which is the standard 'wormhole' solution with two additional terms for our matter sources. When $\Lambda = 0$ and the electromagnetic field vanishes($b = 0$), (9.3) reduces to the standard 'wormhole' solution [178] adapted to the Taub models. The author was unable to find solutions to (8.51) with the aforementioned matter sources which reduce to either the analogues of the Taub 'no boundary' [103] or "arm" solutions [26]. This potentially suggests that there is something special about the 'wormhole'

solution.

Inserting (9.3) into our $\mathcal{S}_{(1)}$ equation results in

$$
\begin{aligned}
&-9\pi \mathrm{b}^2(2\ \frac{\partial \mathcal{S}_{(1)}}{\partial \alpha}-2\ \frac{\partial \mathcal{S}_{(1)}}{\partial \beta_+}+\mathrm{B})-\Lambda e^{4(\alpha+\beta_+)}(2\ \frac{\partial \mathcal{S}_{(1)}}{\partial \alpha}-2\ \frac{\partial \mathcal{S}_{(1)}}{\partial \beta_+}+\mathrm{B})\\
&+6\pi e^{2(\alpha+\beta_+)}(2\ \frac{\partial \mathcal{S}_{(1)}}{\partial \alpha}-2\ \frac{\partial \mathcal{S}_{(1)}}{\partial \beta_+}+\mathrm{B})+3\pi e^{2\alpha-4\beta_+}(2\ \frac{\partial \mathcal{S}_{(1)}}{\partial \alpha}+4\ \frac{\partial \mathcal{S}_{(1)}}{\partial \beta_+}+\mathrm{B}+6)=0,
\end{aligned}
\tag{9.4}
$$

which is satisfied by the very simple expression

$$
\mathcal{S}_{(1)}:=\left(-\frac{\mathrm{B}}{2}-1\right)\alpha-\beta_+, \tag{9.5}
$$

that surprisingly is independent of Λ and b. Another interesting feature of this solution is that it can be absorbed into the terms of (9.3) which are linear in α and β_+ $\big(\mathrm{b}^2(-\alpha-\beta_+)\big)$.

Despite it not being the only solution to (9.4) and it's simple nature we claim that we are justified in employing it to construct our closed form solutions to (9.2) because it generates such fascinating wave functions as we will show shortly. The non-trivial effects that these wave functions imply for the universes that they describe should be chronicled as possible phenomena that a toy model of quantum gravity can induce on the evolution of a quantum universe(s). In addition physically this solution makes sense because the effects of quantum corrections $\mathcal{S}_{(k>0)}$ in our wave function should become negligible compared to the leading order term $\mathcal{S}_{(0)}$ as α increases which is the case as can be seen by comparing (9.5) to (9.3). In addition this exact quantum correction (9.5) is obtained if one solves the vacuum Taub Wheeler Dewitt equation using separation of variables and then constructs a superposition of separable solutions using a specific kernel [178] to integrate the Bessel K functions.

Keeping this in mind we will proceed using (9.5) and insert it into equation (8.53), yielding

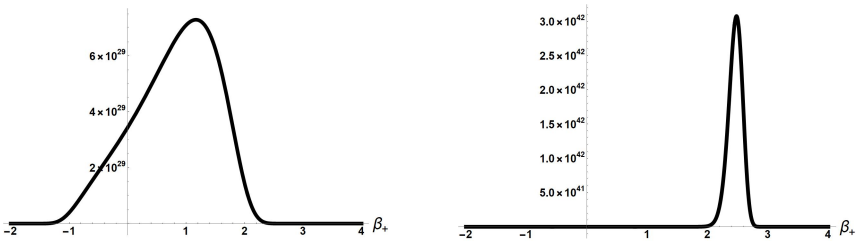

(a) $\alpha = -1 \quad \Lambda = -1 \quad b = 0$ **(b)** $\alpha = -1 \quad \Lambda = -1 \quad b = 5$

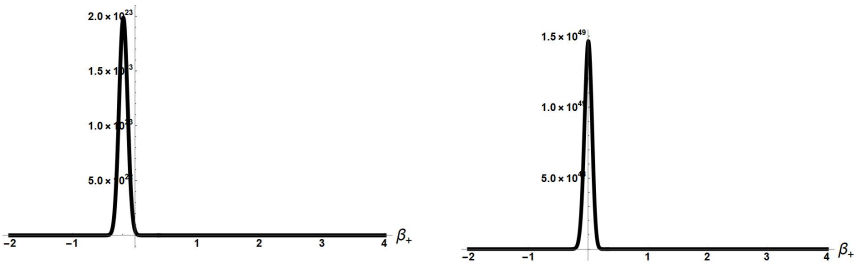

(c) $\alpha = 1.5 \quad \Lambda = -3 \quad b = 0$ **(d)** $\alpha = 1.5 \quad \Lambda = -3 \quad b = 6.5$

Figure 9.2 Plots of (9.7) when our matter sources and α are varied

$$
\begin{aligned}
&- 9\pi \ \left(4\mathrm{b}^2(\frac{\partial \mathcal{S}_{(2)}}{\partial \alpha} - \frac{\partial \mathcal{S}_{(2)}}{\partial \beta_+}) + \mathrm{B}^2\right) - 4\Lambda e^{4(\alpha+\beta_+)}(\frac{\partial \mathcal{S}_{(2)}}{\partial \alpha} - \frac{\partial \mathcal{S}_{(2)}}{\partial \beta_+}) \\
&+ 12 \ \pi \ e^{2\alpha-4\beta_+}\left(2e^{6\beta_+}(\frac{\partial \mathcal{S}_{(2)}}{\partial \alpha} - \frac{\partial \mathcal{S}_{(2)}}{\partial \beta_+}) + \frac{\partial \mathcal{S}_{(2)}}{\partial \alpha} + 2\ \frac{\partial \mathcal{S}_{(2)}}{\partial \beta_+}\right) = 0.
\end{aligned}
\tag{9.6}
$$

When $B = 0$ this equation is satisfied by $\mathcal{S}_{(2)} = 0$ which as was previously shown allows us to construct the following closed form solution to the Taub WDW equation.

$$
\Psi_{matter} = e^{\left(\left(\mathrm{b}^2+1\right)(\alpha+\beta_+)+\frac{\Lambda e^{4(\alpha+\beta_+)}}{36\pi}-\frac{1}{6}\left(2e^{6\quad\beta_+}+1\right)e^{2\alpha-4\beta_+}\right)}. \tag{9.7}
$$

Comparing (9.7) to our two ansätze (8.46) and (8.57) indicates that our closed form solution is a 'ground' state. Figures 9.2a to 9.2d further support this. In our discussion section we will analyze the physical implications of the behavior of these wave functions(figs 9.2a-9.2d) as our matter sources Λ and b^2 are varied.

As of the writing of this dissertation the author found two 'excited' state solutions for the quantum Taub models when an electromagnetic field is present. Using (9.3) when $(\Lambda = 0)$, the author found the following family of conserved quantities which

satisfies (8.59)

$$\phi_{(0)} := \left(-3\mathrm{b}^2 e^{2(\alpha+\beta_+)} - e^{4\alpha-2\beta_+} + e^{4(\alpha+\beta_+)}\right)^n . \tag{9.8}$$

Because (9.8) vanishes for finite values of the Misner variables n is required to be quantized in the sense that it is restricted to only taking on positive integer values and thus our 'excited' states are bound states. In this thesis we will find and analyze the first two closed form 'excited' states. An extension of the work we shall present would be to prove that a countably infinite number of 'excited' states exist when both an electromagnetic field and cosmological constant are present. We will comment on the feasibility of this in the next section.

For the first 'excited' state when $n = 1$ the author found the following solution to the ϕ_1 equation which causes the rest of the ϕ_k equations to be satisfied by zero as will be explained in more detail in the next section

$$\phi_{(1)} := 9\mathrm{b}^2 - 6e^{2(\alpha+\beta_+)}. \tag{9.9}$$

For the case when $n = 2$ the author had to solve up to the ϕ_3 equation to find a closed form solution to (9.2). The sequence of ϕ_ks needed to find the second 'excited' state are given below

$$\phi_{(1)} := 63\mathrm{b}^2 e^{4(\alpha+\beta_+)} - 24e^{6(\alpha+\beta_+)} + 18e^{6\alpha}, \tag{9.10}$$

$$\phi_{(2)} := 108\left(6\mathrm{b}^2 e^{2(\alpha+\beta_+)} + 2e^{4\alpha-2\beta_+} - 9\mathrm{b}^4\right), \tag{9.11}$$

$$\phi_{(3)} := 972\left(4e^{2(\alpha+\beta_+)} - 6\mathrm{b}^2\right). \tag{9.12}$$

We will plot these 'excited' states below in figures 9.3 and discuss the physical

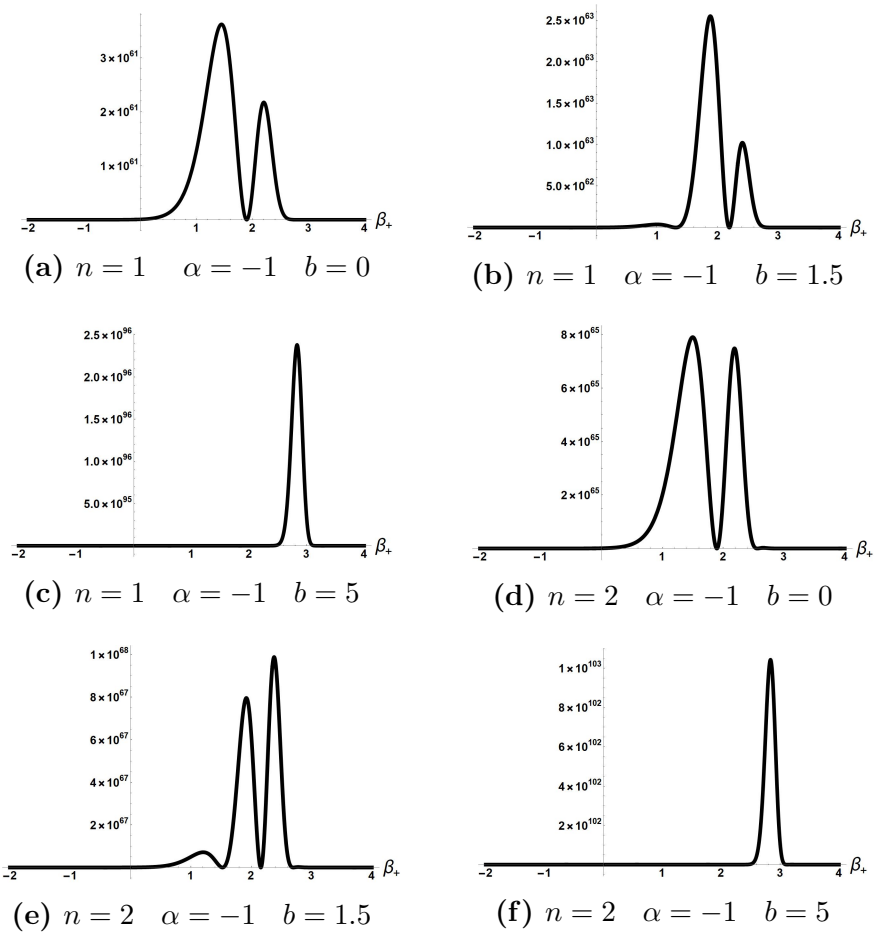

(a) $n = 1 \quad \alpha = -1 \quad b = 0$ **(b)** $n = 1 \quad \alpha = -1 \quad b = 1.5$

(c) $n = 1 \quad \alpha = -1 \quad b = 5$ **(d)** $n = 2 \quad \alpha = -1 \quad b = 0$

(e) $n = 2 \quad \alpha = -1 \quad b = 1.5$ **(f)** $n = 2 \quad \alpha = -1 \quad b = 5$

Figure 9.3 Figures (a)-(c) are of the first closed form 'excited' state when an electromagnetic field is present while figures (d)-(f) are of the second 'excited' state when an electromagnetic field is present. For both sets of figures we varied the values of the electromagnetic field.

consequences of the electromagnetic field b^2 by examining the atheistic characteristics of our wave functions in a similar manner to what was done in [93] at the end of this chapter.

When $B \neq 0$ (9.6) becomes more challenging to solve. To proceed, we will set $b = 0$ and find a suitable coordinate change $u(\alpha, \beta_+)$, $v(\alpha, \beta_+)$ which simplifies our transport equation

$$\frac{\partial \mathcal{S}_{(2)}}{\partial \alpha} = \frac{\partial \mathcal{S}_{(2)}}{\partial u}\frac{\partial u}{\partial \alpha} + \frac{\partial \mathcal{S}_{(2)}}{\partial v}\frac{\partial v}{\partial \alpha}$$
$$\frac{\partial \mathcal{S}_{(2)}}{\partial \beta_+} = \frac{\partial \mathcal{S}_{(2)}}{\partial u}\frac{\partial u}{\partial \beta_+} + \frac{\partial \mathcal{S}_{(2)}}{\partial v}\frac{\partial v}{\partial \beta_+}. \tag{9.13}$$

Inserting (9.13) into (9.6) and choosing $u = e^{\alpha+\beta_+}$, $v = e^{-\alpha+\beta_+}$ results in the following simplification

$$\left(8u^5v^4\Lambda + 12\pi\ v\left(1-4u^3v^3\right)\right)\frac{\partial \mathcal{S}_{(2)}}{\partial v} - 9\pi\ u\ \ \left(\mathrm{B}^2v^3 - 4\frac{\partial \mathcal{S}_{(2)}}{\partial u}\right) = 0 \tag{9.14}$$

whose solutions can be found using Mathematica's DSolve. Once a family of solutions for (9.14) is found one can insert $u = e^{\alpha+\beta_+}$ and $v = e^{-\alpha+\beta_+}$ back into it to obtain

$$f = \frac{3}{8}\pi\ \mathrm{B}^2$$
$$\mathcal{S}_{(2)} := (f)\,\mathrm{RS}\left[\mathrm{x}^3\left(-e^{2\beta_+}\right)\Lambda + 9\pi\ \mathrm{x}^2e^{2\beta_+} - 9\pi\ e^{4\alpha\ \ +6\beta_+} + 9\pi\ e^{4\alpha} + \Lambda e^{6\alpha+8\beta_+}\&, \frac{\log\left(e^{2\alpha+2\beta_+} - \mathrm{x}\right)}{6\pi\ \ \mathrm{x} - \mathrm{x}^2\Lambda}\&\right]$$
$$+ c_1\left(\frac{1}{9}e^{4\alpha-2\beta_+}\left(-9e^{6\beta_+} + \frac{\Lambda e^{2\ \ \alpha+8\beta_+}}{\pi} + 9\right)\right). \tag{9.15}$$

RS stands for Root-sum in (9.15) means summing $\frac{\log\left(e^{2\alpha+2\beta_+}-\mathrm{X}\right)}{6\pi\ \ \mathrm{X}-\mathrm{X}^2\Lambda}$ over the roots of $\mathrm{x}^3\left(-e^{2\beta_+}\right)\Lambda + 9\pi\ \mathrm{x}^2e^{2\beta_+} - 9\pi\ e^{4\alpha\ \ +6\beta_+} + 9\pi\ e^{4\alpha} + \Lambda e^{6\alpha+8\beta_+} = 0$.

9.3 Proof Of Infinite Sequence Of 'Excited' State Solutions For Quantum Taub Models

To construct our 'excited' states we need a family of smooth and globally defined solutions to the equation (8.59). The author was able to obtain the following fam-

ily of such solutions to equation (8.59) when both a cosmological constant and an electromagnetic field are present

$$\phi_{(0)} := \left(27\pi\ \mathrm{b}^2 e^{2(\alpha+\beta_+)} + \Lambda e^{6(\alpha+\beta_+)} - 9\pi\ \left(e^{6\ \ \beta_+} - 1\right) e^{4\alpha-2\beta_+}\right)^n . \tag{9.16}$$

Finding (9.16) represents the second step in proving that a countably infinite number of 'excited' states exist for the quantum Taub models when both an aligned electromagnetic field and cosmological constant are present. As will become apparent to the reader soon, the first step was obtaining a closed form 'ground' state solution for the quantum Taub models when both an aligned electromagnetic field and cosmological constant are present. We will discuss the next steps after we prove that a countably infinite number of smooth and globally defined 'excited' states do exist for the quantum Taub models when only Λ is present. Afterwards though we will study the leading order 'excited' states that this ϕ_0 (9.16) produces.

To begin we will use this ϕ_0

$$\phi_{(0)} := \left(\Lambda e^{6(\alpha+\beta_+)} - 9\pi\ \left(e^{6\ \ \beta_+} - 1\right) e^{4\alpha-2\beta_+}\right)^n . \tag{9.17}$$

Because our $\phi_{(0)}$(9.17) clearly vanishes for some finite values of the Misner variables, in order to ensure that our wave functions are smooth and globally defined we must restrict n to be either zero or a positive integer. As was mentioned before, this manifestation of quantization is one of the reasons why we refer to these states as 'excited' states.

We will now proceed to demonstrate that there are a countably infinite number of closed form solutions to the Taub WDW equation, each corresponding to an 'n' for the case when ϕ_0 is (9.17) and

$$\begin{aligned}\mathcal{S}_{(0)} &:= -\frac{\Lambda e^{4(\alpha+\beta_+)}}{36\pi} + \frac{1}{6}\left(2e^{6\beta_+}+1\right)e^{2\alpha-4\beta_+},\\ \mathcal{S}_{(1)} &:= -\alpha-\beta_+.\end{aligned} \tag{9.18}$$

We will start by observing that the source term for our 'excited' state transport equations (8.61) for $k \geq 1$ reduces to

$$k\left(\frac{\partial\phi_{(k-1)}}{\partial\alpha} - \frac{\partial\phi_{(k-1)}}{\partial\beta_+}\right) + \frac{k}{2}\left(\frac{\partial^2\phi_{(k-1)}}{\partial\alpha^2} - \frac{\partial^2\phi_{(k-1)}}{\partial\beta_+^2}\right), \tag{9.19}$$

because when B=0 the non-trivial solutions to the 'ground' state transport equations, $\mathcal{S}_{(0)}$ and $\mathcal{S}_{(1)}$, allow all of the higher order $\mathcal{S}_{(k\geq 2)}$ transport equations to be satisfied by zero, which results in the $\mathcal{S}_{(\ell)}$ terms in (8.61) to vanish. Thus our 'excited' state transport equation for any kth quantum correction to the nth 'excited' state is

$$-\frac{\partial\phi_{(k)}}{\partial\alpha}\frac{\partial\mathcal{S}_{(0)}}{\partial\alpha} + \frac{\partial\phi_{(k)}}{\partial\beta_+}\frac{\partial\mathcal{S}_{(0)}}{\partial\beta_+} + k\left(\frac{\partial\phi_{(k-1)}}{\partial\alpha} - \frac{\partial\phi_{(k-1)}}{\partial\beta_+}\right) + \frac{k}{2}\left(\frac{\partial^2\phi_{(k-1)}}{\partial\alpha^2} - \frac{\partial^2\phi_{(k-1)}}{\partial\beta_+^2}\right) = 0. \tag{9.20}$$

Because of the linearity and signs of the derivatives present in (9.19) all expressions of the form $x_1 e^{x_2\alpha+x_2\beta_+}$ which are contained, and expressed within ϕ_{k-1} as a sum $\Sigma_i x_i e^{x_i\alpha+x_i\beta_+} + \Sigma_i \cdots$ vanish from the source term of the ϕ_k transport equations. If we insert (9.17) into (9.19) when k=1 it is evident that we obtain a sum of exponentials which is composed of $\frac{1}{2}n(1+n)$ terms, as can be checked by examining the cumbersome resultant expression. In addition the homogeneous portion of the transport equations (9.20) contains a sum of exponentials thanks to (9.18). Thus it is natural to try as an ansatz for ϕ_1 a sum of exponentials composed of $\frac{1}{2}n(1+n)$ terms, $\phi_1 := \sum_{i=1}^{\frac{1}{2}n(n+1)} x_i e^{y_i\alpha+z_i\beta_+}$. The author for n=1, 2, and 3 inserted the aforementioned ansatz into (9.20) when k=1 and was able to find unique solutions for the three, nine, and eighteen coefficients (x_i, y_i, z_i) required to respectively express in closed form the

first quantum correction to the first, second and third $\Lambda \neq 0$ 'excited' quantum Taub states. For the k=2 transport equations the source term for the n=1 case vanished because its respective ϕ_1 was $54\pi\ e^{2\alpha+2\beta_+}$; thus allowing the sequence of 'excited' state transport equations to truncate, resulting in a closed form 'excited' state solution to (9.2). On the other hand for n=2 and n=3 states the author modified the aforementioned ansatz $\sum_{i=1}^{\frac{1}{2}(-k+n+1)(-k+n+2)} x_i e^{y_i\alpha+z_i\beta_+}$ so that it contains the same number of terms as the source of the transport equations it was intended to solve. Using this modified ansatz the author was able to find the three and nine coefficients respectively required to compute ϕ_2 for the second and third 'excited' states. The source term for the the k=3 transport equation vanished when n=2 because its ϕ_2 was $17496\pi^2 e^{4(\alpha+\beta_+)}$, thus allowing us to construct a closed form solution for the second 'excited' state. However when n=3 the source term did not vanish, but rather was composed of only one exponential $c_1 e^{c_2\alpha+c_3\beta_+}$, whose coefficients the author was able to solve for which resulted in ϕ_3 being $14171760\pi^3 e^{6\alpha+6\beta_+}$. We will explicitly present the aforementioned results for the n=1, 2 and 3 states after we prove that a countably infinite number of closed form 'excited' states exist which are of a particular form that we will introduce shortly. Using the three closed form solutions the author found, he was able to notice a pattern in how powers of e^{β_+} and e^{α} varied between terms, and in the total number of terms present for each kth quantum correction given a value of n and deduced the following ansatz for the kth quantum correction given any positive integer value of n

$$\phi_k = \sum_{i=0}^{n-k} \left(\sum_{j=0}^{-i-k+n} b(\{i,j,k\}) e^{(2\alpha(i-k+2n)+2\beta_+(4i+3j+2k-n))} \right). \tag{9.21}$$

In the above expression $b(\{i,j,k\})$ is a constant determined by substituting (9.21) back into the 'excited' state transport equations (9.20). The $b(\{i,j,0\})$ coefficients can be read directly from (9.17).

After we present the explicit n=1, 2, and 3 solutions it will become clear to the

reader how the author was able to deduce this particular form for the solutions of (9.20) when $\Lambda \neq 0$. When we set n=k we obtain

$$\phi_n = e^{2n\alpha+2n\beta_+} b(\{0,0,n\}), \tag{9.22}$$

which results in the source term of the ϕ_{n+1} equation vanishing, and subsequently allowing the ϕ_{n+1} transport equation to be satisfied by zero. This allows one to truncate the infinite sequence of transport equations and show that if (9.21) is indeed the general form for a family of solutions to the transport equations then one only needs to solve n transport equations to obtain the closed form nth 'excited' state of the $\Lambda \neq 0$ quantum Taub models. To prove that there exists a family composed of a countably infinite number of solutions, all with the form of (9.21), we will insert (9.21) into our source term (9.19) to obtain after simplification

$$\begin{aligned} f(i,j,k,n) &= k(i+j+k-n-1)(5i+3j+k+n) \\ &- 6\sum_{i=0}^{-k+n+1}\left(\sum_{j=0}^{-i-k+n+1} f(i,j,k,n) b(\{i,j,k-1\}) e^{(2\alpha(i-k+2n+1)+2\beta_+(4i+3j+2(k-1)-n))}\right). \end{aligned} \tag{9.23}$$

The coefficient of our source term vanishes when $j = 1-i-k+n$, which is the upper limit of our sum over j. Thus we can rewrite our sum for the source term as

$$\begin{aligned} f(i,j,k,n) &= k(i+j+k-n)(5i+3j+k+n) \\ &- 6\sum_{i=0}^{n-k}\left(\sum_{j=0}^{-i-k+n} f(i,j,k,n) b(\{i,j,k-1\}) e^{(2\alpha(i-k+2n+1)+2\beta_+(4i+3j+2(k-1)-n))}\right). \end{aligned} \tag{9.24}$$

We were able to change the range of our sum for i because (k-n-1-k+n)=-1 is below our starting value of j=0. Our next step is to insert (9.21) into (9.20) which after much simplification results in

$$
\begin{aligned}
&- 18\pi \sum_{i=0}^{n-k} \left(\sum_{j=0}^{-i-k+n} (3i+2j+k) b(\{i,j,k\}) e^{(2\alpha(i-k+2n+1)+2\beta_+(4i+3j+2k-n-2))} \right) \\
&+ 36\pi \sum_{i=0}^{n-k} \left(\sum_{j=0}^{-i-k+n} (i+j+k-n) b(\{i,j,k\}) e^{(2\alpha(i-k+2n+1)+2\beta_+(4i+3j+2k-n+1))} \right) \\
&- 6\Lambda \sum_{i=0}^{n-k} \left(\sum_{j=0}^{-i-k+n} (i+j+k-n) b(\{i,j,k\}) e^{(2\alpha(i-k+2n+2)+2\beta_+(4i+3j+2k-n+2))} \right) \\
&- 54\pi \sum_{i=0}^{n-k} \left(\sum_{j=0}^{-i-k+n} f(i,j,k,n) b(\{i,j,k-1\}) e^{(2\alpha(i-k+2n+1)+2\beta_+(4i+3j+2k-n-2))} \right) = 0.
\end{aligned}
\tag{9.25}
$$

For the second and third sum their coefficients vanish when $j = -i-k+n$, thus we can rewrite our kth 'excited' state transport equation for n to be

$$
\begin{aligned}
&- 18\pi \sum_{i=0}^{n-k} \left(\sum_{j=0}^{-i-k+n} (3i+2j+k) b(\{i,j,k\}) e^{(2\alpha(i-k+2n+1)+2\beta_+(4i+3j+2k-n-2))} \right) \\
&+ 36\pi \sum_{i=0}^{n-k-1} \left(\sum_{j=0}^{-i-k+n-1} (i+j+k-n) b(\{i,j,k\}) e^{(2\alpha(i-k+2n+1)+2\beta_+(4i+3j+2k-n+1))} \right) \\
&- 6\Lambda \sum_{i=0}^{n-k-1} \left(\sum_{j=0}^{-i-k+n-1} (i+j+k-n) b(\{i,j,k\}) e^{(2\alpha(i-k+2n+2)+2\beta_+(4i+3j+2k-n+2))} \right) \\
&- 54\pi \sum_{i=0}^{n-k} \left(\sum_{j=0}^{-i-k+n} f(i,j,k,n) b(\{i,j,k-1\}) e^{(2\alpha(i-k+2n+1)+2\beta_+(4i+3j+2k-n-2))} \right) = 0.
\end{aligned}
\tag{9.26}
$$

If we examine the first and fourth sums we see that their summation bounds are the same, the exponentials terms $e^{(2\alpha(i-k+2n+1)+2\beta_+(4i+3j+2k-n-2))}$ they contain are the same, and their coefficients do not vanish within the range which they are summed. Thus if we were to relate the variables $b(\{i,j,k\})$ and $b(\{i,j,k-1\}$ using only the first and fourth sum in (9.25) it is evident we would obtain a $\frac{1}{2}(1-k+n)(2-k+n) \times \frac{1}{2}(1-k+n)(2-k+n)$ diagonal matrix with a non zero determinant

$$\begin{bmatrix} -18\pi\ k & & \\ & \ddots & \\ & & -18\pi\ (3(n-k)+k) \end{bmatrix} \begin{bmatrix} b(\{0,0,k\}) \\ b(\{0,1,k\}) \\ \vdots \\ b(\{n-k,0,k\}) \end{bmatrix}$$

$$= \begin{bmatrix} 54\pi\ k(k-n-1)(k+n)b(\{0,0,k-1\}) \\ 54\pi\ k(k-n)(k+n+3)b(\{0,1,k-1\}) \\ \vdots \\ -54\pi\ k(5(n-k)+k+n)b(\{n-k,0,k-1\}) \end{bmatrix}$$

To prove that a solution of the form (9.21) exists for the kth quantum correction to the nth 'excited' state we must prove that the matrix associated with (9.26) always has a non-zero determinant when both k and n are positive integers, and $1 \leq k \leq n$. Luckily this isn't difficult. All the exponential terms that show up in the second and thirds sums in (9.26) are a subset of the exponentials that appear in the first and fourth sums. This is easy to see, for the second term in our sum if we were to reexpress j as (J-1) we would obtain

$$36\pi \sum_{i=0}^{n-k} \left(\sum_{J=1}^{-i-k+n} (i+J+k-n-1)b(\{i,J-1,k\})e^{(2\alpha(i-k+2n+1)+2\beta_+(4i+3J+2k-n-2))} \right) \tag{9.27}$$

which is a summation of the same exponential terms present in the first and fourth sums of (9.26), except that the range of the variable J which is being summed over is reduced. Hence only a subset of the exponentials which are summed in the first and fourth terms are present in the second term. The same can be easily shown for the 3rd term by substituting into i, I-1

$$-6\Lambda\sum_{\mathrm{I}=1}^{n-k}\left(\sum_{j=0}^{-\mathrm{I}-k+n}(\mathrm{I}+j+k-n-1)b(\{\mathrm{I}-1,j,k\})e^{(2\alpha(\mathrm{I}-k+2n+1)+2\beta_+(4\quad \mathrm{I}+3j+2k-n-2))}\right). \tag{9.28}$$

Now that we established that (9.26) can in principle be expressed as a system of $\frac{1}{2}(1-k+n)(2-k+n)$ linear equations, where the equations are grouped by the exponential term that the known $b(i,j,k-1)$ and unknown $b(i,j,k)$ coefficients are multiplied to; our next task is to deduce the characteristics of the matrix which represents this system. We aim to prove that this matrix is always invertible for the values of n and k we are exclusively considering. To accomplish this we will explicitly write out the matrix elements and show that they clearly are the elements of a triangular matrix with non vanishing diagonal elements.

If we start with the first sum in (9.26) we see that initially the number of terms which are summed are n-k+1 when i=0, then n-k when i=1, then n-k-1 when i=2,etc...; this pattern continues until the single i=n-k term $b(\{n-k,0,k\})$ is summed. With this information for each kth quantum correction we aim to relabel our $b(\{i,j,k\})$ using only a single index $b(\{x(i,j),k\})$ that is a function of both i and j and monotonically increases in units of one by noticing that when the subsequent i index increases by one, then one less term is summed in the j index. Thus to relabel our sum we want to find a labeling scheme such that for every summation over i starting with i=1 we add (-i-k+n+2) to our index $x(i,j)$ before summing over j again. This can be found by solving this recursion relation $\{f(i+1)=f(i)-i-k+n+1, f(0)=0\}$ which yields $-\frac{1}{2}i(i+2k-2n-3)$. This allows us to rewrite the first sum in (9.26) as

$$-18\pi\sum_{i=0}^{n-k}\left(\sum_{j=0}^{-i-k+n}(3i+2j+k)b(\{j-\frac{1}{2}i(i+2k-2n-3),k\})e^{(2\alpha(i-k+2n+1)+2\beta_+(4i+3j+2k-n-2))}\right), \tag{9.29}$$

and subsequently define the diagonal elements of our matrix as

$$M_{\left\{j-\frac{1}{2}i(i+2k-2n-3)+1,j-\frac{1}{2}i(i+2k-2n-3)+1\right\}} = -18 \ \ \pi \ (3i+2j+k) \tag{9.30}$$

For the second term using our aforementioned relabeling of $b(\{i,j,k\})$ and replacing j with J-1 we obtain

$$g(i,J,k,n) = (i+J+k-n-1)$$
$$36\pi \sum_{i=0}^{n-k}\left(\sum_{J=1}^{-i-k+n} g \ e^{(2(\alpha(i-k+2n+1)+\beta_+(4i+3J+2k-n-2)))} b\left(\left\{J-\frac{1}{2}i(i+2 \ \ k-2n-3)-1,k\right\}\right)\right). \tag{9.31}$$

Because the labels of $b(\{x(i,j),k\})$ in (9.29) and (9.31) differ by 1 in our labeling scheme, the terms which correspond to (9.31) are off diagonal terms to the left of the diagonal terms of (9.29). In other words the coefficients of $b(\{x(i,j),k\})$ which are multiplied to the same exponential $e^{(2(\alpha(i-k+2n+1)+\beta_+(4i+3J+2k-n-2)))}$ differ between (9.29) and (9.31) by 1 in $x(i,j)$, thus the terms in (9.31) appears either right before the diagonal terms of (9.29) or not at all because not all of the exponents in (9.29) are summed in (9.31). These one space to the left non diagonal terms are

$$M_{\left\{J-\frac{1}{2}i(i+2k-2n-3)+1,J-\frac{1}{2}i(i+2k-2n-3)\right\}} = 36\pi \ (i+J+k-n-1). \tag{9.32}$$

For the third and final sum we need to consider for our matrix, all of the terms are also to the left of our diagonal terms (9.29). This can be shown by expressing the coefficients in $b(\{x(i,j),k\})$ (9.28) as $b\left(\left\{j-\frac{1}{2}(\mathrm{I}-1)(\mathrm{I}+2k-2n-4),k\right\}\right)$. In relation to the diagonal elements (9.29) these elements will be $-i-k+n+2$ terms to the left

$$M_{\left\{j-\frac{1}{2}I(I+2k-2n-3)+1,j-\frac{1}{2}(\mathrm{I}-1)(\mathrm{I}+2k-2n-4)+1\right\}} = -6\Lambda(\mathrm{I}+j+k-n-1). \qquad (9.33)$$

All of the other elements in our matrix besides (9.33), (9.32), and (9.30) vanish, leaving us with a triangular matrix with non vanishing diagonal elements. Hence we have proved that the system of linear equations for the coefficients for the kth quantum correction to the nth 'excited' states (9.21) are always uniquely solvable. We can obtain explicit values of the $b(\{i,j,0\})$ coefficients from our ϕ_0 (9.17), which enable us to solve the system of linear equations for $b(\{i,j,1\})$, whose solutions allow us to solve for the system of linear equations for $b(\{i,j,2\})$ and etc all the way up to the coefficients $b(\{i,j,n\})$ for the nth quantum correction. Afterwards the rest of the higher order transport equations can be satisfied by zero and thus we can write out a closed form solution for the nth 'excited' state to the Taub WDW equation when $\Lambda \neq 0$.

This concludes our proof for the existence of a countably infinite number of 'excited' states for the Taub models when a cosmological constant is present. Before moving on we should reflect on what the Euclidean-signature semi-classical method has afforded us. Using our modified semi-classical we were able to solve a problem which up to this point has not been solved in closed form using elementary functions. The Taub WDW equation when a cosmological constant is present is not separable PDE, thus it is a non-trivial equation to solve.

By using the Euclidean-signature equations that our modified semi-classical gave us, we were able to prove the existence of solutions to a non-trivial Lorentzian signature PDE without having to perform a Wick rotation. Our ability to construct this proof and obtain our closed form solutions using these Euclidean-signature equations suggests that there is some property inherent in our equations which makes

them easier to solve than their Lorentzian signature counterparts. Thus the success of this method in proving the existence of a countably infinite number of 'excited' states for the Taub models when a cosmological constant is present further motivates applying this method to even more formidable Lorentizan signature problems, such as the functional WDW equation and, Bosonic and Yang Mills [164, 165, 177] field theories.

As previously mentioned, we already have completed both steps one and two for proving the existence of a countably infinite number of solutions to the Taub WDW equation both a cosmological constant and aligned electromagnetic field are present. Because we have a closed form ϕ_0 and 'ground' state solution to the Taub WDW equation when both matter sources are present it is reasonable to assume that a modification of the steps we just performed to obtain the main result of this chapter and arguably of the second portion of this dissertation can be used to prove the existence the aforementioned 'excited' states. Thus we conjecture that a countably 'infinite' number of 'excited' states do exist for the quantum Taub models when both previously mentioned matter sources are present for the operator ordering we choose in this thesis.

We will attach in the appendix a Mathematica code which has as its only input the positive integer 'n' and gives all 'n' non trivial quantum corrections to the nth 'excited' state and its corresponding closed form solution. Using similar techniques and reasoning to our proof, one can find a simpler ansatz for the quantum corrections for the case when $\Lambda = 0$.

$$\phi_k := e^{4\alpha n - 2\alpha k} \sum_{j=0}^{n-k} e^{-6\beta_+ j - 2\beta_+ k + 4\beta_+ n} \quad b_{\{j,k\}} \tag{9.34}$$

The advantage of this simpler ansatz is that it allows us to write a code which we will also include in the appendix that is able to compute exact closed form 'excited' state solutions to the Taub WDW equation far faster than the code which uses the

$\Lambda \neq 0$ ansatz.

Below are the explicit quantum corrections to the first five 'excited' states generated by our code.

$$\begin{aligned} \phi_1 &:= 54\pi\ e^{2(\alpha+\beta_+)} \\ \phi_{k>1} &:= 0 \end{aligned} \tag{9.35}$$

$$\begin{aligned} \phi_2 &:= 17496\pi^2 e^{4(\alpha+\beta_+))} \\ \phi_1 &:= \frac{459}{2}\pi\ \Lambda e^{8\alpha+8\beta_+} - 1944\pi^2 e^{6\alpha+6\beta_+} + 1458\pi^2 e^{6\alpha} \\ \phi_{k>2} &:= 0 \end{aligned} \tag{9.36}$$

$$\begin{aligned} \phi_3 &:= 14171760\pi^3 e^{6(\alpha+\beta_+)} \\ \phi_2 &:= 144342\pi^2\Lambda e^{10\alpha+10\beta_+} + 787320\pi^3 e^{8\alpha+2\beta_+} - 1180980\pi^3 e^{8\alpha+8\beta_+} \\ \phi_1 &:= \frac{1053}{2}\pi\ \Lambda^2 e^{14\alpha+14\beta_+} + \frac{15309}{2}\pi^2\Lambda e^{12\alpha+6\beta_+} - \frac{18225}{2}\pi^2\Lambda e^{12\alpha+12\beta_+} \\ &\quad + 26244\pi^3 e^{10\alpha-2\beta_+} - 65610\pi^3 e^{10\alpha+4\beta_+} + 39366\pi^3 e^{10\alpha+10\beta_+} \\ \phi_{k>3} &:= 0 \end{aligned} \tag{9.37}$$

$$\begin{aligned} \phi_4 &:= 21427701120\pi^4 e^{8(\alpha+\beta_+)} \\ \phi_3 &:= 892820880\pi^4 e^{10\alpha+4\beta_+} - 1428513408\pi^4 e^{10\alpha+10\beta_+} + 178564176\pi^3\Lambda e^{12\alpha+12\beta_+} \\ \phi_2 &:= -59521392\pi^4 e^{12\alpha+6\beta_+} + 39680928\pi^4 e^{12\alpha+12\beta_+} + 21257640\pi^4 e^{12\alpha} \\ &\quad + \frac{1121931}{2}\pi^2\Lambda^2 e^{4(4\alpha+4\beta_+)} + 7164612\pi^3\Lambda e^{14\alpha+8\beta_+} - 9447840\pi^3\Lambda e^{14\alpha+14\beta_+} \\ \phi_1 &:= 393660\pi^4 e^{14\alpha-4\beta_+} - 1417176\pi^4 e^{14\alpha+2\beta_+} + 1653372\pi^4 e^{14\alpha+8\beta_+} - 629856\pi^4 e^{14\alpha+14\beta_+} \\ &\quad + 945\pi\ \ \Lambda^3 e^{20\alpha+20\beta_+} + 21870\pi^2\Lambda^2 e^{18\alpha+12\beta_+} - 24786\pi\ \ {}^2\Lambda^2 e^{18\alpha+18\beta_+} \\ &\quad + 164025\pi^3\Lambda e^{16\alpha+4\beta_+} - 380538\ \ \pi^3\Lambda e^{16\alpha+10\beta_+} + 216513\pi^3\Lambda e^{16\alpha+16\beta_+} \\ \phi_{k>4} &:= 0 \end{aligned} \tag{9.38}$$

$$\phi_5 := 52069313721600\pi^5 e^{10(\alpha+\beta_+)}$$

$$\phi_4 := 1735643790720\pi^5 e^{6(2\alpha+\beta_+)} - 2892739651200\pi^5 e^{12\alpha+12\beta_+} + 367332019200\pi^4\Lambda e^{14\alpha+14\beta_+}$$

$$\phi_3 := 32141551680\pi^5 e^{2(7\alpha+\beta_+)} - 96424655040\pi^5 e^{14\alpha+8\beta_+} + 68874753600\pi^5 e^{14\alpha+14\beta_+}$$
$$+ 1014166575\pi^3\Lambda^2 e^{18\alpha+18\beta_+} + 11861763120\pi^4\Lambda e^{16\alpha+10\beta_+} - 16740391500\pi^4\Lambda e^{16\alpha+16\beta_+}$$

$$\phi_2 := \frac{3072735}{2}\pi^2\Lambda^3 e^{22\alpha+22\beta_+} + \frac{63871335}{2}\pi^3\Lambda^2 e^{20\alpha+14\beta_+}$$
$$- \frac{78830415}{2}\pi^3\Lambda^2 e^{20\alpha+20\beta_+} + 212576400\pi^4\Lambda\ e^{18\alpha+6\beta_+}$$
$$- 542069820\pi^4\Lambda\ e^{18\alpha+12\beta_+} + 336579300\pi^4\Lambda\ e^{18\alpha+18\beta_+} + 446410440\pi^5 e^{16\alpha-2\beta_+}$$
$$- 1785641760\pi^5 e^{16\alpha+4\beta_+} + 2295825120\pi^5 e^{16\alpha+10\beta_+} - 956593800\pi^5 e^{16\alpha+16\beta_+}$$

$$\phi_1 := 1485\pi\ \Lambda^4 e^{26\alpha+26\beta_+} + 47385\pi^2\Lambda^3 e^{24\alpha+18\beta_+} - 52245\pi^2\Lambda^3 e^{24\alpha+24\beta_+} + 557685\pi^3\Lambda^2 e^{22\alpha+10\beta_+}$$
$$- 1246590\pi^3\Lambda^2 e^{22\alpha+16\beta_+} + 688905\pi^3\Lambda^2 e^{22\alpha+22\beta_+} + 2854035\pi^4\Lambda\ e^{20\alpha+2\beta_+}$$
$$- 9743085\pi^4\Lambda\ e^{20\alpha+8\beta_+} + 10924065\pi^4\Lambda e^{20\alpha+14\beta_+} - 4035015\pi^4\Lambda e^{20\alpha+20\beta_+} + 5314410\pi^5 e^{18\alpha-6\beta_+}$$
$$+ 42515280\pi^5 e^{18\alpha+6\beta_+} - 31886460\pi^5 e^{18\alpha+12\beta_+} + 8857350\pi^5 e^{18\alpha+18\beta_+} - 24800580\pi^5 e^{18\alpha}$$

$$\phi_{k>5} := 0$$

(9.39)

The first three plots(figs 9.4a-9.4c) are of a superposition of the first five closed form 'excited' states ψ_n and the 'ground state $\left(\sum_{n=0}^{5} e^{-n^2}\psi_n\right)^2$ for three different value of α.

The last three plots(figs 9.5a-9.5c) are semi-classical 'excited' states with both of our matter sources constructed using (9.16) $\left(\sum_{n=0}^{5} e^{-1.5(n+1.1)^2}\phi_0\Psi_{matter}\right)^2$ for a fixed value of α for three different values of b. We will discuss the qualitative properties of these plots in our discussion section towards the end of this chapter.

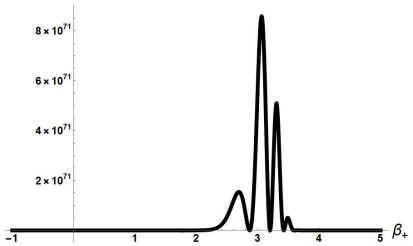

(a) $\alpha = -2 \quad \Lambda = -1$

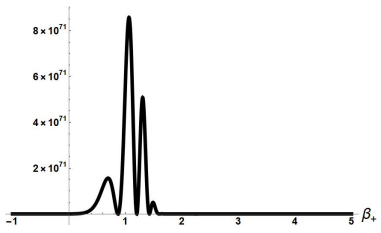

(b) $\alpha = 0 \quad \Lambda = -1$

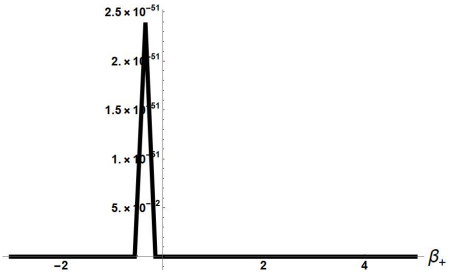

(c) $\alpha = 2.5 \quad \Lambda = -1$

Figure 9.4 Superposition $\left(\sum_{n=0}^{5} e^{-n^2}\psi_n\right)^2$ of the first five closed form 'excited' states ψ_n and the 'ground state for three different value of α.

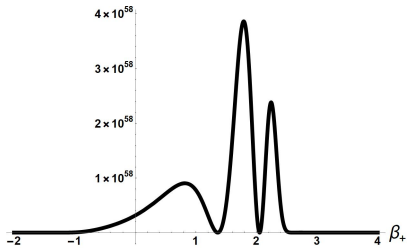

(a) $\alpha = -1 \quad \Lambda = -1 \quad b = 0$

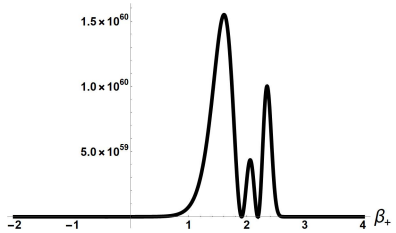

(b) $\alpha = -1 \quad \Lambda = -1 \quad b = 1.5$

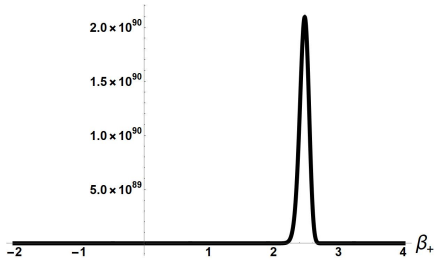

(c) $\alpha = -1 \quad \Lambda = -1 \quad b = 5$

Figure 9.5 Plots of $\left(\sum_{n=0}^{5} e^{-1.5(n+1.1)^2}\phi_0\Psi_{matter}\right)^2$ where Ψ_{matter} is (9.7) and ϕ_0 is (9.16) for three different values of b.

9.4 Quantum Taub 'Wormhole' Model Via Euclidean-Signature semi-classical Method

The goal of this section will be to prove the existence of asymptotic solutions $\overset{(0)}{\Psi}_{\hbar}= e^{-\mathcal{S}_{(0)}-\mathcal{S}_{(1)}-\frac{1}{2!}\mathcal{S}_{(2)}-\cdots}$ to the Taub WDW equation for arbitrary Hartle-Hawking ordering parameter B. Beginning with the 'wormhole' $\mathcal{S}_{(0)}$ and the following $\mathcal{S}_{(1)}$

$$\begin{aligned} \mathcal{S}_{(0)}^{wh} &:= \frac{1}{6}\left(2e^{6\beta_+}+1\right)e^{2\alpha-4\beta_+}, \\ \mathcal{S}_{(1)}^{wh} &:= \left(-\frac{\mathrm{B}}{2}-1\right)\alpha-\beta_+. \end{aligned} \tag{9.40}$$

We will integrate the transport equations along the classical Hamilton Jacobi flows which are produced by (9.40) and use them to show via induction that smooth and globally defined solutions exist for all of the higher order $k \geq 2$ transport equations.

Upon setting $c = 1, G = 1$, and $L = 1$ if we were to apply standard variational techniques to the Einstein-Hilbert action

$$I_{EH} = \frac{1}{16\pi}\int_{\Omega}\sqrt{-\det g}\,(R\,(g_{ab}))\,d^4x \tag{9.41}$$

for the metric (9.1) we would derive the following action

$$I_{\mathrm{ADM}} = \int_I dt\left\{p_\alpha\dot{\alpha}+p_{\beta_+}\dot{\beta}_+ - N\mathcal{H}_\perp\right\}, \tag{9.42}$$

where

$$\mathcal{H}_\perp := \frac{(6\pi)^{1/2}}{4\ e^{3\alpha}}\left(\left(-p_\alpha^2+p_{\beta_+}^2\right)+\ e^{4\alpha}\left[\frac{e^{-8\beta_+}}{3}-\frac{4e^{-2\beta_+}}{3}\ \right]\right). \tag{9.43}$$

If we vary (9.42) with respect to the lapse N which acts as a Lagrange multiplier we obtain the familiar Hamiltonian constraint

$$\mathcal{H}_{\perp}\left(\alpha, \beta_{+}, p_{\alpha}, p_{\beta_{+}}\right) = 0. \tag{9.44}$$

An explicit demonstration of these standard variational techniques applied to the full Bianchi IX models which can trivially be repurposed for metric (9.1) as can be seen in [175].

It can be identified that our Hamililton Jacobi equation (8.51) when both Λ and b vanish is related the Euclidean-signature form of our Hamililtonian constraint

$$N_{\text{Eucl}}\, \mathcal{H}_{Eucl:=} N_{\text{Eucl}}\, \frac{(6\pi)^{1/2}}{4\ e^{3\alpha}} \left(\left(p_{\alpha}^{2} - p_{\beta_{+}}^{2}\right) +\ e^{4\alpha} \left[\frac{e^{-8\beta_{+}}}{3} - \frac{4e^{-2\beta_{+}}}{3} \right] \right) \tag{9.45}$$

by the substitution

$$\begin{aligned} p_{\alpha} &\rightarrow \frac{\partial \mathcal{S}_{(0)}^{wh}}{\partial \alpha}, \\ p_{\beta_{+}} &\rightarrow \frac{\partial \mathcal{S}_{(0)}^{wh}}{\partial \beta_{+}}. \end{aligned} \tag{9.46}$$

Keeping this in mind we can obtain the following differential equations for $\alpha(t)$ and $\beta_{+}(t)$

$$\begin{aligned} \dot{\alpha} &= \frac{(6\pi)^{1/2}}{2e^{3\alpha}} N_{\text{Eucl}}\, p_{\alpha}, \\ \dot{\beta}_{+} &= \frac{-(6\pi)^{1/2}}{2\ e^{3\alpha}} N_{\text{Eucl}}\, p_{\beta_{+}}, \end{aligned} \tag{9.47}$$

where p_{α} and $p_{\beta_{+}}$ are (9.46). We can easily obtain explicit solutions to these flow equations by exploiting our freedom to choose the lapse N_{Eucl} to be any smooth, globally defined nonvanishing function of the Misner variables. As we previously mentioned we have the freedom to choose N_{Eucl} because it acts as a choice of gauge which bestows a physical meaning to our evolution parameter "t". We require our lapse to not vanish in order to ensure that no catastrophic signature changes occur

in our space-time.

Via (9.46) and (9.40) we obtain

$$\begin{aligned} p_\alpha &= \frac{1}{3}\left(2e^{6\beta_+(t)}+1\right)e^{2\alpha(t)-4\beta_+(t)}, \\ p_{\beta_+} &= \frac{2}{3}\left(e^{6\beta_+(t)}-1\right)e^{2\alpha(t)-4\beta_+(t)}, \end{aligned} \tag{9.48}$$

which results in these flow equations for $\alpha(t)$ and $\beta_+(t)$ for general N_{Eucl}

$$\begin{aligned} \dot{\alpha} &= \sqrt{\frac{\pi}{6}}\left(2e^{6\beta_+(t)}+1\right)N_{\text{Eucl}}\, e^{-\alpha(t)-4\beta_+(t)} \\ \dot{\beta}_+ &= -\sqrt{\frac{2\pi}{3}}\left(e^{6\beta_+(t)}-1\right)N_{\text{Eucl}}\, \left(e^{-\alpha(t)-4\beta_+(t)}\right). \end{aligned} \tag{9.49}$$

If we set

$$N_{\text{Eucl}} = \sqrt{\frac{6}{\pi}}e^{\alpha(t)+4\beta_+(t)} \tag{9.50}$$

and insert it into our flow equations (9.49) we obtain

$$\begin{aligned} \dot{\alpha} &= 1+2e^{6\beta_+(t)}, \\ \dot{\beta}_+ &= 2-2e^{6\beta_+(t)}, \end{aligned} \tag{9.51}$$

which can be trivially solved resulting in

$$\begin{aligned} \alpha(t) &= \alpha_0+\frac{1}{6}\log\left(e^{6\beta_{+0}}\left(e^{12t}-1\right)+1\right)+t, \\ \beta_+(t) &= -\frac{1}{6}\log\left(\left(e^{-6\beta_{+0}}-1\right)e^{-12t}+1\right), \end{aligned} \tag{9.52}$$

where α_0 and β_{+0} are the initial values of α and β_+ when t=0. For the following allowable range of initial values $\alpha_0 \in (-\infty,\infty)$, $\beta_{+0} \in (-\infty,\infty)$ our solutions are globally defined and real when the evolution parameter t ranges from $(0,\infty)$. Classically these solutions are the flow in minisuperspace induced by (9.40), measured with respect to our evolution parameter whose physical meaning is derived from our choice of lapse (9.50). Our solutions for the evolution of α and β_+ (9.52) reveal

that the flow in minisuperspace induced by our 'wormhole' solution leads to some interesting geometrical implications for the Euclidean-signature form of our Taub space-time(9.1)

$$\begin{aligned} ds^2 &= N^2_{\text{Eucl}}\, dt^2 + e^{2\alpha(t)} \left(e^{2\beta(t)}\right)_{ab} \omega^a \omega^b \\ \left(e^{2\beta(t)}\right)_{ab} &= \text{diag}\left(e^{2\beta(t)_+}, e^{2\beta(t)_+}, e^{-4\beta(t)_+}\right). \end{aligned} \tag{9.53}$$

Regardless of our initial conditions (α_0, β_{+0}) when our evolution parameter $t \to \infty$, $\alpha \to \infty$ and $\beta_+ \to 0$. Geometrically this means our 'wormhole' flow induces in our metric (9.53) the following evolution; initially the space described by (9.53) has a finite radius dictated by α_0 and a certain amount of anisotropy determined by β_{+0}. However as our evolution parameter grows our space-time will approach a flat isotropic state due to the aforementioned $t \to \infty$ behavior of α and $\beta+$. It is because of this behavior that our $\mathcal{S}^{wh}_{(0)}$ is called the 'wormhole solution'. It should be noted that despite using Euclidean-signature Hamilton Jacobi flows; we are proving the existence of asymptotic solutions to the Lorentzian-signature Wheeler DeWitt equation.

Moving forward with our proof we will choose this natural looking ansatz as our form for the higher order $k \geq 2$ quantum corrections

$$S^{\text{wh}}_{(k)} = 6e^{-2(k-1)\alpha} \Sigma^{\text{wh}}_{(k)}\left(\beta_+\right). \tag{9.54}$$

In terms of this ansatz our 'wormhole' $\mathcal{S}^{wh}_{(0)}$ has the followings $\Sigma_{(0)}$

$$\Sigma^{\text{wh}}_{(0)} = \frac{1}{6}\left(e^{-4\beta_+} + 2e^{2\beta_+}\right) \tag{9.55}$$

so that

$$\mathcal{S}^{\text{wh}}_{(0)} = e^{2\alpha} \Sigma^{\text{wh}}_{(0)}\left(\beta_+\right). \tag{9.56}$$

Using (9.56), (9.55), (9.54), and (9.40) we can rewrite our $3 \geq k \geq 2$ transport

equations as

$$\frac{\partial\Sigma^{\rm wh}_{(0)}}{\partial\beta_+}\frac{\partial\Sigma^{\rm wh}_{(2)}}{\partial\beta_+}+4\Sigma^{\rm wh}_{(0)}\Sigma^{\rm wh}_{(2)}=-\frac{B^2}{4}, \tag{9.57}$$

$$\frac{\partial\Sigma^{\rm wh}_{(0)}}{\partial\beta_+}\frac{\partial\Sigma^{\rm wh}_{(3)}}{\partial\beta_+}+8\Sigma^{\rm wh}_{(0)}\Sigma^{\rm wh}_{(3)}=\frac{3}{2}\frac{\partial^2\Sigma^{\rm wh}_{(2)}}{\partial\beta_+^2}+3\frac{\partial\Sigma^{\rm wh}_{(2)}}{\partial\beta_+}, \tag{9.58}$$

and our $k\geq 4$ equations as

$$\frac{\partial\Sigma^{\rm wh}_{(0)}}{\partial\beta_+}\frac{\partial\Sigma^{\rm wh}_{(k)}}{\partial\beta_+}+4(k-1)\Sigma^{\rm wh}_{(0)}\Sigma^{\rm wh}_{(k)}=\sum_{l=2}^{k-2}\frac{k!\left(4(l-1)(k-l-1)\Sigma^{\rm wh}_{(l)}\Sigma^{\rm wh}_{(k-l)}-\frac{\partial\Sigma^{\rm wh}_{(l)}}{\partial\beta_+}\frac{\partial\Sigma^{\rm wh}_{(k-l)}}{\partial\beta_+}\right)}{2l!\quad(k-l)!}$$
$$-\frac{1}{2}k\left(-2\frac{\partial\Sigma^{\rm wh}_{(k-1)}}{\partial\beta_+}-\frac{\partial^2\Sigma^{\rm wh}_{(k-1)}}{\partial\beta_+^2}+4(k-3)(k-2)\Sigma^{\rm wh}_{(k-1)}\right). \tag{9.59}$$

When $\beta_+=0$, $\frac{\partial\Sigma^{\rm wh}_{(0)}}{\partial\beta_+}=\frac{2e^0}{3}-\frac{2}{3}e^0=0$ and $\Sigma^{\rm wh}_{(0)}(0)=\frac{1}{2}$. Thus we can sequentially write out $\Sigma^{\rm wh}_{(k)}(0)$ as follows

$$\Sigma^{\rm wh}_{(2)}(0)=-\frac{B^2}{8}, \tag{9.60}$$

$$\Sigma^{\rm wh}_{(3)}(0)=\frac{1}{4}\left[\frac{3}{2}\frac{\partial^2\Sigma^{\rm wh}_{(2)}}{\partial\beta_+^2}+3\frac{\partial\Sigma^{\rm wh}_{(2)}}{\partial\beta_+}\right](0), \tag{9.61}$$
$$etc\cdots$$

As the reader can verify using (9.51) and (9.55)

$$-3e^{4\beta_+}\left(\frac{\partial\Sigma^{\rm wh}_{(0)}}{\partial\beta_+}\frac{\partial\Sigma^{\rm wh}_{(k)}}{\partial\beta_+}\right)=\frac{d\Sigma^{\rm wh}_{(k)}}{dt}, \tag{9.62}$$

which allows us to convert (9.57), (9.58) and (9.59) into

$$\frac{d\Sigma^{\rm wh}_{(k)}}{dt}+4\left(-e^{6\beta_+}-\frac{1}{2}\right)(k-1)\Sigma^{\rm wh}_{(k)}=\frac{d\Sigma^{\rm wh}_{(k)}}{dt}-2\frac{d\alpha}{dt}(k-1)\Sigma^{\rm wh}_{(k)}=\Lambda_k \tag{9.63}$$

where Λ_k denotes the right hand side of the original equations (9.57), (9.58), or (9.59) multiplied by $-3e^{4\beta_+}$. If we start with k=2 and integrate (9.63) we obtain

$$\Sigma^{\rm wh}_{(2)}(\beta_+(t) = e^{2\alpha(t)}\left(\Sigma^{\rm wh}_{(2)}(\beta_{+0}) + \int_1^t \frac{3}{4}{\rm B}^2 e^{4\beta_+(s)-2\alpha(s)}\,ds\right). \tag{9.64}$$

As we previously established as $t \to \infty$ so does $\alpha(t)$. Thus in order to ensure that our quantum corrections $\mathcal{S}_{(k\geq 2)}$ are smooth and globally defined we must use our freedom to pick $\Sigma^{\rm wh}_{(2)}(\beta_{+0})$ so that the term proportional to $e^{2\alpha(t)}$ vanishes as $t \to \infty$. Because our range of t is from $(0, \infty)$, in order for our term which is proportional to $e^{2\alpha(t)}$ to vanish we must equate

$$\Sigma^{\rm wh}_{(2)}(\beta_{+0}) = -\int_1^\infty \frac{3}{4}{\rm B}^2 e^{4\ \ \beta_+(s)-2\alpha(s)}\,ds. \tag{9.65}$$

This choice of $\Sigma^{\rm wh}_{(2)}(\beta_{+0})$ allows us to rewrite (9.64) as

$$\Sigma^{\rm wh}_{(2)}(\beta_+(t)) = -e^{2\alpha(t)}\left(\int_t^\infty \frac{3}{4}{\rm B}^2 e^{4\ \ \beta_+(s)-2\alpha(s)}\,ds\right). \tag{9.66}$$

which facilitates us using L'H$\hat{o}$pital's rule to show that the desired limit (9.60) as $t \to \infty$ is reached

$$\begin{aligned}
&-\frac{\left(\int_t^\infty \frac{3}{4}{\rm B}^2 e^{4\ \ \beta_+(s)-2\alpha(s)}\,ds\right)}{e^{-2\alpha(t)}},\\
&-\frac{\frac{3}{4}{\rm B}^2 e^{4\ \ \beta_+(t)-2\alpha(t)}}{2\dot{\alpha}e^{-2\alpha(t)}},\\
&-\frac{\frac{3}{4}{\rm B}^2 e^{4\ \ \beta_+(t)}}{2\dot{\alpha}},\\
&\lim_{t\to\infty}\Sigma^{\rm wh}_{(2)}(\beta_+(t)) = \lim_{t\to\infty} -\frac{\frac{3}{4}{\rm B}^2 e^{4\ \ \beta_+(t)}}{2\dot{\alpha}} = -\frac{B^2}{8},
\end{aligned} \tag{9.67}$$

where $\lim_{t\to\infty}\beta_+(t) = 0$. The reader can easily verify the $\lim_{t\to\infty}\dot{\alpha} = 3$. After

inserting our expressions for $\alpha(t)$ and $\beta_+(t)$ into (9.65)

$$\Sigma^{\text{wh}}_{(2)}(\beta_{+0}) = -\int_1^\infty \frac{3\text{B}^2 e^{-2(\alpha_0+s)}}{4\left(\left(e^{-6\beta_{+0}}-1\right)e^{-12s}+1\right)^{2/3}\sqrt[3]{e^{6\beta_{+0}}\left(e^{12\ \ s}-1\right)+1}}ds \tag{9.68}$$

we can verify that $\Sigma^{\text{wh}}_{(2)}$ is smooth and globally defined by observing that as long as β_{+0} is real that taking the derivative of (9.68) an arbitrary number of times with respect to β_{+0} does not disturb the convergence of this integral(9.68). The $e^{-2\alpha_0}$ is a constant which could have been absorbed into $\Sigma^{\text{wh}}_{(2)}(\beta_{+0})$.

Now that we have shown that $\Sigma^{\text{wh}}_{(2)}$ is smooth and globally defined we can move on to computing the higher order $\Sigma^{\text{wh}}_{(k)}$ terms. Assuming that $\left\{\Sigma^{\text{Wh}}_{(2)},\ldots,\Sigma^{\text{Wh}}_{(k-1)}\right\}$, for $k\geq 2$ have been shown to be smooth and globally defined we can express $\Sigma^{\text{wh}}_{(k)}$ as

$$\Sigma^{\text{wh}}_{(k)}(\beta_+(t)) = e^{2(k-1)\alpha(t)}\left(\Sigma^{\text{wh}}_{(k)}(\beta_{+0}) + \int_1^t e^{-2(k-1)\alpha(s)}\Lambda_{(k)}(s)\ ds\right). \tag{9.69}$$

There is only one choice for $\Sigma^{\text{wh}}_{(k)}(\beta_{+0})$ which allows the kth quantum correction to be smooth and globally defined

$$\Sigma^{\text{wh}}_{(k)}(\beta_{+0}) = -\int_1^\infty e^{-2(k-1)\alpha(s)}\Lambda_{(k)}(s)\ ds. \tag{9.70}$$

Via inspection of (9.58) and (9.59) it can be concluded that our $\Lambda_{(k)}$ term is solely composed of a sum of our aforementioned smooth and globally defined functions $\left\{\Sigma^{\text{Wh}}_{(2)},\ldots,\Sigma^{\text{Wh}}_{(k-1)}\right\}$ and their derivatives with respect to β_+, multiplied by the smooth and globally defined function $-3e^{4\beta_+(t)}$. Thus our source terms for our transport $\Sigma^{\text{wh}}_{(k)}$ equations are always globally defined. Furthermore because of the exponential decay of $e^{-2(k-1)\alpha(s)}$ for $k\geq 2$ as $s\to\infty$, our integral (9.70) always converges and is smooth and globally defined. Using this choice of $\Sigma^{\text{wh}}_{(k)}(\beta_{+0})$ we can rewrite (9.69) as

$$\Sigma^{\mathrm{wh}}_{(k)}(\beta_{+}(t)) = -e^{2(k-1)\alpha(t)}\left(\int_{t}^{\infty} e^{-2(k-1)\alpha(s)}\Lambda_{(k)}(s)ds\right), \tag{9.71}$$

which allows one to easily apply L'Hôpital's rule to show that the desired limit as $\beta_{+} \rightarrow 0$ when $t \rightarrow \infty$ is achieved. If we were to insert our expressions for $\alpha(t)$ into (9.71) it would be straightforward to conclude that arbitrary differentiation with respect to β_{+0} does not disturb its convergence and that (9.71) remains smooth and globally defined.

This conclude ours proof by induction that smooth and globally defined solutions exist for arbitrary ordering parameter B for all of the 'ground' state quantum corrections of the form (9.54) when (9.55), (9.56), and (9.40) hold. In the process we have also proved the existence of a full asymptotic solution of the form $\overset{(0)}{\Psi}_{\hbar} = e^{-\mathcal{S}_{(0)}-\mathcal{S}_{(1)}-\frac{1}{2!}\mathcal{S}_{(2)}-\cdots}$ for any arbitrary ordering parameter. Hopefully the nature of the convergence of this asymptotic solution can be explored in a future work. For information on how to prove that the quantum corrections associated with the 'excited' state transport equations are smooth and globally defined we refer the reader to section 5 of [175] and to the references contained within it.

Even though the vacuum quantum Taub models are solvable [166] using separation of variables for any ordering parameter, it isn't trivial to obtain solutions which possess the forms of (8.46) and (8.57). Via ordinary separation of variables the Taub WDW equation admits two Bessel functions as its solutions which in principle can be used to construct all of the solutions of the quantum Taub models via superposition. However only a limited number of integrals involving Bessel function are known in closed form. In addition even if one can evaluate those integrals numerically there is still the issue of using the correct kernel to obtain wave functions which possess non-trivial characteristics.

These non-trivial characteristics include the wave function's behavior being dependent upon α which as was previously mentioned is our internal clock and also

dictates the size of our Taub universes. Another non-trivial feature is the manifestation of discreteness in our wave functions which is showcased in our 'excited' states that we have computed thus far. The Euclidean-signature semi-classical method is able to bypass the aforementioned difficulties and obtain closed form wave functions which possess these non-trivial characteristics.

We went through the trouble of integrating the transport equations along the flow generated by $\mathcal{S}^{wh}_{(0)}$ in order to prove that smooth and globally defined solutions exist for all of them. However due to the mathematical simplicity present in the quantum Taub models we can directly solve for an arbitrary kth level quantum correction $\mathcal{S}^{wh}_{(k)}(\alpha,\beta_+)$ by solving elementary differential equations. The explicit form of the $\mathcal{S}^{wh}_{(2)}(\alpha,\beta_+)$ transport equation when our ansatz (9.53) is employed is

$$8e^{-4\beta_+}\left(\frac{\partial\Sigma^{\mathrm{wh}}_{(2)}}{\partial\beta_+}-e^{6\beta_+}\left(\frac{\partial\Sigma^{\mathrm{wh}}_{(2)}}{\partial\beta_+}+2\Sigma^{\mathrm{wh}}_{(2)}\right)-\Sigma^{\mathrm{wh}}_{(2)}\right)-3\mathrm{B}^2=0; \tag{9.72}$$

which can be easily solved, yielding

$$\mathcal{S}^{wh}_{(2)}(\alpha,\beta_+):=e^{-2\alpha}\left(\frac{e^{\beta_+}\mathrm{B}^2\sin^{-1}\left(e^{3\beta_+}\right)}{8\sqrt{1-e^{6\ \ \beta_+}}}+\frac{e^{\beta_+}c_1}{\sqrt{1-e^{6\beta_+}}}\right). \tag{9.73}$$

This expression is only smooth and globally defined when a specific value of c_1 is chosen. As $\beta_+\to 0$ the first term of (9.73) which is proportional to $\frac{1}{\sqrt{1-e^{6\beta_+}}}$ approaches $\frac{B^2\pi}{16}$. In order for (9.73) to not blow up we must ensure that $\frac{1}{8}e^{\beta_+}\mathrm{B}^2\sin^{-1}\left(e^{3\beta_+}\right)+e^{\beta_+}c_1$ vanishes when $\beta_+\to 0$, which is accomplished if we set $c_1=-\frac{B^2\pi}{16}$. This results in the following $k=2$ quantum correction

$$\mathcal{S}^{wh}_{(2)}(\alpha,\beta_+):=-e^{-2\alpha}\left(\frac{e^{\beta_+}\mathrm{B}^2\cos^{-1}\left(e^{3\beta_+}\right)}{8\sqrt{1-e^{6\beta_+}}}\right) \tag{9.74}$$

which has the established limit (9.60) when $\beta_+\to 0$ as the reader can verify.

Thanks to the existence and uniqueness theorem for ordinary differential equations, each one of our solutions to the 'ground' state transport equations we found by

integrating along the flow of $\mathcal{S}^{wh}_{(0)}$ are equivalent to the explicit solutions of those same transport equations as long as they are smooth and globally defined. Because we were able to show that picking the right integration constant for a particular $\mathcal{S}^{wh}_{(k)}$ results in it being a smooth and globally defined function, we know that we can obtain smooth and globally defined explicit solutions such as (9.73) by picking a unique constant of integration. Thus all of our results regarding smooth and globally defined solutions to the 'ground' state transport equations we previously obtained also apply to our explicit solutions.

Our $\mathcal{S}^{wh}_{(2)}$ quantum correction has the interesting property that it is undefined in the real plane when $\beta_+ > 0$ due to the domain of $\cos^{-1}\left(e^{3\beta_+}\right)$. However $\cos^{-1}\left(e^{3\beta_+}\right)$ can be analytically continued into the complex plane by expressing it as an integral

$$\cos^{-1}\left(e^{3\beta_+}\right) := \int_{-\infty}^{\beta_+} \frac{3e^{3x}}{\sqrt{1-e^{6x}}}\, dx - \frac{\pi}{2}. \tag{9.75}$$

Despite analytically continuing $\cos^{-1}$ into the complex plane the quantum corrections we computed thus far remain real valued functions because every instance of $\cos^{-1}\left(e^{3\beta_+}\right)$ is multiplied by a term which becomes complex valued when $\beta_+ > 0$, which ultimately results in a real expression.

We can go further and explicitly compute the 'ground' state $k = 3$ quantum correction which is

$$\begin{aligned} f &= \frac{\mathrm{B}^2 e^{-4\alpha+2\beta_+}}{32\left(1-e^{6\beta_+}\right)^{5/2}} \\ \mathcal{S}^{wh}_{(3)}(\alpha,\beta_+) &:= f\Bigg(2e^{6\beta_+}\sqrt{1-e^{6\beta_+}}\mathrm{B}\cos^{-1}\left(e^{3\beta_+}\right)^2 + 2\sqrt{1-e^{6\beta_+}}\mathrm{B}\cosh^{-1}\left(e^{3\beta_+}\right)^2 \\ &+ 3\sqrt{1-e^{6\beta_+}}\left(e^{6\beta_+}-4\right) - 3e^{3\beta_+}\left(2e^{6\beta_+}-5\right)\cos^{-1}\left(e^{3\beta_+}\right)\Bigg) \end{aligned} \tag{9.76}$$

and in principle compute further more complicated explicit expressions for the higher order 'ground' state quantum corrections.

We will now move on and compute the $\phi^{wh}_{(2)}$ quantum correction for the first and second 'excited' states of the wormhole quantum Taub models. We will seek 'excited' state quantum corrections which possess the form

$$\phi^{wh}_{(k)} = e^{(4n-2k)\alpha}\chi_{(k)}\left(\beta_+\right). \tag{9.77}$$

For our $\phi^{wh}_{(0)}$ we will use $\left(\left(e^{6\beta_+}-1\right)e^{4\alpha-2\beta_+}\right)^n$, and when n=1 our $\phi_{(1)}$ is $-6e^{2(\alpha+\beta_+)}$. Thus using (9.74) we can write out the $\phi^{wh}_{(2)}$ transport equation for the first 'excited' wormhole state

$$9e^{3\beta_+}\mathrm{B}^2\left(\sqrt{1-e^{6\beta_+}}\left(e^{3\beta_+}+2e^{9\beta_+}\right)+\left(1-4e^{6\beta_+}\right)\cos^{-1}\left(e^{3\beta_+}\right)\right)=8\ \left(1-e^{6\beta_+}\right)^{5/2}\frac{\partial\chi_{(2)}}{\partial\beta_+}, \tag{9.78}$$

whose solution is

$$\phi^{wh}_2=\chi_{(2)}=-\frac{3\mathrm{B}^2\left(e^{6\beta_+}+e^{3\beta_+}\sqrt{1-e^{6\beta_+}}\left(2e^{6\beta_+}-1\right)\cos^{-1}\left(e^{3\beta_+}\right)-1\right)}{8\left(e^{6\ \ \beta_+}-1\right)^2}. \tag{9.79}$$

For $n=2$, $\phi^{wh}_1=-6e^{6\alpha}\left(4e^{6\beta_+}-3\right)$, which allows us to write down the following $\phi^{wh}_{(2)}$ equation for the second 'excited' state

$$\begin{aligned}&9e^{\beta_+}\left(e^{3\beta_+}\sqrt{1-e^{6\beta_+}}\left(\left(2e^{6\ \beta_+}+1\right)\mathrm{B}^2-576\right)-\left(4e^{6\ \beta_+}-1\right)\mathrm{B}^2\cos^{-1}\left(e^{3\ \ \beta_+}\right)\right)\\&+4\sqrt{1-e^{6\ \beta_+}}\left(e^{6\ \beta_+}\left(4\chi_{(2)}(\beta_+)-\frac{\partial\chi_{(2)}}{\partial\beta_+}\right)+\frac{\partial\chi_{(2)}}{\partial\beta_+}+2\chi_{(2)}(\beta_+)\right)=0,\end{aligned} \tag{9.80}$$

whose solution allows us to write the following as our $\phi^{wh}_{(2)}$ quantum correction for the

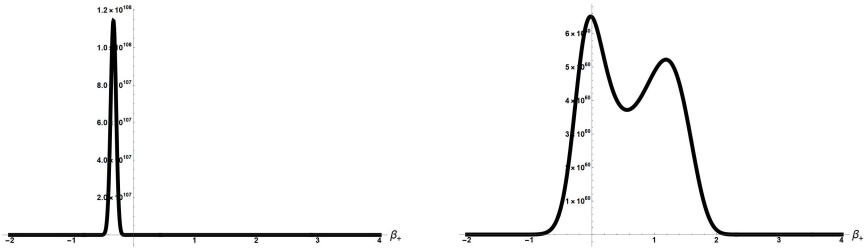

(a) $\alpha = -2 \quad B = -1$ **(b)** $\alpha = -1.1 \quad B = -1$

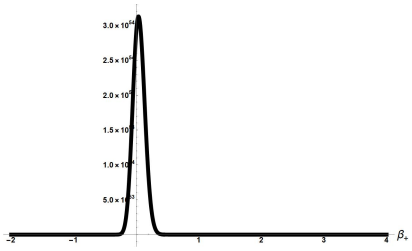

(c) $\alpha = 1 \quad B = -1$

Figure 9.6 Plots of $\left|\psi^{wh}\right|^2$ for the 'wormhole' vacuum quantum Taub 'ground' state constructed out of $\mathcal{S}^{wh}_{(0)}$, $\mathcal{S}^{wh}_{(1)}$,$\mathcal{S}^{wh}_{(2)}$, and $\mathcal{S}^{wh}_{(3)}$.

second 'excited' state for arbitrary Hartle-Hawking ordering parameter B

$$\phi^{wh}_{(2)} = e^{4\alpha}\frac{3e^{-2\beta_+}\left(\left(e^{6\beta_+}-1\right)\left(288-\mathrm{B}^2\right)-e^{3\beta_+}\sqrt{1-e^{6\beta_+}}\left(2e^{6\beta_+}-1\right)\mathrm{B}^2\cos^{-1}\left(e^{3\beta_+}\right)\right)}{4\left(e^{6\beta_+}-1\right)}. \tag{9.81}$$

In principle with the help of a computer algebraic system we can continue to find closed form quantum corrections for the 'ground' state equations and then use those quantum corrections to find additional quantum corrections for the 'excited' state transport equations.

Below we will plot 'ground' and 'excited' states for our 'wormhole' wave functions which include our analytically continued quantum corrections that we calculated above. The first three set of plots(figs 9.6a-9.6c) are of the 'wormhole' 'ground' states when we include the $\mathcal{S}^{wh}_{(2)}$ and $\mathcal{S}^{wh}_{(3)}$ quantum corrections when $B = -1$. The second set of three plots(figs 6a-6c) are of the second 'wormhole' 'excited' state which include the $\mathcal{S}^{wh}_{(2)}$, $\mathcal{S}^{wh}_{(3)}$, and ϕ^{wh}_2 quantum corrections when $B = -1$.

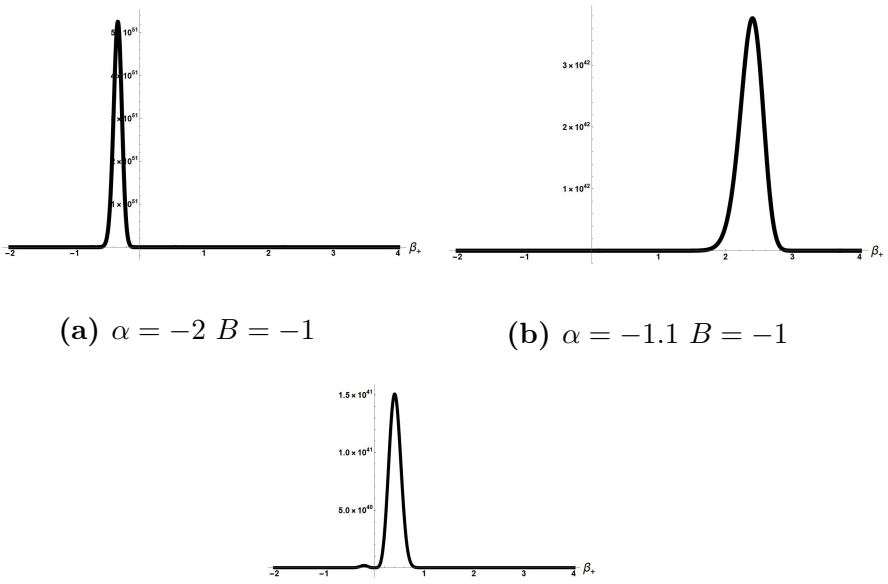

(a) $\alpha = -2$ $B = -1$ **(b)** $\alpha = -1.1$ $B = -1$

(c) $\alpha = 1$ $B = -1$

Figure 9.7 Plots of $\left|\psi^{wh}_{n=2}\right|^2$ for the second 'wormhole' vacuum quantum Taub 'excited' state constructed out of both 'ground' and 'excited' state quantum corrections up to $k = 2$.

We will qualitatively discuss the interesting features of these plots in our discussion section later. For now we will move on and derive the 'no boundary' asymptotic solutions for the quantum Taub models, which have different properties than our wormhole solutions and whose existence have implications for the Bianchi IX models.

9.5 Quantum Taub 'No Boundary' Wave Functions

The 'no boundary' $\mathcal{S}^{\text{nb}}_{(0)}$ solution for the quantum Taub models can easily be found by setting the β_- term in the 'no boundary' $\mathcal{S}_{(0)}$ [102] for the full Bianchi IX models to zero, which results in

$$\mathcal{S}^{\text{nb}}_{(0)} := \frac{1}{6}\left(1 - 4e^{3\beta_+}\right) e^{2\alpha - 4\beta_+}. \tag{9.82}$$

The reader can easily verify that the following $\mathcal{S}^{\text{nb}}_{(1)}$ term satisfies equation (8.52)

when $\mathcal{S}^{\rm nb}_{(0)}$ is inserted into it

$$\mathcal{S}^{\rm nb}_{(1)} := \frac{1}{2}\alpha(4-\mathrm{B}) - \frac{5\beta_+}{2}. \tag{9.83}$$

If we seek a $\mathcal{S}^{\rm nb}_{(2)}$ which possesses the form of our ansatz (9.54) which we used earlier for the 'wormhole case', the resultant $\mathcal{S}_{(2)}$ differential equation is satisfied by a remarkably simple function compared to the 'wormhole' case

$$\mathcal{S}^{\rm nb}_{(2)} := \frac{1}{8}\left(\mathrm{B}^2+9\right)e^{\beta_+-2\alpha}. \tag{9.84}$$

Unlike the 'wormhole' case whose $\Sigma_{(2)}$ was the rather exotic $-\mathrm{B}^2 e^{-2\alpha}\left(\frac{e^{\beta_+}\cos^{-1}\left(e^{3\beta_+}\right)}{8\sqrt{1-e^{6\beta_+}}}\right)$ with its $\cos^{-1}\left(e^{3\beta_+}\right)$ which needs to be analytically continued when $\beta_+ > 0$, 'the no boundary' $\Sigma_{(2)}$ is simply $\frac{1}{8}\left(\mathrm{B}^2+9\right)e^{\beta_+}$. This points to a fundamental difference between the 'wormhole' and 'no boundary' quantum Taub models. In addition this could suggest that the 'wormhole' and the 'no boundary' Bianchi IX models [175] possess significant differences as well. As a result of the simple nature of the $\mathcal{S}^{\rm nb}_{(2)}$ quantum correction we will be able to prove that an asymptotic solution exists for arbitrary ordering parameter for the 'no boundary' case using a more straightforward method than the one we applied to the 'wormhole' case. The existence of this 'no boundary' asymptotic solution for the Taub models is possible evidence that an asymptotic 'no boundary' solution exists for the full quantum Bianchi IX models as well. This is an important observation because the proof of a ' no boundary' solution existing for the Bianchi IX models is still an open problem.

Before we proceed it should be pointed out that if we allow the Hartle-Hawking ordering parameter to take on complex values, then we can form two closed form 'ground' state solutions to the Wheeler DeWitt equation using just (9.82), (9.83) when $B = \pm 3i$. A potential complication though of allowing the Hartle Hawking parameter to assume complex values is that it may fundamentally change the nature of

the Wheeler DeWitt equation in such a way that it yields non-physical solutions. This issue of a complex Hartle-Hawking ordering parameter should be further investigated. For now though we will move forward assuming that the ordering parameter B is an arbitrary real number.

After continuing the process of inserting the explicit forms of the $\mathcal{S}^{\rm nb}_{(k-1)}$ quantum corrections into the kth 'ground' state transport equations; the author found that each kth order quantum correction can be expressed as

$$\mathcal{S}^{\rm nb}_{(k\geq 2)} := g(k)e^{\beta_+(k-1)-2\alpha(k-1)}. \tag{9.85}$$

This is very straightforward to show. First we'll rewrite equation (8.53) as

$$\begin{aligned}
&2\left[\frac{\partial\mathcal{S}_{(0)}}{\partial\alpha}\frac{\partial\mathcal{S}_{(k)}}{\partial\alpha}-\frac{\partial\mathcal{S}_{(0)}}{\partial\beta_+}\frac{\partial\mathcal{S}_{(k)}}{\partial\beta_+}\right]+k\left[B\frac{\partial\mathcal{S}_{(k-1)}}{\partial\alpha}-\frac{\partial^2\mathcal{S}_{(k-1)}}{\partial\alpha^2}+\frac{\partial^2\mathcal{S}_{(k-1)}}{\partial\beta_+^2}\right]\\
&+\sum_{\ell=2}^{k-2}\frac{k!}{\ell!\,(k-\ell)!}\left(\frac{\partial\mathcal{S}_{(\ell)}}{\partial\alpha}\frac{\partial\mathcal{S}_{(k-\ell)}}{\partial\alpha}-\frac{\partial\mathcal{S}_{(\ell)}}{\partial\beta_+}\frac{\partial\mathcal{S}_{(k-\ell)}}{\partial\beta_+}\right)+2k\left(\frac{\partial\mathcal{S}_{(1)}}{\partial\alpha}\frac{\partial\mathcal{S}_{(k-1)}}{\partial\alpha}-\frac{\partial\mathcal{S}_{(1)}}{\partial\beta_+}\frac{\partial\mathcal{S}_{(k-1)}}{\partial\beta_+}\right)\\
&=0.
\end{aligned} \tag{9.86}$$

Next we will insert into (9.86) the following equations (9.85), (9.83) and (9.82) which will yield

$$\sum_{\ell=2}^{k-2}\frac{3(\ell-1)k!\,g(\ell)(k-\ell-1)g(k-\ell)}{\ell!\,(k-\ell)!}+(k-1)(4g(k)-3(k-2)kg(k-1))=0, \tag{9.87}$$

where all of the dependency on α and β_+ has dropped out which has turned the problem of finding higher order quantum corrections into simply an algebraic one.

We can easily solve for g(k)

$$g(k) = \frac{\sum_{\ell=2}^{k-2} \frac{3(\ell-1)k!g(\ell)(k-\ell-1)g(k-\ell)}{\ell!(k-\ell)!}}{4-4k} + \frac{3}{4}(k-2)kg(k-1), \tag{9.88}$$

and it is evident that g(k) is always a well defined number assuming that $(g(2), \ldots, g(k-1))$ are also well defined numbers. All that we need to compute sequentially an arbitrary number of coefficients, $g(k)$, starting with g(2) which can clearly be read off from (9.84) to be $g(2) = \frac{1}{8}\left(\mathrm{B}^2 + 9\right)$. With g(2) known we can write out the following asymptotic 'ground' state solution to the Taub WDW equation

$$\psi^{nb} := e^{\left(-\sum_{k=2}^{\infty} \frac{g(k)e^{\beta_+(k-1)-2\alpha(k-1)}}{k!} - \frac{1}{6}\left(1-4e^{3\beta_+}\right)e^{2\alpha-4\beta_+} - \frac{1}{2}a(4-\mathrm{B}) + \frac{5\beta_+}{2}\right)}. \tag{9.89}$$

Even though the vacuum Taub WDW equation can be solved in closed form for arbitrary ordering parameter, we don't know a-priori which superposition of Bessel functions leads to the wave function which can be well approximated by a finite number of terms of (9.89) or a Borel summation of all of terms.This shows that the Euclidean-signature semi-classical method can even shed light on problems which can in a sense be solved using other techniques.

An outstanding problem in quantum cosmology is whether a smooth and globally defined solution exists for the Bianchi IX WDW equation for any arbitrary ordering parameter of the form (5.19) where its $\mathcal{S}_{(0)}$ is the 'no boundary' solution found in [103]. As previously mentioned Joseph Bae [20] was able to prove the existence of an asymptotic solution to the Bianchi IX WDW equation for the 'wormhole' case. The Taub model can be seen at the classical level as a subset [150] of the Bianchi IX models and therefore by proving that a 'no boundary' asymptotic solution does exist for the Taub model we provide hope that one also exists for the 'no boundary' form of the Bianchi IX models. If a 'no boundary' solution does not exist for the Bianchi

IX it may reveal something interesting about this method of quantizing cosmology.

Attached in the appendix section will be a Mathematica code which explicitly computes this asymptotic solution using (9.88) up to any order k.

We will leave the proof for the existence of asymptotic 'excited' state solutions for another time. For now though we will be content to find the semi-classical ϕ_0 term and the ϕ_1 quantum correction for the 'no boundary' case. The author found the following family of conserved quantities along the flow of $\mathcal{S}^{\mathrm{nb}}_{(0)}$ which satisfies (8.59) as the reader can easily verify

$$\phi_0^{\mathrm{nb}} := \left(\left(e^{3\beta_+} - 1\right) e^{\beta_+ - 2\alpha}\right)^n . \tag{9.90}$$

Because our ϕ_0^{nb} possesses zeros within the domain of real Misner variables we must restrict n to be a positive integer so our wave functions are smooth and globally defined. Using a computer algebraic system and the ansatz (9.77) the ordinary differential equation for ϕ_1 can be solved which yields the following quantum correction

$$\phi_1^{\mathrm{nb}} := -\frac{3ne^{-2\alpha n-2\alpha}\left(e^{\beta_+}\left(e^{3\beta_+}-1\right)\right)^{n+1}\left(4e^{6\beta_+}(n+1)-e^{3\beta_+}(4n+7)+n+2\right)}{4\left(e^{3\beta_+}-1\right)^3}. \tag{9.91}$$

The general form of ϕ_2^{nb} for any n is far too cumbersome to include in this chapter, however below we will display this quantum correction for arbitrary ordering parameter for the first and second 'excited' states.

$$\begin{aligned}
\phi_{2\,n=1}^{\mathrm{nb}} &:= w\Bigg(e^{6\beta_+}\left(\mathrm{B}^2+432e^3-27\right)+\left(e^3-3\right)e^{3\beta_+}\left(\mathrm{B}^2+432e^3-27\right) \\
&\quad + e^6\mathrm{B}^2-3e^3\mathrm{B}^2+3\mathrm{B}^2-27e^6+81e^3+351\Bigg) \\
w &= -e^{-6\alpha}\frac{e^{3\beta_+}\left(e^{3\beta_+}-e^3\right)}{16\left(e^3-1\right)^3}
\end{aligned} \tag{9.92}$$

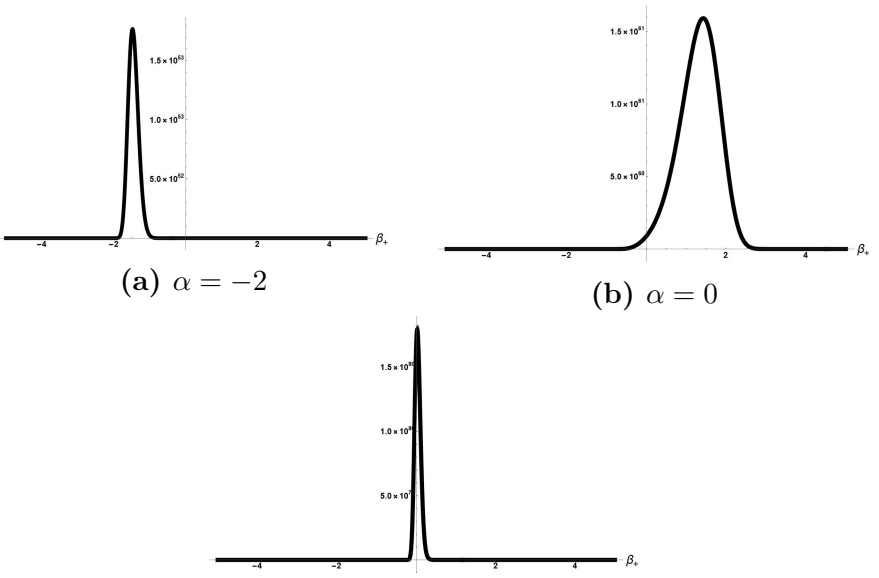

(a) $\alpha = -2$ **(b)** $\alpha = 0$ **(c)** $\alpha = 2$

Figure 9.8 Plots of $\left|\psi^{nb}\right|^2$ for the 'no boundary' vacuum Taub 'ground' state (9.89) which includes quantum corrections up to $k = 2$.

$$
\begin{aligned}
\phi_{2\,n=2}^{\mathrm{nb}} := w\Big(&\left(e^3-1\right)\left(e^{3\beta_+}-1\right)\left(e^{6\beta_+}+\left(e^3-3\right)e^{3\beta_+}+3-3e^3+e^6\right)\mathrm{B}^2 \\
&+27\Big(\left(8-65e^3+88e^6\right)e^{9\beta_+}+\left(e^3-4\right)\left(8-65e^3+88e^6\right)e^{6\beta_+} \\
&-\left(40+70e^3-268e^6+65e^9\right)e^{3\beta_+}+33+8e^3\left(-5-4e^3+e^6\right)\Big)\Big) \\
w = -e^{-8\alpha}&\frac{e^{4\beta_+}\left(e^{3\beta_+}-e^3\right)}{8\left(e^3-1\right)^4}
\end{aligned}
\tag{9.93}
$$

We will now plot some interesting Taub no boundary wave functions composed of (9.93), (9.91), (9.90), and (9.89) which are in the form of (8.46) and (8.57). The first three plots(figs 9.8a-9.8c) are of the 'no boundary' 'ground' states (9.89) computed up to the $\mathcal{S}_{(2)}^{\mathrm{nb}}$ quantum correction for different values of α when B=0.

The next three plots 9.9 are of the second 'excited' state where we include quantum corrections up to $k = 2$ for different values of α.

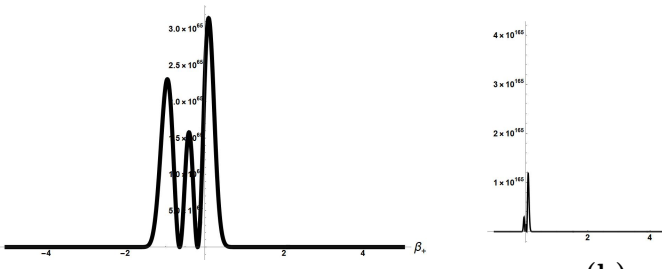

(a) $\alpha = -1.6$

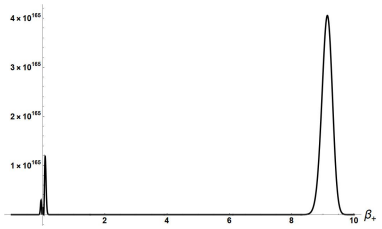

(b) $\alpha = 2.825$

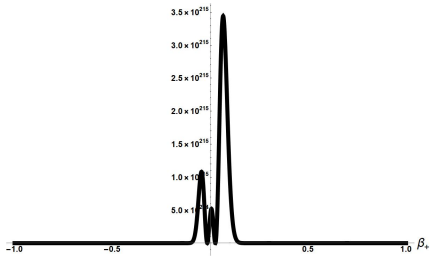

(c) $\alpha = 3$

Figure 9.9 Plots of $\left|\psi^{nb}_{n=2}\right|^2$ for the second 'no boundary' vacuum quantum Taub 'excited' state including terms up to $k = 2$.

In the next section we will discuss qualitatively the behavior of our wave functions and the physical implications that can be extrapolated from them.

9.6 Discussion

To begin analyzing our results we first need to adopt an interpretation for the wave functions we computed. Two interpretations of quantum mechanics which in the past have been used to extrapolate physics from Wheeler Dewitt wave functions within the context of quantum cosmology are the consistent histories approach [105] and pilot wave theory [47]. However, for our purposes, we will use the following admittingly naive interpretation which we will briefly outline. Even though we cannot interpret $|\psi|^2$ as a probability density due to the lack of a known dynamical unitary operator for the symmetry reduced Wheeler Dewitt equation, if we fix α and only consider wave functions which approach zero as $\beta_+ \to \pm\infty$ then our wave functions are reminiscent of normalizable probability densities as can be seen from our plots. Each point in

those plots at a fixed α represents a potential geometric configuration that a quantum universe described by those wave functions can possess. Associated with each of those points in β_+ space at a fixed α is a value of $|\psi|^2$; it is not unreasonable to conjecture that the greater the value of $|\psi|^2$ is, the more likely a Taub universe will possess the geometry dictated by β_+. For example if $|\psi(\alpha, \beta_+ 1)|^2 > |\psi(\alpha, \beta_+ 2)|^2$ we would interpret this to mean that a Taub universe described by ψ when it reaches a size dictated by α is more likely to have a spatial geometry which possesses a level of anisotropy described by the value of $\beta_+ 1$ as opposed to $\beta_+ 2$.

A shortcoming of our interpretation is that it cannot assign numerical values of probability to a micro ensemble of Taub universes with different values of α, because $\int_\infty^\infty |\psi|^2 d\beta_+$ is not conserved in α. Nonetheless we are picking this interpretation because it is intuitive for the solutions we are dealing with and facilitates the elucidation of the points the author wishes to make. This will be the interpretation we use throughout this entire dissertation. In essence the author was inspired to pick this interpretation because he would like to let the bare solutions speak for themselves. The author strongly encourages future work to be done in extrapolating physics for the results presented in this dissertation using both the Bohmian and consistent histories approaches, in conjunction with other quantitative methods. What follows will be an attempt to extrapolate the physical implications of a cosmological constant and an electromagnetic field in the development of a quantum Taub universe from our wave functions by examining their aesthetic characteristics. We interpret the peaks that appear in our wave functions the same way they are interpreted in [93], as possible geometric states a quantum universe can tunnel in and out of.

Our second set of figures in 9.2 emphatically shows how our matter sources can affect the quantum cosmological evolution of a Taub universe. If we compare figures 9.2a and 9.2b we see that the electromagnetic field b^2 causes the wave function originally in figure 9.2a to be peaked at a higher value of anisotropy and be more

narrow. Physically this indicates a quantum mechanism by which an electromagnetic field can increase the level of anisotropy in the early universe. Additionally it can also cause the geometry of a universe to be more defined in the sense that its wave function of the universe becomes sharply peaked at a specific value of β_+ as opposed to being spread out in β_+ space as figure 9.2a is.

The above two effects that our electromagnetic field has on our wave functions in figures(9.2a-9.2b) could have had a profound impact on the formation of pockets of anisotropy in our actual early universe if similar behavior was present in its wave function of the universe. Furthermore, because the electromagnetic field causes the geometry of our quantum Taub universe to be more sharply defined it could have also played a role in the transition of a universe from one which could only be adequately described using quantum mechanics to one which can be described adequately using classical mechanics.

Figures(9.2c-9.2d) sheds interesting light on other effects that our two matter sources can have on the evolution of a quantum universe. For the vacuum quantum Taub 'wormhole' when $\alpha = 1.5$ our wave function sharply peaked at isotropy($\beta_+ = 0$). As α continues to grow that peak at isotropy rapidly sharpens. However when $\Lambda < 0$ no matter how large α becomes the wave function peaks at some non-zero value of β_+. In other words no matter how large α becomes there is always some residual anisotropy present as is shown in figure 9.2c. However in figure 9.2d we see that an electromagnetic field can actually decrease the level of anisotropy present in the early universe at certain stages of its development as measured by our clock α as can be seen by how the wave function is centered at isotropy. This points to how the electromagnetic field in conjunction with other matter sources can have a myriad of different effects on the quantum evolution of a universe.

Moving on to our 'excited' states (figs 9.3a-9.3f) when $\Lambda = 0$ we see even more spectacular effects from our primordial electromagnetic field. When $b^2 = 0$ our 'ex-

cited' states have two peaks which represent two potential geometric configurations our quantum Taub universe can tunnel in and out of. For the vacuum 'wormhole' case as α grows the multiple peaks merge into one central peak located at isotropy$(\beta_+ = 0)$. This behavior makes sense because as we previously mentioned e^{α} classically represents the scale factor of our cosmology and we expect that quantum effects, such as tunneling, would be most prominent when a universe is small and possesses a very high energy density and diminish as it grows in size. Of course no matter how large a universe becomes it is fundamentally quantum mechanical, but the probabilities of those quantum mechanical effects manifesting on large macroscopic scales rapidly diminishes as it grows in size. In other words our 'excited' state quantum Taub universes experience a phase transition over a certain range of α where they transition from a universe where tunneling between different geometric configurations is common to one where it is exceedingly rare.

When our electromagnetic field is turned on we see some profound effects. For $b = 1.5$ an additional peak emerges which represents another likely geometric configuration our quantum Taub universe can tunnel into as can be seen by comparing figures 9.3d and 9.3e. This additional state was created quantum mechanically by our electromagnetic field. This is somewhat similar to how the introduction of noncommutativity in the minisuperspace variables of the quantum Bianchi I [229] and Kantowski Sachs [93] models can cause additional states that can be tunneled in and out of to appear in the form of additional peaks in their respective wave functions. in their respective wave functions As our field grows in strength all of the peaks eventually merge into one central peak as can be seen in figure 9.3f. This effect of an electromagnetic field creating an additional state which a quantum universe can tunnel in and out of can be seen also in figure 9.5b. Thus it appears for 'excited' states of our quantum Taub universes that the effects which a primordial electromagnetic field has on them are highly dependent upon its strength. When the field is somewhat

weak it can create additional states that our quantum universe can tunnel in and out of, and when it is strong it can destroy those states, leaving only one sharply defined state left. Our results encourage studying other anisotropic quantum cosmologies such as the Bianchi I models using the Euclidean-signature semi-classical method when an magnetic field and a cosmological constant are present in order to establish if the plethora of effects we detailed in this dissertation are generic to anisotropic quantum cosmologies.

Using our aforementioned analysis of the first 10 plots the reader can handily interpret in the manner which we have done thus far the wave functions for our superposition of 'excited' states (9.4a-9.4c) and our semi-classical 'excited' states (figs 9.5a-9.5c) when both matter sources are present.

The vacuum 'wormhole' case for arbitrary ordering parameter has some interesting mathematical properties which we have already mentioned. It should be stressed that these properties are only present when $B \neq 0$ and that they manifest themselves differently within our wave functions for different values of the ordering parameter. Nonetheless for $B = -1$ our vacuum 'wormhole' wave functions behave peculiarly in comparison to the ones we computed earlier in this chapter. For large negative $\alpha << 0$ our vacuum 'wormhole' asymptotic wave function which possesses terms up to $\mathcal{S}^{wh}_{(3)}$ behaves as a 'ground' state as we would expect it to as indicated in figure 9.6a. As α continues to grow the wave function behaves as a pseudo-Gaussian traveling to the right in the positive β_+ direction.

However around $\alpha = -1.1$ something drastic happens, a second peak forms which is illustrated in figure 9.6b and thus makes our 'ground' state aesthetically resemble an 'excited' state. This is why we constantly employ ' ' to denote 'ground' and 'excited' states in our work. Unlike in ordinary quantum mechanics the lines between 'ground' and 'excited' states are not as sharply defined. Using our 'ground' state equations we can obtain terms which do not manifest the discretization in their quantum numbers

that we showed to be present in our ϕ_0 terms, and yet the states constructed from them share some properties we expect out of 'excited' states. This further suggests that more theoretical work is necessary to rigorously delineate between the 'ground' and 'excited' states of a theory which possesses a vanishing Hamiltonian. Another interesting feature of our wave functions is that these two peaks which our Taub universe can tunnel in between emerges as our α reaches a threshold, as opposed to being continuously present for small $\alpha < 0$'s as is the case of our closed form 'excited' states(figs 9.4a-9.4c). Our 'excited' states(figs 9.7a-9.7c) which include terms up to $\mathcal{S}^{wh}_{(3)}$ and ϕ^{wh}_2 don't overtly manifest the properties one typically expects from 'excited' states as is exemplified in figures (9.4a-9.5c). At most we see a small second peak form when $\alpha = 1$ in figure 9.7c.

Moving on to our 'no boundary' asymptotic solutions, if we start with our 'ground' state figures (9.8a-9.8c) we see that for small values of α our wave function forms a peak around a negative value of β_+ and is moving to the right from the negative β_+ axis. For larger values of α our wave function forms a peak around a positive value of β_+ as it continues to travel to the right. However at a certain value of α our travelling Gaussian changes direction and eventually resides at the origin as its magnitude continues to grow as α grows. This behavior of our wave function not being bounded from above for real values of the Misner variables poses a complication in our efforts to obtain a physically meaningful picture of what is going on using our method. If we naively interpreted our 'no boundary' states as such using our purely qualitative method we would conclude that the universe described by our wave function can only exist when $\alpha = \infty$ because that state is infinitely more likely to occur then any other geometric configuration because our wave function approaches ∞ as $\alpha \to \infty$. Such an interpretation makes no sense. A potential way to remedy this problem can be by choosing a different way to construct an inner product between $\psi_{nb}s$.

Our 'no boundary' excited states can be interpreted similarly to our other 'excited'

states with the aforementioned caveat. One noteworthy feature of our plots is that in 9.9b our wave function peaks at an extremely anisotropic value of $\beta+$, but then quickly snaps back towards isotropy at $\alpha = 3$. It will require more work to determine if this "snapping" behavior is a generic feature belonging to all quantum Taub 'no boundary' 'excited' states.

9.7 Concluding Remarks

Despite the vast number of results that we presented there now seems to be as many unanswered questions. In the author's own estimation this is a positive sign that the research we conducted is worthwhile and that continued pursuit of it will lead to a further understanding on how matter sources such as an electric/magnetic field and a cosmological constant could have impacted the evolution of the early universe. Because our universe in its most primordial moments of existence was quantum in nature and inhomogeneous, and anisotropic it is important to catalogue all of the possible effects that quantum mechanics can induce on its development so we can have a complete understanding on all of the different ways it could have evolved. By studying the 'ground' and 'excited' states of the quantum Taub models with an aligned electromagnetic field and negative cosmological constant we have reinforced and expanded the known possible phenomena that quantum mechanics could induce on a primordial universe.

From a mathematical point of view we have showcased the strength of the Euclidean-signature semi-classical method for tackling Lorentzian signature problems. The author hopes that the plethora of results obtained in this chapter, in conjunction with all of the results in the second portion of this dissertation, will promote its further development.

In terms of quantum cosmology a good next step would be to apply this method to

the Bianchi I models. Because of the simplicity of the Bianchi I model we can compare the Euclidean-signature semi-classical method to the traditional WKB method. In addition it is worth studying the Bianchi I models to determine if the effects of matter sources on the Taub models that we documented are also present in the Bianch I models. Eventually in order to compute potentially observable quantum corrections in the CMB from a primordial magnetic field we will need to include inhomogeneities and study non-aligned electromagnetic fields. The author believes that the results in this chapter represents a first step to obtaining observable quantum corrections in the CMB from a possible primordial magnetic field.

Chapter 10

Quantum Bianchi IX and VIII With Λ, Aligned Electromagnetic Field, Free Scalar Field, and Stiff Matter

10.1 Bianchi IX And VIII Models

The metric formulations of the Bianchi IX and VIII models are given below

$$
\begin{aligned}
ds^2 &= -N^2 dt^2 + \frac{L^2}{6\pi} e^{2\alpha(t)} \left(e^{2\beta(t)}\right)_{ab} \omega^a \omega^b, \\
\left(e^{2\beta(t)}\right)_{ab} &= e^{2\beta_+(t)} \operatorname{diag}\left(e^{2\sqrt{3}\beta_-(t)}, e^{-2\sqrt{3}\beta_-(t)}, e^{-6\beta_+(t)}\right), \\
\omega^1 &= dx - k\sinh(ky)dz, \\
\omega^2 &= \cos(x)dy - \sin(x)\cosh(ky)dz, \\
\omega^3 &= \sin(x)dy + \cos(x)\cosh(ky)dz,
\end{aligned}
\tag{10.1}
$$

where k=1 is for the Bianchi VIII models and k=i corresponds to the Bianchi IX models. Using the general form of the WDW equations (7.84) and the potentials from table 2 with the inclusion of a stiff matter potential term which has the form prescribed in [227] we can ascertain that the WDW equations for the Bianchi IX and

VIII models with a cosmological constant, aligned electromagnetic field, free scalar field, and stiff matter are

$$\begin{aligned}
&\frac{\partial^2\Psi}{\partial\alpha^2} - B\frac{\partial\Psi}{\partial\alpha} - \frac{\partial^2\Psi}{\partial\beta_+^2} - \frac{\partial^2\Psi}{\partial\beta_-^2} - 12\frac{\partial^2\Psi}{\partial\phi^2} + U_\pm\Psi = 0 \\
&U_\pm = (f)\, e^{6\beta_+}\left(e^{6\beta_+}\sinh^2\left(2\sqrt{3}\ \ \beta_-\right) \pm \cosh\left(2\sqrt{3}\beta_-\right)\right) \\
&+ \frac{2e^{6a}\Lambda}{9\pi} + U_{em} + \frac{1}{4}f + \rho \\
&U_{em} = 2b^2e^{2\alpha-4\beta_+} \vee 2b^2e^{2\left(\alpha\pm\sqrt{3}\beta_-+\beta_+\right)} \\
&f = \frac{4}{3}e^{4\alpha-8\beta_+},
\end{aligned} \tag{10.2}$$

where ρ denotes stiff matter and the plus sign, $+$, in $U_\pm$ corresponds to the Bianchi VIII models and the minus sign, $-$, the Bianchi IX models.

The WDW equation for the Taub models with an exponential scalar field, e^ϕ, and aligned electromagnetic field potential is given below

$$\begin{aligned}
&\frac{\partial^2\Psi}{\partial\alpha^2} - B\frac{\partial\Psi}{\partial\alpha} - \frac{\partial^2\Psi}{\partial\beta_+^2} - 12\frac{\partial^2\Psi}{\partial\phi^2} + V\Psi = 0 \\
&V = \left(\frac{e^{4\alpha-8\beta_+}}{3}\left(1 - 4e^{6\beta_+}\right) + e^{6\alpha+\phi}\right) + 2b^2e^{2\alpha+2\beta_+}.
\end{aligned} \tag{10.3}$$

Beyond free scalar fields being good candidates for clocks, their inclusion can be seen as a first step towards a more general program. Right now we are only considering homogeneous scalar fields for our cosmological models. But as we have shown earlier, the Euclidean-signature semi-classical method can also be applied to models where the scalar field varies with position such as relativistic bosonic ϕ^4 theory. Thus by including a homogeneous scalar field we are testing the waters for the eventual inclusion of a non-homogeneous scalar field in our cosmological models that we wish to study using our modified semi-classical method. By quantizing that scalar field we can introduce primordial fluctuations into our models which is a necessary step for computing quantum cosmological corrections to observables such as the CMB

spectrum. The ability of this method to handle all kinds of scalar fields in general makes it potentially well suited for studying non-homogeneous quantum cosmology.

The Bianchi VIII quantum/classical models have not been as thoroughly studied as the Bianchi IX models we discussed in the last chapter. However, there have been some interesting investigations [23, 155, 186] into them and exact solutions of them have been obtained in both classical and quantum regimes. We shall expand upon what is known for the quantum Bianchi IX and VIII models by including matter sources and applying the Euclidean-signature semi-classical method to them.

This chapter will have the following structure. First we will apply the Euclidean-signature semi-classical method to the Bianchi IX and VIII models with the aforementioned matter sources. Doing so will give us semi-classical solutions to them. The semi-classical wave functions we will obtain in closed form when a negative cosmological constant is present behave similarly in a qualitative sense to the wave functions reported in [189] which were obtained using complexification and are expressed as contour integrals. This supports the idea that our semi-classical wave functions reasonably capture the effects of our matter sources, including our aligned electromagnetic field. In addition, the fact that we were able to find closed form solutions to the Euclidean-signature Hamilton Jacobi equation which can be used to construct semi-classical solutions to the Lorentzian signature symmetry reduced WDW equation without needing to use a Wick rotation further shows the promise of this method to be a useful alternative [175] to Euclidean path integrals [97, 98] for tackling problems in quantum gravity.

Next we will study wave functions of the Bianchi IX models with our matter sources which have as their classical analogues trajectories in minisuperspace in which β_- is fixed at zero. Next we will turn our attention to the Taub models and briefly analyze them when an exponential scalar field and aligned electromagnetic field potentials are present. Finally we will present a few closed form solutions to the WDW

equation for the Bianchi IX and VIII models. We will use the same interpretational scheme that we presented in the last chapter to understand the wave functions in this chapter.

10.2 Bianchi VIII and IX Quantum Cosmology With An Aligned Electromagnetic Field, Scalar Field, Cosmological Constant, And, Stiff Matter

The author found the following solutions to the Euclidean-signature Hamilton Jacobi equations (8.51) when an electromagnetic field, scalar field, cosmological constant, and stiff matter are present

$$\begin{aligned}\mathcal{S}^{1}_{(0\pm)} &= \frac{1}{6}e^{2\alpha-4\beta_{+}}\left(2e^{6\beta_{+}}\cosh\left(2\sqrt{3}\beta_{-}\right)\pm 1\right)\\ &\mp\frac{\Lambda e^{4\alpha+4\beta_{+}}}{36\pi}\mp\alpha \mathrm{b}^{2}\mp\beta_{+}\mathrm{b}^{2}+\frac{\phi\sqrt{\rho}}{2\sqrt{3}},\end{aligned} \tag{10.4}$$

$$\begin{aligned}\mathcal{S}^{2}_{(0\pm)} &= \frac{1}{6}e^{2\alpha-4\beta_{+}}\left(2e^{6\beta_{+}}\cosh\left(2\sqrt{3}\beta_{-}\right)\pm 1\right)\\ &-\frac{\Lambda e^{4\alpha-2\beta_{+}-2\sqrt{3}\beta_{-}}}{36\pi}-\alpha \mathrm{b}^{2}+\frac{\beta_{+}}{2}b^{2}+\frac{\sqrt{3}}{2}\beta_{-}\mathrm{b}^{2}+\frac{\phi\sqrt{\rho}}{2\sqrt{3}},\end{aligned} \tag{10.5}$$

$$\begin{aligned}\mathcal{S}^{3}_{(0\pm)} &= \frac{1}{6}e^{2\alpha-4\beta_{+}}\left(2e^{6\beta_{+}}\cosh\left(2\sqrt{3}\beta_{-}\right)\pm 1\right)\\ &-\frac{\Lambda e^{4\alpha+2\beta_{+}-2\sqrt{3}\beta_{-}}}{36\pi}-\alpha \mathrm{b}^{2}+\frac{\beta_{+}}{2}b^{2}-\frac{\sqrt{3}}{2}\beta_{-}\mathrm{b}^{2}+\frac{\phi\sqrt{\rho}}{2\sqrt{3}}.\end{aligned} \tag{10.6}$$

In our solutions the plus + sign or the top operation in $\pm$ and $\mp$ are for the Bianchi IX models while the bottom symbols/operators are for the Bianchi VIII models. It is interesting to note that in the limit of our matter sources vanishing these solutions approach the well known 'wormhole' [178] Bianchi IX solutions and its analogue for the Bianchi VIII models. The author was unable to find elementary solutions to (8.51) with the aforementioned matters sources that exhibited this property for the Bianchi

IX 'no boundary' [103] or "arm" solutions [26], or for their Bianchi VIII analogues [34]. As we previously mentioned for the Taub models, this suggests that there is something special about the 'wormhole' solution.

Using these expressions we can obtain a semi-classical solution to the WDW equation expressed in the Hartle-Hawking semi general operator ordering which respects the $\frac{2\pi}{3}$ symmetry in β space present in the Bianchi IX potential when our electromagnetic field is zero ($b = 0$) or a solution to the WDW expressed in an alternative operator ordering when $b \neq 0$.

As pointed out by Moncrief and Ryan in [178] and shown explicitly in [96], using a different operator ordering for the Wheeler DeWitt equation than the Hartle-Hawking one [110] allows one to construct wave functions which satisfy it if one possesses pure imaginary solutions to its corresponding Lorentzian signature Hamilton Jacobi equation. We will review the derivation presented in [96] which allows us to construct solutions using just an $\mathcal{S}_{(0)}$. The Hamiltonian constraint for the Bianchi A models can be expressed as

$$H = G^{AB} p_A p_B + U = 0 \tag{10.7}$$

where G^{AB} is the DeWitt supermetric and p_i are the canonical momenta. Likewise the regular Lorentzian signature Hamiliton Jacobi is expressed as

$$G^{AB} \frac{\partial J}{\partial x^A} \frac{\partial J}{\partial x^B} + U = 0. \tag{10.8}$$

Because (10.8) is the Lorentzian signature Hamilton Jacobi equation the signs in its derivatives are the opposite of those for the Euclidean case. That means for the Bianchi VIII and IX models with a cosmological constant, a primordial electromagnetic field, scalar field, and stiff matter (10.8) is satisfied by our previous solutions (10.4), (10.5), and (10.6) multiplied by $\sqrt{-1}$ such that $J = \sqrt{-1}\mathcal{S}^i_{(0)}$. This allows us

to rewrite (10.8) as

$$G^{AB}p_Ap_B + G^{AB}\frac{\partial \mathcal{S}^i}{\partial x^A}\frac{\partial \mathcal{S}^i}{\partial x^B} = G^{AB}(x)\pi^*_A\pi_B = 0 \tag{10.9}$$

where

$$\pi_A = p_A - \sqrt{-1}\frac{\partial\ \mathcal{S}^i}{\partial x^A} \tag{10.10}$$

and is quantized as follows

$$\hat{\pi}_A = -\sqrt{-1}\frac{\partial}{\partial x^A} - \sqrt{-1}\frac{\partial\ \mathcal{S}^i}{\partial x^A}. \tag{10.11}$$

Due to this quantization, wave functions of the form $\Psi = e^{-\mathcal{S}^i_{(0)}}$ mathematically behave in the following way

$$\hat{\pi}_B\Psi = 0. \tag{10.12}$$

Thus we can satisfy the Bianchi VIII and IX WDW equations when a cosmological constant, a primordial electromagnetic field, scalar field, and stiff matter are present if we order the WDW as follows

$$\frac{1}{\sqrt{|G|}}\left[\hat{\pi}^*_A\left(\sqrt{|G|}G^{AB}\hat{\pi}_B\right)\right]\Psi = 0. \tag{10.13}$$

We will first study a semi-classical solution

$$\Psi = \frac{1}{3}\left(e^{-\mathcal{S}^1_{(0\ \ +)}} + e^{-\mathcal{S}^2_{(0\ \ +)}} + e^{-\mathcal{S}^3_{(0\ +)}}\right) \tag{10.14}$$

to the WDW equation(10.2) when $b = 0$ and then turn our attention to a closed form solution which satisfies (10.13) when $b \neq 0$. As we previously mentioned there are two candidates for our evolution parameter α and ϕ. Even though ϕ is in some respects a better variable because classically it is guaranteed to increase monotonically for the Bianchi VIII and IX models we are considering, we will analyze (10.14) using α

because it better facilitates the author's ability to convey the physical implications of our wave functions for this particular case. Below are three plots of (10.14) for three different values of α.

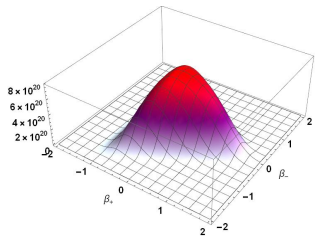

(a) $\alpha = -1 \quad \Lambda = -1$

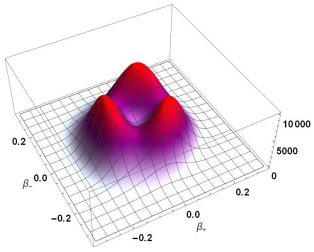

(b) $\alpha = 1.65 \quad \Lambda = -1$

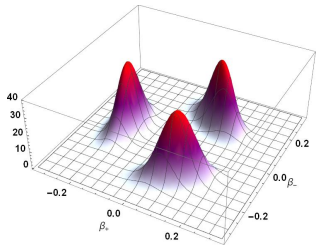

(c) $\alpha = 2 \quad \Lambda = -1$

Figure 10.1 Three different plots of (10.14) for three different values of α where we suppress the the ϕ degree of freedom.

When α is less than 1.6 our wave function's peak is located at the origin in β space which corresponds to isotropy. For negative values of α our wave function is roughly spread evenly around the origin as can be seen in figure (10.1a). Thus we can say that figure (10.1a) describes a universe with a "fuzzy" geometry. As α grows through, our wave function becomes more sharply peaked at the origin. This is expected because geometrical "fuzziness" described by a wave function which is spread out in β space is a quantum effect we intuitively expect to diminish as the universe grows in size dictated by α.

However around $\alpha \approx 1.6$ a dent forms where the wave function used to have an isotropic peak as can be seen in (10.1b) and our wave function begins to split

apart. This is a result of the influence of our negative cosmological constant Λ. As α continues to grow our wave function splits into three parts whose peaks are not centered around the origin. This indicates that the cosmological constant for our wave function acts as a driver of anisotropy by tearing our wave functions away from the origin in β space. This is reminiscent of how a positive cosmological constant causes distant objects which are not gravitational bound to each other in the universe to accelerate away from each other. Of course this is just an analogy because our wave function is in minisuperspace, not space-time.

The wave function shown in (10.1c) is aesthetically similar to the wave functions [189] which were computed by employing Chern-Simons solutions in Ashtekar's variables. Investigating the connection between the caustics which were studied in [189] and these elementary closed form solutions to the Euclidean-signature Hamilton Jacobi equation could potentially yield some interesting results.

In comparison to the exotic and technical methods which were used to compute Bianchi IX wave functions with a negative cosmological constant in [189], the fact that the Euclidean-signature semi-classical method allowed us to compute similar Bianchi IX wave functions in closed form and expressed in terms of elementary functions is an impressive feat. This provides further support that the Euclidean-signature semi-classical method is an effective way to prove the existence of solutions to Lorentzian signature equations.

Another way of visualizing how the cosmological constant is a driver of anisotropy in our wave functions is through the plots in figure (10.2).

Moving on to the case when an electromagnetic field is present we will analyze the solution to (10.13) constructed from (10.4). We don't lose much from not analyzing (10.5) and (10.6) because those are just (10.4) rotated by $\pm\frac{2\pi}{3}$ in β space. In figure

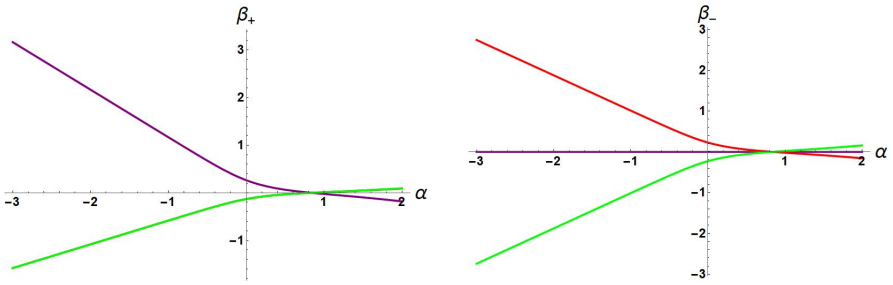

(a) $\Lambda = -1$ **(b)** $\Lambda = -1$

Figure 10.2 Two plots of the wave functions constructed from (10.4), (10.5), and (10.6) which show their maximum values in β space as a function of α. The red line corresponds to (10.6), the green line corresponds to (10.5), and the purple line corresponds to (10.4).

3 are four plots which showcase the possible effects that an aligned electromagnetic field can have on our particular 'ground' state wave functions.

As can be seen by comparing figures (10.3a) and (10.3b) one of the effects of our electromagnetic field is that it causes our wave function to form a peak at a larger value of β_+ than it would otherwise. However, owing to the primordial nature of our electromagnetic field for large values of α this effect is far less drastic as can be seen by comparing figures (10.3c) and (10.3d). This suggests that an electromagnetic field can play a decisive role in increasing the prevalence of anisotropy in the early universe but still allow for a universe which becomes roughly isotropic as it continues to grow in size. To test this assertion, in the future we will need to study other quantum cosmological models with more general electromagnetic fields. In addition we would need to add inhomogeneities to those models. For now this finding contributes towards a theoretical understanding of how a primordial electric/magnetic field could have influenced the seeds of anisotropy in the early universe and how those seeds developed as it grew in size.

Another noticeable effect of our electromagnetic field is that it causes our wave function to be more sharply peaked at smaller values of α than it otherwise would

be as can be seen by comparing figures (10.3a) and (10.3b). This suggest that an electromagnetic field could play a role in causing a universe which initially possesses a "fuzzy" geometry in the sense that its wave function of the universe is evenly spread over β space to transition to one which is sharply peaked at a particular point in β space. This transition from a "fuzzy" geometry to a semi-classical one could occur if the primordial electromagnetic field was something that emerged in an early universe at some point in its evolution or was present in the beginning, but its effects were initially suppressed by Planck or GUT level physics. Such a mechanism being present in general anisotropic quantum cosmologies can help explain how a universe can transition from a state where it can only be accurately described using quantum mechanics to one which can be adequately described by classical mechanics.

A surprising effect of our electromagnetic field is that it can actually reduce the level of anisotropy of a quantum universe at certain values of α. This can be seen by comparing figures (10.3c) and (10.3d). Our cosmological constant has a proclivity towards causing our wave functions to be centered at a negative value of β_+ while our aligned electromagnetic field causes our wave functions to shift toward the positive portion of the β_+ axis. Thus for certain values of α these two competing effects to increase anisotropy can cancel each other out and result in a reduction of anisotropy. This effect may also be caused by an aligned electromagnetic field and other forms of matter. Visually this dual nature concerning the tendencies of our two matter sources to induce anisotropy in our quantum cosmological models can be visualized in figure (10.4).

We should note that this dual nature may be a result of us considering an aligned electromagnetic field and not one which has components in multiple directions.

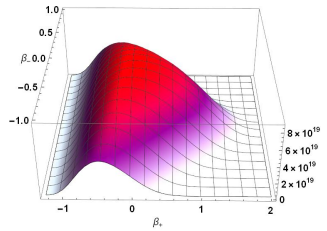

(a) $\alpha = -1 \quad \Lambda = -1 \quad b = 0$

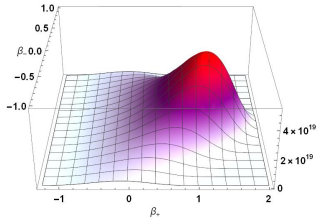

(b) $\alpha = -1 \quad \Lambda = -1 \quad b = 1$

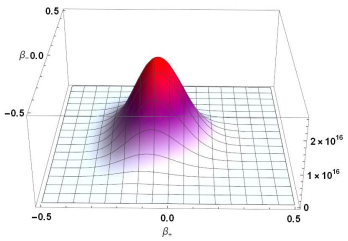

(c) $\alpha = 1 \quad \Lambda = -1 \quad b = 0$

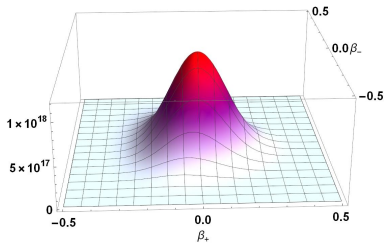

(d) $\alpha = 1 \quad \Lambda = -1 \quad b = 1.4$

Figure 10.3 These are four plots of our wave functions constructed from (10.4) with listed values for their cosmological constant and electromagnetic field.

When both a negative cosmological constant and an electromagnetic field are present, isotropy is more likely to be reached at a smaller value of α than it is when either one or none of the matter sources are present. When an aligned electromagnetic field and a negative cosmological constant are present the magnitude of our wave functions decay as α continues to grow past a point. These results are in concord with those that the author observed in his previous works where he studied the effects of aligned electromagnetic fields on Taub [39], Bianchi II, and $\text{VII}_{h=0}$ [38] quantum cosmologies.

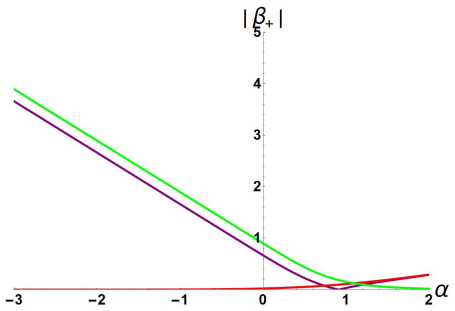

(a) $\alpha = -1 \quad \Lambda = -1 \quad b = 0$

Figure 10.4 This plot shows the maximum values of our wave functions in β space as a function of α. The green plot is of the wave function constructed from (10.4) when no matter sources are present. The purple line is when both a negative cosmological constant $\Lambda = -3$ and an electromagnetic field $b = 2$ are present. The red line is when just an electromagnetic field $b = 2$ is present.

10.3 IX Quantum Cosmology On The β_+ Axis

In this section we will further explore Bianchi IX quantum cosmologies with matter sources by analyzing wave functions which correspond to classical trajectories in minisuperspace where β_- starts at a fixed point in β space. To start we need to pick an $\mathcal{S}_{(0)}$ which induces a flow in minisuperspace which possesses fixed points. To determine this we will write out the classical flow equation for an arbitrary $\mathcal{S}_{(0)}$

$$\begin{aligned} p_\alpha &= \frac{\partial \mathcal{S}_{(0)}}{\partial \alpha}, \\ p_{\beta_+} &= \frac{\partial \mathcal{S}_{(0)}}{\partial \beta_+}, \\ p_{\beta_-} &= \frac{\partial \mathcal{S}_{(0)}}{\partial \beta_-}, \\ p_\phi &= \frac{\partial \mathcal{S}_{(0)}}{\partial \phi,} \end{aligned} \tag{10.15}$$

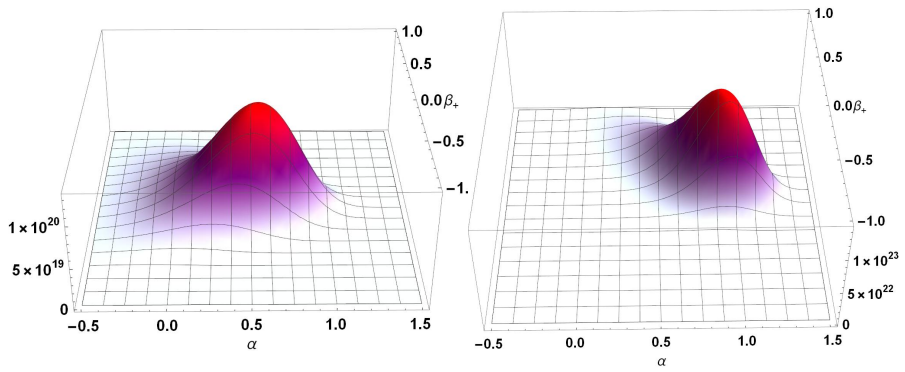

(a) $\phi = 0 \quad b = 0$

(b) $\phi = 0 \quad b = 2$

Figure 10.5 Two plots of (10.23) for two different values for the strength of the electromagnetic field.

$$\begin{aligned}
\dot{\alpha} &= \frac{(6\pi)^{1/2}}{2e^{3\alpha}} N\Big|_{\text{Eucl}} \, p_\alpha, \\
\dot{\beta}_+ &= \frac{-(6\pi)^{1/2}}{2e^{3\alpha}} N\Big|_{\text{Eucl}} \, p_{\beta_+}, \\
\dot{\beta}_- &= \frac{-(6\pi)^{1/2}}{2e^{3\alpha}} N\Big|_{\text{Eucl}} \, p_{\beta_-}, \\
\dot{\phi} &= \frac{-(6\pi)^{1/2}}{2e^{3\alpha}} N\Big|_{\text{Eucl}} \, p_\phi,
\end{aligned} \tag{10.16}$$

where $N|_{\text{Eucl}}$ is the lapse. The lapse $N|_{\text{Eucl}}$ can be any function of the Misner variables and ϕ as long as it never vanishes or changes sign within the range $-\infty$ to ∞ of all four variables. To keep our analysis straightforward we will set $N|_{\text{Eucl}} = \frac{2e^{\alpha}}{(6\pi)^{1/2}}$. Using this lapse and (10.4) results in the following classical flow equations

$$\begin{aligned}
\frac{d\alpha}{dt} = &\frac{1}{3} e^{2\alpha - 4\beta_+} \left(2e^{6\beta_+} \cosh\left(2\sqrt{3} \;\; \beta_- \right) \pm 1 \right) \\
&- \frac{\Lambda e^{4\alpha + 4\beta_+}}{9\pi} - \mathrm{b}^2,
\end{aligned} \tag{10.17}$$

$$\begin{aligned}
\frac{d\beta_+}{dt} = &- 2e^{2\alpha + 2\beta_+} \cosh\left(2\sqrt{3}\beta \;\; _- \right) + \mathrm{bb}^2 + \frac{\Lambda e^{4\alpha + 4\beta_+}}{9\pi} + \\
&\frac{2}{3} e^{2\alpha - 4\beta_+} \left(2e^{6\beta_+} \cosh \;\; \left(2\sqrt{3}\beta_- \right) \pm 1 \right)),
\end{aligned} \tag{10.18}$$

$$\frac{d\beta_-}{dt} = -\frac{2e^{2\alpha+2\beta_+}\sinh\left(2\sqrt{3}\beta_-\right)}{\sqrt{3}}, \tag{10.19}$$

$$\frac{d\phi}{dt} = -\frac{\sqrt{\rho}}{2\sqrt{3}}. \tag{10.20}$$

As it can be seen when $\beta_- = 0$ the time derivative of β_- vanishes which indicates that if β_- is initially zero, then it will remain zero indefinitely. Thus the wave functions we will find and analyze correspond to classical trajectories in minisuperspace where β_- is initially zero.

Despite this we stress that we are not analyzing the LRS Bianchi IX models. Even though we will be eventually setting $\beta_- = 0$ in our calculations, the existence of a β_- axis will impact our wave functions through the derivatives of β_- that will appear in our calculations which do not vanish when $\beta_- = 0$. As the reader can verify, (10.4) is the only $\mathcal{S}_{(0)}$ with matter sources for the Bianchi IX models which possesses this fixed point at $\beta_- = 0$ in its flow equations.

If we start with the case when only an aligned electromagnetic field is present($\Lambda = 0$) we can insert the entirety of (10.4) into (8.52) which will give us a complicated looking transport equation. However because $\beta_- = 0$ is a fixed point on the β_- axis we can set $\beta_- = 0$ for this complicated transport equation which results from inserting (10.4) into (8.52). The resultant transport equation as the reader can verify can be solved by inserting this ansatz into it

$$\mathcal{S}^1_{(1)\ \beta-=0} := x1\alpha + x2\phi, \tag{10.21}$$

which yields the following solution

$$\mathcal{S}^1_{(1)\ \beta-=0} := \frac{1}{2}\alpha(-\mathrm{B}-6) - \frac{\sqrt{3}\mathrm{b}^2\phi}{2\sqrt{\rho}}. \tag{10.22}$$

This is our first quantum correction for our Bianchi IX quantum cosmologies which correspond to classical cosmologies which are formed from a flow in minisuperspace which starts on a fixed point on the β_- axis. The above quantum correction takes into account the existence of the β_- axis in the full Bianchi IX models by taking the full derivative of $\mathcal{S}^1_{(0+)}$ in (8.52). An interesting feature of this quantum correction is how the aligned electromagnetic field b, stiff matter ρ, and the scalar field ϕ are coupled.

Using this first order quantum correction (10.22) and

$$\begin{aligned}\mathcal{S}^1_{(0+)\ \beta-=0} &:= \frac{1}{6}e^{2\alpha-4\beta_+}\left(2e^{6\beta_+}\pm 1\right)\\ &+\alpha \mathrm{b}^2+\beta_+\ \ \mathrm{b}^2+\frac{\phi\sqrt{\rho}}{2\sqrt{3}}.\end{aligned} \tag{10.23}$$

We can study the quantum cosmology of Bianchi IX 'ground' states which are restricted to the β_+ axis. In addition, because our wave functions only possess three minisuperspace variables we can use ϕ as our time parameter to obtain wave functions which are easy to interpret via their aesthetic qualities.

Starting with the Bianchi IX models we form the following wave function

$$\psi^1_{\beta-=0}=e^{-\mathcal{S}^1_{(0+)\ \beta-=0}-\mathcal{S}^1_{(1)\ \beta-=0}} \tag{10.24}$$

and plot them for two different values b of the aligned electromagnetic field as can be seen in (10.5). As can be seen in figure (10.5a) when $b=0$ our wave function is describing a quantum universe which is most likely in a geometric configuration in which its scale factor $\alpha\approx .6$ and $\beta_+=0$. However when we turn on our aligned electromagnetic field its wave function is now peaked at a larger value of both α and β_+.

Next we will examine Bianchi IX 'excited' states which are restricted to the β_+ axis when an electromagnetic field and cosmological constant are present. For notational

convenience we will represent the quantum corrections, ϕ_k, to the 'excited' states as Φ_k. First we insert the entirety of (10.4) into (8.59); then only after taking the derivative of (10.4) with respect to β_- do we set $\beta_- = 0$ which results in the following homogeneous transport equation

$$\begin{aligned}
&\mathrm{b}^2\frac{\partial\phi_{(0)}}{\partial\alpha} - \mathrm{b}^2\frac{\partial\phi_{(0)}}{\partial\beta_+} - \frac{1}{3}e^{2\ \ \alpha-4\beta_+}\frac{\partial\phi_{(0)}}{\partial\alpha}, - \\
&\frac{2}{3}e^{2\alpha+2\beta_+\ \ }\frac{\partial\phi_{(0)}}{\partial\alpha} - \frac{2}{3}e^{2\alpha-4\beta_+}f\left(\beta\ \ _+\right) + \frac{2}{3}e^{2\alpha+2\beta_+}f\left(\beta_+\right), \\
&+2\ \ \sqrt{3}\sqrt{p}\frac{\partial\phi_{(0)}}{\partial\phi} + \frac{\Lambda e^{4\alpha+4\beta_+}}{9\pi}\frac{\partial\phi_{(0)}}{\partial\alpha}, \\
&-\frac{\Lambda e^{4\alpha+4\beta_+}}{9\pi}\frac{\partial\phi_{(0)}}{\partial\beta_+} = 0.
\end{aligned} \tag{10.25}$$

The author found the following solutions to this transport equation

$$\phi_0^1 = \left(9\pi\ e^{4\alpha-2\beta_+} - 9\pi\ e^{4(\alpha+\beta\ \ _+)} + 27\pi\ \mathrm{b}^2 e^{2(\alpha+\beta_+)} + \Lambda e^{6\ \ (\alpha+\beta_+)}\right)^n \tag{10.26}$$

where in order for ϕ_0^1 to be globally defined and smooth we must restrict n to be either a positive integer or zero. Using (10.26) we form the following wave function

$$\Psi^1{}_{\beta-=0} = \phi^1_{0+} e^{-\mathcal{S}^1_{(0+)\ \beta-=0} - \mathcal{S}^1_{(1)\ \beta-=0}} \tag{10.27}$$

which we plot in (10.6). Figure 6 emphatically shows that when both a negative cosmological constant and an electromagnetic field are present the effects of the electromagnetic field are dependent upon its strength. When the field is relatively weak as can be seen (10.6a) and (10.6b) it can cause an additional highly probable geometric state to come into existence which our quantum universe can tunnel in and out of. However when the electromagnetic field is strong it can also destroy a highly probable state, leaving only one highly probable state that a quantum universe can be in. This ability to create an additional state that a quantum universe can tunnel in and out of is similar to how non-commutativity in the minisuperspace variables

can cause new quantum states to emerge in the quantum Kantowski-Sachs [93] and Bianchi I models [229]. Chronicling these effects of our aligned electromagnetic field can help us understand what our early universe could have been like.

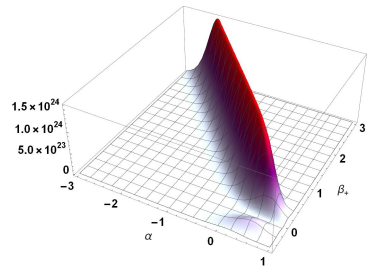

(a) $\phi = 0 \quad \Lambda = -1 \quad b = 0 \quad n = 1$

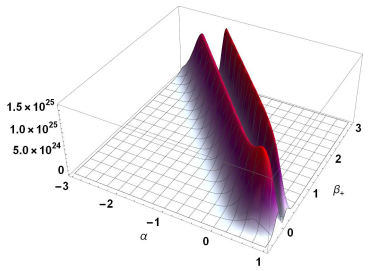

(b) $\phi = 0 \quad \Lambda = -1 \quad b = 1.5 \quad n = 1$

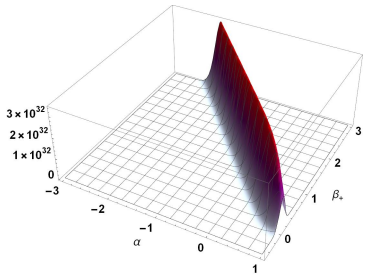

(c) $\phi = 0 \quad \Lambda = -1 \quad b = 3 \quad n = 1$

Figure 10.6 Two plots of (10.27) for the first 'excited' states of our Bianchi IX wave functions restricted to the β_+ axis for two different values of the strength of the electromagnetic field b.

10.4 Quantum Taub Models With A Scalar Field

The author found the following $\mathcal{S}_{(0)}$ for the quantum Taub models when an exponential scalar potential and an aligned electromagnetic field are present

$$\begin{aligned}\mathcal{S}^4_{(0)} := &\frac{1}{6}e^{2\alpha-4\beta_+} + \frac{1}{3}e^{2\alpha+2\beta_+} - \frac{c}{8}\, e^{4\alpha-2\beta_++\phi} \\ &- \alpha \mathrm{b}^2 + \frac{\beta_+ \mathrm{b}^2}{2} - \frac{\mathrm{b}^2\phi}{4},\end{aligned} \tag{10.28}$$

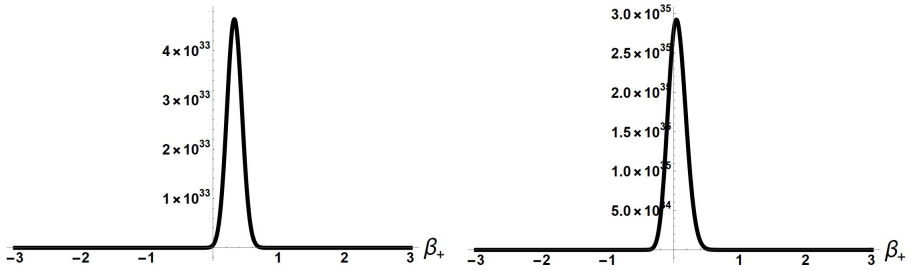

(a) $\alpha = 1 \quad c = -1 \quad \phi = 0$ **(b)** $\alpha = 1 \quad c = -1 \quad \phi = -5$

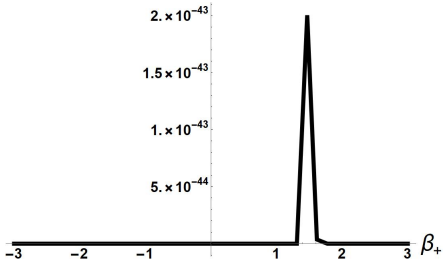

(c) $\alpha = 1 \quad c = -1 \quad \phi = 5$

Figure 10.7 These are three plots of our Taub wave functions when an exponential scalar potential is present.

where c can in principle be any real number. However for the purposes of elucidating the points the author wishes to make we will assume $c < 0$. Utilizing (8.51) the author found the following $\mathcal{S}_{(1)}$ quantum correction to (10.28)

$$\mathcal{S}^4_{(1)} := \frac{1}{2}\alpha(-\mathrm{B} - 2) - \beta_+ - \frac{\phi}{2}. \tag{10.29}$$

The existence of (10.28) and (10.29), suggest that an analogous closed form solution involving an exponential scalar field potential may exist for the Bianchi IX models as well.

First we will plot $e^{-\mathcal{S}^4_{(0)} - \mathcal{S}^4_{(1)}}$ when $B = 0$ and $b = 0$ and use both α and ϕ as our internal clocks.

Our plots (10.7) indicate that as our scalar potential decays the universes described by these wave functions approaches isotropy. However when our scalar potential

increases in magnitude these universes become more anisotropic. Similar qualitative behavior may be present for other types of scalar potentials such as ϕ^n.

These effects are interesting in themselves, however to further determine how typical or robust they are, more general scalar fields need to be studied. To accomplish this in the future various approximate techniques which do not rely on obtaining closed form solutions would need to be employed. However for the meantime these findings encourage further work to be done to determine how scalar fields affect quantum cosmological evolution in anisotropic models.

For the case when an aligned electromagnetic field is present we will use ϕ as our sole internal clock. As can be seen in figure 8, if we use ϕ as our internal clock, the aligned electromagnetic field induces some dramatic effects on our wave functions. If we compare (10.8a) to (10.8b) we see that the electromagnetic field causes the very 'fuzzy' wave function in (10.8a) to become sharp, or peaked at a certain value α and β_+. This effect would be present even if we kept $\phi = 0$. As ϕ increases, our wave functions travel in the negative α direction which indicates that the universes we are describing are more likely to be smaller in size as ϕ grows. In addition as ϕ grows it moves in the positive β_+ direction which indicates its anisotropy in general increases as ϕ increases. The fact that the Euclidean-signature semi-classical method was able to generate such a wealth of information for the solutions of (10.3) further shows its ability to prove [20, 175] the existence of solutions to Lorentzian signature equations.

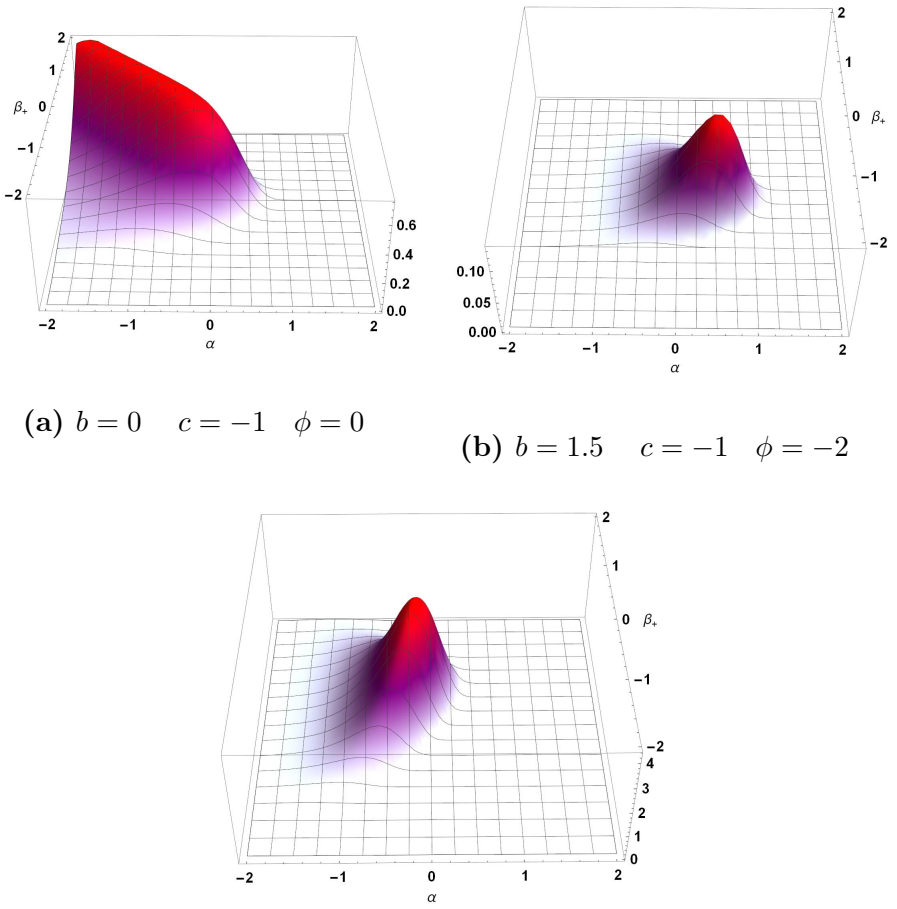

(a) $b = 0 \quad c = -1 \quad \phi = 0$

(b) $b = 1.5 \quad c = -1 \quad \phi = -2$

(c) $b = 1.5 \quad c = -1 \quad \phi = 3$

Figure 10.8 These are three plots of our Taub wave functions when an exponential scalar potential and aligned electromagnetic are present.

10.5 Closed Form Solutions To Bianchi IX and VIII WDW

If we start with (10.4) and set $\Lambda = 0$, and solve the equation which results from inserting (10.4) into (8.52), we obtain the following $\mathcal{S}_{(1)}$ quantum correction

$$\begin{aligned}\mathcal{S}^{1}_{(1\pm)} &:= \alpha \mathrm{x1} + \frac{1}{8}(\mathrm{B} + 2\mathrm{x1} + 6)\log\left(\sinh\left(2 \ \ \sqrt{3}\beta_{-}\right)\right) \\ &+ \beta_{+}\left(\frac{1}{4} \ \ (-\mathrm{B} - 6) - \frac{\mathrm{x1}}{2}\right) \\ &\mp \phi\left(\frac{\sqrt{3} \ \ \mathrm{b}^{2}(\mathrm{B}+2)}{8\sqrt{\rho}} + \frac{\sqrt{3}\mathrm{b}^{2} \ \ \mathrm{x1}}{4\sqrt{\rho}}\right),\end{aligned} \tag{10.30}$$

where x1 is an arbitrary constant, and B is the Hartle-Hawking ordering parameter. Technically this $\mathcal{S}_{(1)}$ term is not smooth and globally defined, however we can form smooth and globally defined wave functions from it if we restrict $(\mathrm{B} + 2\mathrm{x1} + 6)$ to be $-8y$, where y is either zero or a positive integer. Using (8.53) we can obtain solutions to (10.2) of the form $e^{-\mathcal{S}^{1}_{(0\pm)} - \mathcal{S}^{1}_{(1\pm)}}$, when $\Lambda = 0$ and our aligned electromagnetic field is given by $2b^{2}e^{2\alpha - 4\beta_{+}}$ if the constants $(x1, \rho, b, B)$ in (10.30) satisfy the following relations

$$\begin{aligned}&\frac{3\mathrm{b}^{4}(\mathrm{B} - 2\mathrm{x1} + 2)^{2}}{32\rho} - 2\mathrm{B} \ \ \mathrm{x1} + 2\mathrm{x1}^{2} = 0 \\ &\mathrm{B} + 2\mathrm{x1} + 6 = 0.\end{aligned} \tag{10.31}$$

Beyond these closed form solutions we can also construct smooth and globally defined wave functions using (10.4) and (10.30) as long as $(\mathrm{B} + 2\mathrm{x1} + 6)$ is a negative integer which is a multiple of 8. The question of solving the higher order transport equations for the Bianchi IX and VIII models when an aligned electromagnetic field is present in the other two perpendicular directions could be the topic of a future investigation. For now we will be content with this closed form solution for an aligned electromagnetic field.

For the sake of completeness we will report a few other closed form solutions that the author found for the vacuum Bianchi IX and VIII models which were reported in earlier works. For the vacuum Bianchi IX models when $\rho = 0$, $\Lambda = 0$, and $b = 0$, Joseph Bae [20] found two families of quantities which are conserved under the flow produced by (10.4), and thus satisfy (8.59). The author then modified those quantities

so that they are conserved under the flow given by (10.4) for the Bianchi VIII models. Thus we will use the following quantities which satisfy (8.59) for the vacuum Bianchi IX and VIII models

$$\begin{aligned}
&\phi^1_{0\pm} := S^{m1} O^{m2}, \\
&S = \left(e^{4\alpha - 2\beta_+} \left(e^{6\beta_+} \mp \cosh\left(2\sqrt{3} \;\; \beta_- \right) \right) \right), \\
&O = \left(e^{4\alpha - 2\beta_+} \sinh\left(2 \;\; \sqrt{3}\beta_- \right) \right),
\end{aligned} \tag{10.32}$$

where m1 is either zero or a positive integer for the Bianchi IX case, or can be any number for the Bianchi VIII models, m2 is always either zero or a positive integer. Joseph Bae found the following solution to (8.52) for the vacuum Bianchi IX models, which also happens to satisfy (8.52) for the vacuum Bianchi VIII models

$$\mathcal{S}_{(1\ Bae)} := -\frac{1}{2}\alpha(\mathrm{B} + 6). \tag{10.33}$$

Solutions of the form $\phi^1_{0\pm} e^{-\mathcal{S}_{(0\pm)} - \mathcal{S}^1_{(1\ Bae)}}$ exist for the vacuum Bianchi VIII and IX models for the following values of $(B, m1, m2)$

$$\begin{aligned}
&(B = \pm 6, m1 = 0, m2 = 0) \\
&(B = \pm 2\sqrt{33}, m1 = 1, m2 = 0) \\
&(B = \pm 2\sqrt{33}, m1 = 0, m2 = 1)
\end{aligned} \tag{10.34}$$

More information on these closed form solutions can be found in [37].

Chapter 11

Quantum Bianchi II and $\text{VII}_{h=0}$

11.1 Bianchi II and $\text{VII}_{h=0}$ Models

The Bianchi II and $\text{VII}_{h=0}$ models which we will focus on in this chapter have the following one forms respectively

$$\begin{aligned}\omega^1 &= dy + xdz \\ \omega^2 &= dz \\ \omega^3 &= dx,\end{aligned} \tag{11.1}$$

$$\begin{aligned}\omega^1 &= \cos(z)dx + \sin(z)dy \\ \omega^2 &= -\sin(z)dx + \cos(z)dy \\ \omega^3 &= dz.\end{aligned} \tag{11.2}$$

Their corresponding WDW equations are

$$\begin{aligned}&\frac{\partial^2\Psi}{\partial\alpha^2} - B\frac{\partial\Psi}{\partial\alpha} - \frac{\partial^2\Psi}{\partial\beta_+^2} - \frac{\partial^2\Psi}{\partial\beta_-^2} + U_i\Psi = 0, \\ &U_{II} = \frac{1}{12}e^{4\alpha+4\beta_++4\sqrt{3}\beta_-} + 24\Lambda e^{6\alpha} + 2b^2e^{2\alpha+2\beta_++2\sqrt{3}\beta_-} + \rho, \\ &U_{VII} = \frac{4}{3}e^{4(\alpha+\beta_+)}\sinh^2\left(2\sqrt{3}\beta_-\right) + 24\Lambda e^{6\alpha} + 2b^2e^{2\alpha+2\beta_++2\sqrt{3}\beta_-} + \rho,\end{aligned} \tag{11.3}$$

where ρ denotes stiff matter and Λ is scaled differently from (7.84).

This chapter will be organized as follows. We will first apply the Euclidean-signature semi-classical method to rederive closed form solutions to the Bianchi II WDW equation that are similar to the ones first derived by [186]. Afterwards we will show how all of the equations that this method provides can be solved which will give us a family of asymptotic and closed form solutions. In the process we will obtain a novel asymptotic solution to the vacuum Bianchi II WDW equation. Then we will obtain new solutions to the Bianchi II WDW equation when a cosmological constant, primordial aligned electromagnetic field and stiff matter are present and discuss its 'excited' states. Next we will take a detour from applying our modified semi-classical method and turn our attention to the non-commutative quantum Bianchi II models with a primordial aligned electromagnetic field, and stiff matter.

Moving on from Bianchi II we will turn our attention to the quantum Bianchi $\text{VII}_{h=0}$ models. Using the Euclidean-signature semi-classical method we will first study its vacuum 'ground' and 'excited' states. Afterwards we will study its 'ground' states when matter sources are present. Once we have computed all of our wave functions we will interpret [178] them by their aesthetic characteristics. Finally we will provide some concluding remarks.

11.2 'Ground' States Of The Vacuum Bianchi II Wheeler DeWitt Equation

As was reported in [186], there are three solutions to the Euclidean-signature Hamilton Jacobi equation (8.51) that corresponds to the Bianchi II WDW equation (11.3) when $\Lambda = 0$, $b = 0$, and $\rho = 0$, and they are given by

$$\mathcal{S}^{1}_{(0)} := \frac{1}{12} e^{2\left(\alpha+\sqrt{3}\beta_{-}+\beta_{+}\right)}, \tag{11.4}$$

$$\mathcal{S}^{2}_{(0)} := \left(\frac{1}{12} e^{2\alpha+2\sqrt{3}\beta_{-}+2\beta_{+}} + f(2\alpha+2\beta_{+}) \right), \tag{11.5}$$

$$\mathcal{S}^{3}_{(0)} := \left(\frac{1}{12} e^{2\alpha+2\sqrt{3}\beta_{-}+2\beta_{+}} + g(2\alpha+\sqrt{3}\beta_{-}-\beta_{+}) \right), \tag{11.6}$$

where f(x) and g(x) are arbitrary single variable functions. In this section we will study 'ground' state solutions to the Bianchi II Wheeler DeWitt equation obtained using the Euclidean-signature semi-classical method. The superscripts for the $\mathcal{S}_{(k)}$ terms in this chapter will play the role of an index to keep track of them unless stated otherwise.

Starting with (11.4) if we insert it into our first 'ground' state transport equation (8.52) we obtain the following simple differential equation

$$2\frac{\partial \mathcal{S}_{(1)}}{\partial \alpha} - 2\sqrt{3}\frac{\partial \mathcal{S}_{(1)}}{\partial \beta_{-}} - 2\frac{\partial \mathcal{S}_{(1)}}{\partial \beta_{+}} + \mathrm{B} + 6 = 0. \tag{11.7}$$

This transport equation in principle has infinitely many solutions. However for the purposes of trying to find a $\mathcal{S}_{(1)}$ which will allow the solutions to the higher order $k \geq 2$ transport equations to be satisfied by zero, we will choose the following to be our $\mathcal{S}_{(1)}$

$$\mathcal{S}^{1}_{(1)} := \frac{1}{2}\left(-\mathrm{B} + 2\mathrm{x2} + 2\sqrt{3}\mathrm{x3} - 6 \right)\alpha + \mathrm{x2}\beta_{+} + \mathrm{x3}\beta_{-}, \tag{11.8}$$

where x2 and x3 are free parameters, which can be real or complex. We choose this linear form because when we insert it into the $\mathcal{S}_{(2)}$ transport equation (8.53), its source term can be made to vanish by adjusting our free parameters. To clearly illustrate this if we insert (11.8) into the source term of the $\mathcal{S}_{(2)}$ transport equation we obtain the following expression

$$f(x2,x3) = \mathrm{B}^2 - 4\left(2\sqrt{3}(\mathrm{x2}-3)\mathrm{x3} - 6\mathrm{x2} + 2\mathrm{x3}^2 + 9\right), \tag{11.9}$$

which can be easily made to vanish by solving for one of its free parameters (x2,x3) such that f(x2,x3)=0. The constraint of f(x2,x3)=0 was first derived in [186]. If we solve for x2, the following $\mathcal{S}_{(1)}$ will allow all of the higher order transport equations to be satisfied by zero and will allow us to easily write out a closed form solution for any arbitrary ordering parameter B to the Bianchi II Wheeler DeWitt equation

$$\begin{aligned} \mathcal{S}^1_{(1)} &:= \frac{1}{2}\left(-\mathrm{B} + 2\mathrm{x2} + 2\sqrt{3}\mathrm{x3} - 6\right)\alpha + \mathrm{x2}\beta_+ + \mathrm{x3}\beta_- \\ x2 &= \frac{\mathrm{B}^2 - 8\mathrm{x3}^2 + 24\sqrt{3}\mathrm{x3} - 36}{8\left(\sqrt{3}\mathrm{x3} - 3\right)}. \end{aligned} \tag{11.10}$$

This results in us obtaining one of the solutions compatible with the constraint that was first reported in [186] to the Bianchi II WDW equation for any arbitrary ordering parameter B

$$\psi = e^{\left(-\frac{x3\left(2\alpha+\sqrt{3}\beta_- - \beta_+\right)}{\sqrt{3}} - \frac{1}{12}e^{2\left(\alpha+\sqrt{3}\beta_- + \beta_+\right)} - \frac{\left(B^2+12\right)(\alpha+\beta_+)}{8\left(\sqrt{3}x3-3\right)} + \frac{1}{2}\alpha(B+2) - 2\beta_+\right)}. \tag{11.11}$$

A nice feature of this solution is that it still possesses the free parameter x3, which allows one to form a wide variety of wave functions from it using superposition. The above is a procedure that in some cases [39] can be employed to find closed form 'ground' state solutions to the Wheeler DeWitt equation using the Euclidean-signature semi-classical method.

Moving on to (11.5) if we choose f to be $\mathrm{x1}e^{2\alpha+2\beta_+}$ where x1 is a free parameter and apply the same procedure we obtain an $\mathcal{S}_{(1)}$ which possesses one free parameter

$$\mathcal{S}^2_{(1)} := \mathrm{x2}\alpha + \sqrt{3}\beta_- + \left(\frac{\mathrm{B}}{2} + \mathrm{x2}\right)\beta_+, \tag{11.12}$$

and when inserted into (8.53) results in a source term $-\frac{1}{2}B^2 - 6$ which does not vanish for any real values of the ordering parameter, but does vanish when $B = 2\sqrt{3}i$. However if we want a solution involving a real value of the ordering parameter we can use the Euclidean-signature semi-classical method to construct an asymptotic solution to the Bianchi II Wheeler Dewitt equation for any arbitrary ordering parameter for this $\mathcal{S}_{(0)}$ (11.5).

If we choose the following ansatz for our higher order $k \geq 2$ quantum corrections

$$\mathcal{S}^2_{(k)} := g(\mathrm{B})_k e^{\left(-2\alpha(k-1)-2(k-1)\left(\sqrt{3}\beta_- +\beta_+\right)\right)}; \tag{11.13}$$

and insert it into (8.53) we can prove that the problem of solving the higher order transport partial differential equations reduces to solving a recurrence equation, where we are solving for some function, $g(\mathrm{B})_k$, of the Hartle-Hawking ordering parameter. The first step in our proof is to insert (11.13) into the homogeneous portion of equation (8.53) which results in the following expression

$$2(k-1)g(\mathrm{B})_k e^{-2(k-2)\left(\alpha+\sqrt{3}\beta_- +\beta_+\right)}. \tag{11.14}$$

The next step is to rewrite the source terms of equation (8.53) as follows

For $k = 2$

$$2\left[B\frac{\partial\mathcal{S}_{(1)}}{\partial\alpha} - \frac{\partial^2\mathcal{S}_{(1)}}{\partial\alpha^2} + \frac{\partial^2\mathcal{S}_{(1)}}{\partial\beta_+^2} + \frac{\partial^2\mathcal{S}_{(1)}}{\partial\beta_-^2}\right] + 2\left(\frac{\partial\mathcal{S}_{(1)}}{\partial\alpha}\frac{\partial\mathcal{S}_{(1)}}{\partial\alpha} - \frac{\partial\mathcal{S}_{(1)}}{\partial\beta_+}\frac{\partial\mathcal{S}_{(1)}}{\partial\beta_+} - \frac{\partial\mathcal{S}_{(1)}}{\partial\beta_-}\frac{\partial\mathcal{S}_{(1)}}{\partial\beta_-}\right) \tag{11.15}$$

For $k = 3$

$$3\left[B\frac{\partial\mathcal{S}_{(2)}}{\partial\alpha} - \frac{\partial^2\mathcal{S}_{(2)}}{\partial\alpha^2} + \frac{\partial^2\mathcal{S}_{(2)}}{\partial\beta_+^2} + \frac{\partial^2\mathcal{S}_{(2)}}{\partial\beta_-^2}\right] + 6\left(\frac{\partial\mathcal{S}_{(1)}}{\partial\alpha}\frac{\partial\mathcal{S}_{(2)}}{\partial\alpha} - \frac{\partial\mathcal{S}_{(1)}}{\partial\beta_+}\frac{\partial\mathcal{S}_{(2)}}{\partial\beta_+} - \frac{\partial\mathcal{S}_{(1)}}{\partial\beta_-}\frac{\partial\mathcal{S}_{(2)}}{\partial\beta_-}\right) \tag{11.16}$$

For $k > 3$

$$\begin{aligned} &k\left[B\frac{\partial\mathcal{S}_{(k-1)}}{\partial\alpha} - \frac{\partial^2\mathcal{S}_{(k-1)}}{\partial\alpha^2} + \frac{\partial^2\mathcal{S}_{(k-1)}}{\partial\beta_+^2} + \frac{\partial^2\mathcal{S}_{(k-1)}}{\partial\beta_-^2}\right] \\ &+\sum_{\ell=2}^{k-2}\frac{k!}{\ell!\,(k-\ell)!}\left(\frac{\partial\mathcal{S}_{(\ell)}}{\partial\alpha}\frac{\partial\mathcal{S}_{(k-\ell)}}{\partial\alpha} - \frac{\partial\mathcal{S}_{(\ell)}}{\partial\beta_+}\frac{\partial\mathcal{S}_{(k-\ell)}}{\partial\beta_+} - \frac{\partial\mathcal{S}_{(\ell)}}{\partial\beta_-}\frac{\partial\mathcal{S}_{(k-\ell)}}{\partial\beta_-}\right) \\ &+2k\left(\frac{\partial\mathcal{S}_{(1)}}{\partial\alpha}\frac{\partial\mathcal{S}_{(k-1)}}{\partial\alpha} - \frac{\partial\mathcal{S}_{(1)}}{\partial\beta_+}\frac{\partial\mathcal{S}_{(k-1)}}{\partial\beta_+} - \frac{\partial\mathcal{S}_{(1)}}{\partial\beta_-}\frac{\partial\mathcal{S}_{(k-1)}}{\partial\beta_-}\right) \end{aligned} \tag{11.17}$$

As the reader can easily verify if we were to insert (11.13) into the source terms (11.15) and (11.16), the resulting expressions would be some constants which are proportional to the exponential component of (11.13), and thus would allow one to calculate the k=2 and k=3 quantum corrections by simply solving for $g(B)_k$ and inserting it back into (11.13). To prove that this is the case for the higher order $k > 3$ quantum corrections all we need to do is insert our $\mathcal{S}^2_{(k)}$ and our linear $\mathcal{S}^2_{(1)}$ into (11.17). Doing so yields the following amazing simplification

$$\begin{aligned} &-2(k-2)k(\mathrm{B}-6k+12)g(\mathrm{B})_{k-1}e^{-2(k-2)\left(\alpha+\sqrt{3}\beta_-+\beta_+\right)} \\ &+\sum_{\ell=2}^{k-2}\frac{k!}{\ell!\,(k-\ell)!}\left(-12(l-1)(k-l-1)g(\mathrm{B})_l e^{-2(k-2)\left(\alpha+\sqrt{3}\beta_-+\beta_+\right)}g(\mathrm{B})_{k-l}\right) \\ &+2(\mathrm{B}+6)(k-2)kg(\mathrm{B})_{k-1}e^{-2(k-2)\left(\alpha+\sqrt{3}\beta_-+\beta_+\right)}. \end{aligned} \tag{11.18}$$

Putting this all together, and solving for $g(\mathrm{B})_k$ results in

$$g(\mathrm{B})_k = \frac{\sum_{l=2}^{k-2} -\frac{12(l-1)k!(k-l-1)g(B)_l g(B)_{k-l}}{l!(k-l)!}}{2-2k} - 6k(k-2)g(B)_{k-1}. \tag{11.19}$$

As the reader can see, our infinite sequence of linear partial differential equations has become a recurrence relation for our higher order quantum corrections. A computer algebra system like Mathematica can easily compute the terms of this recurrence relation and as a result the $\mathcal{S}^2_{(k)}$ quantum corrections can in principle be obtained to any order k. The above calculation presents an alternative to [20] for obtaining asymptotic solutions to the Wheeler DeWitt equation using the Euclidean-signature semi-classical method.

We have constructed a method to obtain all of the $\mathcal{S}^2_{(k)}$ quantum corrections to the semi-classical wave function $\overset{(0)}{\Psi}_{\hbar} = e^{-\frac{1}{X}\mathcal{S}^2_{(0)}}$, and as a result are able to construct a wide variety of asymptotic solutions to the Bianchi II Wheeler DeWitt equation for any Hartle-Hawking ordering parameter

$$\begin{aligned}
\mathcal{S}^2_{(k,\ k>3)} &:= \left(\frac{\sum_{l=2}^{k-2} -\frac{12(l-1)k!(k-l-1)g(B)_l g(B)_{k-l}}{l!(k-l)!}}{2-2k} - 6k(k-2)g(B)_{k-1} \right) e^{\left(-2\alpha(k-1)-2(k-1)\left(\sqrt{3}\beta_- +\beta_+\right)\right)} \\
\mathcal{S}^2_{(2)} &:= \frac{1}{4}\left(\mathrm{B}^2+12\right) e^{-2\alpha-2\left(\sqrt{3}\beta_- +\beta_+\right)} \\
\mathcal{S}^2_{(3)} &:= -\frac{9}{2}\left(\mathrm{B}^2+12\right) e^{-4\alpha-4\left(\sqrt{3}\beta_- +\beta_+\right)} \\
\overset{(0)}{\Psi}_{\hbar} &= e^{-\frac{1}{X}\mathcal{S}^2_{(0\ \pm)} - \mathcal{S}^2_{(1)} - \frac{X}{2!}\mathcal{S}^2_{(2)} - \frac{X^2}{3!}\mathcal{S}^2_{(3)} - \sum_{k=4}^{\infty}\frac{X^{k-1}}{k!}\mathcal{S}^2_{(k)}}.
\end{aligned} \tag{11.20}$$

It would be instructive to see through some manner of non trivial summation such as a Borel sum if the resulting asymptotic terms converge to some wave function which behaves in an interesting fashion. Regardless of the convergence properties of these terms, the fact that such an asymptotic solution can be found in the first place is remarkable. There are other problems in physics where such a technique for

computing an asymptotic expansion can prove to be very useful.

The explicit forms of the $\mathcal{S}^2_{(2)}$ and $\mathcal{S}^2_{(3)}$ quantum corrections shown above can be easily computed by the reader using (11.14), (11.15), and (11.16). Our quantum corrections possess the important property that they decay as α grows. Because α is related to the spatial size of our Bianchi II universe, physically it makes sense that our quantum corrections become increasingly important the smaller our universe becomes, while conversely becoming negligible in the classical limit of $\alpha >> 0$. Because our solutions are asymptotic we only need to sum up a finite number of terms to get a good approximation for the full wave function. As a result of our solutions being asymptotic we will qualitatively analyze the properties of the following wave functions which are composed from $\mathcal{S}^2_{(0)}$, $\mathcal{S}^2_{(1)}$, and $\mathcal{S}^2_{(2)}$

$$\psi = e^{\left(\frac{1}{24}\left(-3\left(\mathrm{B}^2+12\right)e^{-2\left(\alpha+\sqrt{3}\beta_-+\beta_+\right)}-2e^{2(\alpha+\beta_+)}\left(e^{2\sqrt{3}\beta_-}+12i\mathrm{x1}\right)-24\mathrm{x2}(\alpha+\beta_+)-24\sqrt{3}\beta_--12\beta_+\mathrm{B}\right)\right)}, \tag{11.21}$$

where we made x1 an imaginary number. Because both x1 and x2 are free parameters there are infinitely many different wave functions we can choose to analyze. To narrow things down for our purposes we will set x2 and the ordering parameter B equal to zero, and then form the following wave function $\Psi = \int_{-\infty}^{\infty} e^{-x1^2}\psi dx1$ based on the linearity of the WDW equation resulting in

$$\Psi = \sqrt{\pi}e^{\left(\frac{1}{12}\left(-18e^{-2\left(\alpha+\sqrt{3}\beta_-+\beta_+\right)}-e^{2\left(\alpha+\sqrt{3}\beta_-+\beta_+\right)}-3e^{4(\alpha+\beta_+)}-12\sqrt{3}\beta_-\right)\right)}. \tag{11.22}$$

We will display three plots (figures 1, 2, and 3) of this wave function for different values of α below and discuss them qualitatively towards the end of this chapter.

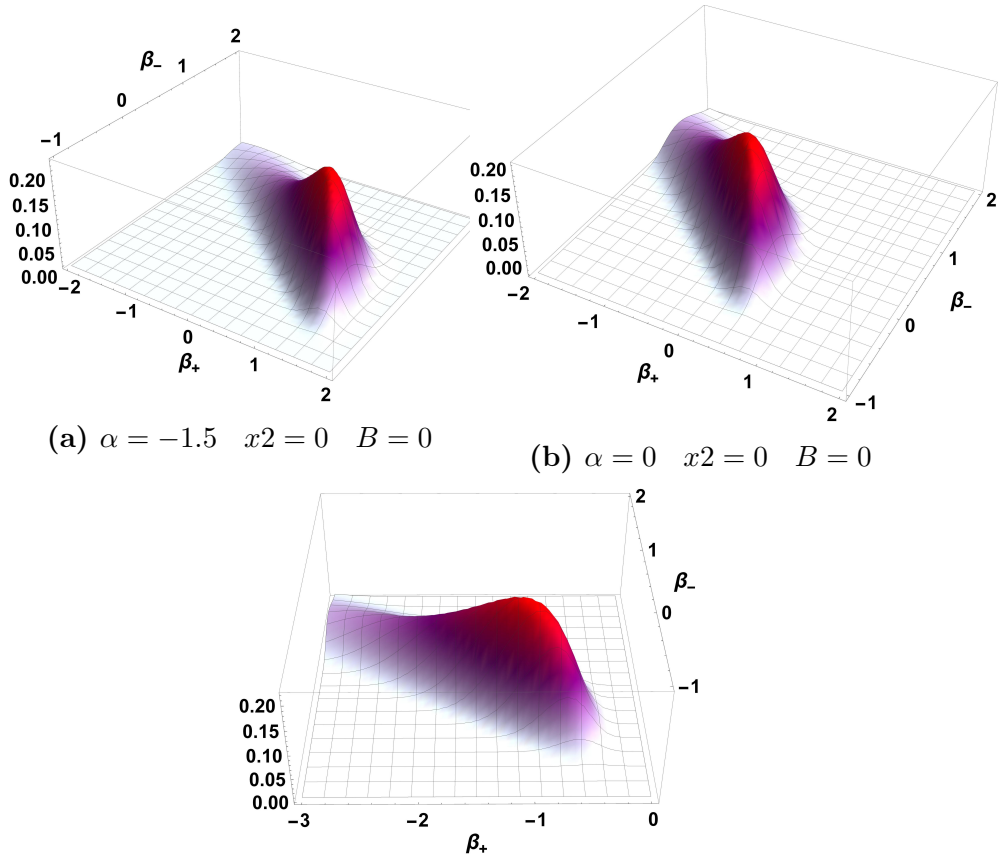

(a) $\alpha = -1.5 \quad x2 = 0 \quad B = 0$

(b) $\alpha = 0 \quad x2 = 0 \quad B = 0$

(c) $\alpha = 1.5 \quad x2 = 0 \quad B = 0$

Figure 11.1 Plot of $|\Psi|^2$ from (11.22) for three different values α.

11.3 Solving The 'Excited' State Transport Equations In Closed Form

Even though the quantum Bianchi II models without any matter sources can be solved in closed form via separation of variables, applying this method has allowed us to obtain explicit quantum corrections to semi-classical wave functions of the form (8.50). For some cases such as the Taub models [178] superpositions of separable solutions can be constructed using integration which yield wave functions having the form of (8.50). Computing an exact expression which looks like $\overset{(0)}{\Psi}_{\hbar}= e^{-\frac{1}{X}\mathcal{S}_{(0)}-\mathcal{S}_{(1)}-\frac{X}{2!}\mathcal{S}_{(2)}-\cdots}$ though is contingent upon knowing how to integrate usually some Bessel function times a kernel such as $e^{-\omega^2}$ in closed form. As we have shown in the previous section our modified semi-classical method allows us to bypass those mathematical difficulties and obtain solutions which are more mathematically transparent. In addition the wave functions that this method obtains for us possess non-trivial characteristics such as their behavior being highly dependent upon α, which as was previously mentioned is our internal clock and also dictates the scale factor of our Bianchi II universes. Another non-trivial feature is the manifestation of discreteness in our wave functions which will be showcased in our 'excited' states later on.

We will now go over how all of the 'excited' state transport equations can be solved for the case when (11.4) is our $\mathcal{S}_{(0)}$. As it can be seen from our 'excited' state transport equations (8.59-8.61), in order to solve them we first need solutions to their ground state counterparts (8.51-8.53). If we insert (11.4) into (8.59) we obtain

$$\left(\frac{\partial\phi_{(0)}}{\partial\alpha}-\sqrt{3}\frac{\partial\phi_{(0)}}{\partial\beta_{-}}-\frac{\partial\phi_{(0)}}{\partial\beta_{+}}\right)=0, \tag{11.23}$$

which is an elementary linear transport equation which has the following solutions

$$\phi^1_{(0)} := f_1\left(\left(3\alpha + \sqrt{3}\beta_-\right), \left(3\beta_+ - \sqrt{3}\beta_-\right)\right), \tag{11.24}$$

where f_1 is a function of both the expressions $3\alpha + \sqrt{3}\beta_-$ and $3\beta_+ - \sqrt{3}\beta_-$. As a result we have infinitely many choices for our $\phi_{(0)}$. We can exploit the properties of the 'excited' state transport equations and our solutions to the 'ground' state equations to pick an ansatz which will give us the forms for all of our $\phi_{(k)}$ terms. Using the same reasoning presented in [175] for the Bianchi IX models we will pick the following to be our ansatz for the higher order $\phi_{(k)}$ terms

$$\phi^1_{(k)} := j(B)_k e^{\left((m_1-2k)\alpha + \frac{1}{\sqrt{3}}(-6k+m_1-m_2)\beta_- + (m_2-2k)\beta_+\right)}. \tag{11.25}$$

The parameters (m_1, m_2) in certain circumstances can plausibly be interpreted as graviton excitation numbers for the ultra long wavelength gravitational wave modes embodied in the (β_+, β_-) anisotropic degrees of freedom [21]. If we assume (m_1, m_2) represent physical quantities then they must be real numbers, despite the fact that states with complex (m_1, m_2) can also satisfy the Wheeler DeWitt equation as will be shown below. Because our ϕ_k terms do not vanish anywhere, m_1 and m_2 can be any real numbers, and if they lead to excited states they would be scattering states. Before we solve for the explicit form of $j(B)_k$ we will pick a different ansatz to showcase the versatility of this method.

If we choose our ϕ^1_0 to be $(\alpha + \sqrt{3}\beta_-)^{m_1}$ $(3\beta_+ - \sqrt{3}\beta_-)^{m_2}$, we can obtain leading order bound states because both of our expressions vanish for real finite values of the Misner variables. Going beyond leading order we can actually find a closed form solution to the Bianchi II Wheeler Dewitt equation by simply inserting $(\alpha + \sqrt{3}\beta_-)^{m_1}$ $(3\beta_+ - \sqrt{3}\beta_-)^{m_2} e^{-\mathcal{S}^1_{(0)} - \mathcal{S}^1_{(1)}}$ into it and noticing that for $m_2 = 1$, $m_1 = 0$, and $x3 =$

$\frac{1}{4}\left(4\sqrt{3}-\sqrt{\mathrm{B}^2+12}\right)$ that it is satisfied by

$$\psi=\frac{1}{3}\left(3\beta_+-\sqrt{3}\beta_-\right)e^{\left(\frac{1}{12}\left(-e^{2\left(\alpha+\sqrt{3}\beta_-+\beta_+\right)}+2\alpha\left(2\sqrt{3}\sqrt{\mathrm{B}^2+12}+3\mathrm{B}-6\right)+\sqrt{\mathrm{B}^2+12}\left(3\beta_-+\sqrt{3}\beta_+\right)-12\left(\sqrt{3}\beta_-+\beta_+\right)\right)\right)}. \tag{11.26}$$

This solution shows that one doesn't have to stick to the type of ansätze used in [175] to find solutions to the Wheeler Dewitt equation using this method. As a matter of fact it may be more advantageous for the sake of finding 'excited' states for the vacuum Bianchi II models after choosing (11.4) to be our $\mathcal{S}_{(0)}$ to use a different ansatz than (11.25) as we will discuss soon.

Moving on, if we pick (11.10) to be the $\mathcal{S}_{(1)}$ for our 'excited' state transport equations, a significant simplification occurs. Because our closed form solution (11.11) is constructed solely from an $\mathcal{S}_{(0)}$ and an $\mathcal{S}_{(1)}$ term all of the higher order $\mathcal{S}_{(k)}$ terms can be set to zero as was explained earlier. This significantly simplifies our 'excited' state transport equations because they depend on those higher order $\mathcal{S}_{(k)}$ terms which we can set to zero. The same is true for any Bianch A model which has a closed form solution where its $\mathcal{S}_{(k>1)}$ terms vanish(an even greater simplification occurs if (11.3) is satisfied by $e^{-\mathcal{S}_{(0)}}$). As a result our sequence of transport equations becomes

$$\begin{aligned}
&-\frac{\partial\phi_{(k)}}{\partial\alpha}\frac{\partial\mathcal{S}_{(0)}}{\partial\alpha}+\frac{\partial\phi_{(k)}}{\partial\beta_+}\frac{\partial\mathcal{S}_{(0)}}{\partial\beta_+}+\frac{\partial\phi_{(k)}}{\partial\beta_-}\frac{\partial\mathcal{S}_{(0)}}{\partial\beta_-}\\
&+k\left(-\frac{\partial\phi_{(k-1)}}{\partial\alpha}\frac{\partial\mathcal{S}_{(1)}}{\partial\alpha}+\frac{\partial\mathcal{S}_{(1)}}{\partial\beta_+}\frac{\partial\mathcal{S}_{(1)}}{\partial\beta_+}+\frac{\partial\phi^{(*)}_{(k-1)}}{\partial\beta_-}\frac{\partial\mathcal{S}_{(1)}}{\partial\beta_-}\right)\\
&+\frac{k}{2}\left(-B\frac{\partial\phi_{(k-1)}}{\partial\alpha}+\frac{\partial^2\phi^{(*)}_{(k-1)}}{\partial\alpha^2}-\frac{\partial^2\phi_{(k-1)}}{\partial\beta_+^2}-\frac{\partial^2\phi_{(k-1)}}{\partial\beta_-^2}\right).
\end{aligned} \tag{11.27}$$

Our situation supremely simplifies further if we can find a ϕ_k which is able to satisfy its associated transport equation when it equals zero. If $\phi_k=0$ satisfies the kth order 'excited' state transport equation then the k+1th order transport equation will

reduce to

$$-\frac{\partial\phi_{(k+1)}}{\partial\alpha}\frac{\partial\mathcal{S}_{(0)}}{\partial\alpha}+\frac{\partial\phi_{(k+1)}}{\partial\beta_+}\frac{\partial\mathcal{S}_{(0)}}{\partial\beta_+}+\frac{\partial\phi_{(k+1)}}{\partial\beta_-}\frac{\partial\mathcal{S}_{(0)}}{\partial\beta_-}=0, \tag{11.28}$$

which is satisfied by $\phi_{k+1}=0$. Thus the k+2th order transport equations reduces to

$$-\frac{\partial\phi_{(k+2)}}{\partial\alpha}\frac{\partial\mathcal{S}_{(0)}}{\partial\alpha}+\frac{\partial\phi_{(k+2)}}{\partial\beta_+}\frac{\partial\mathcal{S}_{(0)}}{\partial\beta_+}+\frac{\partial\phi_{(k+2)}}{\partial\beta_-}\frac{\partial\mathcal{S}_{(0)}}{\partial\beta_-}=0 \tag{11.29}$$

and it is also satisfied by $\phi_{k+2}=0$. When a kth order ϕ_k equation is satisfied by zero, all of the higher order ϕ_{k+n} transport equations can also be satisfied by zero as well. This results in a truncation of the infinite sequence of 'excited' state transport equations to a finite sequence and allows one to find closed form solutions to the Wheeler DeWitt equation for any model to which the above applies to. Inserting our ansatz (11.25) into (11.27) yields

$$\begin{aligned}
&j(\mathrm{B})_{k-1}\Big(3m_1\left(\mathrm{B}^2+8m_2+36\right)-3m_2\left(\mathrm{B}^2+16m_2-36\right)+144k^2\left(\sqrt{3}\mathrm{x}3-3\right)\\
&-144k\left(\sqrt{3}\mathrm{x}3-3\right)+24m_1^2-8\mathrm{x}3(m_1+2m_2)\left(\sqrt{3}m_1-\sqrt{3}m_2-3\mathrm{x}3+6\sqrt{3}\right)\Big)\\
&+24\left(\sqrt{3}\mathrm{x}3-3\right)j(\mathrm{B})_k=0,
\end{aligned} \tag{11.30}$$

which allows us to easily find a simple recurrence relation for $j(\mathrm{B})_k$

$$\begin{aligned}
j(\mathrm{B})_k=&\frac{1}{24\left(\sqrt{3}\mathrm{x}3-3\right)}j(\mathrm{B})_{k-1}\Big(3m_1\left(\mathrm{B}^2+8m_2+36\right)-3m_2\left(\mathrm{B}^2+16m_2-36\right)\\
&+144k^2\left(\sqrt{3}\mathrm{x}3-3\right)-144k\left(\sqrt{3}\mathrm{x}3-3\right)+24m_1^2\\
&-8\mathrm{x}3(m_1+2m_2)\left(\sqrt{3}m_1-\sqrt{3}m_2-3\mathrm{x}3+6\sqrt{3}\right)\Big).
\end{aligned} \tag{11.31}$$

This recursion relation can be solved in closed form using Mathematica in terms of Pochhammer functions. The full expression is too long and cumbersome to express in this chapter. However we will display the explicit form for $j(\mathrm{B})_k$ and all of our ϕ_k's

when our closed form solution (11.11) has x3=0

$$
\begin{aligned}
j(\mathrm{B})_k = \frac{1}{\pi}\Bigg(& (-6)^k \cos\left(\frac{1}{12}\pi\sqrt{m_1\left(\mathrm{B}^2+8m_2+36\right)-m_2\left(\mathrm{B}^2+16m_2-36\right)+8m_1^2+36}\right) \\
& \Gamma\left(k-\frac{1}{12}\sqrt{8m_1^2+\left(\mathrm{B}^2+8m_2+36\right)m_1-m_2\left(\mathrm{B}^2+16m_2-36\right)+36}+\frac{1}{2}\right) \\
& \Gamma\left(k+\frac{1}{12}\left(\sqrt{8m_1^2+\left(\mathrm{B}^2+8m_2+36\right)m_1-m_2\left(\mathrm{B}^2+16m_2-36\right)+36}+6\right)\right)\Bigg) \\
\phi_k = j(\mathrm{B})_k & e^{\left((m_1-2k)\alpha+\frac{1}{\sqrt{3}}(-6k+m_1-m_2)\beta_-+(m_2-2k)\beta_+\right)}.
\end{aligned}
\tag{11.32}
$$

Going back to (11.31) and (11.25) we see that we possess the freedom to pick the values of any of our free parameters m_1, m_2, and x3, for any value of k so that ϕ_k=0. When ϕ_k=0, the solutions to the subsequent transport equations can be satisfied by zero as well, thus truncating the infinite sequence of transport equations to a finite one; enabling us to construct closed form solutions using $\mathcal{S}^1_{(0)}$, $\mathcal{S}^1_{(1)}$, and ϕ_0.....ϕ_{k-1}. Because for every value of k we can set our free parameters so that ϕ_k=0, this enables us to construct a closed form solution using ϕ_0.....ϕ_{k-1}, and because k can take on every possible positive integer value, we have found an infinite family of solutions to the Bianchi II Wheeler DeWitt equation for arbitrary ordering parameter. In addition, because we only need to adjust one of our three free parameters so that $j(\mathrm{B})_k$=0, each one of our solutions has two free parameters which we can vary. If we choose x3 to be the parameter which we adjust so that $j(\mathrm{B})_k$=0, each one of our closed form solutions at a value of k can have their two 'excitation' numbers m_1 and m_2 be any real number. Naturally, this choice makes the most physical sense in terms of forming quantum Bianchi II scattering states. However, if we decide that m_1 and m_2 are not physical quantities, they can be complex numbers and still satisfy the Bianchi II Wheeler DeWitt equation.

Despite in principle solving all of the 'excited' state transport equations for a reasonable looking ϕ_0, $\left(e^{3\alpha+\sqrt{3}\beta_-}\right)^{m_1}\left(e^{3\beta_+-\sqrt{3}\beta_-}\right)^{m_1}$, if one were to graph these wave

functions it wouldn't be straightforward to interpret them as excited states unlike the Bianchi IX [20] and Taub models [39] which can be easily interpreted as excited states. Nonetheless the fact that we can solve these equations in the first place is a big mathematical feat and further shows the prowess of this method for proving the existence of solutions to Lorentzian signature problems.

Furthermore this does not mean no 'excited' states exist for the vacuum Bianchi II models. In this section we chose to use (11.25) as our ϕ_ks because it allowed us to easily solve for all of the 'excited' state transport equations. Because our ϕ_0 is a conserved quantity we could have used any function of it to construct our 'excited' states. There very well could exist a ϕ_0 which results in wave functions that have (11.4) as their semi-classical term that qualitatively behave like 'excited' states. In addition the manifestation of 'excited' states for our choice of ϕ_0 may be dependent on how we define our Hilbert space, which is a task we delineate to a future work.

If we choose a different $\mathcal{S}_{(0)}$ such as the infinitely many choices for (11.5) and (11.6) we may have obtained a simple form for our ϕ_0 which could immediately lead to wave functions that behave as 'excited' states. Studying the perturbations of the LRS Bianchi II models as was done for the Taub models in [21] would also be very useful in establishing the existence of vacuum Bianchi II 'excited' states. As we will see though when matter sources are included, our solutions to the ϕ_0 transport equation does result in wave functions which do behave as 'excited' states.

11.4 Closed Form Bianchi II 'Ground' States With Matter Sources

Using the following ansatz

$$\mathcal{S}^4_{(0)} = -6\Lambda e^{4\alpha-2\sqrt{3}\beta_- -2\beta_+} + \frac{1}{12}e^{2\alpha+2\sqrt{3}\beta_- +2\beta_+} + \alpha \mathrm{x1} + \beta_- \mathrm{x3} + \beta_+ \mathrm{x2} \tag{11.33}$$

the author found the following solutions to the Bianchi II Euclidean-signature Hamilton Jacobi equation corresponding to (11.3)

$$\left(\frac{\partial \mathcal{S}^4_{(0)}}{\partial \alpha}\right)^2 - \left(\frac{\partial \mathcal{S}^4_{(0)}}{\partial \beta_+}\right)^2 - \left(\frac{\partial \mathcal{S}^4_{(0)}}{\partial \beta_-}\right)^2 + \frac{1}{12}e^{4\alpha+4\beta_+ +4\sqrt{3}\beta_-} + 24\Lambda e^{6\alpha} + 2b^2 e^{2\alpha+2\beta_+ +2\sqrt{3}\beta_-} + \rho = 0$$

$$\mathcal{S}^4_{(0)} = -6\Lambda e^{4\alpha-2\sqrt{3}\beta_- -2\beta_+} + \frac{1}{12}e^{2\alpha+2\sqrt{3}\beta_- +2\beta_+} - 2\alpha \mathrm{b}^2 + \frac{1}{2}\beta_- \left(2\sqrt{3}\mathrm{b}^2 + \sqrt{\rho}\right) + \frac{1}{2}\beta_+ \left(2\mathrm{b}^2 - \sqrt{3}\sqrt{\rho}\right). \tag{11.34}$$

If we insert (11.34) into (8.52) we obtain

$$\begin{aligned}
&- 24\Lambda e^{4\alpha-2\left(\sqrt{3}\beta_- +\beta_+\right)}\left(2\frac{\partial \mathcal{S}_{(1)}}{\partial \alpha} + \sqrt{3}\frac{\partial \mathcal{S}_{(1)}}{\partial \beta_-} + \frac{\partial \mathcal{S}_{(1)}}{\partial \beta_+} + \mathrm{B}\right) \\
&+ \frac{1}{6}e^{2\left(\alpha+\sqrt{3}\beta_- +\beta_+\right)}\left(2\frac{\partial \mathcal{S}_{(1)}}{\partial \alpha} - 2\sqrt{3}\frac{\partial \mathcal{S}_{(1)}}{\partial \beta_-} - 2\frac{\partial \mathcal{S}_{(1)}}{\partial \beta_+} + \mathrm{B} + 6\right) \\
&- 4\mathrm{b}^2\frac{\partial \mathcal{S}_{(1)}}{\partial \alpha} - 2\mathrm{b}^2\left(\sqrt{3}\frac{\partial \mathcal{S}_{(1)}}{\partial \beta_-} + \frac{\partial \mathcal{S}_{(1)}}{\partial \beta_+}\right) \\
&+ \sqrt{\rho}\left(\sqrt{3}\frac{\partial \mathcal{S}_{(1)}}{\partial \beta_+} - \frac{\partial \mathcal{S}_{(1)}}{\partial \beta_-}\right) - 2\mathrm{b}^2\mathrm{B} = 0;
\end{aligned} \tag{11.35}$$

which in accordance with our previous reasoning can be satisfied by the following simple solution

$$\mathcal{S}^4_{(1)} := \frac{1}{2}\alpha(-\mathrm{B} - 2) + \frac{\sqrt{3}\beta_-}{2} + \frac{\beta_+}{2}. \tag{11.36}$$

Inserting this into the source term of (8.53) yields $-\frac{B^2}{2}$ which vanishes when $B = 0$. Thus we have the following solution to the Bianchi II WDW equation when a cosmological constant, aligned electromagnetic field and stiff matter are present

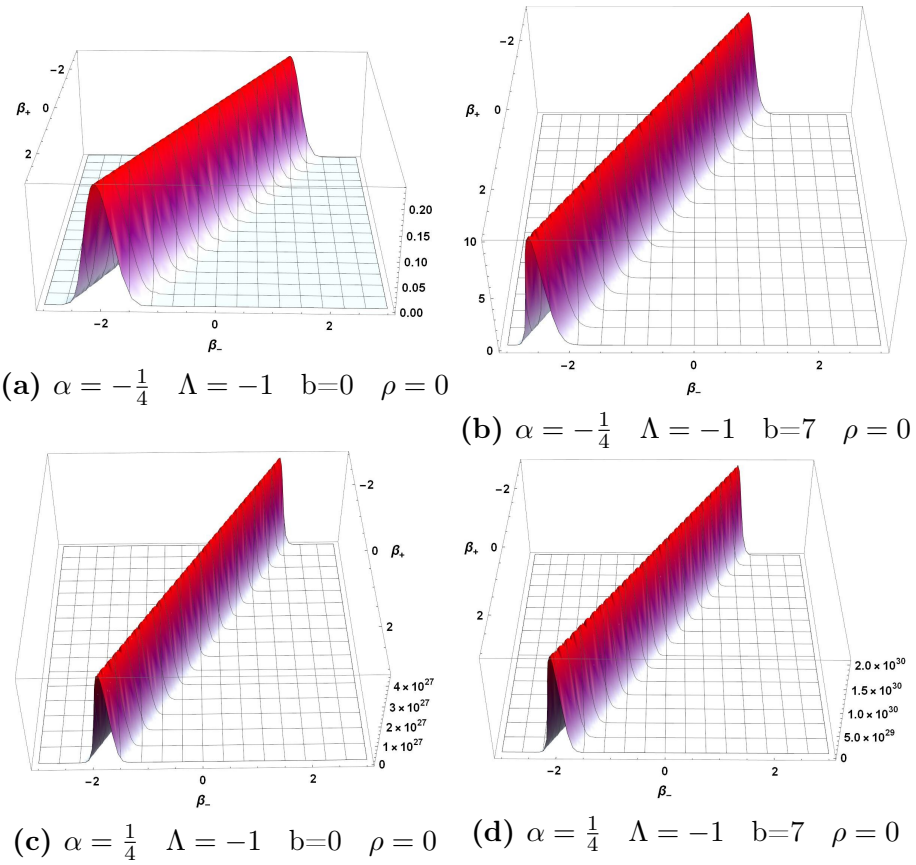

(a) $\alpha = -\frac{1}{4} \quad \Lambda = -1 \quad$ b=0 $\quad \rho = 0$

(b) $\alpha = -\frac{1}{4} \quad \Lambda = -1 \quad$ b=7 $\quad \rho = 0$

(c) $\alpha = \frac{1}{4} \quad \Lambda = -1 \quad$ b=0 $\quad \rho = 0$

(d) $\alpha = \frac{1}{4} \quad \Lambda = -1 \quad$ b=7 $\quad \rho = 0$

Figure 11.2 Plots of (11.37) for $|\Psi|^2$ when our aligned electromagnetic field and α are varied

$$\Psi = e^{6\Lambda e^{4\alpha-2(\sqrt{3}\beta_-+\beta_+)}-\frac{1}{12}e^{2(\alpha+\sqrt{3}\beta_-+\beta_+)}+2\alpha b^2+\alpha-\frac{1}{2}\beta_-\left(2\sqrt{3}b^2+\sqrt{\rho}+\sqrt{3}\right)+\frac{1}{2}\beta_+\left(-2b^2+\sqrt{3}\sqrt{\rho}-1\right)}. \tag{11.37}$$

To understand what effects the aligned electromagnetic field (b^2) has on our wave function (11.37) we construct a series of plots in 11.2, and discuss them at the end of this chapter.

We can obtain a solution for any Hartle-Hawking ordering parameter if we consider the case when only a cosmological constant is present. If we start with the following

semi-classical term

$$\mathcal{S}^5_{(0)} = -6\Lambda e^{4\alpha-2\sqrt{3}\beta_- -2\beta_+} + \frac{1}{12}e^{2\alpha+2\sqrt{3}\beta_- +2\beta_+} \tag{11.38}$$

and insert it into (8.52) we obtain the following $\mathcal{S}^5_{(1)}$

$$\mathcal{S}^5_{(1)} := \frac{1}{2}\alpha(-\mathrm{B}-2) + \beta_-\mathrm{x1} + \beta_+\left(2-\sqrt{3}\mathrm{x1}\right). \tag{11.39}$$

When (11.39) is inserted into (8.53) we obtain this source term $-3\mathrm{B}^2 - 4(1-2\mathrm{x1})^2$ which vanishes when $x1_\pm = \frac{1}{4}\left(2 \pm \sqrt{3}\mathrm{B}i\right)$. This allows us to construct two independent solutions to the Bianchi II WDW equation, one for each of the two possible values of $x1_\pm$ and sum them up to obtain

$$\Psi = \left(e^{\frac{i\beta_- B}{2}} + e^{\frac{1}{2}i\sqrt{3}\beta_+\mathrm{B}}\right) e^{\left(\frac{1}{12}\left(72\Lambda e^{4\alpha-2\left(\sqrt{3}\beta_- +\beta_+\right)} - e^{2\left(\alpha+\sqrt{3}\beta_- +\beta_+\right)} + 6\alpha(\mathrm{B}+2) - 3i\mathrm{B}\left(\beta_- +\sqrt{3}\beta_+\right) - 6\left(\sqrt{3}\beta_- +\beta_+\right)\right)\right)}. \tag{11.40}$$

These solutions non-trivially depend on the ordering parameter. When $B = 0$ these solutions are real, otherwise they are complex. We plot them for three different values of α in 11.3 and will discuss them in detail towards the end of this chapter.

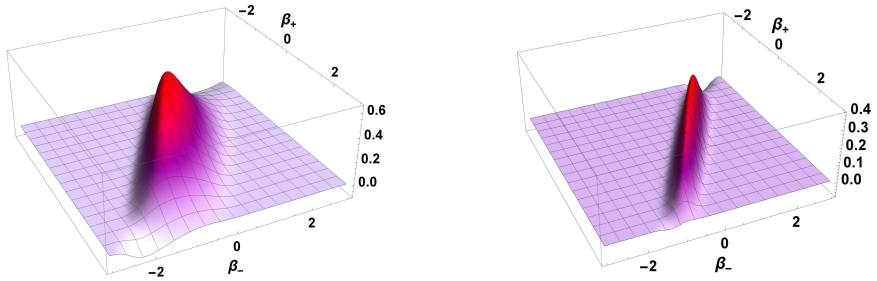

(a) $\alpha = -1 \quad \Lambda = -1 \quad$ B=1

(b) $\alpha = 0 \quad \Lambda = -1 \quad$ B=1

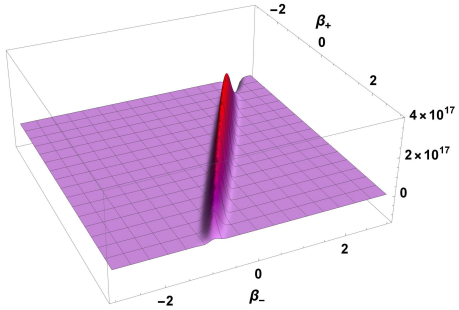

(c) $\alpha = \frac{1}{2} \quad \Lambda = -1 \quad$ B=1

Figure 11.3 Plots of (11.40) for $|\Psi|^2$ for different values of α.

11.5 Closed Form 'Excited' States Of The $\Lambda \neq 0$ Bianchi II Wheeler DeWitt Equation

The author was able to find the following ϕ_0 for the case when only a cosmological constant is present.

$$\phi_0^5 := \left(e^{\frac{1}{3}\left(3\beta_+ - \sqrt{3}\beta_-\right)}\right)^{m_1} \left(48\Lambda e^{6\alpha - 4\sqrt{3}\beta_-} + e^{4(\alpha+\beta_+)}\right)^{m_2}. \tag{11.41}$$

This ϕ_0 suggests that the 'excited' states of the quantum Bianchi II models when a cosmological constant is present have some interesting properties. When $\Lambda > 0$ our 'excited' states are scattering states because none of the terms exponentiated by our graviton excitation numbers m_1 and m_2 vanish for any real values of the Misner variables. However when $\Lambda < 0$ the terms associated with m_1 don't vanish, while the term exponentiated by m_2 does vanish for real values of the Misner variables. Thus for $\Lambda < 0$ our m_1 term can be any real number, while m_2 is restricted to being either zero

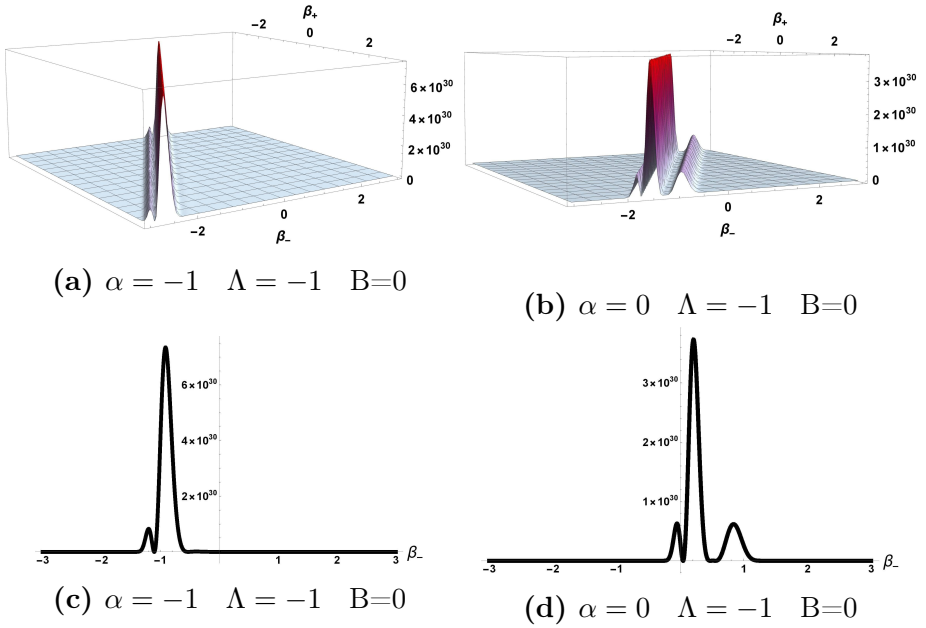

(a) $\alpha = -1 \quad \Lambda = -1 \quad$ B=0

(b) $\alpha = 0 \quad \Lambda = -1 \quad$ B=0

(c) $\alpha = -1 \quad \Lambda = -1 \quad$ B=0

(d) $\alpha = 0 \quad \Lambda = -1 \quad$ B=0

Figure 11.4 Plots of (11.42) when $|\Psi_{Excited}|^2$ for various values of α when $m_1 = -3$ and $m_2 = 1$.

or a positive integer. The 'excited' states for the quantum Bianchi II models when $\Lambda < 0$ are hybrid scattering/bound states. This property is shared with the quantum Bianchi VIII models [40], which the author studied as well. The higher order ϕ_k^5 terms in principle can be found by solving the rest of the transport equations. However, due to $\mathcal{S}^5_{(0)}$ possessing two terms with different α dependence, it is more difficult to solve these transport equations as opposed to the ones we encountered earlier. The author in trying to solve the ϕ_1^5 terms computed an unenlightening integral expression which we will omit. The plots we will show will be leading order in ϕ 'excited' states.

To construct our graphs we will set $m_1 = -3$ and $m_2 = 1$ and graph the modulus squared of the following wave function

$$\Psi_{Excited} = \sum_{m=1}^{10} \left(\phi_0^5\right)^m \Psi, \tag{11.42}$$

where Ψ is our exact wave function (11.40). We will also graph cross sections of our 3D plots when $\beta_+ = 0$.

11.6 Non-Commutative Quantum Bianchi II With Matter Sources

In this section we shall study the quantum non-commutative Bianchi II models when an aligned electromagnetic field and stiff matter are present. To do so we shall use the following deformation of the ordinary commutation relations between the minisuperspace variables

$$[\alpha_{\rm nc}, \beta_{+\rm nc}] = \mathrm{i}\theta_1, \quad [\alpha_{\rm nc}, \beta_{-\rm nc}] = \mathrm{i}\theta_2, \quad [\beta_{-\rm nc}, \beta_{+\rm nc}] = \mathrm{i}\theta_3. \tag{11.43}$$

This type of deformation of the configuration or phase space of a finite dimensional theory is employed in non-commutative quantum mechanics [30, 43, 44]. The non-commutative quantum Bianchi II models with stiff matter were thoroughly investigated in [7]. In this section we will follow their methodology and extend their results by including an aligned electromagnetic field.

The purpose of imposing these non-commutative relations on the minisuperspace of our Bianchi II models is to obtain a better understanding of how non-commutative space-time could have affected cosmological evolution in the early universe. Many theories of quantum gravity predict that space-time itself manifests some form of discretization. One way for this supposed discretization to manifest mathematically is in the coordinates (t, x_i) of space-time possessing non vanishing commutation relations. For example in String Theory/M-Theory a non-commutative gauge theory emerges when describing the low energy excitations of open strings in the presence of a Neveu-Schwarz constant background B field [86, 213]. As a result there has been a renewed interest in the study of non-commutative space-times.

A non-commutative space-time version of general relativity has been proposed [94] and in theory one can use it to directly study the full impact that non-commutative space-time has on classical cosmological evolution. However formulating general rela-

tivity in a non-commutative space-time results in a theory that is incredibly non-linear and very difficult to work with mathematically. A way to obtain some understanding of how non-commutative space-times can affect cosmology was proposed by [93]. Instead of directly studying the cosmology of a theory of gravity with a non-commutative space-time one can study a cosmology with deformed minisuperspace commutative relations as presented in (11.43). The justification for this can be summed up by saying that it is reasonable to expect that a full noncommutative space-time theory of gravity would result in some effects which can be captured by introducing non-commutativity in the minisuperspace of its homogeneous cosmologies. Thus by studying non-commutative minisuperspace homogeneous cosmologies we are studying an effective toy model of a non-commutative theory of gravity with its degrees of freedom reduced by imposing the symmetries present in homogeneous space-times.

To begin the process of solving the non-commutative Bianchi II WDW equation we will implement the following Seiberg-Witten map [213]

$$\alpha_{\rm nc} \to \alpha - \frac{\theta_1}{2} p_{\beta_+} - \frac{\theta_2}{2} p_{\beta_-}, \quad \beta_{-\rm nc} \to \beta_- + \frac{\theta_2}{2} p_\alpha - \frac{\theta_3}{2} p_{\beta_+}, \quad \beta_{+\rm nc} \to \beta_+ + \frac{\theta_1}{2} p_\alpha + \frac{\theta_3}{2} p_{\beta_-}. \tag{11.44}$$

Doing so results in the following modified potential term for (11.3) when $\Lambda = 0$

$$\begin{aligned} \mathrm{U}\left(\Omega, \beta_\pm\right) =& \frac{1}{12} \mathrm{e}^{4\left[\alpha+\beta_+ +\sqrt{3}\beta_- - \frac{\mathrm{i}\theta_1}{2}\left(\frac{\partial}{\partial\alpha} - \frac{\partial}{\partial\beta_+}\right) - \frac{\mathrm{i}\theta_2}{2}\left(\sqrt{3}\frac{\partial}{\partial\alpha} - \frac{\partial}{\partial\beta_-}\right) + \frac{\mathrm{i}\theta_3}{2}\left(\sqrt{3}\frac{\partial}{\partial\beta_+} - \frac{\partial}{\partial\beta_-}\right)\right]} \\ &+ 2b^2 \mathrm{e}^{2\left[\alpha+\beta_+ +\sqrt{3}\beta_- - \frac{\mathrm{i}\theta_1}{2}\left(\frac{\partial}{\partial\alpha} - \frac{\partial}{\partial\beta_+}\right) - \frac{\mathrm{i}\theta_2}{2}\left(\sqrt{3}\frac{\partial}{\partial\alpha} - \frac{\partial}{\partial\beta_-}\right) + \frac{\mathrm{i}\theta_3}{2}\left(\sqrt{3}\frac{\partial}{\partial\beta_+} - \frac{\partial}{\partial\beta_-}\right)\right]} + \rho. \end{aligned} \tag{11.45}$$

After applying the following coordinate transformation

$$\xi = \Omega + \beta_+ + \sqrt{3}\beta_-, \quad \kappa = \Omega + \frac{\sqrt{3}}{3}\beta_-, \quad \lambda = \Omega - 2\beta_+ + \sqrt{3}\beta_- \tag{11.46}$$

and applying the generalized Baker-Campbell-Hausdorff formula

$$\mathrm{e}^{\eta(\hat{\mathrm{A}}+\hat{\mathrm{B}})} = \mathrm{e}^{-\eta^2[\hat{\mathrm{A}},\hat{\mathrm{B}}]}\mathrm{e}^{\eta\hat{\mathrm{A}}}\mathrm{e}^{\eta\hat{\mathrm{B}}} \tag{11.47}$$

we obtain the following WDW equation

$$\begin{aligned}
&- B\frac{\partial\Psi}{\partial\xi} - 3\frac{\partial^2\Psi}{\partial\xi^2} + \frac{2}{3}\frac{\partial^2\Psi}{\partial\kappa^2} - B\frac{\partial\Psi}{\partial\kappa} - 6\frac{\partial^2\Psi}{\partial\lambda^2} - B\frac{\partial\Psi}{\partial\lambda} \\
&+ \frac{1}{12}\mathrm{e}^{4\xi}\mathrm{e}^{-2\mathrm{i}\theta_1\frac{\partial}{\partial\kappa}}\mathrm{e}^{-6\mathrm{i}\theta_1\frac{\partial}{\partial\lambda}}\mathrm{e}^{\frac{-4\sqrt{3}}{3}\mathrm{i}\theta_2\frac{\partial}{\partial\kappa}}\mathrm{e}^{-\frac{2\sqrt{3}}{3}\mathrm{i}\theta_3\frac{\partial}{\partial\kappa}}\mathrm{e}^{-6\sqrt{3}\mathrm{i}\theta_3\frac{\partial}{\partial\lambda}}\Psi \\
&+ 2b^2\mathrm{e}^{2\xi}\mathrm{e}^{-\mathrm{i}\theta_1\frac{\partial}{\partial\kappa}}\mathrm{e}^{-3\mathrm{i}\theta_1\frac{\partial}{\partial\lambda}}\mathrm{e}^{\frac{-2\sqrt{3}}{3}\mathrm{i}\theta_2\frac{\partial}{\partial\kappa}}\mathrm{e}^{-\frac{\sqrt{3}}{3}\mathrm{i}\theta_3\frac{\partial}{\partial\kappa}}\mathrm{e}^{-3\sqrt{3}\mathrm{i}\theta_3\frac{\partial}{\partial\lambda}}\Psi + \rho\Psi = 0.
\end{aligned} \tag{11.48}$$

To solve this equation we will insert this ansatz into it, $\Psi = f(\xi)e^{\mathrm{i}c1\kappa}e^{\mathrm{i}c2\lambda}$ where c1 and c2 are constants while keeping in mind that $\mathrm{e}^{\mathrm{i}\theta\frac{\partial}{\partial\mathrm{x}}}\mathrm{e}^{\eta\mathrm{x}} \equiv \mathrm{e}^{\mathrm{i}\eta\theta}\mathrm{e}^{\eta\mathrm{x}}$, resulting in

$$\begin{aligned}
&f(\xi)\left(24\mathrm{b}^2e^{2e+2w} + e^{4e+4w} + g\right) - 12\left(\mathrm{B}\frac{\partial f}{\partial\xi} + 3\frac{\partial^2 f}{\partial\xi^2}\right) = 0 \\
&w = \frac{1}{2}\left(\theta_1(\mathrm{c1}+3\mathrm{c2}) + \frac{2\theta_2\mathrm{c1}+\theta_3\mathrm{c1}+9\theta_3\mathrm{c2}}{\sqrt{3}}\right) \\
&g = -12i\mathrm{Bc1} - 12i\mathrm{Bc2} + 12\rho - 8\mathrm{c1}^2 + 72\mathrm{c2}^2.
\end{aligned} \tag{11.49}$$

The solution to this equation (11.49) is the following

$$\begin{aligned}
&w = e^{\frac{1}{12}\left(-2\mathrm{B}(\xi+w)-e^{2(\xi+w)}\right)}\left(e^{2(\xi+w)}\right)^{\frac{\sqrt{B^2+g}}{12}} \\
&f(\xi) = (w)\,U\left(\mathrm{b}^2 + \frac{1}{12}\left(\sqrt{\mathrm{B}^2+g}+6\right), \frac{1}{6}\left(\sqrt{\mathrm{B}^2+g}+6\right), \frac{1}{6}e^{2(\xi+w)}\right)
\end{aligned} \tag{11.50}$$

where U is the hypergeometric U function. There is a generalized Laguerre polynomial which also satisfies (11.49) but it yields solutions which do not appear to be physical. Using our ansatz, (11.46), and (11.50) one can express the solutions for the non-commutative Bianchi II WDW equation (11.3 11.45). In what follows we will set $\theta_2 = \theta_1, \quad \theta_3 = \theta_1, \quad \rho = 0$. We will present a series of plots for our non-commutative

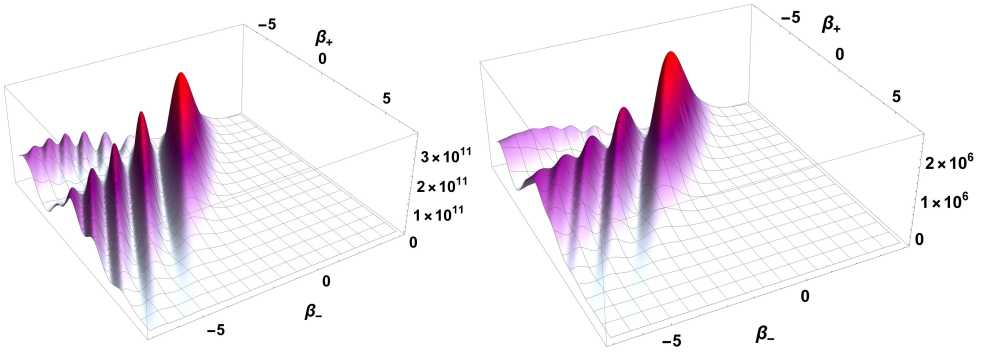

(a) $\alpha = -2 \quad \theta_1 = 1.5 \quad B = 0 \quad b = 0$ **(b)** $\alpha = -2 \quad \theta_1 = 1.5 \quad B = 0 \quad b = 4$

Figure 11.5 These plots of $\left|\int_{-\infty}^{\infty} e^{-1.5(c1-1.3)^2} e^{ic1\kappa} f(\xi) dc1\right|^2$ represent a small subset of the wave functions we can obtain if we manipulate the non-commutative parameters θ_i.

wave $\left|\int_{-\infty}^{\infty} e^{-1.5(c1-1.3)^2} e^{ic1\kappa} f(\xi) dc1\right|^2$ function and discuss them at the end of this chapter.

11.7 Quantum Vacuum Bianchi VII$_{h=0}$ 'Ground' And 'Excited' States

Moving on to the Bianchi VII$_{h=0}$ models, these two solutions were found for its Euclidean-Signature Hamilton-Jacobi equation(6, 14) by [186]

$$\mathcal{S}^6_{(0)} = \frac{1}{3} e^{2(\alpha+\beta_+)} \cosh\left(2\sqrt{3}\beta_-\right) \tag{11.51}$$

$$\mathcal{S}^7_{(0)} = \frac{1}{3} e^{2(\alpha+\beta_+)} \cosh\left(2\sqrt{3}\beta_-\right) + \mathrm{x1} e^{2\alpha+2\beta_+} \tag{11.52}$$

where x1 is an arbitrary constant.

Starting with (11.51) if we insert it into (8.52) and employ the methodology that we used to solve the Bianchi II $\mathcal{S}_{(1)}$ equation (11.7) we obtain

$$\mathcal{S}^{6}_{(1)} = \alpha \mathrm{x1} + \frac{1}{12}\log\left(\sinh\left(2\sqrt{3}\beta_{-}\right)\right)\left(\mathrm{B} + 2\mathrm{x1} - 2\mathrm{x2} + 6\right) + \beta_{+}\mathrm{x2} \tag{11.53}$$

where both x1 and x2 are arbitrary constants. Inserting this term into the source term of equation (8.53) results in an expression which vanishes when our arbitrary constants equals

$$\left\{\mathrm{x1} = \frac{1}{24}\left(-\mathrm{B}^{2} - 12\mathrm{B} - 36\right), \mathrm{x2} = \frac{1}{24}\left(36 - \mathrm{B}^{2}\right)\right\}. \tag{11.54}$$

This allow us to write down the following solution to the Bianchi $\mathrm{VII}_{h=0}$ WDW equation

$$\Psi = e^{\left(\frac{1}{24}(\mathrm{B}+6)(a(\mathrm{B}+6)+\beta_{+}(\mathrm{B}-6)) - \frac{1}{3}e^{2(\alpha+\beta_{+})}\cosh\left(2\sqrt{3}\beta_{-}\right)\right)}. \tag{11.55}$$

This solution was first reported by [186].

For the Bianchi $\mathrm{VII}_{h=0}$ 'excited' states the author found the following solutions to the ϕ_0 equations for (11.51)

$$\phi^{6}_{0} := e^{6m_2\alpha - 6m_1\beta_{+}}\sinh\left(2\sqrt{3}\beta_{-}\right)^{m_1+m_2}. \tag{11.56}$$

Due to $\sinh\left(2\sqrt{3}\beta_{-}\right)$ vanishing we must restrict the values of m_1 and m_2 so that their sum $m_1 + m_2$ always equals a positive integer or zero. Using (11.56) we can construct semi-classical 'excited' states. We can find closed form solutions to the Bianchi $\mathrm{VII}_{h=0}$ WDW equation by inserting $\phi^{6}_{0}\Psi$ into it, where we used (11.55) for our Ψ. By doing so we will find that it is satisfied when $m_1 = \frac{1}{216}\left(\mathrm{B}^{2} + 84\right)$ and $m_2 = \frac{1}{216}\left(132 - \mathrm{B}^{2}\right)$. This leads to the following closed form solution

$$\Psi_{excited} = \sinh\left(2\sqrt{3}\beta_-\right) e^{\left(\frac{1}{72}\left(-24e^{2(\alpha+\beta_+)}\cosh\left(2\sqrt{3}\beta_-\right)+\alpha(\mathrm{B}(\mathrm{B}+36)+372)+\beta_+\left(\mathrm{B}^2-276\right)\right)\right)}. \tag{11.57}$$

This solution has a strange property though. The potential for the Bianchi $\mathrm{VII}_{h=0}$ models is invariant under the reflection of $\beta_- \to -\beta_-$ while our 'excited' state isn't. This is another instance [37] in which the WDW equation admits solutions which do not respect the symmetry of its potential. However $|\Psi_{excited}|^2$ does preserve the symmetry of the potential. This is important because if all of our observables are dependent upon $|\Psi_{excited}|^2$, then the symmetry which is broken by (11.57) may not bear any practical consequences. Nonetheless the physical implications of symmetry breaking solutions of the Wheeler DeWitt equation is a topic which deserves to be investigated more.

Furthermore it is difficult to obtain an 'excited' state wave function which behaves in a way which is easy to interpret qualitatively. Thus we had to pick a specific value of the operator ordering parameter $B \geq 23$ to obtain solutions which are intuitive to interpret. The difficulty in computing 'excited' states for the vacuum Bianchi II and $\mathrm{VII}_{h=0}$ in comparison to the Bianchi IX [20] and Taub models [39] may be a result of topological differences between their space-times or in mathematical difference of the Bianchi Lie algebras which define them.

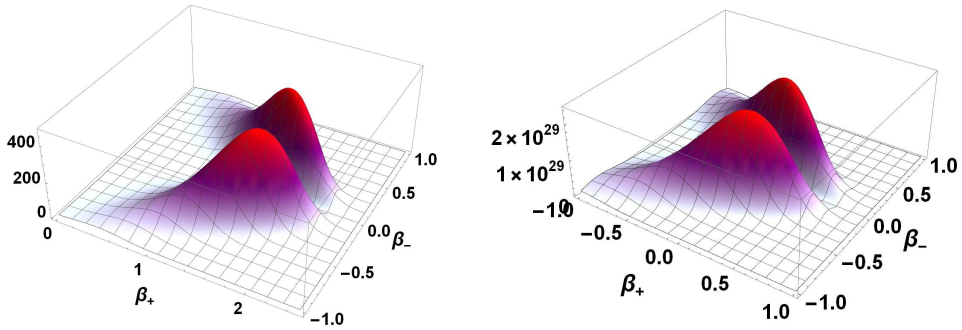

(a) $\alpha = -1$ B=23 **(b)** $\alpha = \frac{1}{2}$ B=23

Figure 11.6 Plots of (11.57) for $|\Psi_{excited}|^2$ for various values of α for a specific value of the ordering parameter.

11.8 Quantum Vacuum Bianchi VII$_{h=0}$ 'Ground' States With Matter Sources

For the case when only an aligned electromagnetic field and stiff matter are present the author found the following solution to the Euclidean-signature Hamiliton Jacobi equation corresponding to (11.3)

$$\mathcal{S}^7_{(0)} = \frac{1}{6}\left(3\mathrm{b}^2\left(-2\alpha+\sqrt{3}\beta_-+\beta_+\right)+2e^{2(\alpha+\beta_+)}\cosh\left(2\sqrt{3}\beta_-\right)+\frac{2\rho(\alpha+\beta_+)}{\mathrm{b}^2}\right). \tag{11.58}$$

Inserting this expression in (8.52) and seeking an $\mathcal{S}_{(1)}$ which is linear in the Misner variables results in

$$\mathcal{S}^7_{(1)} = \frac{2\beta_+\left(3\mathrm{b}^4-\rho\right)}{3\mathrm{b}^4}-\frac{\alpha\left(3\mathrm{b}^4\mathrm{B}+6\mathrm{b}^4+4\rho\right)}{6\mathrm{b}^4}. \tag{11.59}$$

If we insert (11.59) into the source term of (8.53) we obtain $\frac{8\rho}{b^4}-\frac{B^2}{2}-6=0$ which vanishes when our ordering parameter equals $B=\frac{2\sqrt{4\rho-3b^4}}{b^2}$. This allow us to write down the following solution which satisfies (11.3) when $\Lambda=0$ and $B=\frac{2\sqrt{4\rho-3b^4}}{b^2}$

$$\Psi = e^{\left(\frac{1}{6}\left(-3b^2\left(-2\alpha+\sqrt{3}\beta_-+\beta_+\right)-2e^{2(\alpha+\beta_+)}\cosh\left(2\sqrt{3}\beta_-\right)-\frac{2\rho(\alpha+\beta_+)}{b^2}\right)+\frac{2\rho(\alpha+\beta_+)}{3b^4}+\frac{\alpha\sqrt{4\rho-3b^4}}{b^2}+\alpha-2\beta_+\right)}. \tag{11.60}$$

In order for our ordering parameter to be real we require that $\rho \geq \frac{3}{4}b^4$. Nonetheless if one were interested in studying an asymptotic Bianchi $\mathrm{VII}_{h=0}$ wave function, then they may be content to only include the first two terms of the expansion which we have calculated which doesn't require them to impose the stringent requirement that $\rho \geq \frac{3}{4}b^4$.

To accommodate a cosmological constant we have to make our stiff matter term $\rho = 3b^4$, which results in the following $\mathcal{S}_{(0)}$

$$\mathcal{S}^8_{(0)} = -3\Lambda e^{4\alpha+2\sqrt{3}\beta_--2\beta_+} + \frac{1}{3}e^{2(\alpha+\beta_+)}\cosh\left(2\sqrt{3}\beta_-\right) + \frac{1}{2}\mathrm{b}^2\left(\sqrt{3}\beta_- + 3\beta_+\right). \tag{11.61}$$

Using the alternative operator ordering presented in [96] we can satisfy the Bianchi $\mathrm{VII}_{h=0}$ WDW equation when a cosmological constant, aligned electromagnetic field and stiff matter are present using just (11.61). However for our purposes we will only consider semi-classical wave functions $\psi = e^{-\mathcal{S}_{(0)}}$ of the form dictated by (11.3). If we only consider the Bianchi $\mathrm{VII}_{h=0}$ models with a cosmological constant our $\mathcal{S}_{(0)}$ term simplifies to

$$\mathcal{S}^9_{(0)} = \frac{1}{3}e^{2(\alpha+\beta_+)}\cosh\left(2\sqrt{3}\beta_-\right) - 3\Lambda e^{4\alpha\pm_2\sqrt{3}\beta_--2\beta_+}. \tag{11.62}$$

The $\pm$ signs of the β_- term in (11.62) is a result of the fact that the Bianchi $\mathrm{VII}_{h=0}$ potential when only a cosmological constant is present is invariant under reflection of $\beta_- \to -\beta_-$. Via (8.52) and (11.62) we find the following $\mathcal{S}_{(1)}$ term

$$\mathcal{S}^{9}_{(1)} = \frac{1}{2}\alpha(-\mathrm{B}-2) + 2\beta_{+}. \tag{11.63}$$

Using the methodology that we have presented throughout this chapter we can show that a closed form solution to the WDW equation exists when our ordering parameter equals $B = \pm 2\sqrt{3}i$ using just (8.53), (11.62), and (11.63).

In order to determine how our aligned electromagnetic field effects our quantum Bianchi $\mathrm{VII}_{h=0}$ wave functions we will compare the semi-classical wave functions constructed from (11.61) and (11.62). We can group average over the reflection symmetry $\beta_{-} \rightarrow -\beta_{-}$ present in the Bianchi $\mathrm{VII}_{h=0}$ potential when only Λ is present to obtain

$$\Psi = \left(e^{3\Lambda e^{4\alpha+2\sqrt{3}\beta_{-}-2\beta_{+}}} + e^{3\Lambda e^{4\alpha-2(\sqrt{3}\beta_{-}+\beta_{+})}}\right) e^{-\frac{1}{3}e^{2(\alpha+\beta_{+})}\cosh\left(2\sqrt{3}\beta_{-}\right)}. \tag{11.64}$$

In order to see what effects an aligned electromagnetic field has on our Bianchi $\mathrm{VII}_{h=0}$ wave function we will group average the semi-classical wave function constructed using (11.61) despite the fact that the addition of an aligned electromagnetic field breaks the reflection invariance in β_{-} of the potential. Doing so gives us (11.65). We are doing this so we can make a clear comparison between what happens when we just have a cosmological constant vs when we have both a cosmological constant and an aligned electromagnetic field. Specifically we want to highlight how the aligned electromagnetic field affects the anisotropy present in the universes represented by our wave functions. The actual wave function which has an aligned electromagnetic field would only have one branch present.

$$\Psi = \left(e^{3\Lambda e^{4\alpha-2(\sqrt{3}\beta_{-}+\beta_{+})}+\sqrt{3}\beta_{-}\mathrm{b}^{2}} + e^{3\Lambda e^{4\alpha+2\sqrt{3}\beta_{-}-2\beta_{+}}}\right) e^{\left(\frac{1}{6}\left(-2e^{2(\alpha+\beta_{+})}\cosh\left(2\sqrt{3}\beta_{-}\right)-3\mathrm{b}^{2}\left(\sqrt{3}\beta_{-}+3\beta_{+}\right)\right)\right)} \tag{11.65}$$

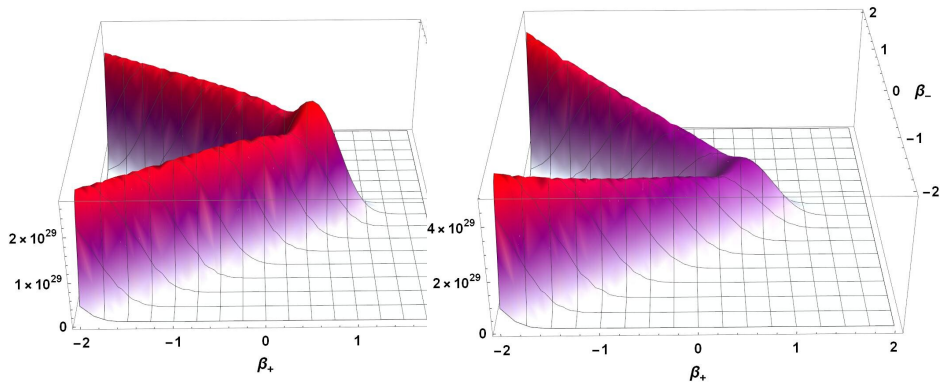

(a) $\alpha = 0 \quad \Lambda = -1 \quad b = 0$ **(b)** $\alpha = 0 \quad \Lambda = -1 \quad b = \frac{2}{5}$

Figure 11.7 Plots of (11.65) for two different values of the electromagnetic field b. Due to the aligned electromagnetic field breaking the reflection symmetry under β_- of the Bianchi $\text{VII}_{h=0}$ potential the actual wave function only has one ridge present as opposed to two, as is shown in figure 20(b). Both ridges are plotted so we can better compare the two wave functions.

11.9 Discussion

The plots for our 'ground' state asymptotic wave functions in figures (11.1a-11.1c) depict a wave travelling down the β_+ axis in the negative direction while the scale factor e^{α} grows. As our clock α "ticks" forward in "time", this universe's geometric probability density will be peaked at an ever increasing negative value of β_+ and a roughly constant value of β_-. A variety of other asymptotic wave functions which behave differently could also be constructed using the methods outlined in III.

Moving on to our Bianchi II solutions with matter sources we notice in figures (11.2a-11.2b) that the aligned electromagnetic field (b^2) causes our wave function to travel in the negative β_- direction. It was noted in [162] that magnetic fields within the context of LRS Bianchi I quantum cosmology induce anisotropy. This is clearly being mirrored for our particular case of the quantum Bianchi II models. However, the opposite can happen as well if our wave functions are centered on the positive portion of the β_- axis because increasing the strength of the aligned electromagnetic field would initially decrease anisotropy by making our β_- approach the origin for certain values of α which we take to be our internal clock. There is mathematical

evidence that this dual nature of the aligned electromagnetic field is a generic feature possessed by wave functions computed using this method as can be seen in the Bianchi IX models [40] and Taub [39] models. If an aligned electromagnetic field was capable of doing something similar in our early universe then this dual behavior might have been responsible for producing some recognizable signature in the CMB. More research into what signatures a primordial magnetic field could have imparted on the CMB within the context of quantum cosmology is needed. Nonetheless these findings are a good start.

In addition to inducing anisotropy the electromagnetic field also makes our wave functions thinner and thus more sharply peaked. This effect of making the wave function of the universe more sharply peaked could have played an important role in the early universe by causing quantum states which otherwise would be geometrically fuzzy, such as those whose wave function possesses multiple peaks [39, 40] to condense to a far more sharply defined state with one narrow central peak. In other words a primordial electromagnetic field might have played an important role in the early universe by facilitating a phase transition from a quantum universe to one that could be adequately described using classical mechanics.

One last feature to point out about the aligned electromagnetic field is that its effects rapidly diminish as α grows. As can be seen in figures 11.2c and 11.2d increasing the strength of the aligned electromagnetic field has milder effects on the wave function then it did in figures 11.2a and 11.2b. This provides a quantum explanation for why an electromagnetic field might have played a large role in the early universe, but played a diminishing role as it grew in size.

For figure 11.3c, in order for it to be of sufficient quality the author had to multiply the wave function by 10^{20}, in actuality its magnitude is far less than the wave functions in figures 11.3a and 11.3b. This is to be expected because a negative cosmological constant naively should act as a powerful force of attraction which resists the ten-

dency of a universe to grow in size. We say naively because as previously mentioned, recent work [111, 112, 172] has been done showing that phenomena expected of classical cosmologies with a positive cosmological constant can be derived from certain quantum cosmological models which possess a negative cosmological constant.

Our wave function (11.40) ($\Lambda < 0$) decaying as α grows indicates that the likelihood that this universe will reach a state when $\alpha >> 0$ is low. Another feature of our figures (11.3a-11.3c) is that as α grows they become thinner. This shows that as α grows larger the universe that these wave functions are supposed to represent become somewhat less fuzzy. Geometric fuzziness is a feature associated with the uncertainty relation of our minisuperspace as a result of quantum mechanics. As a result the larger a universe becomes the less we expect those quantum features of fuzziness to be present.

Our leading order 'excited' states when $\Lambda \neq 0$, figures (11.4a-11.4d), can be interpreted similarly to our other states. One noticeable difference is that their geometry is more "fuzzy" because the wave functions which describe this universe have multiple ridges/peaks. This is most clearly illustrated in the $\alpha = 0$ case where we can see three distinct ridges, one large ridge and two smaller ridges. Figure 11.4d further shows this. The potential geometries this Bianchi II universe can take on are located on one of these three visible ridges. As α grows those ridges appear to fuse and the geometries become slightly more "sharp", while also becoming more unlikely to occur due to the magnitude of the wave function decaying. It is also possible that each one of those ridges represents a "fuzzy" geometric state that our quantum Bianchi II universe can tunnel in and out of.

For the non-commutative quantum Bianchi II models our wave function behaves similarly to other non-commutative quantum cosmological models [93, 218] in the sense that multiple peaks are present when $\theta_i \neq 0$, and only one defined peak is present when $\theta_i = 0$. These multiple peaks indicate that non-commutativity in the

early universe could facilitate the creation of many possible states which a quantum universe can tunnel into.

When we include our aligned electromagnetic field in figure 11.5b it doesn't have much of an effect. However, because we simplified our wave function by setting all three non-commutative parameters θ_i equal to each other, we only looked at a small subset of possible quantum non-commutative universes. There very well could exist a region in θ space such that a primordial electromagnetic field has a profound effect on what states the early universe can tunnel into. Studying the full effects of both non-commutativity and primordial electromagnetic fields in the early universe could shed much light on how our homogeneous and isotropic universe came to be.

Our vacuum Bianchi $\text{VII}_{h=0}$ 'excited' states (figures 11.6a-11.6b) are two Gaussian like peaks which travel in the negative β_+ direction. Thus for a specific value of α our wave function represents a universe which can tunnel in between two relatively defined anisotropic states. This behavior is unusual if compared to that of other [20, 39] 'excited' states computed using this method. Usually for $\alpha < 0$ an 'excited' state possesses multiple peaks that each represent a geometric configuration a universe can tunnel in and out of. However when α grows large, $\alpha >> 0$, those peaks merge into a single peak. This process can be interpreted as one in which a spatially small universe which is quantum in nature evolves into a spatially larger universe which behaves more in line with classical physics. This merger of the peaks never happens for our Bianchi $\text{VII}_{h=0}$ 'excited' state, the two peaks remain separate for all values of α.

This difference in how the 'excited' states of these models behave may be accounted for by the different properties of the groups that the Bianchi $\text{VII}_{h=0}$ and IX models are based on. The Lie algebra corresponding to the Bianchi $\text{VII}_{h=0}$ models is the Lie algebra of the group of isometries of the plane, while the Lie algebra of the Bianchi IX models is associated with the rotational SO(3) group associated with the sphere. The

mathematical differences between these models underlining groups or their topological differences may account for the different behavior of their 'excited' states for large α. By further comparing and contrasting these models, we can learn more about how 'excited' states are defined within the context of this method and in quantum cosmology.

For our quantum Bianchi $\text{VII}_{h=0}$ models with matter sources (figures 11.7a-11.7b) it can be seen that when the aligned electromagnetic field b^2 is zero our wave function is peaked around $\beta_+ = \frac{1}{2}$ and $\beta_- = 0$. However when our aligned electromagnetic field increases in strength the ridges overtake the aforementioned peak and our wave function represents a fuzzier and more anisotropic universe. Making a wave function of the universe less geometrically defined is another potential effect that an electromagnetic field can have. Within the context of non-commutative quantum cosmology this could mean creating additional peaks which otherwise wouldn't be present.

Chapter 12

Definitive Concluding Remarks: Where The Future Lies

The work documented in this dissertation contributes towards a much wider project that is occurring in physics in which Euclidean signature systems are being studied to test the validity of a multitude of conjectured dualities that point to a relationship between gravity and gauge theories. The AdS/CFT correspondence that we discussed earlier is an example of gauge/gravity duality. An important feature of the AdS/CFT correspondence is that it is also a strong/weak correspondence. This means that the observables of a strongly interacting gravitational theory can be computed using a weakly coupled perturbative CFT. On the other hand the observables of a strongly coupled CFT can be obtained by using a weakly interacting gravitational theory. A systematic approach for doing this is currently being investigated, but for a select few problems, [3, 147, 211] this strong/weak correspondence was able to be put into practice and generate some novel results.

This strong/weak correspondence is expected to be a generic feature of gauge/gravity duality. Thus other conjectured manifestations of gauge/gravity duality which are not limited to CFTs or AdS space are also expected to share this feature. It is this

strong/weak correspondence in gauge/gravity duality that dictates the nature of the calculations which are presently performed in holographic [24, 42, 92, 167] cosmology. As a result of the intersection between QFT and gravity, and the two-sidedness of gauge/gravity duality, there are a multitude of avenues for testing the validity and robustness of these conjectures. One such avenue is through lattice simulation [154].

LFT can be used to study correlation functions of non-perturbative quantum field theories in their strong coupling limits. From gauge/gravity duality, these strongly coupled quantum field theories can in theory be related to some weakly interacting gravitational theory. In terms of holographic cosmology, one can relate the observables of a strongly coupled QFT to the cosmological observable known as the CMB power spectrum for the values of its spherical harmonic decomposition, ℓ, which preserve the imprint of phenomenon from an epoch of the pre-recombination universe in which gravity can be considered a weakly interacting theory.

Using standard LFT methods, this investigation into holographic cosmology is limited to strongly coupled QFTs on flat backgrounds. However, with the QFE, we can extend the scope of strongly coupled QFTS that can be considered. Using the QFE we can study strongly coupled QFTs on curved Riemannian manifolds and see if they are related to any known weakly interacting gravitational theories. By taking strongly coupled QFTs which have already been shown to be dual to some cosmological models and studying them on a curved Riemannian manifold we can assess the robustness of these dualities. Studying such strongly coupled QFTs on Riemannian manifolds may also give insights into the Euclidean domain-wall/QFT correspondence that is commonly employed in holographic cosmology. Testing the validity of these dualities for different signatures and geometries is vital towards fully understanding their implications.

A future project that can be undertaken using the QFE is to assess the robustness of the duality between (2+1) quantum gravity and 2D Liouville field theory. If one

Wick rotates (2+1) quantum gravity they get a Euclidean 3-dimensional model of quantum gravity. Using the QFE we can further assess the duality of this Euclidean signature 3-dimensional model of quantum gravity and Liouville field theory on a curved compact 2D manifold. We can also use the results we directly reported on in this dissertation to construct a LFT on an 3D Riemannian manifold and try to establish a correspondence between an 3D strongly coupled QFTs and weakly interacting theories of gravity.

Because we detailed how to discretize an $\mathbb{S}^3$, we can generalize the lattice periodization that was utilized to formulate [56] LFTs on $\mathbb{R} \times \mathbb{S}^2$ to construct LFTs on $\mathbb{R} \times \mathbb{S}^3$ with metric

$$ds^2_{4-cyl} = dt^2 + a^2 d\psi^2 + a^2 \sin^2 \psi (d\theta^2 + \sin^2 \theta d\phi^2), \tag{12.1}$$

where a is the radius of $\mathbb{S}^3$ and the Weyl factor associated with this metric (12.1) is $\Omega^2_{4-cyl} = e^{-2t/a}$. Doing so opens up the possibility that we can investigate a plethora of interesting 4D non-abelian gauge theories. The relationship between non-abelian gauge theories and gravity has been greatly reinforced by double copy theory [41].

Using the QFE we can explore a variety of scattering amplitudes associated with 4D non-abelian gauge theories on curved manifolds. By studying perturbative non-abelian gauge theories on curved manifolds we can assess if the central results pertaining to double copy theory are valid if the gauge theory is both formulated on $\mathbb{R} \times \mathbb{S}^3$ and is Euclidean-signature. Studying the robustness of the double copy theory using the QFE can shed a lot of light on gauge/gravity duality. If double copy theory persists for Euclidean non-abelian gauge theories on curved manifolds then we may be able to investigate it further by studying the scattering amplitudes of additional non-abelian gauge theories besides $\mathcal{N} = 4$ super-Yang-Mills theory. Doing so can help us better understand how to relate these theories to gravity by systematically

modifying their color components.

It might be possible to relate QFE results for $\mathbb{S}^3$ to Lorentzian signature QFTs in curved space-time. As we previously discussed in detail, the 4D space-time metric, g_{ab}, can be decomposed into a spatial metric for an 3D Riemannian surface and two non-dynamical gauge components, the lapse, N, and the shift, N_a. From this decomposition, it was shown that Lorentzian signature general relativity can be understood as the time evolution of a Euclidean signature spatial metric, $h_{ab}(t)$, on a fixed manifold, Σ_0. Using this interpretation of general relativity and the gauge freedom present in both the lapse and the shift, we may be able to formulate our lattice field theories on 4D Lorentzian signature space-times in such a way that they decompose into two portions, one which depends only on the gauge freedom of general relativity and the other which depends solely on the spatial metric. The portion which consists of the spatial metric and the decomposed field theory on it can be solved via the QFE and the portion associated with the gauge components of the metric, g_{ab}, may be handled via methods that don't have to contend with the general issue of discretizing a curved Lorentzian manifold. For more general calculations back reactions can be taken into account using the QFE by introducing some evolution into the Riemannian metric itself.

The case can be made that a considerable portion of theoretical physics is currently devoted to the task of clarifying the meaning and systematizing any of the correspondences which are labeled by arrows that appear in 12.1. As we just discussed, the QFE can contribute towards a better understanding of the two arrows in 12.1 which represent gauge/gravity duality. On the other hand, the Euclidean-signature semi-classical method can potentially aid in both understanding gauge/gravity duality and domain-wall/cosmology correspondence [76, 217].

Even though we exclusively solved the Lorentzian signature WDW equation, we did so by solving equations one usually obtains by applying traditional semi-classical

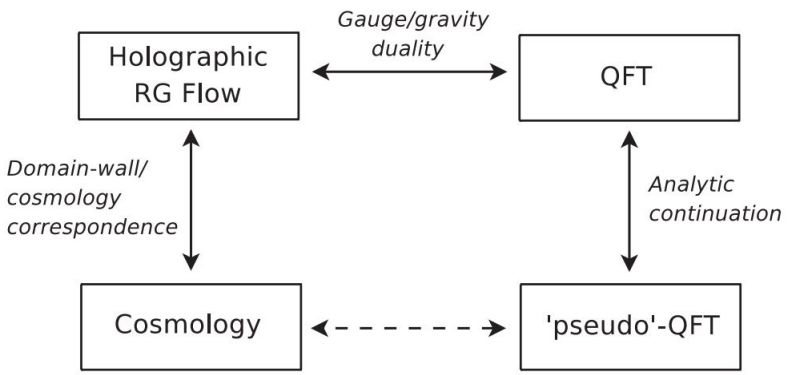

Figure 12.1 A proposed approach for holographic cosmology. It begins with finding a domain-wall space-time which is related to the Lorentziain signature cosmological model originally in question. This corresponding domain-wall space-time may possess [217] Euclidean signature. From there some form of gauge/gravity duality is used to find a QFT which is dual to the domain-wall. If the domain-wall has Euclidean signature then this dual QFT is defined on a Euclidean signature boundary. From there observables in the domain-wall space-time can be computed using its dual QFT. After performing the necessary calculations the results can be analytically continued and be shown through gauge/gravity duality to be the results one would obtain through a QFT dual to the original cosmological solution in question.

methods to the Euclidean signature WDW equation. Thus the results presented in the second part of this dissertation are a two for one deal. By using Euclidean equations to solve the Lorentzian signature WDW equation we have also found solutions to the Euclidean-signature WDW equation. One can take any of the many new $\mathcal{S}_{(0)}$ and ϕ_0 terms that we found and construct the following WKB semi-classical wave functions for the associated Euclidean-signature WDW equation

$$\Psi_{Eucl} = \phi_0 e^{i\mathcal{S}_{(0)}}. \tag{12.2}$$

Many calculations in holographic cosmology were conducted using a single perturbed scalar field with a background FLRW model. However, if holographic cosmology is ever going to become an all encompassing approach to cosmology, the incorporation of more general anisotropic space-times, such as the Bianchi models, is crucial. Using our results for the quantum Taub models with matter sources we can construct an interesting Euclidean anisotropic quantum cosmological model and study it in the hopes of better understanding what type of Euclidean QFT would be dual to this model. The same investigation can also be done for the Euclidean vacuum Bianchi IX models using the results that were found earlier by J.Bae. Testing the robustness of gauge/gravity duality using more general anisotropic theories of cosmology can only allow us to develop a more complete understanding of what holography really means.

In addition to further contributing towards the study of gauge/gravity duality by allowing us to better understand certain Euclidean-signature gravitational models whose dual gauge theories we can later search for, the Euclidean signature semi-classical method can also help us better understand the quantum aspect of domain-wall/cosmology correspondence. It was recently shown [112] that a classical history that corresponds to a Lorentzian signature dS universe can be extrapolated from

a quantized Euclidean signature AdS domain-wall through analytical continuation. For this particular example both the domain-wall and cosmology were isotropic and homogeneous. If the analogous calculation can be done for an anisotropic Euclidean domain-wall our modified semi-classical method can be a powerful tool to further assess this correspondence.

In this dissertation, the author has showcased a multitude of original results which are highly non-trivial within the context of the broader projects his two advisers are working on. Those projects, the QFE and the modified/Euclidean-signature semi-classical method, are highly original and significant endeavors, which have the potential to shed much light on important aspects of physics. Beyond the potential applications to gauge/gravity duality and holography more applications for these two methods are given in the introductory section.

To recap the work that the author did. We first furnished a conformal mapping between $\mathbb{R}^3$ and a general 3D spheroid. Using that mapping and direct Monte-Carlo integration we obtained estimates of the fourth-order Binder cumulant of the critical 3D Ising model on an $\mathbb{S}^3$ and a 3-ball with no boundary. The Binder cumultant is an important observable that one can compute in a CFT and we plan to compare it to results obtained from applying the QFE to ϕ^4 theory on an $\mathbb{S}^3$ at its Wilson-Fisher critical fixed point. To move towards that goal, we uncovered a way to construct a Delaunay simplicial approximation to $\mathbb{S}^3$ while preserving its largest discrete isometry group and found out how to obtain the correct magnitude, and signs of the weights which are assigned to the links and vertices that make up this simplicial approximation. We then ordered the simplicies in such a way that the boundary condition $\partial\mathcal{K} = 0$ for our simplicial complex is satisfied.

Afterwards we proved the existence of an infinite number of smooth and globally defined 'excited' states for the Taub models when a cosmological constant is present. It was then shown that an asymptotic solution exists for the 'no boundary' Taub

models. From there we found new semi-classical solutions to the Bianchi IX models when both a cosmological constant, aligned electromagnetic field and stiff matter were present. We did similar calculations for the Bianchi II and $\text{VII}_{h=0}$ models. By doing so we showed that the Euclidean-signature semi-classical method can be applied to more general situations than it was previously applied to in the past and thus we were able to accomplish furthering the framework and assessing it.

Appendix

12.1 Making Contact With Physical Cosmology

The formalism of quantum cosmology we presented and the matter sources we included to originally assess, and further develop the Euclidean-signature semi-classical method can be seen as representing a first step towards using this method to investigate subjects which are of a great deal of interest to cosmologists. For example, there has been a significant effort to constrain the magnitude of hypothesized primordial magnetic fields (PMFs) which could have seeded the early universe, thus enabling the formation [49, 151, 236] of the micro-Gauss strength magnetic fields we observe in galaxies [104, 149, 236] today. These hypothesized PMFs may have been generated during the inflationary [196, 225, 226] epoch or even earlier as a result of phase transitions [119, 195, 228] occurring at the GUT epoch; other mechanisms [109, 214] for magnetogenesis have been proposed as well. Trying to constrain the strength of these theorized PMFs coincides with trying to detect and determine which signatures they can induce in the CMB.

There are two mains routes through which PMFs can induce distinctive signatures in the CMB. One route is through their stress energy tensor altering the gravitational perturbations of the pre-recombination universe, thus modifying the signatures that we see from baryon acoustic oscillations (BAO). Another route is through the Lorentz force influencing the behavior of the pre-recombination plasma. These two broad

effects of the PMFs can manifest themselves in a plethora of ways as a result of the turbulent and ever changing conditions of the early universe. These effects will manifest themselves differently than those originating from standard cosmological perturbations. One reason for this is that the stress energy tensor of the PMFs induces scalar, vector, and tensor perturbations in which the vector perturbations don't rapidly decay. Another reason is that perturbations of magnetic origins are not suppressed by Silk dampening. One more difference is that their effect on the CMB temperature and polarization spectrums are most prominent on small scales. Thus high resolution CMB data is the best way to constrain the strength of PMFs.

The nature of the signatures that PMFs would produce are dependent upon the strength and form they possess. In the scientific literature PMFs have mainly taken on two forms, a homogeneous aligned field [2, 130] similar to the ones we introduced in our quantum Bianchi models and a stochastic background, which is treated on an equal footing to other stochastic perturbations. The stochastic PMFs can take on many forms such as being helical, non-helical, scale invariant, etc.

By exploring the anisotropies present in the thermal and polarization power spectrums of the CMB using the latest Planck and SPT data the strength of a non-helical PMF at the time of recombination was recently constrained [168] to be $B_{1Mpc} < 1.52nG$ at the 95 percent C.L. The $1Mpc$ refers to the comoving field amplitude at a scale of $1Mpc$ and is obtained from smoothing

$$\begin{aligned} &\lambda = 1Mpc, \\ &B^2_{1\mathrm{Mpc}} = \int \frac{d^3k}{(2\pi)^3} \mathrm{e}^{-k^2\lambda^2} P_B(k), \end{aligned} \tag{12.3}$$

the power spectrum of the PMF, $P_B(k)$, which is obtained from the two-point function of the PMF expressed in Fourier space

$$\left\langle B_i(\boldsymbol{k}) B_j^*(\boldsymbol{k}') \right\rangle = \delta_{\mathrm{D}}(\boldsymbol{k} - \boldsymbol{k}') \left(\delta_{ij} - \hat{k}_i \hat{k}_j\right) P_B(k). \tag{12.4}$$

This constraint was obtained by taking into account two types of anisotropies that PMFs can induce in the CMB spectrums, passive and compensated. Passive constraints are prominent on super- and sub-cosmic horizon scales prior to neutrinos decoupling from the photon-baryon fluid. They arise from the Lorentz force of the PMFs affecting evolution of the photon-baryon-neutrino fluid before decoupling and due to its stress-energy tensor. These anistropies persist after neutrino decoupling in the form of a constant suppression of the amplitudes of the inflationary non-magnetic perturbations. Thus the presence of a PMF would induce a distinctive signature in the CMB through these passive modes.

Compensated modes are generated after neutrinos decouple from matter. They are called compensated because the decoupled neutrinos act as an independent matter source which can induce anisotropy in the very early universe which negates or compensates for the anisotropy generated by the PMF on super-horizon scales. Compensated modes can induce anisotropies on sub-horizon scales by altering the velocity of the baryon fluid via the Doppler effect which is why the study we cited [168] went to large ℓ in order to constrain the PMF using high resolution CMB data.

Another signature of a PMF would be non-gaussianity [59] in the modes which make up the CMB power spectrum. The presence of non-gaussianity means that the modes are correlated with each other and that higher statistical moments can be extrapolated from the CMB anisotropies. One such quantity is the third order statistic known as the CMB bispectrum. By using the bispectrum of the polarization data from the 2015 Planck results, the strength of the PMF was constrained [5] to be under $5nG$ depending on the method which was used to analyze magnetically-induced non-gaussianity.

Far more stringent limits on the magnitude of a particular PMF were obtained by first showing that one can induce small-scale baryonic density fluctuations in the pre-recombination universe. These fluctuations result in an inhomogeneous recombination

event occurring which may alter the large scale CMB temperature anisotropies to a detectable degree. Using this information and through numerical simulations, the following bound [127] was set for the strength of a present day remnant of a PMF integrated over all scales: $B < 47pG$.

The study of quantum cosmology has the potential to shed further light on PMFs. This is especially true of PMFs generated during the GUT epoch. The GUT epoch has a characteristic energy scale of $(10^{16}GeV - 10^{17}GeV)$ while the inflationary epoch has an energy scale of $(10^{14}GeV)$. Thus it is expected that the effects of quantum gravity should manifest more strongly during the GUT epoch than the inflationary one, which has been the subject of a previous investigation which we will touch upon shortly. Even though WDW quantum gravity is not the most fundamental theory of quantum gravity, it is probably a decent description of nature for energies somewhat less [137] than the Planck scale $(10^{19}GeV)$. Therefore the author hopes that quantum cosmology can shed further light on magnetogenesis during the GUT era. The understanding of quantum cosmology that the author has obtained while working on his doctoral work can serve as a good basis for beginning this venture.

Previous efforts [138] to obtain quantum corrections to the CMB power spectrum have resulted in corrections which are exceedingly small relative to expected systematic errors, such as cosmic variance, which are inherent to cosmological observation. A popular model to extrapolate quantum corrections from is the flat FLRW model with a single scalar field and a simple potential which yields chaotic inflation

$$\mathcal{H}_0\Psi_0(\alpha,\phi) = \frac{e^{-3\alpha}}{2}\left[\frac{1}{m_{\mathrm{P}}^2}\frac{\partial^2}{\partial\alpha^2} - \frac{\partial^2}{\partial\phi^2} + e^{6\alpha}m^2\phi^2\right]\Psi_0(\alpha,\phi) = 0. \tag{12.5}$$

After introducing scalar field perturbations

$$\phi \to \phi(t) + \delta\phi(\mathbf{x},t), \tag{12.6}$$

and expanding the inhomogeneous modes, $\delta\phi(\mathbf{x},t)$, as a Fourier decomposition

$$\delta\phi(\mathbf{x},t)=\sum_{k=1}^{\infty}f_k(t)e^{i\mathbf{k}\cdot\mathbf{x}}, \tag{12.7}$$

the following equation can be obtained from (12.5)

$$\left[\mathcal{H}_0+\sum_{k=1}^{\infty}\mathcal{H}_k\right]\Psi\left(\alpha,\phi,f_k\right)=0, \tag{12.8}$$

where $\mathcal{H}_k$ [108, 136] is the Hamiltonian which governs the evolution of the perturbations

$$\mathcal{H}_k=\frac{1}{2}e^{-3\alpha}\left[-\frac{\partial^2}{\partial f_k^2}+\left(k^2e^{4\alpha}+m^2e^{6\alpha}\right)f_k^2\right]. \tag{12.9}$$

Next one can apply the quantum analogue of the slow roll condition, $\frac{\partial^2\psi}{\partial\phi^2}<<|V(\phi)|$, to (12.8) and obtain the following equation

$$\frac{1}{2}e^{-3\alpha}\left[\frac{1}{m_{\mathrm{P}}^2}\frac{\partial^2}{\partial\alpha^2}+e^{6\alpha}m_{\mathrm{P}}^2H^2-\frac{\partial^2}{\partial f_k^2}+\left(k^2e^{4\alpha}+m^2e^{6\alpha}\right)f_k^2\right]\Psi_k\left(\alpha,f_k\right)=0, \tag{12.10}$$

where m_{P} is the Planck mass, k is the wave number, and H is the quasi static Hubble scale during inflation.

Applying the Born-Oppenheimer approximation [135] to this WDW equation results in a sequence of equations that can be solved in a manner similar to those generated by the Euclidean-signature semi-classical method. Using WKB time

$$\frac{\partial}{\partial t}:=-e^{-3\alpha}\frac{\partial S_0}{\partial\alpha}\frac{\partial}{\partial\alpha}, \tag{12.11}$$

these equations can be expressed as sequence of Schrödinger equations with additional gravitational quantum corrections [204] added on to them at each order. The first order equation one obtains with this method is exactly the Schrödinger equation expressed in WKB time. The higher order equations have terms which spoil the

unitarity of the Schrödinger equation. However the dominant quantum correction to the CMB is going to come [29, 139] mainly from the gravitational correction to the Schrödinger equation which does not violate unitarity. Thus one can use the standard inner product from quantum mechanics to compute this dominant contribution which ultimately for our purposes results in the following spectrum

$$\Delta^2_{(1)}(k) \simeq \Delta^2_{(0)}(k)\left[1 - \frac{123.83}{k^3}\frac{H^2}{m_{\rm P}^2} + \frac{1}{k^6}\mathcal{O}\left(\frac{H^4}{m_{\rm P}^4}\right)\right]^2, \tag{12.12}$$

where $\Delta^2_{(0)}(k)$ is the standard CMB power spectrum one obtains for this model of chaotic inflation when no quantum gravitational effects are taken into account. The quantum correction (12.12) was obtained from truncating a more complicated expression which vanishes when $k \approx 5.74(H/m_{\rm P})^{2/3}$. This vanishing of the power spectrum indicates a breakdown in our approximation and thus we should avoid scales close to the aforementioned k. If we wish to study smaller scales we would need to take into account higher order quantum corrections.

As it can be seen, the effects of the quantum corrections to the CMB spectrum are immensely suppressed as a result of the Planck scale $m_{\rm P} \approx 10^{19} GeV$. In addition the spectrum is no longer scale invariant. The quantum correction to the CMB spectrum is largest when the scale, k, is small because the large (inverse of k) size modes were the first to enter the horizon and thus were exposed to gravitational quantum effects for the longest time. Using the standard inflationary scale [143] of $10^{14} GeV$ we obtain the following scale dependent expression for the quantum correction

$$\Delta^2_{(1)}(k) \simeq \Delta^2_{(0)}(k)\left[1 - 1.76 \times 10^{-9}\frac{1}{k^3} + \frac{\mathcal{O}\left(10^{-15}\right)}{k^6}\right]^2, \tag{12.13}$$

which is way too small to be observable given the systematic error we face [192] of only being able to observe one universe. Despite this calculation not giving us any physics that we can observe in the CMB it can be used to compare different models

of quantum gravity. Because loop quantum gravity predicts a radical alteration to space-time the quantum corrections obtained from that theory are much larger and can possibly be observed. Thus calculations of this type can allow us to compare different theories of quantum gravity with each other while giving us results which we may be able to observe.

Because the quantum Bianchi models were the main conduit through which we applied, assessed, and further developed the Euclidean-signature semi-classical method, it is appropriate to discuss whether the classical Bianchi models can be accurate representations of our actual universe. There has been a lot of recent work [4, 8, 210] done on constraining classical Bianchi models using the CMB. The observables one tries to constrain in these models are the components of the shear tensor, σ_{ab}. In terms of the CMB, the shear tensor is a measure of how the redshift of a photon is dependent upon the direction from which it is travelling from.

The Bianchi models which have been investigated the most in the literature are the Bianchi VII_h models. This is because they admit both flat and open topologies. Furthermore, depending on the value of h, these models admit [27] a plethora of other Bianchi models as their sub types such as the Bianchi $VII_{h=0}$, V, and I models. The Bianchi IX models and its sub type, the Taub models, have not been subject to constraint using recent CMB data. The reason for this is because these closed models induce only a quadrupole, $(l = 2)$, contribution to the CMB temperature distribution and polarization, and thus are difficult to constrain compared to the open and flat Bianchi models.

For space-times which are near isotropic, the shear tensor can be broken up into four modes, the scalar, vector, regular tensor and irregular tensor modes. What differentiates the regular from the irregular tensor modes is their initial behavior. Regular tensor modes initially grow in size while irregular tensors modes decay monotonically. Modes which decay monotonically are larger at recombination than modes which over-

all decay more slowly and thus can be better constrained using CMB data. Using both CMB temperature and polarization data all four modes of the shear tensor were constrained in [210]. Only taking into account the vorticity which is determined by the vector mode, the aforementioned studies found that the odds against anisotropic expansion were 270:1. Taking into account all four modes, one arrives at an astounding 121000 to 1 odds against anisotropic expansion.

This result which strongly disfavors our universe being a Bianchi universe is further corroborated [8] by a 2019 study on Bianchi I models. For the Bianchi I models, which correspond to the LRS Bianchi $VII_{h=0}$ models, a modified Friedmann equation was constructed and included a term which scales like stiff matter, $\Omega_{0\sigma}a^{-6}$, which measures the anisotropic expansion. Using CMB data the authors of [8] constrained the present value of that stiff matter term corresponding to anisotropic expansion to be $\Omega_{0\sigma} < 10^{-15}$ which is too small to alter either matter-radiation equality or the size and locations of the peaks corresponding to matter perturbations in the CMB power spectrum. If big bang nucleogenesis is taken into account the constraint becomes tighter $\Omega_{0\sigma} < 10^{-23}$. It should be noted that these constraints are model (GR) dependent.

From the data obtained from Planck and accepting the assumptions that general relativity is the correct classical description of gravity, and that dark energy is not an anisotropic matter source it is incredibly unlikely that our universe had a period of anisotropic expansion; thus it is unlikely that Bianchi models will serve as the best description of our universe. Nonetheless Bianchi models are incredibly important to study and if these two assumptions are challenged the chances that our universe had a period of anisotropic expansion could dramatically increase. If strong evidence for anisotropic expansion was found it would cause us to rethink a lot of what we know about the universe. For example there is a cosmic no-hair theorem [219, 232] which implies that if inflation did occur in the early universe that it would have reduced

the universe's anisotropy to the point that any residual anisotropy left over after inflation would have no observational consequences. Finding evidence of an epoch of anisotropic expansion can fundamentally change our understanding of inflation and perhaps more importantly its underlying physics.

As we demonstrated, the Bianchi models are a rich set of systems one can use to ascertain what effects quantum gravity possibly induces on cosmic evolution. Because of their richness they are excellent tools to differentiate different models of quantum gravity. As implied in the aforementioned investigation [138], general observational effects of quantum gravity don't become prominent unless one probes energy scales which approach the Planck length. Thus until we are able to overcome the hurdle of observing phenomena which approaches the Planck length Bianchi models will remain valuable tools to further study and understand quantum gravity.

12.2 Binder Code

Using the following code and the CFT data reported for the five operators included in table 1 of [141] we performed 100,000 Monte Carlo evaluations with our accuracy goal set to 5 and calculated $\langle \sigma^4 \rangle$ to be 1.591463 with an error of 0.000050. This allows us to obtain the following estimate of the fourth-order Binder cumulant

$$U_4 = 0.391765 \pm 0.000035. \tag{12.14}$$

The code below can be easily modified to include the additional CFT data [216] that we used to compute (4.40).

This code defines the $h_{\Delta,\ell}(r,\eta)$ which we wish to calculate through the recursion relation given in (5.30). The only input for the user is "n", which is the order one wishes to compute the recursion relation up to.

```
H[\[CapitalDelta]\[CapitalDelta]_,
```

```
LL_] := {n = 12;,
 recursion[a_] := Normal[Series[a /. hh -> h, {r, 0, n}]],
 Nest[recursion, {h[\[CapitalDelta]_,
      L_] := ((LegendreP[L, \[Eta]]/(
        Sqrt[1 - rr^2] Sqrt[-4 \[Eta]^2 rr^2 + (1 + rr^2)^2]) +
        Sum[((-((
              2^(1 - 4 k)
                k ((2 k)!)^2 Pochhammer[1 + L,
                2 k])/((k!)^4 Pochhammer[1/2 + L, 2 k])))*(r)^(2*
                k)/(\[CapitalDelta] - (1 - L - 2*k)))*
          hh[1 - L, L + 2*k], {k, 1, n/2}]
        +
        Sum[((-((
              k (1/2 - k + L) Pochhammer[1/2, k]^2 Pochhammer[
                1/4 (3 - 2 k + 2 L),
                k]^2)/((1/2 + k + L) (k!)^2 Pochhammer[
                1/4 (1 - 2 k + 2 L), k]^2)))*(r)^(2*
                k)/(\[CapitalDelta] - ((3/2) - k)))*
          hh[(3/2) + k, L], {k, 1, n/2}] +
        Sum[((-((
              2^(1 - 4 k)
                k ((2 k)!)^2 Pochhammer[1 - 2 k + L,
                2 k])/((k!)^4 Pochhammer[3/2 - 2 k + L,
                2 k])))*(r)^(2*
                k)/(\[CapitalDelta] - (2 + L - 2*k)))*
          hh[2 + L, L - 2*k], {k, 1,
          L/2}])), \[CapitalDelta] = \
```

```
\[CapitalDelta]\[CapitalDelta];,
      L = LL;, (((LegendreP[L, \[Eta]]/(
          Sqrt[1 - rr^2] Sqrt[-4 \[Eta]^2 rr^2 + (1 + rr^2)^2]) +
          Sum[((-((
                2^(1 - 4 k)
                  k ((2 k)!)^2 Pochhammer[1 + L,
                  2*k])/((k!)^4 Pochhammer[1/2 + L, 2*k])))*(r)^(2*
                  k)/(\[CapitalDelta] - (1 - L - 2*k)))*
            hh[1 - L, L + 2*k], {k, 1, n/2}]
          +
          Sum[((-((
                k (1/2 - k + L) Pochhammer[1/2, k]^2 Pochhammer[
                  1/4 (3 - 2 k + 2 L),
                  k]^2)/((1/2 + k + L) (k!)^2 Pochhammer[
                  1/4 (1 - 2 k + 2 L), k]^2)))*(r)^(2*
                  k)/(\[CapitalDelta] - ((3/2) - k)))*
            hh[(3/2) + k, L], {k, 1, n/2}] +
          Sum[((-((
                2^(1 - 4 k)
                  k ((2 k)!)^2 Pochhammer[1 - 2 k + L,
                  2 k])/((k!)^4 Pochhammer[3/2 - 2 k + L,
                  2 k])))*(r)^(2*
                  k)/(\[CapitalDelta] - (2 + L - 2*k)))*
            hh[2 + L, L - 2*k], {k, 1, L/2}])))}[[4]], n/2]}[[3]]
```

This code is the numerator that appears in the four-point function for the critical 3D Ising model and is computed in accordance with (5.28)

```
G = (1 + (H[1.412625, 0]*(((4*r)^(1.412625))*(1.0518537)^2)) + (H[
       3.82966, 0] (((4*r)^(3.82966))*(0.053029)^2)) + (H[3,
       2]*(((4*r)^(3)) ((0.5181489/Sqrt[0.946539])^2))) + (H[5.509,
       2] (((4*r)^(5.509))*(0.0172)^2)) + (H[5.02274,
       4] (((4*r)^(5.02274))*(0.1319)^2)));
```

This last piece of code plots the four-point function, showing that our computation of the four-point function agrees with [209].

```
{FourPointFunction = (G/(1 +
            Abs[z]^1.0362978 + (Abs[z]^1.0362978/
               Abs[1 - z])^1.0362978) /. rr -> r /.
        r -> Abs[
          z/(1 + Sqrt[1 - z])^2] /. \[Eta] -> (z/(1 + Sqrt[1 - z])^2 +
            Conjugate[z]/(1 + Sqrt[1 - Conjugate[z]])^2)/(2*
           Abs[z/(1 + Sqrt[1 - z])^2]) /. z -> x + I*y);,
  Plot3D[FourPointFunction, {x, -1, .5}, {y, -1, 1},
   RegionFunction -> Function[{x, y}, Sqrt[x^2 + y^2] < 1 && x < 1/2],
    PlotRange -> All]}[[2]]
```

12.3 Taub 'Excited' And 'No Boundary' Code

This code produces the n non-trivial quantum corrections to the nth 'excited' state of the $\Lambda \neq 0$ Taub models which can be used to construct a closed form solution when the operator ordering parameter $B = 0$. The only required inputs from the user is setting n equal to a positive integer and choosing an option h. When h=2 it gives the 'excited' state quantum corrections. When h=3 it gives the closed form 'excited' solution to the Taub WDW equation when a cosmological constant is present. When

h=4 it gives zero indicating that the solution given by h=3 does indeed satisfy the WDW equation;

```
{{n = 2, h = 3};,
  Table[{Subscript[S,
        0] = ((-9 E^(4 \[Alpha] - 2 \[Beta]) (-1 +
              E^(6 \[Beta])) \[Pi] +
           E^(6 (\[Alpha] + \[Beta])) \[CapitalLambda]))^(n);,
     Subscript[S, k] =
       Sum[Sum[b[{i, j}]*
          E^(6*n*\[Alpha] - 2*(n - i)*\[Alpha] -
             2*k*\[Alpha] + -2*n*\[Beta] + 6*j*\[Beta] +
             8*\[Beta]*i + 4*\[Beta]*k), {j, 0, n - k - i}], {i, 0,
         n - k}];,
     asd = ((-D[Subscript[S, k], \[Alpha]]*
            D[1/6 E^(2 \[Alpha] - 4 \[Beta]) (1 +
                 2 E^(6 \[Beta])) - (E^(4 (\[Alpha] + \[Beta])) \
\[CapitalLambda])/(36 \[Pi]), \[Alpha]] +
           D[Subscript[S, k], \[Beta]]*
            D[1/6 E^(2 \[Alpha] - 4 \[Beta]) (1 +
                 2 E^(6 \[Beta])) - (E^(4 (\[Alpha] + \[Beta])) \
\[CapitalLambda])/(36 \[Pi]), \[Beta]]) +
         k*(D[Subscript[S, -1 + k], \[Alpha]] -
            D[Subscript[S, -1 + k], \[Beta]]) + (k/
            2)*(D[D[Subscript[S, -1 + k], \[Alpha]], \[Alpha]] -
            D[D[Subscript[
               S, -1 + k], \[Beta]], \[Beta]]));, \[Alpha] =
       Log[x];, \[Beta] = Log[y];,
```

```
    Subscript[S,
       k] = ((Sum[
          Sum[b[{i, j}]*

            E^(6*n*\[Alpha] - 2*(n - i)*\[Alpha] -
               2*k*\[Alpha] + -2*n*\[Beta] + 6*j*\[Beta] +
               8*\[Beta]*i + 4*\[Beta]*k), {j, 0, n - k - i}], {i, 0,
            n - k}]) /.
        Solve[Simplify[
           MonomialList[Simplify[asd], {x, y, 1/x, 1/y}]] ==
          Table[0, {i, 1,
            Length[Flatten[
              Table[Table[b[{i, j}], {j, 0, n - k - i}], {i, 0,
                n - k}], 1]]}],
         Flatten[Table[
           Table[b[{i, j}], {j, 0, n - k - i}], {i, 0, n - k}],
          1]]);, ClearAll[\[Alpha]];, ClearAll[\[Beta]];,
    Subscript[S, k] =
     Expand[Simplify[
       First[Subscript[S, k] /. {x -> E^(\[Alpha]),
          y -> E^(\[Beta])}]]], ClearAll[x];, ClearAll[y];};, {k, 1,
   n}];
  o[n] = Table[Subscript[S, g] /. {\[Beta] -> \!\(TraditionalForm\`
\*SubscriptBox[\(\[Beta]\), \(+\)]\)}, {g, 0, n}],
  psi = (Table[1/k!, {k, 0, n}].o[n]) E^(-(1/6) E^(
     2 \[Alpha] -
      4 SubPlus[\[Beta]]) (1 + 2 E^(6 SubPlus[\[Beta]])) + (
```

```
    E^(4 (\[Alpha] + SubPlus[\[Beta]])) \[CapitalLambda])/(
    36 \[Pi]) + \[Alpha] + SubPlus[\[Beta]]),
  FullSimplify[
   D[D[psi, \[Alpha]], \[Alpha]] -
    D[D[psi, SubPlus[\[Beta]]],
     SubPlus[\[Beta]]] + (1/3 E^(4 \[Alpha] - 8 SubPlus[\[Beta]]) -
       4/3 E^(4 \[Alpha] - 2 SubPlus[\[Beta]]) + (
       2 E^(6 \[Alpha]) \[CapitalLambda])/(9 \[Pi])) (psi)]}[[h]]
```

This code produces the n non-trivial quantum corrections to the nth 'excited' state of the $\Lambda = 0$ Taub models which can be used to construct a closed form solution when $B = 0$. The only required inputs from the user is setting n equal to a positive integer and choosing an option h. When h=2 it gives the 'excited' state quantum corrections. When h=3 it gives the closed form 'excited' solution to the Taub WDW equation. When h=4 it gives zero indicating that the solution given by h=3 does indeed satisfy the WDW equation

```
{{n = 2, h = 3},
  Table[{Subscript[S,
        0] = ((-9 E^(4 \[Alpha] - 2 \[Beta]) (-1 +
             E^(6 \[Beta])) \[Pi]))^(n);,
     Subscript[S, k] =
       E^(4*\[Alpha]*n - 2*\[Alpha]*k)*
        Sum[E^(-6*\[Beta]*j - 2*\[Beta]*k + 4*\[Beta]*n)*b[j, k], {j,
          0, n - k}];,
     asd = ((-D[Subscript[S, k], \[Alpha]]*
           D[1/6 E^(2 \[Alpha] - 4 \[Beta]) (1 +
               2 E^(6 \[Beta])), \[Alpha]] +
```

```
          D[Subscript[S, k], \[Beta]]*
           D[1/6 E^(2 \[Alpha] - 4 \[Beta]) (1 +
               2 E^(6 \[Beta])), \[Beta]]) +
         k*(D[Subscript[S, -1 + k], \[Alpha]] -
           D[Subscript[S, -1 + k], \[Beta]]) + (k/
           2)*(D[D[Subscript[S, -1 + k], \[Alpha]], \[Alpha]] -
           D[D[Subscript[
              S, -1 + k], \[Beta]], \[Beta]]));, \[Alpha] =
       Log[x];, \[Beta] = Log[y];,
     Subscript[S,
       k] = ((E^(4*\[Alpha]*n - 2*\[Alpha]*k)*
          Sum[E^(-6*\[Beta]*j - 2*\[Beta]*k + 4*\[Beta]*n)*
            b[j, k], {j, 0, n - k}]) /.
        Solve[Simplify[
           MonomialList[Simplify[asd], {x, y, 1/x, 1/y}]] ==
          Table[0, {i, 1,
            Length[Flatten[Table[b[j, k], {j, 0, n - k}], 1]]}],
         Flatten[Table[b[j, k], {j, 0, n - k}], 1]]);,
     ClearAll[\[Alpha]];, ClearAll[\[Beta]];,
     Subscript[S, k] =
      Expand[Simplify[
        First[Subscript[S, k] /. {x -> E^(\[Alpha]),
          y -> E^(\[Beta])}]]], ClearAll[x];, ClearAll[y];};, {k, 1,
    n}];
  o[n] = Table[Subscript[S, g] /. {\[Beta] -> \!\(TraditionalForm\`
\*SubscriptBox[\(\[Beta]\), \(+\)]\)}, {g, 0, n}],
  psi = (Table[1/k!, {k, 0, n}].o[n]) E^(-(1/6) E^(
```

```
      2 \[Alpha] -
       4 SubPlus[\[Beta]]) (1 + 2 E^(6 SubPlus[\[Beta]])) + \[Alpha] +
      SubPlus[\[Beta]]),
  FullSimplify[
   D[D[psi, \[Alpha]], \[Alpha]] -
    D[D[psi, SubPlus[\[Beta]]],
     SubPlus[\[Beta]]] + (1/3 E^(4 \[Alpha] - 8 SubPlus[\[Beta]]) -
       4/3 E^(4 \[Alpha] - 2 SubPlus[\[Beta]])) (psi)]}[[h]]
```

This last piece of codes computes the higher order $-\mathcal{S}^{nb}_{(k\geq 3)}$ terms of the asymptotic series present in the exponent of our 'ground' state 'no boundary' wave functions $\psi^{nb} := e^{\left(-\sum_{k=2}^{\infty}\frac{g(k)e^{\beta_+}(k-1)-2\alpha(k-1)}{k!}-\frac{1}{6}\left(1-4e^{3\beta_+}\right)e^{2\alpha-4\beta_+}-\frac{1}{2}a(4-\mathrm{B})+\frac{5\beta_+}{2}\right)}$. The only input from the user is an n which is positive integer greater than 2.

```
{n = 5, Total[{g[2] = 1/8 (9 + BB^2),
     Table[{g[k] = 3/4 (-2 + k) k g[-1 + k] + \!\(
\*UnderoverscriptBox[\(\[Sum]\), \(L = 2\), \(\(-2\) + k\)]\(50
\*FractionBox[\(3\ \((\(-1\) + k - L)\)\ \((\(-1\) + L)\)\ \(k!\)\ g[
                k - L]\ g[L]\), \(\(\((k - L)\)!\)\ \(L!\)\)]/\((\n
              4\  - \ 4\ k)\)\)\), (1/(k!)) g[k]*
         E^(-2 \[Alpha] (-1 + k) + \[Beta] (-1 + k))}[[2]], {k, 3,
       n}]}[[2]]]}[[2]]
```

Bibliography

[1] R Abraham, JE Marsden, and T Ratiu. Manifolds, tensor analysis and applications, (massachusetts, 1983.

[2] Julian Adamek, Ruth Durrer, Elisa Fenu, and Marc Vonlanthen. A large scale coherent magnetic field: interactions with free streaming particles and limits from the cmb. *Journal of Cosmology and Astroparticle Physics*, 2011(06):017, 2011.

[3] Allan Adams, Lincoln D Carr, Thomas Schaefer, Peter Steinberg, and John E Thomas. Strongly correlated quantum fluids: ultracold quantum gases, quantum chromodynamic plasmas and holographic duality. *New Journal of Physics*, 14(11):115009, 2012.

[4] PAR Ade, N Aghanim, M Arnaud, M Ashdown, J Aumont, C Baccigalupi, AJ Banday, RB Barreiro, N Bartolo, S Basak, et al. Planck 2015 results-xviii. background geometry and topology of the universe. *Astronomy & Astrophysics*, 594:A18, 2016.

[5] Peter AR Ade, N Aghanim, M Arnaud, F Arroja, M Ashdown, J Aumont, C Baccigalupi, M Ballardini, AJ Banday, RB Barreiro, et al. Planck 2015 results-xix. constraints on primordial magnetic fields. *Astronomy & Astrophysics*, 594:A19, 2016.

[6] Peter AR Ade, N Aghanim, M Arnaud, Mark Ashdown, J Aumont, C Baccigalupi, AJ Banday, RB Barreiro, JG Bartlett, N Bartolo, et al. Planck 2015 results-xiii. cosmological parameters. *Astronomy & Astrophysics*, 594:A13, 2016.

[7] M Aguero, JAS Aguilar, C Ortiz, M Sabido, and J Socorro. Noncommutative bianchi type ii quantum cosmology. *International Journal of Theoretical Physics*, 46(11):2928–2934, 2007.

[8] Özgür Akarsu, Suresh Kumar, Shivani Sharma, and Luigi Tedesco. Constraints on a bianchi type i spacetime extension of the standard λ cdm model. *Physical Review D*, 100(2):023532, 2019.

[9] PM Alsing, JR McDonald, DX Gu, WA Miller, and ST Yau. Simplicial ricci flow. *Commu. Math. Phys*, 329(2):579–608, 2014.

[10] Thomas Appelquist, Richard Brower, Simon Catterall, George Fleming, Joel Giedt, Anna Hasenfratz, Julius Kuti, Ethan Neil, and David Schaich. Lattice gauge theories at the energy frontier. *arXiv preprint arXiv:1309.1206*, 2013.

[11] Thomas Appelquist, Richard C Brower, George T Fleming, Anna Hasenfratz, Xiao-Yong Jin, Joe Kiskis, Ethan T Neil, James C Osborn, Claudio Rebbi, Enrico Rinaldi, et al. Strongly interacting dynamics and the search for new physics at the lhc. *Physical Review D*, 93(11):114514, 2016.

[12] Douglas N Arnold, Richard S Falk, and Ragnar Winther. Finite element exterior calculus, homological techniques, and applications. *Acta numerica*, 15:1–155, 2006.

[13] Richard Arnowitt, Stanley Deser, and Charles W Misner. Dynamical structure and definition of energy in general relativity. *Physical Review*, 116(5):1322, 1959.

[14] Richard Arnowitt, Stanley Deser, and Charles W Misner. Gravitation: an introduction to current research, 1962.

[15] Richard L Arnowitt, SD Deser, and Charles W Misner. The dynamics of general relativity. Technical report, 1962.

[16] Abhay Ashtekar, Tomasz Pawlowski, and Parampreet Singh. Quantum nature of the big bang. *Physical review letters*, 96(14):141301, 2006.

[17] Abhay Ashtekar, Tomasz Pawlowski, and Parampreet Singh. Quantum nature of the big bang: an analytical and numerical investigation. *Physical Review D*, 73(12):124038, 2006.

[18] Abhay Ashtekar, Tomasz Pawlowski, and Parampreet Singh. Quantum nature of the big bang: improved dynamics. *Physical Review D*, 74(8):084003, 2006.

[19] Joseph H Bae. Quantizing the homogeneous linear perturbations about taub using the jacobi method of second variation. *arXiv preprint arXiv:1410.3446*, 2014.

[20] Joseph H Bae. Mixmaster revisited: wormhole solutions to the bianchi ix wheeler–dewitt equation using the euclidean-signature semi-classical method. *Classical and Quantum Gravity*, 32(7):075006, 2015.

[21] Joseph H Bae. Quantizing the homogeneous linear perturbations about taub using the jacobi method of second variation and the method of invariants. *Classical and Quantum Gravity*, 32(14):145002, 2015.

[22] Joseph Hongchul Bae. *Wormhole Solutions to the Bianchi IXWheeler-DeWitt Equation using theEuclidean-Signature Semi-Classical Method*. Yale University, 2015.

[23] AK Banerjee and NO Santos. Spatially homogeneous cosmological models. *General Relativity and Gravitation*, 16(3):217–224, 1984.

[24] T Banks and W Fischler. Holographic cosmology 3.0. *Physica Scripta*, 2005(T117):56, 2005.

[25] C. Bradford Barber, David P. Dobkin, and Hannu Huhdanpaa. The quickhull algorithm for convex hulls. *ACM TRANSACTIONS ON MATHEMATICAL SOFTWARE*, 22(4):469–483, 1996. http:
www.qhull.org.

[26] J Fernando Barbero and Michael P Ryan Jr. Minisuperspace examples of quantization using canonical variables of the ashtekar-type: Structure and solutions. *Physical Review D*, 53(10):5670, 1996.

[27] JD Barrow. Juszkiewicz, and dh sonoda. *Mon. Not. R. Astron. Soc*, 213:917, 1985.

[28] John D Barrow. Chaotic behaviour in general relativity. *Physics Reports*, 85(1):1–49, 1982.

[29] Andrei O Barvinsky and Claus Kiefer. Wheeler-dewitt equation and feynman diagrams. *Nuclear Physics B*, 526(1-3):509–539, 1998.

[30] Catarina Bastos, Orfeu Bertolami, Nuno Costa Dias, and Joao Nuno Prata. Weyl–wigner formulation of noncommutative quantum mechanics. *Journal of mathematical physics*, 49(7):072101, 2008.

[31] Marco Valerio Battisti and Giovanni Montani. Quantum dynamics of the taub universe in a generalized uncertainty principle framework. *Physical Review D*, 77(2):023518, 2008.

[32] VA Belinskii, GW Gibbons, Don N Page, and CN Pope. Asymptotically euclidean bianchi ix metrics in quantum gravity. *Physics Letters B*, 76(4):433–435, 1978.

[33] Vladimir A Belinskii, Isaac M Khalatnikov, and Evgeny M Lifshitz. Oscillatory approach to a singular point in the relativistic cosmology. *Advances in Physics*, 19(80):525–573, 1970.

[34] J Bene and R Graham. Supersymmetric homogeneous quantum cosmologies coupled to a scalar field. *Physical Review D*, 49(2):799, 1994.

[35] Charles L Bennett, Davin Larson, Janet L Weiland, N Jarosik, G Hinshaw, N Odegard, KM Smith, RS Hill, B Gold, M Halpern, et al. Nine-year wilkinson microwave anisotropy probe (wmap) observations: final maps and results. *The Astrophysical Journal Supplement Series*, 208(2):20, 2013.

[36] Daniel Berkowitz. Conformal invariance and the ising model on a 3 sphere in connection with the quantum elemental method. *arXiv preprint arXiv:1808.05862*, 2018.

[37] Daniel Berkowitz. New solutions to the bianchi ix wheeler dewitt equation and leading order solutions for

\

lambda

\ne 0*andaprimordialmagneticfield.arXivpreprintarXiv* : 1910.11970, 2019.

[38] Daniel Berkowitz. Towards uncovering generic effects of matter sources in anisotropic quantum cosmologies via bianchi ii and vii _{$h = 0$} models. *arXiv preprint arXiv:2011.05972*, 2020.

[39] Daniel Berkowitz. Towards uncovering generic effects of matter sources in anisotropic quantum cosmologies via taub models. *arXiv preprint arXiv:2011.04229*, 2020.

[40] Daniel Berkowitz. Bianchi ix and viii quantum cosmology with a cosmological constant, aligned electromagnetic field, and scalar field. *arXiv preprint arXiv:2102.02343*, 2021.

[41] Zvi Bern, John Joseph M Carrasco, and Henrik Johansson. Perturbative quantum gravity as a double copy of gauge theory. *Physical review letters*, 105(6):061602, 2010.

[42] Heliudson Bernardo. Trans-planckian censorship conjecture in holographic cosmology. *Physical Review D*, 101(6):066002, 2020.

[43] O Bertolami, JG Rosa, CML De Aragao, P Castorina, and D Zappala. Noncommutative gravitational quantum well. *Physical Review D*, 72(2):025010, 2005.

[44] O Bertolami, JG Rosa, CML De AragÃO, P Castorina, and D Zappala. Scaling of variables and the relation between noncommutative parameters in noncommutative quantum mechanics. *Modern Physics Letters A*, 21(10):795–802, 2006.

[45] Tirthabir Biswas and Anupam Mazumdar. Inflation with a negative cosmological constant. *Physical Review D*, 80(2):023519, 2009.

[46] Philippe Blanchard and Erwin Brüning. Some remarks on the history and objectives of the calculus of variations. In *Variational Methods in Mathematical Physics*, pages 1–14. Springer, 1992.

[47] David Bohm. A suggested interpretation of the quantum theory in terms of" hidden" variables. i. *Physical review*, 85(2):166, 1952.

[48] Martin Bojowald. *Canonical gravity and applications: cosmology, black holes, and quantum gravity*. Cambridge University Press, 2010.

[49] Axel Brandenburg and Kandaswamy Subramanian. Astrophysical magnetic fields and nonlinear dynamo theory. *Physics Reports*, 417(1-4):1–209, 2005.

[50] RC Brower, GT Fleming, and Herbert Neuberger. Lattice radial quantization: 3d ising. *Physics Letters B*, 721(4-5):299–305, 2013.

[51] Richard Brower, Claudio Rebbi, and David Schaich. Hybrid monte carlo simulation on the graphene hexagonal lattice. *arXiv preprint arXiv:1204.5424*, 2012.

[52] Richard C Brower, Michael Cheng, and George T Fleming. Improved lattice radial quantization. *arXiv preprint arXiv:1407.7597*, 2014.

[53] Richard C Brower, Michael Cheng, and George T Fleming. Quantum finite elements: 2d ising cft on a spherical manifold. *PoS LATTICE2014*, 318, 2015.

[54] Richard C Brower, Michael Cheng, Evan S Weinberg, George T Fleming, Andrew D Gasbarro, Timothy G Raben, and Chung-I Tan. Lattice ϕ 4 field theory on riemann manifolds: Numerical tests for the 2d ising cft on s 2. *Physical Review D*, 98(1):014502, 2018.

[55] Richard C Brower, George Fleming, Andrew Gasbarro, Timothy Raben, Chung-I Tan, and Evan Weinberg. Quantum finite elements for lattice field theory. *arXiv preprint arXiv:1601.01367*, 2016.

[56] Richard C Brower, George T Fleming, Andrew D Gasbarro, Dean Howarth, Timothy G Raben, Chung-I Tan, and Evan S Weinberg. Radial lattice quantization of 3d ϕ^4 field theory. *arXiv preprint arXiv:2006.15636*, 2020.

[57] Richard C Brower, George T Fleming, Andrew D Gasbarro, Dean Howarth, Timothy G Raben, Chung-I Tan, and Evan S Weinberg. Radial lattice quantization of 3d ϕ^4 field theory. *arXiv preprint arXiv:2006.15636 [hep-lat]*, 6 2020.

[58] Richard C Brower, George T Fleming, and Herbert Neuberger. Radial quantization for conformal field theories on the lattice. *arXiv preprint arXiv:1212.1757*, 2012.

[59] Iain Brown and Robert Crittenden. Non-gaussianity from cosmic magnetic fields. *Physical Review D*, 72(6):063002, 2005.

[60] Iosif L Buchbinder, Sergei D Odintsov, and Ilya Lvovitch Shapiro. Renormalization group approach to quantum field theory in curved space-time. *La Rivista del Nuovo Cimento (1978-1999)*, 12(10):1–112, 1989.

[61] Giuseppe Buttazzo, Mariano Giaquinta, Stefan Hildebrandt, et al. *One-dimensional variational problems: an introduction*. Number 15. Oxford University Press, 1998.

[62] John Cardy. *Scaling and renormalization in statistical physics*, volume 5. Cambridge university press, 1996.

[63] John L Cardy. Conformal invariance and surface critical behavior. *Nuclear Physics B*, 240(4):514–532, 1984.

[64] John L Cardy. Universal amplitudes in finite-size scaling: generalisation to arbitrary dimensionality. In *Current Physics–Sources and Comments*, volume 2, pages 370–373. Elsevier, 1988.

[65] Valerio Cascioli, Giovanni Montani, and Riccardo Moriconi. Wkb approximation for the polymer quantization of the taub model. *arXiv preprint arXiv:1903.09417*, 2019.

[66] David F Chernoff and John D Barrow. Chaos in the mixmaster universe. *Physical Review Letters*, 50(2):134, 1983.

[67] Roberta Chiovoloni, Giovanni Montani, and Valerio Cascioli. Quantum dynamics of the corner of the bianchi ix model in the wkb approximation. *Physical Review D*, 102(8):083519, 2020.

[68] NH Christ, R Friedberg, and TD Lee. Gauge theory on a random lattice. *Nuclear Physics B*, 210(3):310–336, 1982.

[69] NH Christ, R Friedberg, and T_D Lee. Random lattice field theory: General formulation. *Nuclear Physics B*, 202(1):89–125, 1982.

[70] NH Christ, R Friedberg, and TD Lee. Weights of links and plaquettes in a random lattice. *Nuclear Physics B*, 210(3):337–346, 1982.

[71] Andrew G Cohen, David B Kaplan, and Ann E Nelson. Effective field theory, black holes, and the cosmological constant. *Physical Review Letters*, 82(25):4971, 1999.

[72] Wikimedia Commons. Delaunay circumcircles centers, 1 April 2012.

[73] Neil J Cornish and Janna J Levin. The mixmaster universe is chaotic. *Physical Review Letters*, 78(6):998, 1997.

[74] Catarina Cosme, JM Viana Parente Lopes, and João Penedones. Conformal symmetry of the critical 3d ising model inside a sphere. *Journal of High Energy Physics*, 2015(8):1–15, 2015.

[75] Oliver Coussaert, Marc Henneaux, and Peter van Driel. The asymptotic dynamics of three-dimensional einstein gravity with a negative cosmological constant. *Classical and Quantum Gravity*, 12(12):2961, 1995.

[76] Mirjam Cvetič and Harald H Soleng. Naked singularities in dilatonic domain wall space-times. *Physical Review D*, 51(10):5768, 1995.

[77] Mattias Dahl. The positive mass theorem for ale manifolds. *Banach Center Publications*, 41(1):133–142, 1997.

[78] Thibault Damour and Philippe Spindel. Quantum supersymmetric bianchi ix cosmology. *Physical Review D*, 90(10):103509, 2014.

[79] Mariaveronica De Angelis and Giovanni Montani. Dynamics of quantum anisotropies in a taub universe in the wkb approximation. *Physical Review D*, 101(10):103532, 2020.

[80] P De Bernardis, PAR Ade, JJ Bock, JR Bond, J Borrill, A Boscaleri, K Coble, CR Contaldi, BP Crill, G De Troia, et al. Multiple peaks in the angular power spectrum of the cosmic microwave background: Significance and consequences for cosmology. *The Astrophysical Journal*, 564(2):559, 2002.

[81] Youjin Deng and Henk WJ Blöte. Conformal invariance and the ising model on a spheroid. *Physical Review E*, 67(3):036107, 2003.

[82] Youjin Deng, Henk WJ Blöte, and MP Nightingale. Surface and bulk transitions in three-dimensional o (n) models. *Physical Review E*, 72(1):016128, 2005.

[83] Mathieu Desbrun, Anil N Hirani, Melvin Leok, and Jerrold E Marsden. Discrete exterior calculus. *arXiv preprint math/0508341*, 2005.

[84] Bryce S DeWitt. Quantum theory of gravity. i. the canonical theory. *Physical Review*, 160(5):1113, 1967.

[85] HW Diehl and M Shpot. Massive field-theory approach to surface critical behavior in three-dimensional systems. *Nuclear Physics B*, 528(3):595–647, 1998.

[86] Michael R Douglas and Chris Hull. D-branes and the noncommutative torus. *Journal of High Energy Physics*, 1998(02):008, 1998.

[87] Sheer El-Showk, Miguel F Paulos, David Poland, Slava Rychkov, David Simmons-Duffin, and Alessandro Vichi. Solving the 3d ising model with the conformal bootstrap. *Physical Review D*, 86(2):025022, 2012.

[88] Sheer El-Showk, Miguel F Paulos, David Poland, Slava Rychkov, David Simmons-Duffin, and Alessandro Vichi. Solving the 3d ising model with the conformal bootstrap

ii.

c

c-minimization and precise critical exponents. *Journal of Statistical Physics*, 157(4):869–914, 2014.

[89] Giampiero Esposito, Alexander Yu Kamenshchik, Igor V Mishakov, and Giuseppe Pollifrone. Relativistic gauge conditions in quantum cosmology. *Physical Review D*, 52(4):2183, 1995.

[90] WD Evans. M. dimassi and j. sjöstrand spectral asymptotics in the semi-classical limit (lms lecture note series no. 268, cambridge, 1999), xi+ 227 pp., 0 521 66544 2 (paperback), 24.95. *Proceedings of the Edinburgh Mathematical Society*, 43(2):448–448, 2000.

[91] Arthur E Fischer and Jerrold E Marsden. The initial value problem and the dynamical formulation of general relativity. 1979.

[92] Willy Fischler and Leonard Susskind. Holography and cosmology. *arXiv preprint hep-th/9806039*, 1998.

[93] H Garcia-Compean, O Obregon, and C Ramirez. Noncommutative quantum cosmology. *Physical review letters*, 88(16):161301, 2002.

[94] H Garcia-Compean, O Obregon, C Ramirez, and M Sabido. Noncommutative self-dual gravity. *Physical Review D*, 68(4):044015, 2003.

[95] Andrew David Gasbarro. *Studies of Conformal Behaviorin Strongly Interacting Quantum Field Theories*. PhD thesis, Yale University, 2018.

[96] Giacomo Giampieri. A new solution of the wheeler-de witt equation. *Physics Letters B*, 261(4):411–414, 1991.

[97] Gary W Gibbons and Stephen W Hawking. *Euclidean quantum gravity*. World Scientific, 1993.

[98] Gary W Gibbons and Christopher N Pope. The positive action conjecture and asymptotically euclidean metrics in quantum gravity. *Communications in Mathematical Physics*, 66(3):267–290, 1979.

[99] Ferdinando Gliozzi, Pedro Liendo, Marco Meineri, and Antonio Rago. Boundary and interface cfts from the conformal bootstrap. *Journal of High Energy Physics*, 2015(5):36, 2015.

[100] Robert Graham. Supersymmetric bianchi type ix cosmology. *Physical review letters*, 67(11):1381, 1991.

[101] Robert Graham. Supersymmetric general bianchi type ix cosmology with a cosmological term. *Physics Letters B*, 277(4):393–397, 1992.

[102] Robert Graham. Anisotropic diagonal bianchi type-ix minisuperspace with n= 4 supersymmetry. *Physical Review D*, 48(4):1602, 1993.

[103] Robert Graham and Julius Bene. Supersymmetric bianchi type ix cosmology with a scalar field. *Physics Letters B*, 302(2-3):183–188, 1993.

[104] Dario Grasso and Hector R Rubinstein. Magnetic fields in the early universe. *Physics Reports*, 348(3):163–266, 2001.

[105] Robert B Griffiths. Consistent histories and the interpretation of quantum mechanics. *Journal of Statistical Physics*, 36(1-2):219–272, 1984.

[106] Andrea L Guerrieri, Anastasios C Petkou, and Congkao Wen. The free σ cfts. *Journal of High Energy Physics*, 2016(9):1–26, 2016.

[107] Monica Guica, Thomas Hartman, Wei Song, and Andrew Strominger. The kerr/cft correspondence. *Physical Review D*, 80(12):124008, 2009.

[108] Jonathan J Halliwell and Stephen William Hawking. Origin of structure in the universe. *Physical Review D*, 31(8):1777, 1985.

[109] ER Harrison. Generation of magnetic fields in the radiation era. *Monthly Notices of the Royal Astronomical Society*, 147(3):279–286, 1970.

[110] James B Hartle and Stephen W Hawking. Wave function of the universe. *Physical Review D*, 28(12):2960, 1983.

[111] James B Hartle, SW Hawking, and Thomas Hertog. Accelerated expansion from negative\lambda. *arXiv preprint arXiv:1205.3807*, 2012.

[112] James B Hartle, SW Hawking, and Thomas Hertog. Quantum probabilities for inflation from holography. *Journal of Cosmology and Astroparticle Physics*, 2014(01):015, 2014.

[113] Martin Hasenbusch. Thermodynamic casimir force: A monte carlo study of the crossover between the ordinary and the normal surface universality class. *Physical Review B*, 83(13):134425, 2011.

[114] Stephen W Hawking. Quantum gravity and path integrals. *Physical Review D*, 18(6):1747, 1978.

[115] Stephen W Hawking. The path-integral approach to quantum gravity. In *General relativity*. 1979.

[116] Bernard Helffer and Johannes Sjostrand. Multiple wells in the semi-classical limit i. *Communications in Partial Differential Equations*, 9(4):337–408, 1984.

[117] Bernard Hellfer. Semi-classical analysis for the schrodinger operator and applications. *Lecture Notes in Math.*, 1336, 1988.

[118] Gary Hinshaw, D Larson, Eiichiro Komatsu, David N Spergel, CLaa Bennett, Joanna Dunkley, MR Nolta, M Halpern, RS Hill, N Odegard, et al. Nine-year wilkinson

microwave anisotropy probe (wmap) observations: cosmological parameter results. *The Astrophysical Journal Supplement Series*, 208(2):19, 2013.

[119] Craig J Hogan. Magnetohydrodynamic effects of a first-order cosmological phase transition. *Physical Review Letters*, 51(16):1488, 1983.

[120] Matthijs Hogervorst. Dimensional reduction for conformal blocks. *Journal of High Energy Physics*, 2016(9):1–16, 2016.

[121] Matthijs Hogervorst and Slava Rychkov. Radial coordinates for conformal blocks. *Physical Review D*, 87(10):106004, 2013.

[122] Lotte Hollands and Andrew Neitzke. Exact wkb and abelianization for the

t_3

t 3 equation. *Communications in Mathematical Physics*, 380(1):131–186, 2020.

[123] Héctor Javier Hortúa and Leonardo Castañeda. Reduced bispectrum seeded by helical primordial magnetic fields. *Journal of Cosmology and Astroparticle Physics*, 2017(06):020, 2017.

[124] Lane P Hughston and Kenneth C Jacobs. Homogeneous electromagnetic and massive-vector fields in bianchi cosmologies. *The Astrophysical Journal*, 160:147, 1970.

[125] I Jack and H Osborn. General background field calculations with fermion fields. *Nuclear Physics B*, 249(3):472–506, 1985.

[126] Ian Jack and H Osborn. Background field calculations in curved spacetime:(i). general formalism and application to scalar fields. *Nuclear physics B*, 234(2):331–364, 1984.

[127] Karsten Jedamzik and Andrey Saveliev. Stringent limit on primordial magnetic

fields from the cosmic microwave background radiation. *Physical review letters*, 123(2):021301, 2019.

[128] Jose Beltrán Jiménez and Antonio L Maroto. Cosmological electromagnetic fields and dark energy. *Journal of Cosmology and Astroparticle Physics*, 2009(03):016, 2009.

[129] Tina Kahniashvili, Arthur Kosowsky, Andrew Mack, and Ruth Durrer. Cmb signatures of a primordial magnetic field. In *AIP Conference Proceedings*, volume 555, pages 451–456. American Institute of Physics, 2001.

[130] Tina Kahniashvili, George Lavrelashvili, and Bharat Ratra. Cmb temperature anisotropy from broken spatial isotropy due to a homogeneous cosmological magnetic field. *Physical Review D*, 78(6):063012, 2008.

[131] A Yu Kamenshchik and IV Mishakov. Fermions in one-loop quantum cosmology. *Physical Review D*, 47(4):1380, 1993.

[132] A Karagiorgos, T Pailas, N Dimakis, GO Papadopoulos, Petros A Terzis, and T Christodoulakis. Quantum cosmology of bianchi viii, ix lrs geometries. *Journal of Cosmology and Astroparticle Physics*, 2019(04):006, 2019.

[133] A Karagiorgos, T Pailas, N Dimakis, Petros A Terzis, and T Christodoulakis. Quantum cosmology of a bianchi iii lrs geometry coupled to a source free electromagnetic field. *Journal of Cosmology and Astroparticle Physics*, 2018(03):030, 2018.

[134] Ryan Kerner and Robert B Mann. Tunnelling, temperature, and taub-nut black holes. *Physical Review D*, 73(10):104010, 2006.

[135] C Kiefer. Quantum gravity 2nd ed. *Oxford University Press*, 78:190, 2007.

[136] Claus Kiefer. Continuous measurement of mini-superspace variables by higher multipoles. *Classical and Quantum Gravity*, 4(5):1369, 1987.

[137] Claus Kiefer. Quantum geometrodynamics: whence, whither? *General Relativity and Gravitation*, 41(4):877–901, 2009.

[138] Claus Kiefer and Manuel Kraemer. Quantum gravitational contributions to the cosmic microwave background anisotropy spectrum. *Physical review letters*, 108(2):021301, 2012.

[139] Claus Kiefer and Tejinder P Singh. Quantum gravitational corrections to the functional schrödinger equation. *Physical Review D*, 44(4):1067, 1991.

[140] Takeshi Kobayashi and Martin S Sloth. Early cosmological evolution of primordial electromagnetic fields. *Physical Review D*, 100(2):023524, 2019.

[141] Zohar Komargodski and David Simmons-Duffin. The random-bond ising model in 2.01 and 3 dimensions. *Journal of Physics A: Mathematical and Theoretical*, 50(15):154001, 2017.

[142] Zohar Komargodski and David Simmons-Duffin. The Random-Bond Ising Model in 2.01 and 3 Dimensions. *J. Phys. A*, 50(15):154001, 2017.

[143] Eiichiro Komatsu, J Dunkley, MR Nolta, CL Bennett, B Gold, G Hinshaw, N Jarosik, D Larson, M Limon, L Page, et al. Five-year wilkinson microwave anisotropy probe* observations: cosmological interpretation. *The Astrophysical Journal Supplement Series*, 180(2):330, 2009.

[144] Filip Kos, David Poland, and David Simmons-Duffin. Bootstrapping mixed correlators in the 3d ising model. *Journal of High Energy Physics*, 2014(11):109, 2014.

[145] Filip Kos, David Poland, and David Simmons-Duffin. Bootstrapping mixed correlators in the 3d ising model. *Journal of High Energy Physics*, 2014(11):109, 2014.

[146] Filip Kos, David Poland, David Simmons-Duffin, and Alessandro Vichi. Precision

islands in the ising and o (n) models. *Journal of High Energy Physics*, 2016(8):1–16, 2016.

[147] PK Kovtun, Dan T Son, and Andrei O Starinets. Viscosity in strongly interacting quantum field theories from black hole physics. *Physical review letters*, 94(11):111601, 2005.

[148] Hulikal R Krishnamurthy, HS Mani, and Harish C Verma. Exact solution of the schrodinger equation for a particle in a tetrahedral box. *Journal of Physics A: Mathematical and General*, 15(7):2131, 1982.

[149] Philipp P Kronberg. Extragalactic magnetic fields. *Reports on Progress in Physics*, 57(4):325, 1994.

[150] Karel V Kuchař and Michael P Ryan Jr. Is minisuperspace quantization valid?: Taub in mixmaster. *Physical Review D*, 40(12):3982, 1989.

[151] Russell M Kulsrud and Ellen G Zweibel. On the origin of cosmic magnetic fields. *Reports on Progress in Physics*, 71(4):046901, 2008.

[152] Julius Kuti. The higgs particle and the lattice. In *31st International Symposium on Lattice Field Theory LATTICE 2013*, volume 187, page 004. SISSA Medialab, 2014.

[153] LD Landau. Lifshitz 1958 quantum mechanics. *Oxford: Pergamon Press) p*, 422:817–22.

[154] Joseph KL Lee, Luigi Del Debbio, Andreas Jttner, Antonin Portelli, and Kostas Skenderis. Towards a holographic description of cosmology: Renormalisation of the energy-momentum tensor of the dual qft. *arXiv preprint arXiv:1909.13867*, 2019.

[155] Dieter Lorenz. Exact bianchi type-viii and type-ix cosmological models with matter and electromagnetic fields. *Physical Review D*, 22(8):1848, 1980.

[156] Jorma Louko. Quantum cosmology with electromagnetism. *Physical Review D*, 38(2):478, 1988.

[157] Martin Lüscher. Dimensional regularisation in the presence of large background fields. *Annals of Physics*, 142(2):359–392, 1982.

[158] Martin Lüscher. Advanced lattice qcd. *arXiv preprint hep-lat/9802029*, 1998.

[159] Matthew Luzum and Paul Romatschke. Conformal relativistic viscous hydrodynamics: Applications to rhic results at s nn= 200 gev. *Physical Review C*, 78(3):034915, 2008.

[160] Malcolm MacCallum. The mathematics of anisotropic spatially-homogeneous cosmologies. In *Physics of the Expanding Universe*, pages 1–59. Springer, 1979.

[161] A Macias, O Obregón, and J Socorro. Supersymmetric quantum cosmology. *International Journal of Modern Physics A*, 8(24):4291–4317, 1993.

[162] Mark S Madsen. Magnetic fields in cosmology. *Monthly Notices of the Royal Astronomical Society*, 237(1):109–117, 1989.

[163] Juan Maldacena. The large-n limit of superconformal field theories and supergravity. *International journal of theoretical physics*, 38(4):1113–1133, 1999.

[164] Antonella Marini, Rachel Maitra, and Vincent Moncrief. Euclidean signature semiclassical methods for bosonic field theories: interacting scalar fields. *arXiv preprint arXiv:1601.01765*, 2016.

[165] Antonella Marini, Rachel Maitra, and Vincent Moncrief. A euclidean signature semiclassical program. *Communications in Analysis and Geometry*, 28(4):979–1056, 2020.

[166] Sergio E Martinez and Michael P Ryan Jr. An exact solution for a quantum taub model. *rctm*, page 262, 1983.

[167] Paul McFadden and Kostas Skenderis. Holography for cosmology. *Physical Review D*, 81(2):021301, 2010.

[168] Teppei Minoda, Kiyotomo Ichiki, and Hiroyuki Tashiro. Small-scale cmb anisotropies induced by the primordial magnetic fields. *Journal of Cosmology and Astroparticle Physics*, 2021(03):093, 2021.

[169] Charles W Misner. Mixmaster universe. *Physical Review Letters*, 22(20):1071, 1969.

[170] Charles W Misner. Quantum cosmology. i. *Physical Review*, 186(5):1319, 1969.

[171] Charles W Misner, Kip S Thorne, John Archibald Wheeler, and WH Gravitation. Freeman and company. *San Francisco*, page 891, 1973.

[172] Audrey T Mithani and Alex Vilenkin. Inflation with negative potentials and the signature reversal symmetry. *Journal of Cosmology and Astroparticle Physics*, 2013(04):024, 2013.

[173] Koichi Miyamoto, Toyokazu Sekiguchi, Hiroyuki Tashiro, and Shuichiro Yokoyama. Cmb distortion anisotropies due to the decay of primordial magnetic fields. *Physical Review D*, 89(6):063508, 2014.

[174] Mamdouh S Mohamed, Anil N Hirani, and Ravi Samtaney. Numerical convergence of discrete exterior calculus on arbitrary surface meshes. *International Journal for Computational Methods in Engineering Science and Mechanics*, 19(3):194–206, 2018.

[175] Vincent Moncrief. Euclidean-signature semi-classical methods for quantum cosmol¬ ogy. *Surveys in Differential Geometry; commemorating the 100th anniver¬ sary of the development of General Relativity (S_ T. Yau and L. Bieri, eds.),(Invited Submission)*, 2014.

[176] Vincent Moncrief, Antonella Marini, and Rachel Maitra. Modified semi-classical

methods for nonlinear quantum oscillations problems. *Journal of mathematical physics*, 53(10):103516, 2012.

[177] Vincent Moncrief, Antonella Marini, and Rachel Maitra. Orbit space curvature as a source of mass in quantum gauge theory. *Annals of Mathematical Sciences and Applications*, 4(2):313–366, 2019.

[178] Vincent Moncrief and Michael P Ryan Jr. Amplitude-real-phase exact solutions for quantum mixmaster universes. *Physical Review D*, 44(8):2375, 1991.

[179] Ali Mostafazadeh. Quantum mechanics of klein–gordon-type fields and quantum cosmology. *Annals of Physics*, 309(1):1–48, 2004.

[180] AE Motter and PS Letelier. Mixmaster chaos. *Physics Letters A*, 285(3-4):127–131, 2001.

[181] Niall Ó Murchadha and James W York Jr. Initial-value problem of general relativity. i. general formulation and physical interpretation. *Physical Review D*, 10(2):428, 1974.

[182] Muhammad Muzammil. Canonical formulation of general relativity. *Research Gate preprint https://www.researchgate.net/publication/338170258_Canonical_Formulation_of_General_Relati* 2019.

[183] Yu Nakayama. Scale invariance vs conformal invariance. *Physics Reports*, 569:1–93, 2015.

[184] Andrii Neronov and Ievgen Vovk. Evidence for strong extragalactic magnetic fields from fermi observations of tev blazars. *Science*, 328(5974):73–75, 2010.

[185] Ezra Newman, L Tamburino, and T Unti. Empty-space generalization of the schwarzschild metric. *Journal of Mathematical Physics*, 4(7):915–923, 1963.

[186] O Obregón and J Socorro. $\psi=$ we$\pm\phi$ quantum cosmological solutions for class a bianchi models. *International Journal of Theoretical Physics*, 35(7):1381–1388, 1996.

[187] Lars Onsager. Crystal statistics. i. a two-dimensional model with an order-disorder transition. *Physical Review*, 65(3-4):117, 1944.

[188] Daniela Paoletti and Fabio Finelli. Cmb constraints on a stochastic background of primordial magnetic fields. *Physical Review D*, 83(12):123533, 2011.

[189] Robert Paternoga and Robert Graham. Exact quantum states for the diagonal bianchi type ix model with negative cosmological constant. *Physical Review D*, 54(8):4805, 1996.

[190] Matej Pavšič. Wheeler–dewitt equation in five dimensions and modified qed. *Physics Letters B*, 717(4-5):441–446, 2012.

[191] Joao Penedones, Emilio Trevisani, and Masahito Yamazaki. Recursion relations for conformal blocks. *Journal of High Energy Physics*, 2016(9):1–51, 2016.

[192] Patrick Peter and Jean-Philippe Uzan. *Primordial cosmology*. Oxford University Press, 2013.

[193] Joseph Polchinski. Scale and conformal invariance in quantum field theory. *Nuclear Physics B*, 303(2):226–236, 1988.

[194] Alexander M Polyakov. Conformal symmetry of critical fluctuations. *JETP Lett.*, 12:381–383, 1970.

[195] Jean M Quashnock, Abraham Loeb, and David N Spergel. Magnetic field generation during the cosmological qcd phase transition. *The Astrophysical Journal*, 344:L49–L51, 1989.

[196] Bharat Ratra. Cosmological'seed'magnetic field from inflation. *The Astrophysical Journal*, 391:L1–L4, 1992.

[197] T Regge and C Teitelboim. Improved hamiltonian for general relativity. *Physics Letters B*, 53(1):101–105, 1974.

[198] Tullio Regge and Claudio Teitelboim. Role of surface integrals in the hamiltonian formulation of general relativity. *Annals of physics*, 88(1):286–318, 1974.

[199] Thomas Reisz. A convergence theorem for lattice feynman integrals with massless propagators. *Communications in mathematical physics*, 116(4):573–606, 1988.

[200] Thomas Reisz. A power counting theorem for feynman integrals on the lattice. *Communications in mathematical physics*, 116(1):81–126, 1988.

[201] Thomas Reisz. Renormalization of feynman integrals on the lattice. *Communications in mathematical physics*, 117(1):79–108, 1988.

[202] Thomas Reisz. Lattice gauge theory: renormalization to all orders in the loop expansion. *Nuclear Physics B*, 318(2):417–463, 1989.

[203] Valentina Riva and J Cardy. Scale and conformal invariance in field theory: a physical counterexample. *Physics Letters B*, 622(3-4):339–342, 2005.

[204] Jose-Luis Rosales. Quantum state correction of relic gravitons from quantum gravity. *Physical Review D*, 55(8):4791, 1997.

[205] Carlo Rovelli and Francesca Vidotto. *Covariant loop quantum gravity: an elementary introduction to quantum gravity and spinfoam theory*. Cambridge University Press, 2014.

[206] Michael P Ryan Jr. The oscillatory regime near the singularity in bianchi-type ix universes. *Annals of Physics*, 70(2):301–322, 1972.

[207] Michael P Ryan Jr and Sergio M Waller. On the hamiltonian formulation of class b bianchi cosmological models. *arXiv preprint gr-qc/9709012*, 1997.

[208] Slava Rychkov. *EPFL lectures on conformal field theory in $D \geq 3$ dimensions*. Springer, 2017.

[209] Slava Rychkov, David Simmons-Duffin, and Bernardo Zan. Non-gaussianity of the critical 3d ising model. *SciPost Physics*, 2(1):1–9, 2017.

[210] Daniela Saadeh, Stephen M Feeney, Andrew Pontzen, Hiranya V Peiris, and Jason D McEwen. How isotropic is the universe? *Physical review letters*, 117(13):131302, 2016.

[211] Subir Sachdev. What can gauge-gravity duality teach us about condensed matter physics? *Annu. Rev. Condens. Matter Phys.*, 3(1):9–33, 2012.

[212] Richard M Schoen and Shing-Tung Yau. Proof of the positive-action conjecture in quantum relativity. *Physical Review Letters*, 42(9):547, 1979.

[213] Nathan Seiberg and Edward Witten. String theory and noncommutative geometry. *Journal of High Energy Physics*, 1999(09):032, 1999.

[214] H Sicotte. Large-scale magnetic fields in texture-seeded cosmological models. *Monthly Notices of the Royal Astronomical Society*, 287(1):1–9, 1997.

[215] David Simmons-Duffin. The lightcone bootstrap and the spectrum of the 3d ising cft. *Journal of High Energy Physics*, 2017(3):1–85, 2017.

[216] David Simmons-Duffin. The Lightcone Bootstrap and the Spectrum of the 3d Ising CFT. *JHEP*, 03:086, 2017.

[217] Kostas Skenderis and Paul K Townsend. Pseudo-supersymmetry and the domain-wall/cosmology correspondence. *Journal of Physics A: Mathematical and Theoretical*, 40(25):6733, 2007.

[218] J Socorro, Luis O Pimentel, C Ortiz, and M Aguero. Scalar field in the bianchi i: non-commutative classical and quantum cosmology. *International Journal of Theoretical Physics*, 48(12):3567, 2009.

[219] AA Starobinskii. Isotropization of arbitrary cosmological expansion given an effective cosmological constant. *ZhETF Pisma Redaktsiiu*, 37:55–58, 1983.

[220] Gilbert Strang and G Fix. An analysis of the finite element method 2nd edition. *Wellesley-Cambridge, Englewood Cliffs*, 2008.

[221] Andrew Strominger. The ds/cft correspondence. *Journal of High Energy Physics*, 2001(10):034, 2001.

[222] Abraham H Taub. Empty space-times admitting a three parameter group of motions. *Ann. Math*, 53(3):472–490, 1951.

[223] F Tavecchio, G Ghisellini, L Foschini, G Bonnoli, G Ghirlanda, and P Coppi. The intergalactic magnetic field constrained by fermi/large area telescope observations of the tev blazar 1es 0229+ 200. *Monthly Notices of the Royal Astronomical Society: Letters*, 406(1):L70–L74, 2010.

[224] JW Turner. On the quantum particle in a polyhedral box. *Journal of Physics A: Mathematical and General*, 17(14):2791, 1984.

[225] Michael S Turner, Erick J Weinberg, and Lawrence M Widrow. Bubble nucleation in first-order inflation and other cosmological phase transitions. *Physical Review D*, 46(6):2384, 1992.

[226] Michael S Turner and Lawrence M Widrow. Inflation-produced, large-scale magnetic fields. *Physical Review D*, 37(10):2743, 1988.

[227] Claes Uggla, Michael Bradley, and Mattias Marklund. Classifying einstein's field

equations with applications to cosmology and astrophysics. *Classical and Quantum Gravity*, 12(10):2525, 1995.

[228] Tanmay Vachaspati. Magnetic fields from cosmological phase transitions. *Physics Letters B*, 265(3-4):258–261, 1991.

[229] B Vakili, N Khosravi, and HR Sepangi. Bianchi spacetimes in noncommutative phase space. *Classical and Quantum Gravity*, 24(4):931, 2007.

[230] Alexander Vilenkin. Interpretation of the wave function of the universe. *Physical Review D*, 39(4):1116, 1989.

[231] Luca Visinelli, Sunny Vagnozzi, and Ulf Danielsson. Revisiting a negative cosmological constant from low-redshift data. *Symmetry*, 11(8):1035, 2019.

[232] Robert M Wald. Asymptotic behavior of homogeneous cosmological models in the presence of a positive cosmological constant. *Physical Review D*, 28(8):2118, 1983.

[233] Robert M Wald. General relativity(book). *Chicago, University of Chicago Press, 1984, 504 p*, 1984.

[234] SM Waller. Bianchi type-ix electromagnetic universes. *Physical Review D*, 29(2):176, 1984.

[235] John A Wheeler. Superspace and the nature of quantum geometrodynamics. *pp 615-724 of Topics in Nonlinear Physics. Zabusky, Norman J.(ed.). New York, Springer-Verlag New York, Inc., 1968.*, 1969.

[236] Lawrence M Widrow. Origin of galactic and extragalactic magnetic fields. *Reviews of Modern Physics*, 74(3):775, 2002.

[237] Xiao Zhang. Positive mass conjecture for five-dimensional lorentzian manifolds. *Journal of Mathematical Physics*, 40(7):3540–3552, 1999.